Investigating the mechanisms involved in the anti-obesity effect of conjugated linoleic acid (CLA) isomers in 3T3-L1 adipocytes, and in obese *db/db* and lean C57BL/6 mice

by

Azadeh Yeganeh

A Thesis submitted to the Faculty of Graduate Studies of

The University of Manitoba

in partial fulfillment of the requirements for the degree of

DOCTOR OF PHILOSOPHY

Department of Physiology and Pathophysiology

University of Manitoba

Winnipeg

ABSTRACT

The high rate of obesity is having a significant impact on human health. Understanding the underlying biological mechanisms that regulate adipogenesis and adipocyte lipid metabolism is necessary to identify novel approaches that promote weight loss. Conjugated linoleic acid (CLA) is an example of a naturally-derived product reported to exhibit an anti-obesity effect.

For this thesis, it was hypothesized that the anti-obesity effects of the *t*10-*c*12 CLA isomer is due to lipid droplet dynamics alteration through activation of the Wnt/β-catenin pathway, which leads to weight loss via affecting adipogenesis and/or adipocyte death. Testing of this hypothesis was achieved by examining the effects of the most biologically active CLA isomers, *cis*-9, *trans*-11 (*c*9-*t*11), *trans*-10, *cis*-12 (*t*10-*c*12) CLA using *in vitro* (3T3-L1 cell line) and *in vivo* (mouse) models.

In 3T3-L1 preadipocytes, both *c*9-*t*11 and *t*10-*c*12 CLA stimulated early stage differentiation, while *t*10-*c*12 CLA inhibited late differentiation as indicated by fewer lipid droplets, lower adipokine levels, and decreased levels of perilipin-1 and phospho-perilipin-1 compared to null. The *t*10-*c*12 CLA isomer decreased hormone-sensitive lipase (HSL) levels and inhibited lipolysis by activating protein kinase Cα (PKCα). As well, *t*10-*c*12-CLA inhibited adipocyte differentiation by stabilizing β-catenin, which sequesters peroxisome proliferator-activated receptor-γ in an inactive complex.

Reduced body weight in both *db/db* and C57B/L6 mice fed *t*10-*c*12 CLA was due to less white and brown fat mass without changes in lean body mass or an alteration in

feed intake compared to their respective control. *t*10-*c*12 CLA did not stimulate cell death in white adipose tissue. Immune cell infiltration was decreased in calorie restricted pair weight control mice, but not with CLA. *t*10-*c*12 CLA-induced weight loss did not improve hyperglycemia in *db/db* mice.

In conclusion, the anti-adipogenic effects of *t*10-*c*12 CLA *in vitro* result from stabilization of β-catenin, which alters lipid droplet dynamics through HSL levels and perilipin-1 phosphorylation via the activation of PKCα. In contrast, *t*10-*c*12 CLA promotes loss of adipose tissue *in vivo*, possibly by activating β-catenin, but without influencing either adipogenesis or adipocyte clearance. This study suggests a novel mechanism for the anti-obesity effect of *t*10-*c*12 CLA, and highlights the possible side-effects associated with *t*10-*c*12 CLA consumption.

ACKNOWLEDGEMENTS#

I would like to thank my advisors Dr. Peter Zahradka and Dr. Carla Taylor, for their guidance, encouragment and support during my PhD work. I greatly appreciate their feedback throughout the past years; this project would not have been completed without their constant support. I am forever indebted to them for giving me a chance to study under their guidance and work in their respective labs. They taught me how to be a great scientist as well as how to be a better person. Thank you very much for all of your understanding, patience, constant encouragement and all your help.

I would like to thank my thesis committee members: Dr. Elissavet Kardami, Dr. Peter Cattini and Dr. Jeffry Wigle for their valuable advice and guidance. Particularly, .I would like to thank Dr. Kardami and her lab members Robert Fandrich & Barbara Nickel for providing some of the materials and equipment which helped me complete my project and for all your help and advice.

My special thanks to Leslee Tworek for keeping the lab going and providing the peaceful environment and also helping with the lipolysis assay. Thank you to Amy Klann and Amy Wu for their help with the animal study, which certainly I would not be able to accomplish without their assistance. Thank you to Jenna Poole for helping me with the animal study and with Western blotting. And thank you to past and present Zahradka/Taylor lab members for being very good friends; I was very fortunate to work with you and have you as my friends.

I would like to extend my thanks to my family and friends for all of their encouragement. My special thanks to my loving husband Behzad. My sincerest thanks to my son, Omid, who is my greatest joy in life, for all his encouragment, understanding, support and patience. I would not

have been able to complete this work without your love and support. I dedicate this thesis to my son, Omid.

TABLE OF CONTENTS

LIST OF FIGURES

LIST OF TABLES

LIST OF ABBREVIATIONS

ACRP30	Adiponectin or Adipocyte complement related protein 30 kDa
ADRP	Adipophilin
ADSCs	Adipocyte-derived stem (stromal) cells
A-FABP	Adipocyte fatty acid binding protein
AMP	Adenosine-5'-monophosphate
AMPK	Adenosine monophosphate-activated protein kinase
ANOVA	Analysis of variance
aP2	A-FABP or Adipocyte protein 2
APC	Adenomatous polyposis coli
APC	Allophycocyanin
APS	Ammonium persulfate
ASCs	Adipose stem cells
ATGL	Adipose triglyceride lipase
ATP	Adenosine-5'-triphosphate
BAT	Brown adipose tissue
BCA	Bicinchoninic Acid
BMI	Body mass index
BMP	Bone morphogenetic protein
BSA	Bovine serum albumin

*c*9-*t*11 CLA	*cis* 9-*trans* 11 conjugated linoleic acid
CamKII	Ca^{2+}/calmodulin-dependent protein kinase
cAMP	Cyclic adenosine monophosphate
C/EBP-α	CCAAT/ enhancer binding protein-α
C/EBP-β	CCAAT/ enhancer binding protein-β
CIDE	Cell death-inducing DNA fragmentation factor-α-like effector
CIP	Calf intestinal alkaline phosphatase
CKI-α	Casein kinase I-α
CLA	Conjugated linoleic acid
CREB	cAMP response element binding protein
CRP	C-reactive protein
CTL	Control
CVD	Cardiovascular disease
DC	Dendritic cell
DEX	Dexamethasone
ddH_2O	Double distilled water
DIO	Diet induced obesity
DMEM	Dulbecco's modified Eagle's medium
DNA	Deoxyribonucleic acid
Dsh/Dvl	Dishevelled

eEF2	Eukaryotic translation elongation factor 2
ER	Endoplasmic reticulum
ERK	Extracellular signaling-regulated kinase
FBS	Fetal bovine serum
FFA	Free fatty acid
FGF	Fibroblast growth factor
FITC	Fluorescein isothiocyanate
FZ	Frizzled receptor
GAPDH	Glyceraldehyde 3-phosphate dehydrogenase
GLUT	Glucose transporter
GPR-1	G protein-coupled receptor 1
GSK-3	Glycogen synthase kinase-3
HEPES	4-(2-Hydroxyethyl)piperazine-1-ethanesulfonic acid
HFD	High fat diet
HLB	Hypotonic lysis buffer
HOMA-IR	Homeostasis model assessment –insulin resistance
HRP	Horseradish peroxidase
HSL	Hormone sensitive lipase
IF	Immunofluorescence
iNOS	Inducible nitric oxide synthase

IGF-1	Insulin-like growth factor-1
IL	Interleukin
IRS	Insulin-receptor substrate
INS	Insulin
IP	Immunoprecipitation
JNK	c-Jun amino terminal kinase
LC3	Light chain 3
kDa	Kilodalton
LEF/TCF	Lymphoid-enhancer-binding factor/T-cell-specific transcription factor
LPS	Lipopolysaccharide
LRP	Low-density lipoprotein receptor-related
MAPK	Mitogen activated protein kinase
MHC	Major histocompatibility complex
MIX	Methylisobutylxanthine
MCP-1	Monocyte chemoattractant protein-1
MEF	Mouse embryonic fibroblast
NF-κB	Nuclear factor-kappa B
NKT	Natural killer T cells
OCT	Optimal cutting temperature
PBS	Phosphate-buffered saline

PE	Phycoerythrin
PI3K	Phosphatidylinositol 3-kinase
PGC1α	PPARγ-coactivator-1α
PKA	Protein kinase A
PKB	Protein kinase B
PLIN	Perilipin
PMSF	Phenylmethylsulfonyl fluoride
PPARγ	Peroxisomal proliferator - activated receptor γ
PRDM16	PR-domain-containing 16
PTCH	Patched receptor
PW	Pair weight
QMR	Quantitative magnetic resonance
RNA	Ribonucleic acid
RXR	Retinoid X receptor
SB	Sample buffer
SDS	Sodium dodecyl sulfate
SDS-PAGE	Sodium dodecyl sulphate-polyacrylamide gel electrophoresis
SFRP	Soluble frizzled-related proteins
SOCS-3	Suppressor of cytokine signaling-3
SVF	Stromal vascular fraction

*t*10-*c*12 CLA	*trans* 10-*cis*12 conjugated linoleic acid
TBST	Tris-buffered saline with Tween-20
TBX-1	T-box protein-1
TG	Triglycerides/ Triacylglycerol
TGF-β	Transforming growth factor-β
TMEM26	Transmembrane protein 26
TNF-α	Tumor necrosis factor-α
TZD	Thiazolidinedione
UCP	Uncoupling protein
VCAM-1	Vascular cell adhesion molecule-1
VLDL	Very low-density lipoprotein
WAT	White adipose tissue
WHO	World Health Organization
ZDF	Zucker diabetic fatty

1. Literature review

1.1 Adipose tissue and its formation

1.1.1 Adipose tissue in health and disease

Adipose tissue is necessary for maintaining normal physiology. It is the largest energy reserve in the body. This tissue contains a unique cell type (adipocyte) that is involved in the storage and mobilization of lipids. When energy is needed, triglycerides (TG) stored in the adipocytes are hydrolysed by lipases to produce free fatty acids (FFA), which are then transported via the circulation to tissues that oxidize them in the mitochondria for energy production. In addition, adipose tissue is an active endocrine organ that secretes hormones and cytokines involved in the regulation of appetite and metabolism, energy expenditure, insulin sensitivity, inflammation and coagulation (Hauner 2005). Adipose tissue is a highly dynamic tissue that can change its metabolism rapidly in response to the body's energy status. In adipose tissue, mature adipocytes account for the majority of the mass and volume, but they contribute less than 20% to the total cell number (Eto, Suga et al. 2009). The rest of the cells in adipose tissue are referred to as the stromal vascular fraction (SVF), which consists of a heterogeneous population of stem cells, fibroblasts, endothelial cells, macrophages and various immune cells such as lymphocytes. Adipose tissue plays an important role in both healthy and disease states. Genetic disorders that lead to a loss of fat in certain depots, called lipodystrophy, are associated with insulin resistance, dyslipidemia and cardiovascular disease (CVD) (Capeau, Magre et al. 2005), all conditions that also occur when there is an excess of fat mass (obesity) (Pedersen 2013). Therefore, maintaining functional and healthy adipose tissue is a key factor for overall health.

Adipose tissue can be classified by its morphological appearance as either white adipose tissue (WAT) or brown adipose tissue (BAT).

1.1.2 White adipose tissue (WAT)

WAT originates from multipotent mesenchymal stem cells and mostly develops after birth. Morphologically, WAT contains mature white adipocytes with a unilocular lipid droplet, a thin cytoplasm and few mitochondria. As a result of the high plasticity of adipocytes, WAT can rapidly expand in size; thus, in obese individuals, adipose tissue represents the second largest organ in the body after the skin (Mueller 2014). Developmentally, WAT originates from the mesoderm, except the facial adipose tissue that originates from neuro-ectodermal cells (Billon and Dani 2012). There are various distinct fat depots in the body that can be distinguished by different properties such as adipocyte number and size, insulin sensitivity, glucose and lipid metabolism, lipolytic rates, and adipokine secretion (Hausman, DiGirolamo et al. 2001; Laviola, Perrini et al. 2006).

There is no clear system for distinguishing the location of different fat depots. Thus, the depots' names vary between studies. Experts in the field divide WAT into 5 different depots: 1) Anterior subcutaneous WAT, which includes intrascapular and axillary WAT, 2) Inguinal WAT, which is attached dorsally along the pelvis to the thigh of the back limb, 3) Perigonadal WAT that surrounds the uterus and ovaries in females and the epididymis and testes in males, 4) Perirenal WAT, located within the abdominal cavity along the dorsal wall of the abdomen behind the kidney, also known as the retroperitoneal depot, and 5) Mesenteric WAT, which lines the surface of the intestines.

In most of the reports, the combination of perigonadal, perirenal and mesenteric fat is called visceral fat. WAT accumulation in different depots can affect pathogenesis during obesity. These fat depots are differentially distributed in males and females.

Females in general have more fat than males (Gallagher, Visser et al. 1996; Jackson, Stanforth et al. 2002). Female accumulation of WAT occurs mostly as glutofemoral subcutaneous WAT (pear phenotype), which is associated with insulin sensitivity and a reduced risk of diabetes and CVD. In males, accumulation of visceral WAT (apple phenotype) is typical, and is associated with greater risk for metabolic disorders. In addition, substantial amounts of the primary sex hormones (estrogen and testosterone) are detected in adipose tissue (Simpson 2003; Stocco 2012), which may affect the distribution of different depots and thus lead to specific phenotypes in males and females. One of the important distinctions between different depots is their blood flow and innervation density in various fat depots (Hausman, DiGirolamo et al. 2001; Laviola, Perrini et al. 2006). Inguinal WAT and mesenteric WAT show greater blood flow and innervation density compared to other depots (Hausman, DiGirolamo et al. 2001).

WAT depots respond differently to increased calorie intake; visceral WAT is more prone to adipocyte hypertrophy, which correlates with higher metabolic risk, while inguinal (subcutaneous) WAT is more susceptible to hyperplasia of adipocytes, which leads to production of new healthy adipocytes (Joe, Yi et al. 2009). Interestingly, Tchoukalova et al. (2010) have shown that subcutaneous WAT located in the upper body and abdominal area is more prone to hypertrophy in response to overfeeding compared to femoral subcutaneous WAT, which has a higher rate of hyperplasia.

Recently another type of adipocyte has been identified within WAT, mostly in the inguinal adipose tissue of mice and subcutaneous adipose tissue of humans, referred to as brown-like adipocytes which are also known as brite or beige adipocytes. Beige adipocytes morphologically resemble white adipocytes but are involved in thermogenesis upon stimulation (e.g., cold exposure and/or β_3-adrenergic receptor activation) (Himms-Hagen, Melnyk et al. 2000; Barbatelli, Murano et al. 2010) and have more mitochondria compared to white adipocytes (Wu, Bostrom et al. 2012). Studies show the inter-conversion between beige and white adipocytes is possible when the WAT switches from energy storage to energy expenditure in the presence of thermogenic stimuli. Beige adipocytes are similar to white adipocytes with respect to having a unilocular large lipid droplet and expressing the white adipose tissue specific marker PPARγ during the basal state. However, upon appropriate stimulation, brown adipocytes change to a multilocular lipid droplet morphology and express brown adipocyte specific genes such as uncoupling protein-1 (UCP-1). Beige adipocytes also have their own distinct gene profile as they express T-box protein-1 (TBX-1) and transmembrane protein 26 (TMEM26), which are not expressed in white or brown adipocytes (Barbatelli, Murano et al. 2010; Park, Kim et al. 2014).

1.1.3 Brown adipose tissue (BAT)

BAT has a distinct developmental pattern compared to WAT. Unlike WAT, BAT develops and differentiates during fetal development. Its primary function is non-shivering thermogenesis, which protects the newborn against cold. The amount of BAT declines with age in both humans and rodents (Cannon and Nedergaard 2004), although it

is always detectable in adults, even at low levels. BAT is located in depots located in the interscapular, sub-scapular and cervical regions. BAT is also detected around the aorta and kidneys (Fitzgibbons, Kogan et al. 2011). Interscapular BAT is located between the shoulders and can be easily dissected in animal studies, while the perirenal BAT is hard to remove without removing the kidneys (Park, Kim et al. 2014).

Some important characteristics of BAT are the presence of multilocular lipid droplets, rich vascularization and innervation, and elevated mitochondrial density. Sympathetic nervous system activation and exposure to cold are the two main stimulators of BAT (Golozoubova, Hohtola et al. 2001; Nedergaard, Golozoubova et al. 2001; Golozoubova, Cannon et al. 2006). Production of heat by BAT is executed in the mitochondria, with UCP-1 being the main mediator of this process. UCP-1 is a trans-membrane protein located in the inner membrane of mitochondria that regulates acute non-shivering thermogenesis by dissipating the proton electrochemical gradient across the inner membrane of mitochondria, thereby converting chemical energy into heat (Tseng, Cypess et al. 2010). Different forms of UCP are present in other tissues, such as non-thermogenic UCP-2, which is found in a variety of tissues including WAT, and UCP-3 in skeletal muscle (Boss, Samec et al. 1997; Fleury, Neverova et al. 1997).

1.1.4 White adipocyte turnover

Adipose tissue is a highly dynamic and active organ. Thus, the view that adipocytes are just terminally differentiated cells that modulate their lipid content in response to changes in energy balance with no turnover no longer holds. In fact, it has been reported that adipocytes have a turnover rate of 10% per year (Spalding, Arner et al.

2008). Increases in adipocyte numbers occur in obesity, and the adipocyte numbers are also tightly regulated during weight loss. This well-maintained turnover of adipocytes is achieved by balancing both adipocyte production (adipogenesis) and adipocyte death. The importance of adipogenesis and the mechanisms regulating adipocyte death will be discussed in the next sections.

1.1.4.1 Adipocyte progenitor cells (stem cells)

Rodbell et al. (1964) were the first to digest rat WAT for the purpose of separating mature adipocytes from the non-adipocyte cells that make up the SVF. Later on, culturing human SVF resulted in the differentiation of fibroblastic SVF into lipid filled adipocytes (Ng, Poznanski et al. 1971). Early work by Hausman et al. (1980) revealed that a wide range of cells common to red bone marrow were involved in the development of adipose tissue, among them endothelial cells, macrophages, fibroblasts and perivascular mesenchymal cells. After the discovery of stem cell-specific surface markers, other investigators showed that adipose tissue and bone marrow–derived mesenchymal stem cells have a similar protein expression profile (Gronthos, Franklin et al. 2001; De Ugarte, Alfonso et al. 2003). Many studies showed that adipocyte-derived stem (stromal) cells (ADSCs) or adipose stem cells (ASCs), which are the adherent population of SVF, have the ability to differentiate into many cell types *in vitro*, including adipocytes, osteoblasts, chondrocytes, and skeletal myocytes (Gimble, Katz et al. 2007). The pattern of cell surface marker expression also confirms that ADSC/ASC cultures are a heterogeneous population of cells (Zuk, Zhu et al. 2002; Guilak, Lott et al. 2006; Mitchell, McIntosh et al. 2006).

ADSC/ASC of SVF has been characterized in greater detail using flow cytometry and fluorescence-activated cell sorting (FACS), which use cell surface markers to identify and isolate specific populations of live cells. Rodehffer et al. (2008) were the first to use FACS to characterize ADSC/ASC from subcutaneous WAT, and this led to the discovery of two stromal cell populations with adipogenic activity *in vitro*. Both populations are negative for blood and endothelial specific markers (CD45, CD31, Ter119), while positive for mesenchymal and stem cell markers (CD29, CD34, Sca-1). The only difference between the two populations is CD24 expression. One cell population is characterized by $CD45^{-}CD31^{-}Ter119^{-}CD29^{+}CD34^{+}Sca\text{-}1^{+}CD24^{-}$, and is known as the $CD24^{-}$ population. These cells have adipogenic ability *in vitro* but they failed to differentiate into adipocytes when they were injected into the underdeveloped perigonadal adipose tissue of lipodystrophic mice. The other cell population is characterized by the cell surface marker profile of $CD45^{-}CD31^{-}Ter119^{-}CD29^{+}CD34^{+}Sca\text{-}1^{+}CD24^{+}$, and is known as the $CD24^{+}$ population. This cell population is highly adipogenic and capable of differentiating into functional adipocytes in lipodystrophic mice. Furthermore, the $CD24^{+}$ cells are PPARγ and C/EBPα negative and have the ability to give rise to the $CD24^{-}$ population. In contrast, the $CD24^{-}$ population lacks this characteristic and expresses PPARγ and C/EBPα (Berry and Rodeheffer 2013). Based on these findings, Rodeheffer et al. (2008) concluded that the $CD24^{+}$ population contains adipocyte progenitor cells that can differentiate into adipocytes only in a WAT environment, while the $CD24^{-}$ population represents preadipocytes already committed to the adipocyte lineage and thus have low adipogenic ability.

1.1.4.2 Adipogenesis

Obesity is a result of both an increase in adipocyte size (hypertrophy) and an increase in adipocyte number (hyperplasia) (Joe, Yi et al. 2009; Wang, Tao et al. 2013). WAT development begins in the embryo, although the bulk of tissue expansion mostly occurs after birth, when specialized fat storing cells are needed. Spalding et al. (2008) showed that approximately 10% of the body's adipocytes are regenerated each year and this regeneration of new fat cells could be affected by environmental factors such as nutritional status (Faust, Johnson et al. 1978; Faust, Miller et al. 1984; Miller, Faust et al. 1984).

Adipocytes are derived from multipotent mesenchymal stem cells (Pittenger, Mackay et al. 1999). Stem cells and the mature adipocytes have very distinct characteristics, although characterization of the specific intermediates at the molecular level has been difficult.

Adipogenesis occurs in two phases, determination (or commitment) and terminal differentiation. During the determination process, pluripotent stem cells undergo a multi-step process, which results in restriction to the adipocyte lineage, although they do not express any adipocyte markers yet. At this point, the pluripotent stem cells convert to preadipocytes, but remain morphologically indistinguishable. At the same time, the cells lose their pluripotent ability. There are many factors that can trigger the process of commitment; these factors may be secreted by cells within the stromal vascular population, such as macrophages and adipocytes undergoing hypertrophy.

In the second phase, terminal differentiation, preadipocytes are exposed to differentiation inducers, which trigger two rounds of mitotic clonal expansion. This leads

to a 4-fold increase in cell number. Subsequently, the preadipocytes differentiate into mature adipocytes, which exhibit the characteristics associated with mature adipocytes such as lipid transport and synthesis, insulin sensitivity and the production of adipokines. Overall, adipogenesis is a sequential and temporally defined process, which involves multiple signaling cascades. Unlike terminal differentiation of preadipocytes to adipocytes, which is well studied, the specific details of the commitment phase, when the pluripotent stem cells become restricted to the adipocyte lineage, are not known. The process of adipogenesis has been reviewed in detail in various articles (Siersbaek, Nielsen et al. 2012; Tang and Lane 2012).

Our current understanding of the molecular regulation of adipocytes was obtained through the use of adipocyte cell culture models: 1) pluripotent stem cell lines that are not committed to the adipocyte linage, such as C3H10T1/2, which was isolated from C3H mouse embryos (Reznikoff, Brankow et al. 1973), and 2) preadipocyte cell lines, which are already restricted to the adipogenic lineage, such as 3T3-L1 and 3T3-F442A. The 3T3-L1 line, which was cloned from heterogeneous Swiss 3T3 cells that had been derived from dissociated near-term mouse embryos, is the most commonly used preadipocyte cell line (Green and Meuth 1974). Differentiation of 3T3-L1 cells can be divided into four separate stages: pre-confluent proliferation, confluence, hormonal induction, and terminal differentiation (Cornelius, MacDougald et al. 1994). Many factors and pathways are involved, which will be discussed in the following sections. Adipogenesis of 3T3-L1 cells is induced by adding an adipogenic cocktail containing dexamethasone (DEX) (Miller, Hackenberg et al. 1978; Rubin, Hirsch et al. 1978),

insulin (INS) (Green and Kehinde 1975) and methylisobutylxanthine (MIX) (Russell and Ho 1976); this cocktail significantly enhances the adipogenesis process. However, while this method of differentiation is effective for preadipocyte cell lines, primary cells require the addition of indomethacin (Peroxisome proliferator activated receptor γ (PPARγ) agonist), which leads to the accumulation of lipid in mesenchymal stem cells that are not committed to an adipogenic lineage (Styner, Sen et al. 2010).

Although studies of 3T3-L1 preadipocyte differentiation have provided tremendous knowledge in regards to molecular mechanisms and regulation of adipogenesis, studying adipogenesis *in vitro* has limitations. A particular issue is the need to stimulate the cells with a reagent cocktail in order to trigger differentiation. At this time, the role of the individual factors in the cocktail as they relate to adipogenesis *in vivo* has not yet been resolved. Thus, one of the limitations associated with the use of this stimulation cocktail *in vitro* is the lack of clarity regarding how these factors contribute to the induction of adipogenesis *in vivo*. In addition, lipid droplet formation will be observed within 48 hours when cells undergo adipogenesis in culture, while this process may take over 35 days *in vivo* (Greenwood and Hirsch 1974; Wang, Tao et al. 2013).

1.1.4.3 Adipocyte clearance

Similar to many other cell types, adipocytes have a half-life of about 4-5 years (Spalding, Arner et al. 2008). Different mechanisms are involved in adipocyte clearance and include programmed cell death or inflammation. These pathways are regulated by different factors such as diet (Feng, Tang et al. 2011). The importance of adipogenesis

has been discussed previously in detail; therefore, the mechanisms regulating adipocyte death will be discussed in the next sections.

1.1.4.3.1 Necrosis

Necrosis is an irreversible process that leads to cell death (Proskuryakov, Konoplyannikov et al. 2003) due to factors such as injury, radiation or chemicals. Adipocyte cell death primarily occurs through necrosis rather than other types of cell death (Loftus, Kuhajda et al. 1998). Due to the release of cellular contents into the extracellular matrix, necrotic cell death is associated with macrophage accumulation in WAT (Cinti, Mitchell et al. 2005), which leads to induction of "crown-like structures" which consist of a dying adipocyte surrounded by macrophages. This type of cell death is associated with inflammation and is closely tied to the metabolic complications of obesity. Since the macrophages are also responsible for removing the lipid droplets of the dead adipocyte; lipid accumulates in the macrophages, resulting in the formation of foam-like cells (Prieur, Mok et al. 2011), which are specifically found in subcutaneous and omental fat depots of obese humans (Shapiro, Pecht et al. 2013). Cinti et al. (2005) reported that obese humans and mice have a 30-fold increase in necrosis-like cell death in WAT compared to their lean counterparts. A positive correlation between necrosis-like cell death and adipocyte cell size has also been observed in obese mice and humans (Cinti, Mitchell et al. 2005).

1.1.4.3.2 Apoptosis

Another type of cell death that adipocytes can undergo is apoptosis. Apoptosis is a type of programmed cell death that is observed in physiological processes involved in the removal of selected cells in an efficient manner, without releasing their contents into the surrounding extracellular space (Della-Fera, Qian et al. 2001). Apoptosis can be initiated by many pathways, all of which trigger an energy-dependent enzymatic cascade that leads to the breakdown of DNA, lipids and other macromolecules (Fuchs and Steller 2011). These pathways involve activation of the tumor necrosis factor alpha (TNF-α) receptor, also known as death receptor, which initiates the apoptosis cascade through activation of caspase-8 and caspase-3 (Della-Fera, Qian et al. 2001). TNF-α induced apoptosis is mediated by caspase-3 and occurs in both preadipocytes and mature adipocytes (Della-Fera, Qian et al. 2001). There is evidence that suggests PPARγ is involved in the induction of apoptosis in large adipocytes (Qian, Hausman et al. 1998). Adipocyte apoptosis is elevated in the WAT of diet-induced obese mice and obese humans with type 2 diabetes (Keuper, Bluher et al. 2011; Bluher, Kloting et al. 2014).

1.1.4.3.3 Autophagy

Autophagy is a catabolic process by which cytoplasmic macromolecules and organelles undergo lysosomal degradation, thus supplying energy during development and under conditions of nutrient shortage (Mizushima and Levine 2010). Despite its role in survival, autophagy also contributes to caspase-independent cell death, a process that is linked with autophagosome accumulation in cells (Shimizu, Kanaseki et al. 2004). Three distinct forms of autophagy have been identified: chaperone-mediated autophagy,

microautophagy and macroautophagy (Klionsky, Abdalla et al. 2012). Each form of autophagy is associated with a different way of delivering material to the lysosome. Long term starvation and oxidative stress induce chaperone-mediated autophagy, which selectively degrades cytosolic proteins in lysosomes (Kaushik and Cuervo 2012). In contrast, macroautophagy is involved in degrading damaged proteins and cytoplasmic organels such as mitochondria and endoplasmic reticulum (Mizushima and Levine 2010). The mechanisms involved in microautophagy are not clear yet. Autophagy-related (Atg) proteins are the basic component of the autophagy process, which requires the involvement of a ubiqutin-like protein conjugation system (Mizushima, Noda et al. 1998). Vesicle elongation into a lysosome requires two ubiqutin-like conjugation sytems, one of which forms the Atg12–Atg5 conjugate through the action of E3 ligase of microtubule-associated protein 1 light chain 3 (LC3) (Klionsky, Abdalla et al. 2012). The second system conjugates LC3 with phosphatidylethanolamine, which leads to the conversion of soluble LC3 (LC3I) to its lipidated form, LC3II, so it that can be incorporated into the autophagosome membrane (Hanada, Noda et al. 2007; Kroemer, Marino et al. 2010).

Increased autophagy was observed during normal 3T3-L1 preadipocyte and Mouse embryonic fibroblast (MEF) differentiation (Baerga, Zhang et al. 2009). Mice with a global knockout of Atg5 died one day after birth and post mortem analysis of WAT revealed a reduction in perilipin-1 in adipose tissue compared to wild type (Baerga, Zhang et al. 2009). Deletion of Atg7 in 3T3-L1 preadipocytes and MEFs blocks adipogenesis (Singh, Xiang et al. 2009). Adipose tissue-specific deletion of Atg7 in mice showed that autophagy is involved in the regulation of fat mass as these animals were

resistant to diet-induced obesity. It also revealed that autophagy contributes to the balance between WAT and BAT, as the white adipocytes of Atg7$^{-/-}$ mice contained multiple lipid droplets, a higher numbers of mitochondria and increased β-oxidation compared to the wild type (Zhang, Goldman et al. 2009). Overall, Atg7$^{-/-}$ mice had improved insulin sensitivity, and lower plasma TG and leptin levels, although no changes in adiponectin levels were detected. However, inconsistent with the improvement in metabolic markers, the Atg7$^{-/-}$ mice had higher macrophage infiltration in WAT when challenged with a high fat diet (Zhang, Goldman et al. 2009). These findings suggest that autophagy may regulate adipocyte death by mediating the macrophage survival (Zhang, Goldman et al. 2009; Ma, Panda et al. 2011). However, the direct relationship between autophagy and cell death is still not clear and thus remains controversial (Shen and Codogno 2011). Certain evidence suggests there are interactions between processes active in autophagy and other types of cell death, but these are not fully understood at this time (Jain, Paczulla et al. 2013). The role of autophagy in adipose tissue biology has been recently reviewed (Zhang, Zeng et al. 2012).

1.1.5 Transcriptional regulation of adipogenesis

After induction of adipogenesis in confluent preadipocytes with the adipogenic cocktail, the cells synchronously re-enter the cell cycle and express a cascade of transcription factors, which ultimately lead to preadipocyte differentiation and expression of the adipocyte phenotype. The two most important transcription factor families that regulate adipogenesis are highlighted in the next sections.

1.1.5.1 CCAAT/enhancer binding proteins (C/EBP)

The C/EBP family is known to control numerous activities in various tissues, including cell growth (Tanaka, Yoshida et al. 1997), differentiation (Smink and Leutz 2010) and immune processes (Friedman 2007). C/EBPα was the first to be identified in this family. To date five more C/EBPs have been identified; four of these six members are expressed in adipocytes and have been shown to be involved in adipogenesis, including C/EBPα, C/EBPβ, C/EBPδ and C/EBPζ (also known as CHOP-10) (Tsukada, Yoshida et al. 2011). One of the main characteristics of the C/EBP family is that all the members have similar abilities to bind to the CCAAT motif found in various gene promoters including those for stearoyl-CoA desaturase, glucose transporter-4 (GLUT-4), adipocyte protein 2 (aP2), phosphoenolpyruvate carboxykinase and UCP (Christy, Yang et al. 1989; Kaestner, Christy et al. 1990; Park, Gurney et al. 1993; Park, Song et al. 1999). The C/EBP family is also characterized by a transactivation domain, a DNA-binding basic site and a leucine-rich dimerization domain. The well conserved leucine-rich domain and its role in dimerization are required for DNA binding (Landschulz, Johnson et al. 1989).

C/EBPβ and C/EBPδ are early regulators of adipogenesis; their expression rapidly increases within four hours following induction of differentiation (Tang and Lane 1999). The importance of these factors is revealed by the fact that over-expression of either factor in preadipocytes enhances adipogenesis in cell culture (Yeh, Cao et al. 1995; Darlington, Ross et al. 1998). However, knocking out C/EBPβ or C/EBPδ in mice has no effect on body weight and they have normal fat depots (Tanaka, Yoshida et al. 1997). These data suggest that C/EBPβ and C/EBPδ functions are not as critical for adipocyte

differentiation *in vivo*, however, the double knock out C/EBPβ$^{-/-}$/C/EBPδ$^{-/-}$ mice had lower body weight and smaller adipose depots (Tanaka, Yoshida et al. 1997). Despite the small adipose depots, the adipocytes were of normal size and functional, which suggests a role for C/EBPβ and C/EBPδ in adipocyte hyperplasia. The role of C/EBPβ in modulating adipocyte differentiation through regulation of gene transcription has been recently reviewed in detail (Guo, Li et al. 2015).

C/EBPα is a multi-functional transcriptional activator that plays a critical role in preadipocyte differentiation (Rangwala and Lazar 2000). Phosphorylation of C/EBPα by glycogen synthase kinase 3β (GSK3β), on the insulin-dependent sites Thr222 and Thr 226, is required to fulfill its role in adipogenesis (Ross, Erickson et al. 1999). It has been shown that in the absence of hormonal stimulation, conditional expression of C/EBPα is sufficient for induction of adipogenesis (Freytag and Geddes 1992; Freytag, Paielli et al. 1994; Lin and Lane 1994). Furthermore, inhibition of C/EBPα by siRNA blocks adipocyte differentiation (Lin and Lane 1992). It was also reported that C/EBPα$^{-/-}$ mice are unable to accumulate lipids in hepatocytes and adipocytes and die within 8 hours after birth (Wang, Finegold et al. 1995; Flodby, Barlow et al. 1996). C/EBPβ and C/EBPδ are responsible for the transcriptional activation of C/EBPα, after which its expression is maintained through auto-activation (Christy, Kaestner et al. 1991).

C/EBPζ (CHOP-10), unlike other members of C/EBP family, is rich in proline and glycine residues at its DNA binding site, and this inhibits its DNA binding ability. CHOP-10 can heterodimerize with C/EBPβ, which leads to its inactivation and the inhibition of adipogenesis (Darlington, Ross et al. 1998). Over expression of CHOP-10 in 3T3-L1 cells inhibits adipogenesis. In addition, CHOP-10 knockout mice showed an

increase in fat mass compared with wild-type mice on a high fat diet (Han, Murthy et al. 2013).

1.1.5.2 Peroxisome proliferator-activated receptors γ (PPAR γ)

Within the transcriptional cascade of adipogenesis, PPARγ is the master regulator that is required for development of the adipocyte phenotype both *in vivo* and *in vitro*. PPARγ is a member of the nuclear hormone receptor family, which includes retinoic acid receptors and thyroid hormone receptors (Aranda and Pascual 2001), and is responsible for activating a number of genes involved in fatty acid and TG synthesis and uptake, such as aP2 (Tontonoz, Graves et al. 1994; Tontonoz, Hu et al. 1994), and acyl-CoA synthase (Schoonjans, Watanabe et al. 1995) and lipoprotein lipase (Schoonjans, Peinado-Onsurbe et al. 1996). It has been reported that over-expression of PPARγ is sufficient to induce an adipocyte-like phenotype in non-adipogenic cell types (Tontonoz and Spiegelman 2008). Up to now, three isoforms of PPARγ have been identified, PPARγ1, PPARγ2 and PPARγ3; all three isoforms are transcribed from a common gene but with a different promoter start site (Zhu, Qi et al. 1995). PPARγ2 is the primary adipocyte-specific isoform with an extra 30 amino acids at its N-terminus compared to the ubiquitous PPARγ1, which is found in other cell types besides adipocytes (Tontonoz and Spiegelman 2008). PPARγ1 and PPARγ2 are expressed in adipocytes at the same level, so it was expected that both would have similar effects on adipogenesis. However, ectopic expression of PPARγ2 into PPARγ null 3T3-L1 preadipocytes restored adipogenesis, while over-expression of PPARγ1 had almost no effect (Ren, Collingwood et al. 2002). Thus, PPARγ2 is exclusively responsible for induction of adipogenesis.

Similar to C/EBPα, after activation, PPARγ2 maintains its expression by auto-activation. PPARγ and C/EBPα cross-activate each other through their respective C/EBP regulatory elements (Schwarz, Reginato et al. 1997; Elberg, Gimble et al. 2000).

The PPARγ ligand-binding domain is a wide region, thus various ligands can bind to it, such as fatty acids and fatty acid derivatives, including prostaglandins. In the absence of ligand, PPARγ binds to NCor, which leads to a repressive complex (Nolte, Wisely et al. 1998). The retinoid X receptor (RXR) heterodimerizes with PPARγ after ligand binding and acts as its co-activator (Mukherjee, Davies et al. 1997). It is also reported that LG100268, the RXR ligand, can promote 3T3-L1 preadipocyte differentiation (Schulman, Shao et al. 1998). Thiazolidinediones (TZDs) are the most effective synthetic ligands for PPARγ, and are used in the management of type 2 diabetes (Lehmann, Moore et al. 1995). In addition, Ohno et al. (Ohno, Shinoda et al. 2012) showed that mice treated with TZDs had elevated expression of brown adipocyte specific genes in WAT.

Phosphorylation of PPARγ does not alter adipocyte differentiation, although it mediates other metabolic actions. Choi et al. (2010) showed that phosphorylation of PPARγ at Ser 273 contributes to insulin sensitization by influencing specific PPARγ target genes such as adiponectin and adipsin.

1.1.6 Signaling pathways involved in adipogenesis

The induction and progression of adipogenesis *in vivo* and *in vitro* are controlled by important transcription factors as discussed previously, and developmental signaling systems. The stages of differentiation and levels of these factors mediate their exact

effects. Some of the important signaling pathways involved in adipogenesis are discussed in the next sections.

1.1.6.1 Insulin and insulin growth factor-1 (IGF-1) signaling

Insulin has important effects on adipogenesis, and it is one of the ingredients of the adipogenic cocktail used to stimulate adipocyte differentiation in cell culture. Preadipocytes express higher levels of insulin growth factor-1 (IGF-1) receptor compared to insulin receptor. Thus, in the early stages of adipocyte differentiation, insulin acts mostly through the IGF-1 receptor. However, after the preadipocytes have differentiated into adipocytes this ratio changes and more insulin receptor is expressed (Smith, Wise et al. 1988).

IGF-1 activates several intracellular signaling pathways. Upon ligand binding, the IGF-1 receptor is auto-phosphorylated intracellularly at the kinase domain and becomes activated (LeRoith, Werner et al. 1995). Subsequently, various protein substrates are activated, such as the insulin receptor substrate (IRS) family, which includes IRS1, IRS2, IRS3 and IRS4. These IRSs play an important role in adipogenesis with IRS1 the most important and the IRS4 the least (Tseng, Kriauciunas et al. 2004). It has been reported that *in vitro* double knockouts *Irs1/Irs2* or *Irs1/Irs3* inhibit adipogenesis (Tseng, Kriauciunas et al. 2004). Phosphatidylinositol 3-kinase (PI3K) and AKT/protein kinase B (PKB) are downstream of IRS in the insulin signaling cascade; their down-regulation leads to inhibition of adipogenesis (Garofalo, Orena et al. 2003). Mammalian target of rapamycin (mTOR) is another downstream target of insulin signaling. mTOR can inhibit PPARγ transactivation and block adipogenesis (Kim and Chen 2004). Therefore,

PI3K/AKT signaling and the mTOR pathway are the two sides of the insulin signaling cascade that have to act in parallel to maintain adipogenesis. In addition, insulin/IGF-1 signaling can affect adipogenesis by activating C/EBPβ (Tang, Gronborg et al. 2005) and CREB through their phosphorylation (Petersen, Madsen et al. 2008). It is also reported that AKT can regulate adipogenesis by phosphorylating the anti-adipogenic members of nuclear proteins, such as the forkhead family members FOXO1 and FOXO2, which results in their inactivation (Fan, Imamura et al. 2009; Gerin, Bommer et al. 2009).

1.1.6.2 Transforming growth factor-β (TGF-β) and bone morphogenetic protein signaling (BMPs)

The transforming growth factor-β (TGF-β) superfamily regulates the differentiation of many cell types, including osteoblasts, chondrocytes and adipocytes (Massague, Seoane et al. 2005). High levels of TGF-β and transducers such as SMADs (Mothers Against Decapentaplegic Homology) are expressed in adipocytes and adipose tissue (Samad, Yamamoto et al. 1997). TGF-β family members signal through SMAD-dependent and independent mechanisms (Derynck and Zhang 2003). Activation of TGF-β serine/threonine kinase receptors results in SMAD activation followed by its translocation to the nucleus, where the SMADs regulate the transcription of responsive genes (Shi and Massague 2003; Schmierer, Tournier et al. 2008). All three forms of SMAD are present in adipocytes, including the receptor regulated SMADs (R-SMADs), SMAD1, SMAD2, SMAD3, SMAD5 and SMAD8, the common-mediator SMAD (Co-SMAD), SMAD4, which operates by oligomerising with R-SMADsn and the inhibitory SMADs (I-SMADs), SMAD6 and SMAD7, which inhibit Co-SMAD and R-SMAD

activity (Zamani and Brown 2011). It has been shown that SMAD3 binds to C/EBPs and inhibits transactivation of PPARγ (Choy, Skillington et al. 2000; Choy and Derynck 2003). There is a discrepancy between *in vitro* and *in vivo* studies of TGF-β. TGF-β mediated SMAD3 phosphorylation leads to inhibition of adipogenesis *in vitro* in 3T3-F442A cells (Choy, Skillington et al. 2000). In contrast, SMAD3 knockout mice are resistant to diet-induced obesity and, when kept on a standard diet, showed elevation of brown-like cells in WAT (Yadav, Quijano et al. 2011). On the other hand, TGF-β overexpressing mice showed a lipodystrophy-like syndrome and impaired adipose tissue development (Clouthier, Comerford et al. 1997).

Bone morphogenetic proteins (BMPs) are members of the TGF-β superfamily, and polymorphisms in their respective genes are associated with obesity in humans (Bottcher, Unbehauen et al. 2009). BMPs are mainly involved in commitment of mesenchymal cells depending on the concentration and type of BMPs and the type of precursor cells. Similar to TGF-β, BMPs induce adipogenesis by activating SMAD1, SMAD5 and SMAD8, and also through activation of p38 MAPK (Hata, Nishimura et al. 2003). It has been shown that BMP4 induces adipogenesis, while inhibiting myogenesis (Kang, Bennett et al. 2007). Tang et al. (2004) showed that BMP4 expression in multipotent mesenchymal cells, specifically the C3H10T1/2 cell line, resulted in their commitment to the adipocyte lineage, and when treated with differentiation inducers they express adipocyte markers. Similar results have been obtained with BMP2 (Huang, Song et al. 2009). BMP4 acts differently on mature adipocytes and results in induction of BAT (Hao, Yuan et al. 2012; Herzig and Wolfrum 2013). Qine et al. (2013) confirmed the roles of BMP4 in mature adipocytes and showed that forced expression of BMP4 in

WAT reduced WAT mass and adipocyte size. In these transgenic mice, the white adipocytes exhibited characteristics of brown adipocytes and expressed higher levels of brown and beige adipocyte markers including UCP-1, PR-domain-containing 16 (PRDM16), PPARγ-coactivator-1-α (PGC1α) and TBX-1. Another member of the BMP family is BMP2, and its function is dependent on the presence of other factors; when BMP2 treatment occurs in combination with a PPARγ agonist there is induction of adipogenesis in 3T3-L1 preadipocytes and the multipotent mesenchymal C3H10T1/2 cell line (Sottile and Seuwen 2000; Hata, Nishimura et al. 2003). In contrast, treatment of 3T3-F442A preadipocytes with a combination of BMP2 and retinoic acid promotes osteogenesis (Skillington, Choy et al. 2002). BMP7 is another member of the BMP family that is capable of inducing BAT (Tseng, Kokkotou et al. 2008; Schulz, Huang et al. 2011). Tseng et al. (2008) showed that over-expression of BMP7 *in vivo* led to an increase in BAT and expression of BAT related proteins such as PRDM16 and PGC1α. On the other hand, BMP7 knockout embryos had a minimal level of BAT and UCP-1 was not detectable (Tseng, Kokkotou et al. 2008).

1.1.6.3 Hedgehog Signaling

Hedgehog is a protein involved in a key intracellular signaling pathway that was originally discovered in Drosophila (Nusslein-Volhard and Wieschaus 1980). There are three mammalian homologs of hedgehog: Sonic hedgehog, Indian hedgehog and Desert hedgehog, all of which are involved in the fate of mesenchymal cells (James 2013). Among them, Sonic hedgehog plays a critical role during embryological development. All members of the hedgehog family initiate a signaling cascade by binding to the

Patched receptor (PTCH), a 7-transmembrane protein, followed by phosphorylation and nuclear localization of glioblastoma (Gli) (Cohen 2003; Varjosalo and Taipale 2008). It is known that hedgehog signaling inhibits adipogenesis at the stem cell and adipocyte levels. It has been shown that expression of Gli1, Gli2, Gli3 and PTCH is significantly reduced during adipogenesis (Fontaine, Cousin et al. 2008). In contrast, activation of hedgehog signaling inhibits adipocyte differentiation and reduces levels of adipokines such as adipocyte fatty acid binding protein, adipsin, adiponectin and leptin (Fontaine, Cousin et al. 2008). Studies have shown that the anti-adipogenic effect of hedgehog signaling is mediated by transcription factors of the GATA family, which target C/EBPα and PPARγ2 expression (Tong, Tsai et al. 2005; Fontaine, Cousin et al. 2008). Other studies suggest that hedgehog signaling inhibits adipogenesis of ASCs at the expense of osteoblastogenesis with the assistance of BMP signaling (Zhao, Qiao et al. 2006; James, Leucht et al. 2010).

1.1.6.4 Fibroblast Growth Factors (FGF)

The FGF family consists of 23 members which signal through four receptors (Ornitz and Itoh 2001). These signaling molecules regulate several physiological and developmental events; however, their role in adipocyte development is not clear yet. There is evidence showing that the involvement of FGFs 1, 2 (also known as basic-FGF), 10, 16 and 19 in adipose tissue development. It has been reported that treatment of mature adipocytes with high concentrations of FGF-2 reduces adipocyte characteristics, including a significant reduction in PPARγ expression and adiponectin levels (Xing, Northrop et al. 1997). This ability of FGFs to inhibit adipogenesis was observed when

FGFs were added at different stages of differentiation. Injection of FGF-2 to ear cartilage and muscle resulted in *de novo* adipogenesis (Kawaguchi, Toriyama et al. 1998). In contrast, Xiao et al. (2010) showed that bone marrow stromal cells isolated from FGF-2 knockout mice were more readily converted to the adipogenic lineage than an osteoblastogenic lineage as they showed elevated expression of PPARγ2 mRNA as well as aP2 and adiponectin. These findings suggest that FGFs stimulate adipogenesis at the commitment phase, while inhibiting adipogenesis when the cells have entered the differentiation phase. Hutley et al. (2004) identified FGF-1 as a factor that is secreted from microvascular endothelial cells and stimulates the proliferation of human preadipocytes, which subsequently promotes their differentiation. The same group showed that, although preadipocytes express FGF receptors, they do not express FGF-1; the primary source of FGF in adipose tissue is microvascular endothelial cells (Hutley, Shurety et al. 2004). On the other hand, 3T3-L1 cells produce high levels of FGF-1, and inhibition of FGF-1 production in 3T3-L1 reduces their adipogenic potential (Hutley, Shurety et al. 2004). FGF-10 mRNA is abundant in WAT, where it induces mitogenesis in primary preadipocytes. FGF10 knockout (*Fgf10*$^{-/-}$) mice showed impaired adipogenesis, which could be rescued with an active form of C/EBPβ (Sakaue, Konishi et al. 2002). FGF-16 and FGF-19 are predominantly expressed in BAT and their role in BAT development has been studied (Konishi, Mikami et al. 2000; Tomlinson, Fu et al. 2002). FGF-16 was identified as a growth factor that exclusively regulates the proliferation of rat embryonic BAT (Konishi, Mikami et al. 2000). FGF-19 overexpressing transgenic mice had increased feed intake and showed specific reduction

in the WAT mass, while the BAT mass was increased. Increased energy expenditure in FGF-19 transgenic mice was also observed (Tomlinson, Fu et al. 2002).

1.2 White adipose tissue functions

The two important characteristic of adipocytes that play a critical role in maintaining and regulating their function are lipid droplet storage and adipokine secretion and these will be discussed in the following sections.

1.2.1 Lipid droplets

Lipid droplets are cytosolic organelles comprised of a hydrophobic lipid core containing TG and cholesterol ester coated with a phospholipid monolayer. Lipid droplets have very diverse sizes depending on cell type; they can have diameters as big as 150 μm in the cytoplasm of white adipocytes, or around 1 μm in fibroblast and less than 0.4 μm in normal yeast cells (Zweytick, Athenstaedt et al. 2000). Lipid droplets are not just inert fat depots; they are highly dynamic and actively involved in cellular metabolism and physiology (Miyanari, Atsuzawa et al. 2007; Samsa, Mondotte et al. 2009). Lipid droplets originate from the endoplasmic reticulum (ER), although the exact mechanism is not known yet. In addition, they are a site for *de novo* synthesis of TG, since TG synthetic enzymes have been detected in lipid droplets (Wilfling, Wang et al. 2013). The surface of the lipid droplet is coated with different proteins, which play critical roles in the structure and function of the lipid droplet (Yang, Galea et al. 2012). Some of these functions include synthesis and mobilization of lipids, and interactions with cytosolic proteins and other cellular organelles such as the ER and mitochondria.

There are many proteins that are associated with lipid droplets. There are reports showing that lipid droplets contain from 40 to 300 different proteins, depending on the species (Beller, Riedel et al. 2006; Bouchoux, Beilstein et al. 2011; Ding, Wu et al. 2012; Krahmer, Hilger et al. 2013). Among them, there are three major families of lipid droplet associated proteins: perilipin (PLIN), cell death-inducing DNA fragmentation factor-α-like effector (CIDE) and fatty acid binding proteins (FABP).

1.2.1.1 Perilipins (PLIN)

Perilipin is derived from a Greek word meaning "surrounding lipid". Perilipins are well conserved and the most abundant cytosolic lipid droplet coat protein across species. The various proteins that form the perilipin family share a similar N-terminal sequence (Lu, Gruia-Gray et al. 2001; Miura, Gan et al. 2002). Perilipin-1 (PLIN-1) was the first member of the perilipin family identified. Later, it was shown that the mammalian genome encodes five perilipins (Lu, Gruia-Gray et al. 2001; Miura, Gan et al. 2002). Perilipin-1 (PLIN-1) is highly expressed in WAT and BAT. Perilipin-2 (PLIN-2, also known as ADRP and adipophilin) is ubiquitously expressed. Perilipin-3 (PLIN-3, also known as TIP47) is expressed in liver, enterocytes, macrophages and testes (Liu, Qi et al. 2012). Perilipin-4 (PLIN-4, also known as S3-12) is expressed in adipocytes. Perilipin-5 (PLIN-5, also known as LSDP5, OXPAT, MLDP and PAT-1), the newest member of perilipin family, is primarily expressed in oxidative tissue, such as heart, liver, BAT and skeletal muscle (Bickel, Tansey et al. 2009). The cellular locations of perilipins can differ. Perilipin-1 and perilipin-2 are mostly localized on lipid droplets (Londos, Sztalryd et al. 2005), while perilipin-3, perilipin-4 and perilipin-5 are localized on both

lipid droplets and the ER (Skinner, Shew et al. 2009). Mitochondrial localization of perilipin-5 in muscle cells has also been shown (Wang, Sreenivasan et al. 2011).

Perilipin-1 plays an important role in lipolysis and fat loss in adipocytes. Perilipin-1 covers the surface of lipid droplets and restricts the access of lipases such as hormone sensitive lipase (HSL) to lipid droplets, thus maintaining TG levels under basal conditions (Souza, Muliro et al. 2002; Zhang, Souza et al. 2003). When cAMP levels increase in adipocytes, perilipin-1 is phosphorylated by Protein kinase A (PKA) (Greenberg, Egan et al. 1991) on different serine sites (Greenberg, Egan et al. 1993; Lu, Gruia-Gray et al. 2001). As a result, the protection that was provided by perilipin-1 is removed and TG gets exposed to lipases. In agreement with this finding, Brasaemle et al. (2000) showed that over-expression of perilipin-1 in 3T3-L1 preadipocytes elevates TG accumulation by reducing lipolysis and increasing TG synthesis. It has been reported that phosphorylation of perilipin-1 at Ser 492 by PKA is required for docking of HSL onto lipid droplets (Sztalryd, Xu et al. 2003). This leads to dispersion of lipid droplets, which increases the surface area available for lipase action (Marcinkiewicz, Gauthier et al. 2006). Phosphorylation of perilipin-1 by PKA also promotes lipolysis in fibroblasts that do not express HSL (Souza, Muliro et al. 2002; Tansey, Huml et al. 2003; Zhang, Souza et al. 2003); this finding suggests that PKA-mediated perilipin phosphorylation may recruit other lipases than HSL. Perilipin-1 is also phosphorylated by cGMP-depending kinase (PKG), although the detailed mechanism is not known yet (Sengenes, Bouloumie et al. 2003).

Besides its important role as a scaffold and cofactor for lipases, perilipin is also involved in lipid droplet growth and expansion. It has been shown that large lipid

droplets contain mostly perilipin-1 and perilipin-2, while perilipin-3, 4 and 5 are more abundant on the surface of smaller lipid droplets (Wolins, Quaynor et al. 2005). The importance of perilipin-1 in lipid droplet biology was demonstrated in perilipin-$1^{-/-}$ mice. Martinez and colleagues (2000) have shown that the perilipin-$1^{-/-}$ mice have lower body mass index (BMI) and 62% less WAT, despite increased feed intake. These mice have elevated basal lipolysis in WAT compared to wild type. In addition, stimulation of lipolysis by β-adrenergic agonists in WAT of perilipin-$1^{-/-}$ mice was reduced. Interestingly, the lipid droplets in perilipin-$1^{-/-}$ mice were mostly coated with perilipin-2. Perilipin-2 is the most abundant perilipin in liver. Studies have shown that perilipin-2 targeted mutant mice, in response to short and long-term high fat diet, were protected and did not accumulate lipid droplets in the liver (Chang, Li et al. 2006; McManaman, Bales et al. 2013). In the absence of perilipin-2, the lipid droplets were coated with perilipin-3 and 5, which are less effective in protecting lipid droplets from lipases. It has been reported that perilipin-2 prevents the association of adipose triglyceride lipase (ATGL) with lipid droplets (Listenberger, Ostermeyer-Fay et al. 2007). Thus, as might be expected, over-expression of perilipin-2 leads to lipid droplet accumulation in the liver (Sun, Miller et al. 2012).

Perilipin-4 and perilipin-1 share some sequence similarity; both were first identified in adipocytes, and are induced by PPARγ during adipogenesis (Wolins, Skinner et al. 2003; Dalen, Schoonjans et al. 2004). Chen et al. (2013) showed that perilipin-4 is not a necessary asset in adipocyte differentiation, as its loss did not affect adipogenesis and/or related metabolism. In contrast, loss of perilipin-4 reduces cardiac perilipin-5 expression and thus reduces cardiac lipid droplets (Chen, Chang et al. 2013).

1.2.1.2 Cell death-inducing DNA fragmentation factor-α-like effectors (CIDEs)

The CIDE family proteins are new members of lipid droplet -associated proteins, and include Cidea, Cideb and Cidec, also known as fat-specific protein of 27kDa (Fsp27). The CIDEs family has been found on lipid droplets and on the ER; they recently emerged as regulators of lipid droplet size, lipid storage and energy homeostasis (Gong, Sun et al. 2009).

Cidea is highly expressed in BAT (Wu, Zhang et al. 2008), while its very close homolog, Cidec, is highly expressed in WAT and only moderately expressed in BAT (Toh, Gong et al. 2008). Cidec is responsible for formation of large unilocular lipid droplet. It is highly expressed at sites of contact between lipid droplets and promotes lipid transfer from small lipid droplets to larger ones (Gong, Sun et al. 2011). The deletion of Cidec from WAT and BAT *in vivo* leads to increased basal lipolysis, while hormonally-stimulated lipolysis was unaffected (Toh, Gong et al. 2008) or only moderately decreased (Nishino, Tamori et al. 2008). Cidec$^{-/-}$ mice showed changes in WAT morphology, as vascularization and multilocularization of lipid droplet were increased and WAT became structurally similar to BAT (Nishino, Tamori et al. 2008; Toh, Gong et al. 2008). These mice also showed improvement in whole body and hepatic insulin sensitivity. Wu et al. (2014) showed that over-expression of Cidea in Cidec$^{-/-}$ mice restored the normal WAT phenotype and promoted lipid accumulation. In addition, Cidea and Cidec double knockout mice (Cidea$^{-/-}$/Cidec$^{-/-}$) were extremely lean and had less than 20% of the normal adipose mass, while the Cidec$^{-/-}$ mice had less than 45% of normal adipose mass. Furthermore, knocking-out Cidec in *ob/ob* mice (*Cidec*$^{-/-}$*/ob/ob*) resulted in lean mice

with small adipocytes and multilocular lipid droplets (Zhou, Park et al. 2015). The B-cell and T-cell receptor and chemokine signaling pathways were significantly reduced in *Cidec*$^{-/-}$/*ob/ob* mice compare to *ob/ob* mice, while the animals were insulin resistance. These findings suggest that WAT inflammation and insulin resistance are regulated through distinct pathways.

Deletion of Cidea and Cideb in mice led to a lean phenotype and the mice were resistant to diet-induced obesity (Zhou, Yon Toh et al. 2003; Li, Ye et al. 2007). Qi et al. suggested that deletion of Cidea leads to stabilization of adenosine monophosphate-activated protein kinase (AMPK) and this promotes FA oxidation, which results in the lean phenotype (Qi, Gong et al. 2008). The lean phenotype that was observed in Cideb$^{-/-}$ mice was explained by a decrease in the level of mature very-low-density lipoprotein (VLDL) in the liver of these mice, and increased hepatic oxidation (Ye, Li et al. 2009).

1.2.1.3 Fatty acid binding proteins (FABPs)

Fatty acid binding proteins (FABPs) are a large family of intracellular proteins that selectively bind to hydrophobic ligands such as saturated and unsaturated long-chain fatty acids, eicosanoids and retinoids (Chmurzynska 2006; Smathers and Petersen 2011). FABPs are abundantly expressed 14-15 kDa lipid chaperones that are linked to metabolic and inflammatory pathways (Haunerland and Spener 2004; Makowski and Hotamisligil 2005; Chmurzynska 2006). FABPs are well conserved across species as they have been found in *Drosophila melanogaster* and *Caenorhabditis elegans* as well as in mice and humans.

Different members of the FABP family have been identified and named based on

the tissue where they are predominantly expressed in relation to active lipid metabolism. The FABP family includes nine members, liver FABP (L-FABP), intestinal FABP (I-FABP), heart FABP (H-FABP), adipocyte FABP (A-FABP), epidermal FABP (E-FABP), ileal FABP (Il-FABP), brain FABP (B-FABP), peripheral myelin FABP (M-FABP) and testis FABP (T-FABP). Although each FABP is expressed mostly in the specified tissue, tissues can express more than one type of FABP. Adipocytes express mostly A-FABP, however, E-FABP is also expressed in adipocytes at a low level. Studies have shown that under certain conditions A-FABP, L-FABP, H-FABP and E-FABP can transport fatty acids into the nucleus where they activate transcription factors such as members of the PPAR family, including PPARγ, PPARα and PPARδ. The PPARs form a positive feedback loop, since expression of FABPs is also controlled by these transcription factors (Motojima 2000; Tan, Shaw et al. 2002; Schachtrup, Emmler et al. 2004). However, Ayers et al. (2007) have shown that a decrease in A-FABP expression leads to a negative feedback loop and enhanced PPARγ activity in the macrophage.

A-FABP, also known as FABP4, was first identified in mature adipocytes and adipose tissue (Spiegelman, Frank et al. 1983; Hunt, Ro et al. 1986). A-FABP is also named adipocyte P2 (aP2), since it shares 67% similarity with another FABP family member, peripheral myelin FABP (M-FABP/FABP8) (Hunt, Ro et al. 1986). A-FABP is considered to be an adipokine since it is primarily produced and released from adipocytes. A-FABP can represent about 6% of total cytosolic protein in cultured primary differentiated adipocytes (Baxa, Sha et al. 1989). Although A-FABP is mainly expressed in adipocytes, macrophages (Fu, Luo et al. 2002) and endothelial cells (Elmasri, Karaaslan et al. 2009) also express significant amounts of A-FABP. Fatty acids, PPARγ

agonists and insulin are the main regulators of A-FABP mRNA during adipocyte differentiation (Bernlohr, Bolanowski et al. 1985; Elmasri, Karaaslan et al. 2009). Furthermore, C/EBP β can interact with the *AFABP* promoter and stimulate transcription of the gene (Christy, Yang et al. 1989). In addition, cAMP inhibits the negative regulatory element in the *AFABP* promoter during 3T3-L1 preadipocyte differentiation (Yang, Christy et al. 1989). The level of A-FABP is different in various adipose depots, with higher levels in subcutaneous (inguinal) depots compared to visceral depots in lean and obese subjects (Fisher, Eriksson et al. 2001). A-FABP has a high binding affinity to long-chain FFA (Coe and Bernlohr 1998), which play an important role in A-FABP and HSL protein-protein interactions, and thus the hydrolytic activity of HSL (Shen, Liang et al. 2001). Interestingly, *AFABP*$^{-/-}$ mice become extremely obese, however, they do not develop insulin resistance or diabetes (Hotamisligil, Johnson et al. 1996). In these mice, E-FABP levels are elevated to compensate for the loss of A-FABP (Hotamisligil, Johnson et al. 1996). Double knock-out *AFABP*$^{-/-}$/*EFABP*$^{-/-}$ mice also showed a similar phenotype to *AFABP*$^{-/-}$ mice with resistance to diabetes (Maeda, Cao et al. 2005). Furthermore, knock-out of *AFABP*$^{-/-}$ in the *ob/ob* background promotes an extreme state of obesity, while A-FABP deficiency is still able to improve insulin sensitivity despite extreme obesity (Uysal, Scheja et al. 2000). This group showed that despite the obese phenotype, *ob/ob-AFABP*$^{-/-}$ mice do not exhibit impaired β-cell function. Baar et al. (Baar, Dingfelder et al. 2005) suggested that A-FABP elimination leads to decreased adipocyte FFA efflux, thus glucose is preferentially used over fatty acids.

1.2.1.4 Regulation of lipid droplet dynamics in adipocytes

Adipose tissue is the body's largest energy storage unit. This energy is stored in fat cells as TG. There are two major sources for the TG stored in adipose tissue, *de novo* lipogenesis from non-lipid precursors and FA uptake from the circulation. TG are transported in VLDLs and chylomicrons and it is hydrolyzed by lipoprotein lipase (LPL) to FFA, which are taken up by adipocytes and re-esterified to TG. Whether obtained from the circulation or synthesized *de novo* by fatty acid synthase, all TG are stored in lipid droplets within the cytosol of adipocytes. During the fasting state, TG stored in lipid droplets are hydrolyzed into FFA and glycerol through lipolysis. The FFAs are taken up by other organs for ATP generation and glycerol is metabolized in the liver (Lafontan and Langin 2009).

Lipolysis is tightly regulated by three major enzymes, adipose triglyceride lipase (ATGL), hormone-sensitive lipase (HSL) and monoacylglycerol lipase. The coordinated activation of these three lipases is required for complete hydrolysis of TG and release of FFA and glycerol. ATGL is mainly responsible for removal of the first FA during TG hydrolysis (Zimmermann, Strauss et al. 2004; Schweiger, Schreiber et al. 2006), whereas HSL action is more specific for release of a FA from diacylglycerols. Monoacylglycerol lipase completes the process by removing the remaining FA from the glycerol backbone. During the fed state, HSL is located in the cytosol and is inactive. Under these conditions, perilipin-1 coats the lipid droplet and prevents access of these lipases to the TG. Perilipin-1 also binds to CGI-58 (comparative gene identification-58), an ATGL coactivator (Yamaguchi 2010), thus preventing the first step of lipolysis. During the

fasting state, perilipin-1 is phosphorylated, which leads to CGI-58 release and activation of ATGL; this also facilitates translocation of perilipin-1 from the lipid droplet, which allows access of phosphorylated HSL to the lipid droplet (Brasaemle, Rubin et al. 2000).

There are many factors that regulate lipid hydrolysis, such as sympathetic and sensory nerve fibres, catecholamines and insulin. The intracellular signaling cascade that controls lipolysis is another important component of this metabolic process. One of the main players involved in regulating lipolysis is PKA, a cAMP-dependent kinase. Upon activation of adenylyl cyclase by hormonal or sympathetic stimulation, the intracellular levels of cAMP increase and this leads to activation of PKA (Trewhella 2006). PKA phosphorylates perilipin-1 at several residues leading to release of CGI-58 and dissociation of perilipin-1 from the surface of the lipid droplet (Subramanian, Rothenberg et al. 2004; Granneman, Moore et al. 2007; Miyoshi, Perfield et al. 2007). In addition, activation of PKA leads to phosphorylation and translocation of HSL to the lipid droplet surface, and this allows induction of lipolysis (Belfrage, Fredrikson et al. 1981). Regulation of lipolysis by different kinases and lipases is shown in Figure 1.

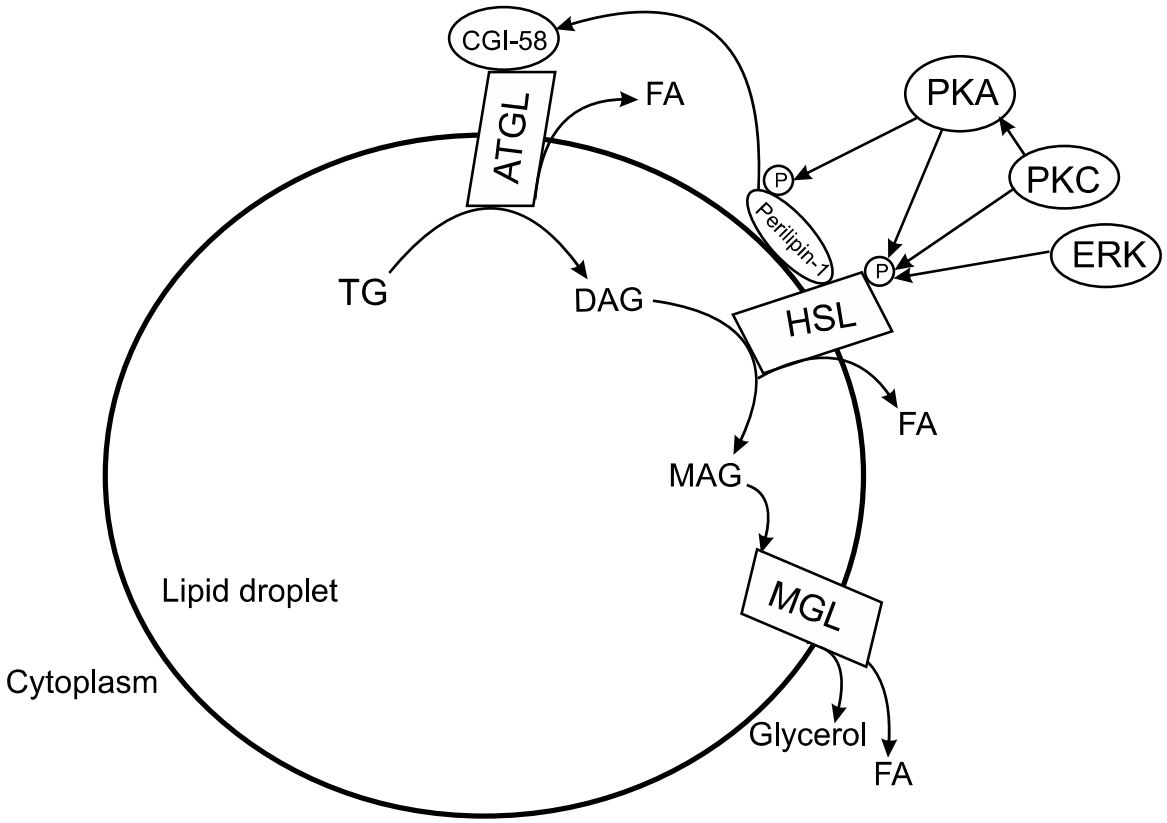

Figure 1. Regulation of lipolysis in adipocytes.

When lipolysis is stimulated, perlipin-1 becomes phosphorylated and activates ATGL through binding of CGI-58. Perilipin-1 phophorylation also activates HSL. TG are subsequently processed to DAG through the action of ATGL and subsequently to MAG by HSL, with FA released at each step. Lastly, MAG is processed to Glycerol and FA by MGL.

PKC is another important intracellular regulator of many different processes, but its role in lipolysis is not clear. There is evidence that PKC activity stimulates adenylyl cyclase in rat adipocytes, which can contribute to promotion of lipolysis by increasing cAMP levels and subsequently activating PKA (Naghshineh, Noguchi et al. 1986). However, inhibition of either PKA or PKC does not impair lipolysis, but their activation increases glycerol release in 3T3-L1 adipocytes (Fricke, Heitland et al. 2004). In contrast, Unal et al. (2008) showed that PKCα depletion results in activation of PKA in adipocytes. Further investigation is required to explain the exact role of PKC in the regulation of lipolysis in adipocytes, however, this may be difficult to achieve due to the fact PKC consists of several distinct isoforms. In brief, the PKC family consists of at least 12 distinct enzymes which are grouped into three categories. The conventional PKCs (α, βI, βII, γ) require both calcium and diacylglycerol for activity. In contrast, the novel PKCs (δ, ε, η, θ) only require diacylglycerol, while the atypical PKCs (ζ, ι/λ) require neither calcium nor diacylglycerol for activity (Steinberg 2008; Newton 2010; Pearce, Komander et al. 2010; Lipp and Reither 2011; Hui, Kaestner et al. 2014). Because of this complexity, associating a specific PKC with a certain process is difficult. With respect to adipocytes, PKCα, βI, βII and ε are associated with adipogenesis (Schmitz-Peiffer 2013). PKC has also been shown to modulate lipid metabolism in adipocytes. Specifically, PKC activation blocks lipolysis through inhibition of PKA (Schmitz-Peiffer 2013). Unfortunately, the latter studies did not examine the contribution of the various PKC isoforms. How these kinases contribute to adipocyte metabolism thus remains to be elucidated.

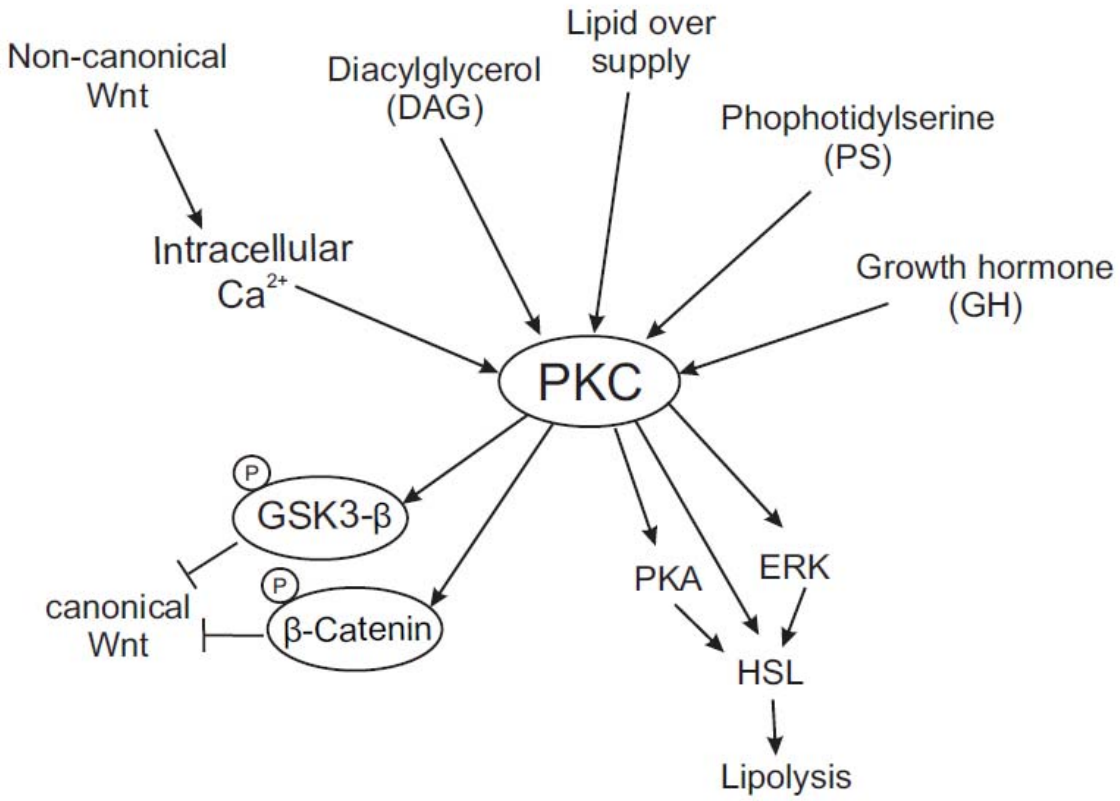

Figure 2. Stimulators of PKC and downstream effects on Wnt signaling pathways and lipolysis.

1.2.2 Adipokines

In addition to storing excessive energy, adipose tissue is a dynamic endocrine organ, which secretes many factors into the bloodstream. These factors are named adipokines. There are over 600 well known and less well known adipokines that contribute to normal physiological processes and pathological conditions, including adiponectin, leptin, resistin, adipsin, chemerin, vasfatin, omentin, vaspin, lipin, angiotensinogen, various prostaglandins, plasminogen activator inhibitor-1, interleukin

(IL)-17D among a long list of interleukins, TNF-α, BMP-7, IGF-1, fibronectin, monocyte chemoattractant protein-1 (MCP-1) and macrophage migration inhibitory factor. These adipokines are involved in the regulation of metabolism, immune response, inflammation, hypertension, cell adhesion, adipogenesis and bone morphogenesis, cell and tissue growth, and many other functions. The amount of adipokine production depends on both the origin of the adipocytes (subcutaneous or visceral adipose) and the size of the adipocytes as illustrated in two recent reviews (White and Tchoukalova 2014).

1.2.2.1 Adiponectin

Adipocyte complement related protein 30 kDa (ACRP30), adipose-specific secreted protein, AdipoQ and gelatin binding protein 28 kDa (GBP28) are different names for adiponectin. Adiponectin was identified independently by four groups using a variety of different approaches (Scherer, Williams et al. 1995; Hu, Liang et al. 1996; Maeda, Okubo et al. 1996; Nakano, Tobe et al. 1996). Adiponectin is synthesized primarily in white adipose as a monomer. It undergoes post-translational modifications that lead to higher molecular weight complexes. Adiponectin can be found as both full length and globular adiponectin; the latter is formed by proteolytic cleavage of full length adiponectin (Fruebis, Tsao et al. 2001). Trimers of full-length adiponectin are assembled in the ER. These low molecular weight complexes can oligomerize into high molecular weight hexamers and 18-mer complexes (Waki, Yamauchi et al. 2003; Schraw, Wang et al. 2008). Almost all adiponectin appears to be present as full-length adiponectin within the circulation and only a small amount of globular adiponectin can be detected in human plasma (Fruebis, Tsao et al. 2001).

Adiponectin circulates in human serum at a concentration of 3-30 μg/ml; this is a much higher concentration than other adipokines (e.g., ng/ml for leptin). Levels of circulating adiponectin in females are two to three times higher compared to males (Scherer, Williams et al. 1995; Combs, Berg et al. 2003). Adiponectin has been studied intensively since it showed a protective effect against CVD and higher levels of adiponectin in females may be responsible for the lower incidence of CVD in females compared to males (Maas and Appelman 2010). Lower plasma concentrations of adiponectin occur in individuals with obesity, type 2 diabetes, and coronary heart disease compared to healthy individuals (Hu, Liang et al. 1996; Arita, Kihara et al. 1999; Yamauchi, Kamon et al. 2001). However, treatment with insulin-sensitizing TZD can increase expression and secretion of adiponectin (Maeda, Takahashi et al. 2001; Combs, Wagner et al. 2002; Yu, Javorschi et al. 2002). A low adiponectin concentration is associated with a higher degree of visceral adiposity in children and adolescents independent of pubertal stage (Medina-Bravo, Meza-Santibanez et al. 2011). These findings indicate that adiponectin could potentially serve as a link between obesity and obesity-related disorders such as coronary artery disease (Hotta, Funahashi et al. 2000; Kumada, Kihara et al. 2003), hypertension (Ouchi, Ohishi et al. 2003), diabetes and metabolic syndrome (Trujillo and Scherer 2005).

Hrabak et al. (2011) investigated the role of adiponectin and inflammation in obese children, and found that they had lower adiponectin levels and higher amounts of inflammatory markers in their white blood cells. In addition, Wu et al. (2011) showed an association between obesity and a single nucleotide polymorphism in the adiponectin gene. Specifically, the allelic frequency of the adiponectin gene +45 single nucleotide

polymorphism was significantly different in obese versus healthy children. This finding suggests that adiponectin gene single nucleotide polymorphisms may be associated with the pathogenesis of obesity in children (Wu, Yan et al. 2011). Polymorphisms have also been shown to correlate with obesity in adult populations (Enns, Taylor et al. 2011). There is evidence that weight loss causes an increase in adiponectin levels, thus exhibiting a negative correlation with changes in BMI, and waist and hip circumference (Rolland, Hession et al. 2011).

The mechanism by which low levels of adiponectin are related to insulin resistance and type 2 diabetes is not clear. However, stimulation of glucose metabolism by adiponectin through phosphorylation and activation of AMPK in skeletal muscle (Tomas, Tsao et al. 2002), liver (Yamauchi, Kamon et al. 2002), and adipocytes (Wu, Motoshima et al. 2003) has been shown. The role of adiponectin in inflammation has also been studied. Downregulation of adiponectin by TNF-α, a pro-inflammatory cytokine that is increased in the WAT of obese subjects, has been suggested (Kappes and Loffler 2000; Wang, Poole et al. 2004). On the other hand, Masaki et al. (2004) showed that in mice adiponectin reduces the production and activity of TNF-α, which leads to a negative feedback loop. Moreover, production of IL-6, a pro-inflammatory cytokine, is inhibited by adiponectin in porcine macrophages (Wulster-Radcliffe, Ajuwon et al. 2004). In contrast, adiponectin induces the production of the anti-inflammatory cytokines IL-10 and IL-1 receptor antagonist in human macrophages (Wolf, Wolf et al. 2004). Ge et al. (2011) showed that in mice adiponectin influences the secretion of other adipokines that could affect the inflammatory state of adipose tissue. They showed that over-expression of adiponectin in WAT reduces pro-inflammatory factors such as IL-17β, IL-21, TNF-α

and growth factors such as thrombopoietin and colony stimulating factor 2 (granulocyte-macrophage) in comparison to wild type mice. In addition, the SVF of these mice secretes lower levels of other growth factors such as Fms-related tyrosine kinase 1 (vascular endothelial growth factor/vascular permeability factor receptor), and chemokines such as chemokine (C-C motif) ligand 5, intercellular adhesion molecule-1 and pro-inflammatory factors (IL-6, IL-12p70) (Ge, Ryken et al. 2011). The adiponectin-knockout mouse shows the reverse expression pattern. Specifically, the SVF of the adiponectin-knockout mouse secretes higher levels of Fms-related tyrosine kinase 1 (vascular endothelial growth factor/vascular permeability factor receptor), as well as chemokine (C-C motif) ligand 5, intercellular adhesion molecule-1 and other pro-inflammatory factors (IL-6, IL-12p70) (Ge, Ryken et al. 2011).

1.2.2.2 Leptin

The *ob* gene codes for leptin, a 16-kDa protein that controls appetite (Zhang, Proenca et al. 1994). Leptin promotes basal metabolism and β-oxidation (Matarese 2000). Leptin was the first adipokine to be discovered, in 1994. Adipocytes are the main site for leptin production and therefore they play an important role in maintaining leptin levels (typical concentration in human serum is approximately 1–10 ng/ml). In addition to adipose tissue, leptin is found in the circulation and cerebrospinal fluid. Unlike adiponectin, leptin levels are positively correlated with BMI and degree of adiposity (Maffei, Halaas et al. 1995; Friedman and Halaas 1998). Despite the higher concentration of leptin in obesity, it is unable to block weight gain effectively. This condition is termed leptin resistance. Transgenic mice with mutations in either the gene for leptin (*ob/ob*

mice) or the leptin receptor (*db/db* mice) show extreme obesity (Cefalu 2001; Shore 2007). In humans, there are very rare cases of leptin mutations, similar to *ob/ob* mice, which lead to leptin deficiency, and where administration of leptin decreases adiposity. Secretion of leptin followed by activation of its receptor leads to expression of suppressor of cytokine signalling 3 (SOCS3) in *ob/ob* mice, which in turn inhibits further leptin signal transduction and leads to leptin resistance (Howard and Flier 2006).

Leptin plays an important role in the induction of inflammation and related complications. Elevated leptin levels lead to increased monocyte recruitment in mice (Gruen, Hao et al. 2007) and induction of oxidative stress in postmenopausal women (Porreca, Di Febbo et al. 2004). There is evidence that increased leptin levels in cultures of murine or human marrow cells lead to secretion of pro-inflammatory cytokines such as TNF-α and IL-6 (Gainsford, Willson et al. 1996). Leptin may also influence production of certain adipokines, such as adipsin. In contrast, circulating levels of visfatin and vaspin in humans did not change when leptin levels declined because of severe starvation; this suggests that these adipokines are regulated independent of leptin in humans (Kang, Magkos et al. 2011).

The role of leptin in immune function has also been studied. Leptin is structurally similar to IL-2, IL-6 and IL-15 (Friedman and Halaas 1998; Matarese 2000). The structural similarities between the leptin receptor and hematopoietic cytokine receptors suggest leptin can influence immune function. It has been shown that *ob/ob* and *db/db* mice are susceptible to infection and resistant to autoimmunity due to a leptin or leptin receptor defect (Matarese, La Cava et al. 2002; Ikejima, Sasaki et al. 2005). These animals have thymic and lymph node atrophy, reduced numbers of bone marrow

precursors and impaired cell-mediated immune responses (Mandel and Mahmoud 1978; Chandra 1980; Howard, Lord et al. 1999; Matarese 2000). De Rosa et al. (2007) showed that freshly isolated T cells from human thymus expressed high levels of leptin and its receptor. They also showed that leptin can negatively affect T cell proliferation.

1.2.2.3 Adipsin

Adipsin, a serine protease homologue, exhibits an apparent molecular weight of 44 and 37 kDa due to glycosylation of a core 28 kDa polypeptide (Spiegelman, Frank et al. 1983; Bernlohr, Angus et al. 1984). Adipsin is produced in a non-glycosylated (28 kDa) form and its glycosylation (44-37 kDa) occurs before secretion (Cook, Min et al. 1987). Adipsin was the first hormone shown to be secreted by adipose tissue and later named as an adipokine (Cook, Min et al. 1987). Adipsin was later identified as complement factor D in human subjects since they share 98% amino acid sequence similarity and exhibit the same enzymatic activity (Rosen, Cook et al. 1989; White, Damm et al. 1992). Adipose tissue is the main source of adipsin secretion but it is detectable in the sciatic nerve and bloodstream (Cook, Groves et al. 1985; Zezulak and Green 1985). There is evidence showing that adipsin is expressed in both adipose tissue and monocytes-macrophages (White, Damm et al. 1992). Recently, Blogowski et al. (2013) examined the levels of selected complement cascade-derived molecules, including adipsin, in plasma and the two main adipose tissue depots, subcutaneous and visceral. Interestingly, they found that the concentrations of adipsin detected in both adipose tissue depots were significantly lower than in the blood. They also found differences in the concentration of adipsin between the fat depots, with subcutaneous depots having higher

concentrations of adipsin than the visceral depot. In addition, the plasma concentration of adipsin was negatively correlated with a patient's age and body adiposity mass, while being positively correlated with the waist-to-hip ratio. These associations confirm that adipsin may be important in age related complications such as diabetes.

Adipsin can regulate blood glucose since it causes the translocation of glucose transporters from the cytosol to the plasma membrane (Germinario, Sniderman et al. 1993). Levels of adipsin mRNA are insulin dependent, as its gene is expressed more during fasting and diabetes in the rat (Flier, Cook et al. 1987). It is also known that insulin assists adipsin secretion by 3T3-L1 adipocytes by increasing the number of glucose transporters. The increase in intracellular glucose promotes adipsin glycosylation (Kitagawa, Rosen et al. 1989). On the other hand, adipsin mRNA is decreased in the hyperglycemic and hyperinsulinemic states (Flier, Cook et al. 1987). Adipsin mRNA levels are significantly decreased in genetically obese mice (*db/db* and *ob/ob*) and also in a mouse model of chemically-induced obesity, but the changes are not as large as when obesity is generated by overfeeding normal rats (Flier, Cook et al. 1987). These finding suggests that it maybe possible to use adipsin to distinguish between obesity disorders that arise from genetic or metabolic disorders compared to simply overfeeding. Recently, Lo et al. (2014) showed that the levels of adipsin in the blood are decreased in mice fed a high fat diet. Among wild type and adipsin$^{-/-}$ mice, the adipsin$^{-/-}$ mice showed a slight but significant increase in weight on a high fat diet. As previously stated, adipsin is an important factor in the complement pathway and the receptors for these complement-derived peptides are widely expressed on different immune cell types (Ricklin, Hajishengallis et al. 2010). Lo et al. (2014) reported that the degree of adipose tissue

inflammation in adipsin$^{-/-}$ mice was decreased compare to wild type. The T cell co-receptor gene showed no difference between adipsin$^{-/-}$ mice and wild type. They also showed that adipsin$^{-/-}$ mice had lower levels of insulin due to decreases in β-cell function that affect insulin secretion.

Harada et al. (2003) showed that in WAT and BAT of HSL$^{-/-}$ mice there is a 60-90% decrease in adipsin mRNA levels. These observations suggest that adipsin levels may be affected by lipid metabolism.

1.2.2.4 Chemerin

Chemerin was first known as tazarotene-induced gene 2 protein, since it was discovered in psoriatic skin lesions (Nagpal, Patel et al. 1997). It also was known as retinoic acid receptor responder2. Later, it was named chemerin when it was identified as an agonist of the orphan receptor CMKLR1 also known as ChemeR23 (Wittamer, Franssen et al. 2003). Chemerin binds to three G-protein coupled receptors named CMKLR1 (ChemeR23) (Wittamer, Franssen et al. 2003), G protein-coupled receptor 1 (GPR1) (Barnea, Strapps et al. 2008) and C-C chemokine receptor-like 2 (Zabel, Nakae et al. 2008). Chemerin is produced as preprochemerin which contains 163 amino acids. After cleavage of the 20 amino acids forming its N-terminal signal peptide, chemerin is secreted as the 143 amino acid prochemerin (Wittamer, Franssen et al. 2003). Different proteases cleave the C-terminal of prochemerin, which results in active chemerin as well as other isoforms.

Chemerin was identified as an *endocrine* agent and particularly an adipokine since adipocytes are the main source of chemerin secretion (Goralski, McCarthy et al.

2007). Chemerin mRNA is significantly increased by 60-fold during differentiation of 3T3-L1 adipocytes (Bozaoglu, Bolton et al. 2007) and human preadipocytes (Sell, Laurencikiene et al. 2009). Chemerin and its mRNA are highly expressed in all of the WAT depots. In addition, Hansen et al. (2014) showed an intermediate level of chemerin in the BAT as well as liver, spleen and lungs. Like many other adipokines, chemerin levels are dysregulated in obesity. Serum levels of chemerin in obese human subjects and chemerin mRNA in adipose tissue of diet induced obese rats are increased (Bozaoglu, Bolton et al. 2007). Serum chemerin levels have been positively correlated with BMI (Bozaoglu, Bolton et al. 2007), blood pressure, serum lipid, insulin and cholesterol levels (Bozaoglu, Segal et al. 2009).

The *autocrine* function of chemerin involves regulating adipogenesis and adipocyte metabolism via activation of ChemR23 in both humans and mice (Bozaoglu, Bolton et al. 2007). In two separate studies, Goralski et al. (2007) and Muruganandan et al (2010) demonstrated that knocking down chemerin in 3T3-L1 preadipocytes and human multi-potent bone marrow-derived stromal cells leads to prevention of adipogenesis. This inhibition of adipogenesis cannot be rescued by the forced expression of PPARγ (Muruganandan, Roman et al. 2010). Chemerin expression is important for induction of adipogenesis in the first days of adipocyte differentiation (mitotic clonal expansion), since chemerin knock down in late differentiation does not affect adipogenesis (Muruganandan, Roman et al. 2010).

Chemerin has also been described as a *paracrine* agent, since it has chemoattractant properties (Zabel, Allen et al. 2005) and thus promotes macrophage infiltration during obesity. In support of these observations, it has been reported that

ChemR23 is expressed on macrophages and immature dendritic cells (DC) (Wittamer, Franssen et al. 2003). Furthermore, pro-inflammatory cytokines such as TNF-α increase chemerin levels in human adipocytes (Sell, Laurencikiene et al. 2009). There is evidence to show that chemerin could be the link between obesity and related complications such as type 2 diabetes (Roman, Parlee et al. 2012).

1.2.2.5 Resistin

In 2001, three research groups independently identified resistin (Steppan, Brown et al. 2001), although it was originally called Adipose tissue-specific secretory factor (Kim, Lee et al. 2001) and Found in inflammatory zone 3 (Holcomb, Kabakoff et al. 2000). All the groups classified resistin as a member of the newly discovered family of cysteine-rich secretory proteins. In human serum, resistin is present in two forms as low and high molecular weight (Gerber, Boettner et al. 2005). While resistin is secreted mainly from adipose tissue in rodents (Steppan, Brown et al. 2001), humans have high expression of resistin in mononuclear blood cells such as macrophages and leukocytes (Fain, Cheema et al. 2003; Patel, Buckels et al. 2003). Resistin production in macrophages is regulated directly by PPARγ (Patel, Buckels et al. 2003). Resistin production is associated with the expression of pro-inflammatory cytokines such as TNF-α, IL-1 and IL-6 (Lehrke, Reilly et al. 2004; Anderson, Mehta et al. 2007) and various other inflammatory stimuli such as lipopolysaccharide (LPS), TG and LDL cholesterol levels in human (de Luis, Gonzalez Sagrado et al. 2011). In line with previous findings, it has been reported that resistin and its mRNA are higher in visceral (abdominal) adipose tissue, a depot that is associated more with inflammation in obesity compared to the

inguinal adipose tissue depot (McTernan, McTernan et al. 2002; McTernan, McTernan et al. 2002). Resistin also promotes formation of foam cells, therefore, it is related to the development of atherosclerosis and occurrence of heart disease and stroke (Korah, Ibrahim et al. 2011; Krecki, Krzeminska-Pakula et al. 2011).

Resistin was named after its function for inducing resistance to insulin, and thus could be the link between obesity and diabetes (Steppan, Brown et al. 2001). Several groups showed an elevation of resistin in obese and diabetic subjects (Steppan, Brown et al. 2001; Gerber, Boettner et al. 2005), and it is suggested to be an indicator of metabolic syndrome (Malo, Ukkola et al. 2011). Although the first groups showed that resistin levels increase during obesity, there are other groups that reported opposite results in several models of obesity (Le Lay, Boucher et al. 2001; Way, Gorgun et al. 2001). However, resistin levels increase during differentiation of 3T3-L1 preadipocytes and primary adipocytes (Kim, Lee et al. 2001). Addition of resistin into 3T3-L1 differentiating medium inhibits differentiation to adipocytes, which suggests resistin has a role as a negative feedback regulator of adipogenesis and adipose tissue formation (Kim, Lee et al. 2001).

1.2.2.6 Visfatin

Human visfatin, previously known as pre-B-cell colony-enhancing factor (PBEF) (Samal, Sun et al. 1994) or nicotinamide phosphoribosyltransferase (NAMPT) (Luk, Malam et al. 2008), is a 52 kDa protein, which acts as an *endocrine*, *autocrine* as well as *paracrine* agent with many different functions. Visfatin was named NAMPT due to its significant sequence and functional homology with nicotinamide

phosphoribosyltransferase, an enzyme involved in nicotinamide adeninedinucleotide (NAD) biosynthesis. Visfatin was identified as PBEF, since it is secreted by activated lymphocytes, and was found to play a role in stimulating cytokine release in chronic and acute inflammatory diseases such as rheumatoid arthritis, inflammatory bowel disease and lung injury (Jia, Li et al. 2004; Nowell, Richards et al. 2006; Moschen, Kaser et al. 2007).

Visfatin is found in very high levels in the visceral adipose tissue (Fukuhara, Matsuda et al. 2005) and 3T3-L1 adipocytes (Tanaka, Nozaki et al. 2007). It has been reported that visfatin levels increase in obese adults with visceral fat accumulation (Fukuhara, Matsuda et al. 2005) and also in obese children with recently diagnosed type 1 diabetes (Redondo, Rodriguez et al. 2014), although opposite results were observed where circulating visfatin in obese subjects was lower than in healthy ones (Pagano, Pilon et al. 2006). There is evidence showing that during intervention and weight loss a decrease in visfatin levels is accompanied by a parallel decrease of other inflammatory markers such as TNF-α and C-reactive protein (CRP) (Petelin, Bizjak et al. 2014).

Fukuhara et al. (2005) were the first and only group to report an insulin-like effect of visfatin. They showed that visfatin functions as a non-competitive insulin inhibitor that binds to the insulin receptor at a site distinct from that of insulin. Due to the fact their findings were not confirmed by other researchers, their report was eventually retracted. However, several other groups have reported the insulin mimicking effects of visfatin, but its mechanism is not known yet. Lan et al. (2011) investigated the role of visfatin on insulin resistance, and reported that plasma levels of visfatin are higher in non-diabetic hypertensive patients with insulin resistance compared to those without insulin resistance.

They also showed that visfatin is independently correlated with HOMA-IR (homeostatic model assessment - insulin resistance). Recently, Gouranton et al. (2014) showed that visfatin was involved in the TNF-α mediated inhibition of insulin signalling in 3T3-L1 adipocytes. They suggested that modulation of protein-tyrosine phosphatase 1B by visfatin is responsible for the decrease in glucose uptake and Akt phosphorylation in 3T3-L1 adipocytes.

Some of the contrasting findings in studies of the more recently identified adipokines could be due to differences in the methodologies used to measure the adipokine concentrations (radioimmunoassay vs enzyme linked immunoassay), and the circadian rhythm for secretion of hormones also should be considered. There are many other adipokines that have not been discussed here and that remain to be discussed. Recently, the various roles of adipokines in obesity, type 2 diabetes and CVD were discussed and reviewed in detail in several excellent review articles (Northcott, Yeganeh et al. 2012; DeClercq, Enns et al. 2013; Molica, Morel et al. 2014; Ogawa, Damrongrungruang et al. 2014).

1.3 Adipose tissue pathophysiology

1.3.1 Obesity

Obesity is a worldwide concern. The prevalence of obesity has doubled from 1980 to 2008 (Stevens, Singh et al. 2012); this rate is continuing to accelerate as indicated in recent studies that show a very high incidence of obesity and overweight worldwide (Flegal, Carroll et al. 2012; Perez Rodrigo 2013). Obesity is characterized by an excess of WAT. In normal, healthy individuals, fat mass contributes to 9-18% of body

weight in males and 14-28% of body weight in females; these numbers may increase up to 60-70% in extremely obese individuals (Hausman, DiGirolamo et al. 2001).

BMI, a measure of weight relative to height (kg/m^2), is used by the World Health Organization (WHO), to assess body weight and for most people it correlates with the amount of body fat. A BMI ranging from of 18.5 to 24.9 kg/m^2 is considered healthy, a BMI between 25.0 to 29.9 kg/m^2 is overweight and individuals with a BMI of over 30 kg/m^2 are obese (WHO 2009). According to the WHO, 65% of the world's population is at risk for diseases and death caused by overweight and obesity (WHO 2009). It was estimated that, in 2005, there were over 1 billion overweight and more than 300 million obese individuals globally. Among all countries, the Americas, Europe and the Eastern Mediterranean have the highest average BMI (Perez Rodrigo 2013).

The WHO considers overweight and obesity as one of the leading global risks for mortality in the world, accounting for 5% of deaths worldwide due to coronary artery disease, type 2 diabetes, hypertension, certain forms of cancer, dyslipidemia and sleep apnea. Epidemiological studies indicate a high BMI is the underlying cause of 44% of diabetes events, 23% of ischaemic heart disease incidence and 7–41% of certain cancer events (WHO 2009). Obesity, as a source of these complications, exerts a tremendous burden on health care utilization and costs. Therefore, healthcare and health services are targeting obesity in order to minimize the risk of new cases of diabetes (especially type 2 diabetes), heart disease and other obesity-related complications.

According to the organization for Economic Co-operation and Development (OECD), different strategies would prevent obesity in the world, although varying levels of success have been observed in different countries. In 2010, the OECD reported these

strategies were able to prevent 155 000 deaths from chronic diseases in Japan, 75 000 in Italy, 70 000 in England, 55 000 in Mexico and 40 000 in Canada (Sassi 2010). Unfortunately, Canada was less successful in preventing chronic disease caused by obesity, although Canada has been spending the highest amount on preventive strategies in comparison to other countries such as Japan (Sassi 2010). According to Statistics Canada, in 2008, 66% of women and 54% of men were overweight, and 25% of women and 23% of men were obese. Sadly these numbers are increasing; this increase in the incidence of obesity is estimated to contribute at least $1.8 billion to health care costs in Canada. The burden of obesity is 2-6% of healthcare costs in different countries, which could otherwise contribute to economic productivity and development (Sassi 2010). Although the most recent studies suggest that the rate of obesity is no longer increasing, the general rate remains very high globally (Perez Rodrigo 2013).

1.3.2 Childhood obesity

Childhood obesity has become a concern all around the world. The International Association for the Study of Obesity (Obesity. 2013) estimated 200 million school-age children worldwide are overweight and 40-50 million of them are obese. In 2013, the prevelance of childhood obesity had increased 47.1% since 1980 (Ng, Fleming et al. 2014). This rate is rising all around the world and varies in different regions depending on economic status, climate and traditional food sources. The rate of obesity is less than 5% in Africa and parts of Asia, less than 20% in Europe and less than 30% in the Americas and some Middle East countries (Worldobesity 2015). Obesity in Canada increased 3-fold in the past 35 years (Statcan 2004). In Canada, over 30% of children

between 5 to 18 years old are either overweight or obese (Childhoodobesityfoundation 2014). A number of studies have shown that one of the factors for the increasing prevalence of obesity in adulthood is childhood obesity and parental obesity (Parsons, Power et al. 1999; Nicklas, Baranowski et al. 2001; Magrone and Jirillo 2015). The occurrence of adult obesity is 8% for individuals who were obese during childhood but did not have obese parents, and this number increases to 79% for an adult with childhood obesity and who had at least one obese parent (Whitaker, Wright et al. 1997). Both over and undernutition by the mother during the prenatal and perinatal period have now been shown to contribute in postnatal and adulthood obesity (Magrone and Jirillo 2015). With respect to the etiology of childhood obesity, mothers with diabetes and who smoked during pregnancy have an increased risk of having a child who develops obesity and type 2 diabetes. In addition, childhood obesity is a risk factor for adulthood CVD (Ayer, Charakida et al. 2015). Epigenetics, the interaction of genes with the environment, is another important factor in childhood obesity and can be dependent and independent of parental obesity (Speakman and O'Rahilly 2012; Aguilera, Olza et al. 2013). The main focus of obese individuals (children and adults) is on weight loss, however, the method used to manage weight has a great influence on outcomes. To date, lifestyle and behavior modification have been shown to produce the most lasting results. The childhood obesity epidemic is growing and further research is required to find ways to manage and address this important disease. Recently, the roles of childhood obesity in type 2 diabetes CVD and other obesity-related complications were discussed and reviewed in detail in several excellent articles (Drummond and Gibney 2013; Lobstein, Jackson-Leach et al. 2015; Magrone and Jirillo 2015; Savona-Ventura and Savona-Ventura 2015).

1.3.3 Association of obesity with diabetes and cardiovascular diseases

Improvements in medical care, the increased age of the population and public health intervention are some of the factors that influence the type of diseases that affect a population. In developed countries, the types of diseases have shifted from infectious disease such as diarrhea and pneumonia to non-communicable diseases such as diabetes, cardiovascular diseases and cancer. Among all the other risk factors, obesity is one of the main reasons for the increasing prevalence of non-communicable diseases (WHO 2009).

A decrease in the response of tissues to insulin action, which is a characteristic of both pre-diabetes and diabetes, is responsible for 6% of deaths globally (WHO 2009). Diabetes is responsible for 22% of ischaemic heart disease and 16% of stroke deaths (WHO 2009). A direct effect of increased BMI is the incidence of type 2 diabetes in the United States, where two thirds of adults diagnosed with type 2 diabetes have a BMI of 27 kg/m² or greater (National Task Force on the and Treatment of 2000). Approximately 41 500 Canadian die due to diabetes every year (C.D.A. 2006). CVD is a leading cause of death worldwide. According to a WHO report, mortality of over half of the patients with type 2 diabetes (52%) is caused by cardiovascular diseases (Morrish, Wang et al. 2001). Obesity and type 2 diabetes are also linked to other complications such as hypertension, hyperglycemia and dyslipidemia. The presence of these multiple risk factors contribute to a condition termed metabolic syndrome (Reaven 1988; Reilly and Rader 2003).

Visceral obesity, which leads to dysfunctional adipose tissue, is the driving force for metabolic syndrome development (Bosello and Zamboni 2000). In addition, ectopic fat deposition in other organs such as liver, kidney, heart and skeletal muscle adds to

these complications by causing lipotoxicity, a process where accumulation of excess FFA in certain tissues like the heart, kidney and pancreas leads to impairment of their normal functions (Yang, Jansson et al. 2004; Suganami, Tanaka et al. 2012), thus resulting in cellular dysfunction and cell death. These changes have consequences such as the release of fatty acids, hormones and pro/anti-inflammatory molecules from adipocytes and/or other affected tissues. These changes in endocrine balance can induce insulin resistance, type 2 diabetes, inflammation, dyslipidemia, and, possibly, endothelial dysfunction and vascular damage leading to hypertension and atherosclerosis (Northcott, Yeganeh et al. 2012). During obesity, adipose tissue is in an inflammatory state, and secretes predominantly pro-inflammatory cytokines, such as TNF-α, IL-6 and CRP. Studies have shown that the level of pro-inflammatory cytokines is increased in the plasma of obese individuals (Dandona, Weinstock et al. 1998; Kern, Ranganathan et al. 2001; Pradhan, Manson et al. 2001). Although adipocytes are mostly responsible for the secretion of pro-inflammatory cytokines, macrophages that accumulate in the adipose tissue of obese subjects also contribute to the levels of pro-inflammatory cytokines (Weisberg, McCann et al. 2003; Xu, Barnes et al. 2003). These pro-inflammatory cytokines can promote development of atherosclerotic lesions by stimulating vascular smooth muscle cell migration to the endothelial layer at sites of injury (Zernecke and Weber 2005).

Hypertension is another important risk factor for CVD (Chobanian, Bakris et al. 2003). The Framingham Offspring Study indicates that adiposity is a significant independent predictor of hypertension in men (Garrison, Kannel et al. 1987). This study also showed that obesity contributed to 78% of cases of hypertension in men and 64% in women (Garrison, Kannel et al. 1987). Sharma et al (2001) showed that obesity has a

direct association with the increasing prevalence of diabetes and hypertension. Furthermore, their finding showed that methods of controlling blood pressure were less effective in obese and overweight patients.

1.3.4 Obesity and adipocyte dysfunction

Adipocytes have a high capacity to store TG, as well as hydrolyze TG and release FFAs. In the lean state, there is a balance between storing and releasing TG. However, when caloric intake exceeds energy expenditure this balance is changed and adipocyte TG deposition is increased; this leads to adipocyte hypertrophy, which in turn alters adipocyte properties. If this high TG deposition continues, the adipocyte will eventually reach a limit in size and the additional TG will be shunted to non-adipose tissues such as liver and skeletal muscle. This process can lead to lipotoxicity in those organs.

As adipocytes enlarge, their ability to function as endocrine cells is affected. The effect of obesity and adipocyte dysfunction with respect to secretion of adipokines was discussed in the adipokine section (1.2.2). Here, the effect of adipocyte dysfunction on the secretion of inflammation-related adipokines in WAT is discussed. TNFα and MCP-1 are the two important factors that are secreted in higher amounts in the obese state from enlarged adipocytes (Gustafson, Gogg et al. 2009) . TNFα inhibits phosphorylation of IRS1, an essential step for insulin signaling, and thus plays an important role in the development of obesity-induced insulin resistance (Hotamisligil and Spiegelman 1994). MCP-1 enhances macrophage infiltration into adipose tissue during obesity as reported in mice (Xu, Barnes et al. 2003) and humans (Curat, Miranville et al. 2004). However, MCP-1 knockout mice revealed that other factors are also involved in promoting

macrophage infiltration during obesity (Inouye, Shi et al. 2007). A role for other pro-inflammatory cytokines such as IL-1β and IL-6 on obesity-related inflammation has also been reported (Lagathu, Yvan-Charvet et al. 2006). Studies have shown that adipose tissue in the obese state exhibits greater adipocyte hypertrophy, angiogenesis, extracellular matrix over-production and immune cell infiltration (Nishimura, Manabe et al. 2008; Schenk, Saberi et al. 2008).

1.3.5 Contribution of adipocytes to immune cell function in inflammation

In addition to secreting immune factors into the circulation, adipose tissue expresses receptors for many immune molecules (Schaffler and Scholmerich 2010). Therefore, adipose tissue may be considered an element of the immune system. Several different immune cells contribute to the inflammatory state present in obesity, including macrophages, neutrophils, mast cells, eosinophils, dendritic cells, T cells, B cells and natural killer cells.

1.3.5.1 Macrophages

Macrophages are the most abundant leukocyte in adipose tissue, and considered the core of inflammation in obesity (Chawla, Nguyen et al. 2011). Generally, in lean subjects, macrophages account for 10-15% of the SVF in adipose tissue, and this number increases to 40-50% of the SVF in obese mice and humans (Weisberg, McCann et al. 2003). In addition to their numbers, the macrophage phenotype can change during obesity. In normal lean adipose tissue, the majority of macrophages are the anti-inflammatory, IL-10-producing M2 macrophages, whereas in obesity, the M1

macrophages that produce MCP-1, TNFα, IL-1β and IL-6 are more abundant (Lumeng, Bodzin et al. 2007). One of the unique characteristics of M1 macrophages is the expression of the cell surface marker CD11c, in addition to macrophage-specific markers such as F4/80 and CD11b (Lumeng, Bodzin et al. 2007). Macrophages accumulate around necrotic adipocytes and form crown-like structures that facilitate adipocyte cell death. A significant positive correlation between the increased numbers of cells expressing macrophage markers and both adipocyte size and body mass has been demonstrated (Weisberg, McCann et al. 2003). This finding suggests there is a strong association between macrophage infiltration and the development of obesity.

1.3.5.2 Dendritic cells (DCs)

In addition to macrophages, other innate immune cells are involved in promoting inflammation in the obesity state, such as dendritic cells. DCs are antigen-presenting cells that function to process foreign antigens onto a cell surface molecule, the major histocompatibility complex (MHC), and present it to T cells (Hackstein and Thomson 2004). The adipose tissue of obese mice, including diet-induced obese (DIO), *ob/ob* and *db/db*, is infiltrated by DCs that express $CD11c^{high}$, $F4/80^{low}$ (Bertola, Ciucci et al. 2012). There is also evidence showing that this increase in dendritic infiltration can promote additional macrophage recruitment (Stefanovic-Racic, Yang et al. 2012). Further investigation is required to enlighten our understanding of the role of DCs in adipose tissue inflammation in obesity.

1.3.5.3 T cells

Adaptive immune cells also play a role in adipose tissue inflammation. T cells develop in the thymus and their main function is to distinguish between self and foreign antigens. T cells can be distinguished from other lymphocytes by the specific cell surface marker CD3. Increases in T cell numbers in WAT in the obese state have been reported (Bornstein, Abu-Asab et al. 2000). Moreover, adipose tissue infiltrated by T cells produces chemokines that lead to further recruitment of macrophages (Yang, Youm et al. 2010).

1.3.5.4 Natural killer T cells (NKT)

Natural killer T (NKT) cells are innate-type T cells that bridge innate and adaptive responses. The classical type of NKT cell contributes to adipose tissue inflammation in obesity by recognizing lipids presented by the surface marker CD1d (Gumperz 2006). There is a controversy regarding the role of NKT cells with respect to adipose tissue inflammation. Mantell et al. (2011) showed that CD1d knockout mice on a high fat diet (HFD) had normal body weight, glucose sensitivity, fat mass and adipose tissue inflammation, which suggests that NKT cells do not play a vital role in the induction of obesity-related inflammation. On the other hand, Wu et al. (2012) reported that CD1d knockout mice had less adipose tissue inflammation and insulin resistance. It is also suggested that the presence of NKT in mouse and human adipose tissue prevents insulin resistance (Schipper, Rakhshandehroo et al. 2012). The exact role of NKT cells in adipose tissue inflammation thus remains unclear and requires further investigation.

1.3.6 Animal models of obesity

The incidence of obesity and related diseases is increasing worldwide. The use of animal models serves as a foundation for assisting researchers to understand the basic mechanisms of these diseases in a physiologically-relevant environment such as an animal body. Animal models are also valuable test beds for investigating pharmaceuticals and novel anti-obesity drugs. In these models, obesity can be induced by dietary manipulations or genetic interventions. Rodents such as mice and rats are widely used as models of obesity.

1.3.6.1 Diet-induced obesity (DIO) models

DIO animal models are polygenic models of obesity that more closely reassemble human obesity. In these animals, obesity is induced by positive energy balance, through either a HFD, high fructose diet or cafeteria diet (also known as Western diet, which is a combination of HFD and high fructose diet) (Rothwell and Stock 1988). Among mouse models, the male C57BL/6J mouse is the best candidate and considered an obesity-prone strain, since it accumulates fat when allowed access to the HFD *ad libitum* while otherwise maintaining a lean phenotype if fed a standard diet. The HFD-induced obese C57BL/6J mouse exhibits abnormalities similar to human metabolic syndrome, such as hyperinsulinemia and insulin resistance (Collins, Martin et al. 2004). Hypertrophy and hyperplasia of adipocytes is also observed in HFD-induced obese C57BL/6J mice (Collins, Martin et al. 2004). On the other hand, A/J or C57BL/KsJ mice are resistant to developing obesity even with access to a HFD *ad libitum* (Surwit, Feinglos et al. 1995). Outbred Sprague-Dawley rats are a strain that also have been used as a model of DIO.

Animals in this strain maintain body weights similar to the control; this group is called diet resistance Sprague-Dawley rats (Sclafani and Springer 1976; Chang, Graham et al. 1990). The obese prone Sprague-Dawley rat shows the obese phenotype after 4 weeks of HFD and this is accompanied by leptin resistance, hyperinsulinemia, hyperglycemia and hypertriglyceridemia (Chang, Graham et al. 1990). Animals placed on the high fructose and cafeteria diets show similar phenotypes to those on a HFD, while the effects of the cafeteria diet are more pronounced (Kretschmer, Schelling et al. 2005).

1.3.6.2 Genetically obese models

Genetically obese rodents are monogenic models. There is a common argument against these obesity models since they are not truely representative of human obesity, which is usually polygenic (Hinney, Vogel et al. 2010). However, these models develop severe adiposity and exhibit distinct phenotypes that could be important in different aspects of obesity research.

Leptin is one of the most important genes manipulated in mice. The Jackson Laboratory was the first to discover the C57BL/6J mouse with a mutation in the leptin gene, which is also known as the obese (ob) gene (Ingalls, Dickie et al. 1950). Leptin mutant (*ob/ob*) mice are normal neonatally, but by 4 weeks of age start to gain weight (Chatzigeorgiou, Halapas et al. 2009). They can reach a body weight almost three times that of their wild type littermates (Jackson 2014). Leptin deficient mice have uncontrollable food intake (hyperphagy) and reduced energy expenditure. Obesity is the first observable characteristic in this animal, which is followed by insulin resistance, moderate hyperglycemia and hyperinsulinemia.

The *db/db* mouse has a G-to-T point mutation in the leptin receptor gene, which leads to impaired leptin signaling (Chen, Charlat et al. 1996; Lee, Proenca et al. 1996). *Db/db* mice develop hyperinsulinemia and insulin resistance at about 2 weeks of age and become obese by the age of 4 weeks. At about 4-8 weeks of age, they exhibit hyperglycaemia due to pancreatic β-cells failure (Bates, Kulkarni et al. 2005). Therefore, in addition to being an obesity model, they can be used as a model of diabetes. The maximum life span of *db/db* mice is about 8-10 months. The *db/db* mice have a phenotype similar to *ob/ob* mice, but they develop insulin resistance earlier in life.

Leptin receptor defects also occur in rats; the obese *fa/fa* Zucker and Koletsky rats have mutations on the extracellular domain of the leptin receptor (Phillips, Liu et al. 1996). Similar to the *db/db* mouse, the *fa/fa* Zucker rat has elevated circulating leptin levels, but they are leptin resistance due to a defective leptin receptor. These animals develop severe obesity early in their lives as a result of hyperphagia and exhibit reduced energy expenditure (White and Martin 1997). The *fa/fa* Zucker rat is obese and insulin resistant, but not diabetic, since they have normal fasting glucose levels (Bray 1977). Due to an unknown mutation, the Koletsky rat is more prone to hypertension and develops severe insulin resistance (da Silva, Bjorbaek et al. 1998).

Another animal model that is being used in the field of obesity and diabetes is the Zucker Diabetic Fatty (ZDF) rat, a mutant from a colony of outbred *fa/fa* Zucker rats. The ZDF rat demonstrates early diabetes due to dysregulation of glucose metabolism. The rate of development of the diabetic phenotype is depend on diet and sex, as HFD is required for development of diabetes and males are more prone to develop diabetes than females (Corsetti, Sparks et al. 2000). The early diabetes in the ZDF rat is possibly due to

alternations in the GLUT-4 gene in skeletal muscle (Zierath, Ryder et al. 1998).

There are several other animal models with obesity and metabolic disease phenotypes that have been reviewed in detail in several excellent articles (Lutz and Woods 2012; Nilsson, Raun et al. 2012).

1.4 Wnt signaling

The wingless-type MMTV integration site (Wnt) is a 19-member family of secreted glycoproteins that have important functions in stem cell biology, cell fate and development. Wnts act as paracrine and autocrine agents that bind to a cell surface receptor and activate either a canonical or non-canonical intracellular signal transduction pathway.

1.4.1 Canonical Wnt (Wnt/β-catenin)

Canonical Wnt is activated by binding of Wnt ligands to the heterodimeric cell surface receptor composed of low-density lipoprotein receptor-related 5 (LRP5), LRP6 and the seven trans-membrane Frizzled (Fz) receptor (Yang-Snyder, Miller et al. 1996). This complex exhibits the characteristics of a G-protein coupled receptor (Huang and Klein 2004). In the canonical pathway, activation of Fz leads to recruitment of a cytoplasmic phosphoprotein called dishevelled (Dsh/Dvl) (Yang-Snyder, Miller et al. 1996). Dsh plays an important role in regulating Wnt signaling in relation to other non-canonical pathways, although its mechanism of action is still unclear. The canonical pathway is regulated by the accumulation and translocation of the adherens junction associated-protein β-catenin. In the absence of Wnt ligands, the degradation complex

consisting of Axin and adenomatous polyposis coli (APC) is active and facilitates the phosphorylation of β-catenin by casein kinase I-α (CKIα) and GSK3β (He, Semenov et al. 2004; Gordon and Nusse 2006). This sequential phosphorylation of β-catenin leads to its ubiquitination and subsequently its degradation by the proteasome (He, Semenov et al. 2004). PKCα also phosphorylates β-catenin at N-terminal serine residues (Ser 33/37) and promotes β-catenin degradation (Gwak, Cho et al. 2006; Gwak, Jung et al. 2009). However, in the presence of canonical Wnt ligands such as Wnt1, Wnt3a, Wnt5b, Wnt7a and Wnt10b, activation of Fz and LRP5/6 leads to the disruption of the Axin/APC/GSK3β complex (Gordon and Nusse 2006). β-catenin accumulates in the cytoplasm since it is not degraded and is then translocated into the nucleus (Hatsell, Rowlands et al. 2003). β-catenin has no nuclear export sequence and the mechanism of its transportation into the nucleus is not clear yet. In the nucleus, β-catenin acts as a transcriptional co-activator and binds to the lymphoid-enhancer-binding factor/T-cell-specific transcription factor (LEF/TCF) family of transcription factors to activate Wnt responsive genes such as Myc and Cyclin D1 (Harland and Gerhart 1997; Reya and Clevers 2005).

1.4.2 Non-canonical Wnt

The non-canonical Wnt pathway is also known as the β-catenin independent pathway, and all the steps in this signaling pathway are not clearly elucidated yet. Wnt4, Wnt5a and Wnt11 are the ligands known to signal through the non-canonical pathway (Dawson, Aflaki et al. 2013). Downstream of Dsh, Wnt signaling can branch either into the canonical signaling pathway or to either of the two main non-canonical signaling

pathway branches. The Planar Cell Polarity pathway signals through the Rho/ROCK or Rac/JNK pathways, while the Wnt/Ca^{2+} pathway is mediated through Calcineurin, Ca^{2+}/calmodulin-dependent protein kinase (CamKII) and PKC pathways (Komiya and Habas 2008). It is known that the CamKII-mediated non-canonical pathway inhibits β-catenin dependent Wnt signaling at the transcriptional level (Ishitani, Ninomiya-Tsuji et al. 1999). There are other pathways that overlap with Planar Cell Polarity and Wnt/Ca^{2+} signaling, although the relationship to these branches of Wnt signaling is not clear. Details of the non-canonical signaling pathway have been reviewed (Komiya and Habas 2008; Colaianni, Brunetti et al. 2014).

1.4.3 Extracellular regulators of Wnt

There are a number of secreted proteins in the extracellular matrix that can bind to Wnts or the Wnt receptors and thus either activate or inhibit the resultant signaling cascade. The factors that bind to Wnts and inhibit their binding to either of the Fz or LRP5/6 receptors are the Dickkopf (Dkk) proteins (Glinka, Wu et al. 1998), Wnt-Inhibitor Factor (WIF) (Hsieh, Kodjabachian et al. 1999) and Soluble Frizzled-Related Proteins (SFRP) (Hoang, Thomas et al. 1998). In contrast, Norrin (Xu, Wang et al. 2004) and R-Spondin (Kazanskaya, Glinka et al. 2004) are the factors that can bind to the LRP5/6 receptor and activate the canonical Wnt signaling independent of Wnt protein binding. Expression of these factors varies in different adipose depots; for example, SFRP-2 is higher in mouse visceral adipose tissue compared to the subcutaneous adipose tissue (Gesta, Bluher et al. 2006). These distinctions may explain the lower rate of adipogenesis in visceral adipose depots compared to subcutaneous adipose tissue.

1.4.4 Wnt and adipocyte lineage commitment

Studies have shown that canonical Wnt signaling inhibits adipogenesis in WAT at the expense of myogenesis and osteogenesis. It has been reported that adipose tissue-specific over-expression of Wnt10b, which is expressed only in preadipocyte and mesenchymal stem cells, leads to a 50% reduction of adipose tissue mass and increased bone mass (Longo, Wright et al. 2004). In addition, over-expression of Wnt10b in mesenchymal cells and MEFs *in vitro* inhibits adipogenesis in WAT and promotes ostogenesis (Kang, Bennett et al. 2007). In agreement with other findings, studies have shown that down-regulation of Wnt10b due to targeted deletion (Vertino, Taylor-Jones et al. 2005) or aging (Taylor-Jones, McGehee et al. 2002) leads to increased adipogenesis and white adipocyte characteristics in muscle tissue and myofibres. It was also reported that knocking out the LRP6 receptor in MEFs results in increased adipocyte differentiation (Kawai, Mushiake et al. 2007). In support of these findings, Wang and colleagues (Wang, Jin et al. 2010) showed that activation of the histone methyltransferase enhancer of zeste homologue 2 in primary preadipocytes, which leads to down regulation of Wnt10b and other canonical Wnts ligands such as Wnt 1, 6 and 10a, is a required step for adipocyte differentiation. In contrast, Bowers et al. (2008) used pluripotent C3H10T1/2 cells and committed A33 preadipocyte cells derived from C3H10T1/2 cells to show that several genes involved in the Wnt signaling pathway were differentially expressed in these two cell lines. Interestingly, they revealed that R-spondins-2 and -3, activators of canonical Wnt signaling, increased A33 proliferation and nuclear β-catenin accumulation, an effect not seen in C3H10T1/2 cells. Furthermore, they showed that

activation of Wnt/β-catenin signaling leads to expression of BMP-4, which in turn stimulates adipogenesis. Bone marrow-derived cells isolated postnatally from β-catenin knockout mice had a higher rate of adipogenesis compared to the wild-type, which may explain the higher adiposity and reduced bone mass in β-catenin knockout mice (Song, Liu et al. 2012).

1.4.5 Wnt and preadipocyte differentiation

The role of Wnt signaling in the regulation of preadipocyte differentiation has also been studied. Inhibition of adipogenesis in 3T3-L1 preadipocytes was achieved by activation of the canonical Wnt pathway via over-expression of Wnt1 or mutant β-catenin (Ross, Hemati et al. 2000). On the other hand, inhibition of GSK3β in 3T3-L1 preadipocytes blocked adipogenesis (Bennett, Ross et al. 2002). The high level of Fz1, Fz2 or Fz5 expression in preadipocytes compared to mature adipocytes suggests that they have an important role in mediating Wnt effects (Bennett, Ross et al. 2002); this finding suggests that both canonical and non-canonical Wnt signaling can influence adipogenesis. Canonical pathway mediated inhibition of adipogenesis leads to induction of PPARγ and C/EBPα, and the cascade of gene expression stimulated by these transcription factors is disrupted (Kang, Bennett et al. 2007). Furthermore, PPARγ is involved in β-catenin proteasomal degradation independent of GSK3β activity (Liu, Wang et al. 2006). The ligand-binding domain of PPARγ directly binds to the TCF/LEF binding domain of β-catenin; this complex facilitates β-catenin proteasomal degradation (Liu, Wang et al. 2006). With respect to non-canonical Wnt signaling, there are reports that show Wnt 5a, a non-canonical Wnt ligand, blocks adipogenesis in bone marrow

mesenchymal cells through CamKII and NEMO-like kinase by inhibiting the transcriptional activity of PPARγ (Takada, Mihara et al. 2007). Similar results were reported for 3T3-L1 preadipocyte differentiation (Wakabayashi, Okamura et al. 2009). In addition to its role in adipocyte development, Wnt protects 3T3-L1 preadipocytes during starvation induced by serum deficiency through increased expression of IGF-1 and IGF-2, which protect the preadipocytes from apoptosis (Longo, Kennell et al. 2002). Some anti-adipogenic dietary compounds such as curcumin have been shown to activate Wnt/β-catenin signaling and promote nuclear localization of β-catenin in 3T3-L1 adipocytes. Curcumin also increases mRNA of upstream and downstream effectors of Wnt/β-catenin signaling, such as Wnt10b, Fz2, LRP5, cMyc and cyclin D1 in 3T3-L1preadipocytes, which inhibits adipogenesis (Ahn, Lee et al. 2010).

1.4.6 Wnt signaling and brown adipogenesis

The importance of Wnt signaling in BAT formation was revealed when over-expression of Wnt10b from the FABP4 promoter completely blocked brown adipose tissue development *in vivo* (Longo, Wright et al. 2004). Kang et al. (2005) showed that in BAT, activation of Wnt signaling reduces PGC1α expression, which in turn suppresses UCP-1 expression. The same group also reported that over-expression of Wnt10b from the UCP-1 promoter leads to development of BAT with the characteristics of WAT. In addition, Tseng et al. (2004) showed that brown adipocytes isolated from *Irs*1 or *Irs*3 knockout mice moderately differentiated into brown adipocytes; this effect occurred in parallel with increased Wnt10a expression and a reduction of PGC1α expression. A complete deficiency in brown adipocyte differentiation was observed in brown

adipocytes isolated from double knockout *Irs*1$^{-/-}$/*Irs*3$^{-/-}$ mice, where the cells also showed a dramatic increase in the levels of Wnt10a. These findings suggest that canonical Wnt signaling inhibits brown adipogenesis and stimulates the appearance of white adipocyte properties in BAT.

1.5 Conjugated Linoleic Acid (CLA)

Conjugated linoleic acid (CLA) describes a mixture of positional and geometric isomers of octadecadienic (linoleic) acid, a fatty acid with 18 carbons and two double bonds at the 9th and the 12th carbons. CLAs are found in a number of different foods, with the highest concentrations found in the meats and milk of ruminant animals (cow, sheep, goat) (Steinhart, Rickert et al. 2003). Among the 28 possible isomers of CLA, the *cis*-9, *trans*11 (*c*9-*t*11) isomer is the most abundant isomer in food, contributing ~90% to the CLA in the diet (Dhiman, Nam et al. 2005). The *c*9-*t*11 and *trans*-10, *cis*-12 (*t*10-*c*12) isomers show the greatest biological activity (Wallace, McKain et al. 2007). The *t*10-*c*12 CLA isomer is produced synthetically from linoleic acid extracted from safflower or sunflower oils. This produces a mixture of 44% *t*10-*c*12-CLA and 40% *c*9-*t*11-CLA, which is used in natural health supplements (Pariza, Park et al. 2001).

*c*9-*t*11 CLA is mostly responsible for the positive health benefits associated with CLA such as reducing the risk of CVD, as well as the anti-carcinogenic and anti-inflammatory properties (Choi, Park et al. 2002; Ntambi, Choi et al. 2002; Gebauer, Chardigny et al. 2011; Bocking, Harb et al. 2014). On the other hand, *t*10-*c*12 CLA is associated with the anti-obesity effects of CLA, which include reducing body fat and increasing lean muscle mass (Nall, Wu et al. 2009).

1.5.1 CLA and obesity

After the discovery by Dr. Pariza in the 1980s (Pariza and Hargraves 1985) that CLA was an anti-carcinogenic agent, there was a tremendous interest in the effects of CLA on other diseases, including metabolic diseases such as obesity. Several *in vivo* and *in vitro* studies have demonstrated that CLA treatment reduces adiposity or TG accumulation, respectively. There were differences among the studies such as dose, different percentages of the CLA isomers and duration of the CLA treatments, but all of them agreed that the *t*10-*c*12 isomer is responsible for CLA's effects on body composition (Park, Storkson et al. 1999). Animal studies have shown that supplementing CLA at doses ranging from 0.5 to 1.5% w/w of the diet for 3-4 weeks leads to effective weight loss in mice, chicken, hamsters and pigs (Wahle, Heys et al. 2004). Studies done in mice have shown the most substantial decreases in body weight, where supplementing only 0.5% w/w CLA for 6 weeks resulted in a 40-80% decline in adipose, with the retroperitoneal depot being the most sensitive to CLA (West, Delany et al. 1998). The effect of CLA on genetically obese animal models was also investigated. Wendel et al. (2008) showed that feeding *ob/ob* mice with a mixture of CLA isomers (1.5% w/w) for 4 weeks significantly reduced body weight compared with the control diet. They also reported that the effect of CLA on weight loss was more significant than leptin administration. Significant weight loss was also observed in *fa/fa* Zucker rats fed a 1.5% w/w CLA isomer mixture for 14 days when compared with *fa/fa* Zucker rats given TZD (Houseknecht, Vanden Heuvel et al. 1998).

Promising evidence from animal studies moved CLA research to the next phase, clinical trials, but the outcomes from human studies were not as consistent and promising as animal studies. The majority of human studies used a CLA isomer mixture and they showed no significant effect on body weight, although some reported a 4-20% reduction in body fat mass depending the duration of the study, age, the initial body weight and dose of CLA (McCrorie, Keaveney et al. 2011; Dilzer and Park 2012).

The fundamental discrepancy between human and animal studies is the dose of CLA. Mouse studies provide up to 0.5% w/w CLA in the diet, and this would correspond to about 56 g CLA per day for a 70 kg subject, while the highest amount of CLA administrated in human studies was 6.8 g per day (Blankson, Stakkestad et al. 2000). However, based on our animal study, we calculated that a 43 g mouse provided with a 0.5% w/w CLA diet consumed 0.0165 g CLA per day, which is about 27 g CLA per day for a 70 kg subject or about 4 times higher than the maximum amount of CLA administrated in human study. Another factor is metabolic rate; the metabolic rate of mice is 7 time higher than humans, which theoretically allows them to lose fat 7 times faster than humans (Terpstra 2001). These factors could possibly explain the differences between human studies and studies conducted in mice; however, there are major differences in CLA studies among the rodents (mice and rats), which will be discussed in the following section and there is no clear explanation for those differences yet.

1.5.2 CLA and adipocytes

One of the morphological factors that influences adipocyte function is adipocyte size. Noto et al. (2007) showed that *fa/fa* Zucker rats fed a diet supplemented with a 1.5%

w/w CLA isomer mixture had smaller adipocyte size compared to animals on the control diet, and DeClercq et al. (2010) showed that the *t*10-*c*12 isomer is responsible for this outcome. This change in adipocyte size was also shown in mouse models, as female ICR mice fed 0.5% w/w *t*10-*c*12 CLA for 3 weeks had a lower percentage of large adipocytes compared with the mice fed control diet (Xu, Storkson et al. 2003). Similarly, CD2F1/Cr male mice given diets supplemented with 0.5% w/w *t*10-*c*12 CLA isomer for 1-7 weeks had fewer large adipocytes (Russell, McGee et al. 2007). In addition, C57BL/6 male mice fed 0.5% w/w *t*10-*c*12 CLA for 2 weeks had a 95% reduction in cell volume (LaRosa, Miner et al. 2006).

There are studies showing that CLA influences the two main functions of adipocytes, adipokine production and lipid accumulation. It has been shown that *t*10-*c*12 CLA treatment of 3T3-L1 cells, which are of mouse origin, significantly reduces leptin secretion and similar effects have been observed in mice fed a 0.5% w/w *t*10-*c*12 CLA diet (Kang and Pariza 2001). *Fa/fa* Zucker rats fed a 1% w/w CLA isomer mixture had significantly increased plasma adiponectin levels (Nagao, Inoue et al. 2003). However, when *fa/fa* Zucker rats were supplemented with 1% w/w *t*10-*c*12 CLA, a reduction of leptin and adiponectin mRNA in WAT was observed, while their plasma levels were unchanged (Gudbrandsen, Rodriguez et al. 2009). In contrast, resistin mRNA levels were increased in the WAT of those obese rats (Gudbrandsen, Rodriguez et al. 2009). The effect of CLA on more recently identified adipokines has not been investigated.

With respect to lipid accumulation, supplementation with a CLA mixture or *t*10-*c*12 CLA alone reduced protein levels of enzymes involved in lipogenesis such as lipoprotein lipase, acetyl-CoA carboxylase, fatty acid synthase and stearoyl-CoA

desaturase in C57BL/6 mice, primary human preadipocytes and 3T3-L1 cells, respectively (Evans, Lin et al. 2002; Brown, Boysen et al. 2003; Brown, Boysen et al. 2004; LaRosa, Miner et al. 2006). There are reports suggesting that *t*10-*c*12 CLA (30 μM) but not *c*9-*t*11 CLA (30 μM) stimulates lipolysis in differentiated 3T3-L1 (mature adipocyte) and newly differentiated human adipocytes from the SVF (Chung, Brown et al. 2005; den Hartigh, Han et al. 2013). *t*10-*c*12 CLA-induced lipolysis is paralleled by smaller lipid droplets and replacement of large, perilipin-1 coated lipid droplets with perilipin-2 coated lipid droplets in the cytosol. These effects were accompanied by translocation of perilipin-1 into the cytosol followed by a significant reduction in its protein levels (Chung, Brown et al. 2005). In agreement with previous findings, Cai et al. (2012) also showed that mice fed a 1.5% w/w CLA isomer mixture for 13 days had lower epididymal WAT, and reduced perilipin-1 mRNA and protein levels while there were significant increases in perilipin-2 mRNA levels. The mechanism by which perilipin responds to CLA remains unknown.

1.5.3 Mechanisms for the anti-obesity effect of CLA

Several potential mechanisms by which mixtures of CLA isomers or *t*10-*c*12 CLA alone can impact adiposity have been proposed. The mechanisms with the best evidence are discussed below.

One of the proposed mechanisms for reducing adiposity with *t*10-*c*12 CLA is increasing energy expenditure, which could be achieved by increasing basal metabolism or thermogenesis or physical activity. There is no evidence to support that CLA can increase physical activity. Increased basal metabolism following supplementation with a

CLA isomer mixture has been reported in mice (Terpstra, Javadi et al. 2003), while the results from human studies are not consistent (Lambert, Goedecke et al. 2007; Nazare, de la Perriere et al. 2007). Thermogenesis is promoted by uncoupling proteins, which are involved in proton transport into the inner mitochondria membrane. UCP-2 is the most abundant UCP in WAT and its levels are positively correlated with adiposity (Fleury, Neverova et al. 1997). Several studies reported that a mixture of CLA isomers or *t*10-*c*12 CLA supplementation up-regulate UCP-2 transcription and translation in the WAT and BAT of mice (Ealey, El-Sohemy et al. 2002; Takahashi, Kushiro et al. 2002), however, these changes were not observed in rat models (Ealey, El-Sohemy et al. 2002).

There is a body of evidence suggesting that *t*10-*c*12 CLA but not *c*9-*t*11 CLA inhibits adipogenesis. Treatment of differentiated 3T3-L1 (mature adipocytes) and differentiated primary human preadipocytes with *t*10-*c*12 CLA leads to a significant reduction in PPARγ mRNA and protein levels (Kang, Liu et al. 2003; Kennedy, Chung et al. 2008), and downstream PPARγ responsive genes (Miller, Siripurkpong et al. 2008). Similar results were observed in rodents (Liu, Purushotham et al. 2007). While the effect of *t*10-*c*12 CLA on PPARγ expression is established, the exact mechanism is not clear yet. Post-translational regulation of PPARγ by *t*10-*c*12 CLA has been suggested. There is moderate activation of PPARγ with *t*10-*c*12 CLA as well as *c*9-*t*11 CLA (Clement, Poirier et al. 2002). CLA isomers completely block the effects of rosiglitazone and darglitazone, two specific PPARγ agonists (Granlund, Juvet et al. 2003; Kennedy, Chung et al. 2008). Kennedy et al. (2008) showed that acute treatment (24 hours) with *t*10-*c*12 CLA increases PPARγ phosphorylation at Ser 112, a MAPK-dependent site, with no changes in its protein levels. This finding explains the effect of CLA on PPARγ

responsive genes, which fail to express due to inhibition of the PPARγ transcriptional activity.

Apoptosis is another mechanism that might be responsible for the anti-obesity actions of CLA. The effects of CLA on stimulating apoptosis in adipocytes have been shown in various models, both *in vitro* and *in vivo*. A reduction in pig back fat was induced by feeding a mixture of CLA isomers and this involved stimulation of adipocyte apoptosis as indicated by chromatin condensation, DNA fragmentation and elevation of apoptotic regulators such as cleaved caspase-3 and cytosolic cytochrome c (Qi, Yang et al. 2014). Mice fed a 1% w/w mixture of CLA isomers had elevated apoptosis in the WAT, measured by terminal deoxynucleotidyl transferase-mediated dUTP-biotin nick end-labeling (TUNEL) assay, accompanied by increases in TNFα, which is known to induce apoptosis (Tsuboyama-Kasaoka, Takahashi et al. 2000). Furthermore, Evans et al. (2000) showed that a mixture of CLA isomers (50-200 μM) reduced preadipocyte proliferation in 3T3-L1 cells. When similar treatments were applied to post-confluent preadipocytes, higher rates of apoptosis and fewer cells in S-phase were observed. Similar results were achieved at even lower concentrations of CLA (1-10 μM) by Fischer-Prosovszky et al. (2007). In all experiments, *t*10-*c*12 CLA showed higher apoptotic potency than *c*9-*t*11 CLA.

It is also suggested that CLA modulates adiposity via an increase in lipolysis and an inhibition of lipogenesis; these two mechanisms have been discussed previously.

1.5.4 CLA, diabetes and inflammation

The effects of CLA on diabetes have also been examined. As previously stated, increased obesity leads to an increase in diabetes prevalence. Since this insulin resistant state occurs due to increases in adipose tissue mass, it is presumed that reductions in body weight could decrease insulin resistance (Taylor and Zahradka 2004). While the effect of CLA on obesity and weight loss is established, its anti-diabetic actions conflict across species and some data suggest there are isomeric differences (Roche, Noone et al. 2002). Supplementation with a 1% w/w mixture of CLA isomers in the diet of obese Zucker rats reduced hyperinsulinemia and normalized impaired glucose tolerance (Houseknecht, Vanden Heuvel et al. 1998; Nagao, Inoue et al. 2003). In addition, Noto et al. (2004) showed that a 1% w/w mixture of CLA isomers in the diet of obese Zucker rats improved oral glucose tolerance and preserved pancreatic β-cells. On the other hand, CLAs have been shown to induce insulin resistance in cultured 3T3-L1 adipocytes (Kang, Liu et al. 2003), mice (LaRosa, Miner et al. 2006) and humans (Moloney, Yeow et al. 2004). In contrast, *ob/ob* mice fed *c*9-*t*11 CLA had less insulin resistance and a marked reduction in pro-inflammatory markers in the WAT, such as TNFα and nuclear factor-kappa B (NF-κB) (Moloney, Toomey et al. 2007). In contrast, the *t*10-*c*12 CLA-rich diet induced insulin resistance and promoted inflammation in C57BL/6 mice (LaRosa, Miner et al. 2006). One of the mechanisms by which CLA suppresses PPARγ expression is through induction of NF-κB, which directly antagonizes PPARγ (Takada, Suzawa et al. 2005). In addition to inflammatory cytokines such as TNFα and IL-6, CLA supplementation also alters immune cell populations in WAT. Poirier et al. (2006) reported that a *t*10-*c*12 CLA rich-diet induced inflammation in mouse WAT and also promoted macrophage

proliferation and infiltration into adipose tissue. This pro-inflammatory effect of CLA on macrophages was shown to be PPARγ-dependent (Yu, Correll et al. 2002). It was subsequently revealed that increases in macrophage numbers in *t*10-*c*12 CLA fed animals were a secondary effect and it was due to the effect of *t*10-*c*12 CLA on adipocytes and not a direct effect of *t*10-*c*12 CLA on macrophages (Belda, Thompson et al. 2012). The role of CLA isomers on other immune cells involved in inflammation in obesity was not studied.

Another mechanism by which CLA could possibly affect diabetes is through activation of PKC. PKCs have been shown to play an important role in regulating the upstream and downstream targets of insulin signaling (Sampson and Cooper 2006). Treatment of human prostate cancer cell lines with *c*9-*t*11, *t*10-*c*12 CLA or mixtures of these isomers modulated the cellular location of PKCs, and in some experiments progression of cancer was inhibitied (Song, Sneddon et al. 2004). In addition, an increase in the membrane localization of PKCα has been reported in adipocytes isolated from mammary glands of rats fed CLA isomers (Ip, Masso-Welch et al. 1999). Further evidence supporting the ability of CLA to influence PKC activity was obtained in a related study and showed *t*10-*c*12 CLA affects the regulation of PKC isoforms in 3T3-L1 adipocytes (Hunt 2008).

Claims that CLA is beneficial for human health (McCrorie, Keaveney et al. 2011; Dilzer and Park 2012) remain controversial because CLA treatment studies with rodent models show quite different results compared to human clinical trials where the reduction in body weight obtained with CLA supplementation was not as significant as in animal models. In addition, similar to mice, the manifestation of pro-diabetic effects of *t*10-*c*12

CLA isomer in a diabetes-prone population has been questioned (McCrorie, Keaveney et al. 2011).

2. Rationale

The incidence of obesity is increasing dramatically and it is becoming a global phenomenon. Obesity contributes to an increased prevalence of type 2 diabetes, cardiovascular disease, hypertension and certain cancers. Visceral obesity, in particular, is a major risk factor for metabolic syndrome, a combination of various dysregulated parameters. The intensive research to find new therapeutic approaches to control this global health risk has led to greater research efforts to understand adipose tissue and its role in initiating and regulating these metabolic consequences.

Reduced adiposity and/or improved adipose function have been observed in different animal models with CLA treatment. The *c*9-*t*11 and *t*10-*c*12 CLA isomers exhibit the greatest biological activity. Several studies have demonstrated that *t*10-*c*12 CLA treatment during adipocyte differentiation reduces lipid accumulation in both mouse and human adipocytes (Evans, Lin et al. 2002; Brown, Boysen et al. 2003; Brown, Boysen et al. 2004; LaRosa, Miner et al. 2006); however, the mechanism of action is not clear yet.

The Wnt signalling pathway has a major role in both commitment and differentiation of adipocytes. Specifically, Wnt inhibits the commitment of stem cells to the adipocyte lineage (preadipocytes) (Kang, Bennett et al. 2007); in addition, Wnt inhibits the differentiation of preadipocytes to mature adipocytes by blocking PPARγ/CEBPα expression (Bennett, Ross et al. 2002). However, Bennett et al. (2002)

showed that the level of Frz1 is elevated during the clonal expansion period of 3T3-L1 adipogenesis, which suggests increased activation of Wnt/β-catenin signaling at this time. Therefore, Wnt/β-catenin transiently affects adipogenesis.

One of the main characteristics of adipocytes is a TG filled lipid droplet. The lipid droplets are surrounded by proteins such as perilipin-1 and the phosphorylation state of perilipin-1 has an important role in protection of lipid droplets from lipolysis (Souza, Muliro et al. 2002; Zhang, Souza et al. 2003). Perilipin-1 is also involved in controlling lipid droplet size and therefore could be involved in the regulation of adipocyte size (Wolins, Quaynor et al. 2005). Previously, we showed that the *t*10-*c*12 CLA isomer inhibits 3T3-L1 differentiation (Yeganeh 2008). Also, DeClercq et al. (2010) showed that the *t*10-*c*12 and *c*9-*t*11 CLA isomers have completely opposite effects on the adipocytes of obese rats. Specifically, the *t*10-*c*12 CLA treated rats had smaller and healthier adipocytes compared with *c*9-*t*11 CLA fed animals. They also showed that the number of adipocytes was increased in *t*10-*c*12 CLA fed obese rats. However, *t*10-*c*12 CLA treatment in 3T3-L1 cells has been associated with a decrease in adipocyte number (Granlund, Juvet et al. 2003), but the mechanism responsible for these inconsistencies is not known. Unpublished data from our group showed that *db/db* mice fed *t*10-*c*12 CLA become extremely lean despite having a high food intake. These data also indicated that CLA isomers have the ability to alter PKC localization and level in adipose tissue and 3T3-L1 cells (Hunt 2009). In agreement with these findings, Song et al. (Song, Sneddon et al. 2004) reported that CLA isomers modulate PKC isoforms in a cancer cell line. It is also reported that PKC phosphorylates β-catenin at Ser33/37 and this modification

negatively regulates Wnt/β-catenin signaling by promoting β-catenin degradation (Cho, Park et al. 2008).

The role of Wnt/β-catenin signaling in the anti-adipogeneic actions of other compounds such as curcumin has been studied previously (Ahn, Lee et al. 2010), while its role in the anti-obesity effects of CLA has not been examined. Therefore, we propose to investigate the mechanisms by which CLA isomers affect adiposity through an examination of the effects of CLA isomers in the regulation of Wnt/β-catenin signaling at the commitment phase and also during differentiation. We will study the effects of *t*10-*c*12 CLA and *c*9-*t*11 CLA on adipogenesis in relation to Wnt activation both *in vivo* and *in vitro* using the *db/db* mouse model and 3T3-L1 cells, respectively.

3. Hypotheses

3.1 Overall hypothesis

The anti-obesity effects of the *t*10-*c*12 CLA isomer result from an alteration of lipid droplet dynamics through activation of the Wnt/β-catenin pathway, which leads to weight loss through a reduction in adipogenesis and/or an increase in adipocyte death.

3.2 Specific hypotheses

1. *t*10-*c*12 CLA reduces lipid droplet accumulation by inhibiting perilipin phosphorylation in 3T3-L1 adipocytes. (Section 6.1-6.8)
2. *t*10-*c*12 CLA inhibits differentiation of 3T3-L1 preadipocytes by activating the Wnt/β-catenin signaling pathway in the late stages of adipogenesis. (Section 6.9-6.13)

3. Extreme loss of fat depots in *db/db* mice fed *t*10-*c*12 CLA is due to activation of Wnt/ β-catenin signaling in the stromal vascular cells that inhibits preadipocyte differentiation and promotes adipocyte death. (Section 6.14-6.23)

4. Objectives

1. Examine the effect of CLA isomers on lipid droplet proteins and lipid droplet hydrolysis during adipogenesis in 3T3-L1 adipocytes.
    a. Examine the effect of CLA isomers on lipid droplet protein levels during adipocyte differentiation, focusing on perilipin.
    b. Evaluate the effect of CLA isomers on perilipin phosphorylation and localization.
    c. Determine the effect of CLA isomers on TG hydrolysis in mature 3T3-L1 adipocytes.
    d. Investigate the effect of CLA isomers on adipocyte cell size.

2. Examine the effect of CLA isomers on the Wnt/β-catenin pathway and its regulation of adipogenesis in 3T3-L1 adipocytes.
    a. Evaluate the effect of CLA isomers on β-catenin and on its phosphorylation and its localization during 3T3-L1 preadipocyte differentiation.
    b. Examine the effect of CLA isomers on upstream effectors and downstream targets of Wnt/ β-catenin, including SFRP, LRP5/6, Wnt10b and cyclin D1.

c. Investigate the effect of CLA isomers on Wnt-independent effects of β-catenin on adipocyte differentiation.

3. Identify the mechanism that leads to fat loss by *t*10-*c*12 CLA in *db/db* mice.
    a. Investigate the effect of CLA isomers on fat loss in different white and brown fat depots, and overall body composition.
    b. Investigate the effect of CLA isomers on metabolic rate by measuring body temperature and investigating the presence of metabolically active beige adipocytes.
    c. Evaluate the effect of CLA isomers on blood glucose levels during fat loss.
    d. Investigate the effect of CLA isomers on adipocyte turnover in fat depots.
    e. Examine the effect of CLA isomers on adipocyte stem cell populations compared to preadipocyte populations in various fat depots.
    f. Examine the effect of CLA isomers on different populations of immune cells in the fat depots.
    g. Characterize macrophage polarization in adipose tissue and its regulation by CLA isomers.

4. Resolve which stages of differentiation are sensitive to CLA.
    a. Compare the effect of CLA isomers at the commitment phase and terminal differentiation in two models, 3T3-L1 preadipocytes (*in vitro*) and *db/db* mice (*in vivo*).

5. Material and methods

5.1. Cell culture and differentiation

3T3-L1 cells were purchased from ATCC and were grown in DMEM (Dulbecco's modified Eagle's medium) supplemented with 20 mM HEPES, 100 units/ml penicillin and 100 μg/ml streptomycin. Ten percent calf serum was added to the medium in the growth stage and 10% fetal bovine serum (FBS) was used during differentiation. The cells were maintained in a humidified atmosphere with 95% air/5% CO_2. To induce differentiation, the cells were allowed to reach confluence and, after two days, cells were placed into Induction Medium, which consisted of DMEM (supplemented with 10% FBS) with 0.5 mM 1-methyl 3-isobutylxanthine (MIX), 0.25 μM dexamethasone, and 10 μg/ml insulin. This was considered day 0. After two days, the media (10% FBS-DMEM) were refreshed, but only 10 μg/ml insulin was added. The media were refreshed every 48 hours until the end of the experiment. Cells started differentiating on day 4; cells could be cultured up to day 12, although most experiments were terminated by day 8.

5.2. Cell treatments

For experiments investigating the contribution of PKC to the actions of CLA with respect to adipogenesis and lipid accumulation, the cells were treated with adipogenic Induction Medium after addition of PKC βI inhibitor (inhibits PKC βI), LY333531 (inhibits PKC βI and βII), bisindolylmaleimide I (Bis: inhibits PKCα, βI, βII, γ, δ, ε) or Gö6976 (inhibits PKCα) (See Table 1). Cells were lysed on day 2 and then at intervals until the morphologic features of differentiation were established (Day 8); the medium

was changed every 2 days and treatments added concurrently. CLA treatment was achieved by adding 60 μM *t*10-*c*12 CLA or *c*9-*t*11 CLA directly to the media on day 0 and every 48 hours with the media change. The specific concentration of the CLA isomers was based on the previous experiments in 3T3-L1 cells in our laboratory (Yeganeh, Stelmack et al. 2012).

5.3. Alkaline phosphatase treatment

The perilipin-1 antibody detects total perilipin-1 (phosphorylated and unphosphorylated perilipin-1). However, the upper phosphorylated band seen in Western blotting with this antibody has not been characterized. Thus, to validate the phosphorylated band of perilipin-1 in Western blotting alkaline phosphatase treatment was applied as follows. 3T3-L1 cells were grown and differentiated as described in section 5.1 above. Mature adipocytes were lysed with hypotonic lysis buffer (HLB) (100 mM Tris pH 7.4, 2 mM EDTA, and 1× Halt Protease Inhibitors) and were used as a stock protein lysate. Twenty μl of protein lysate was mixed with 2 μl of Cut Smart® Buffer (NEB B7204S) and 1 μl of calf intestinal alkaline phosphatase (CIP) (NEB M0290S), and incubated at 37°C for 40 minutes, at which time 20 μl of 2× sample buffer (2×SB) (20% glycerol, 0.05 M Tris pH 6.8 and 10% SDS) was added to the mixture. In parallel, 20 μl stock protein lysate was mixed with 1 mM phenylmethylsulfonyl fluoride (PMSF), 0.5% Tween-20, and 1× Halt Protease Inhibitors (null sample), after which 20 μl of 2×SB was also added. Perilipin-1 levels were examined by Western blotting.

5.4. Lipolysis assay

Lipolysis was quantified by measuring glycerol release into the culture medium (Bio Vision Lipolysis kit) on day 8 of differentiation without (basal unstimulated) or with CLA treatment. For long-term treatment, 60 μM *c*9-*t*11 or 60 μM *t*10-*c*12 CLA were included during the 8 day differentiation period, while short-term (acute) treatment involved incubating mature (8 day) adipocytes with 60 μM *c*9-*t*11 or 60 μM *t*10-*c*12 CLA for 24 hours. Cells treated with 100 nM isoproterenol during the final 24 hours of the treatment period were the positive control. Cells were lysed and the total protein content was used to normalize the glycerol release. The extent of differentiation was determined by the level of adiponectin expressed by the cells.

5.5. Live cell microscopy and cell size measurement

Photographs of 3T3-L1 cells were taken before the cells were lysed. Digital images were captured with an AMG-EVOS-XL (Life Technologies), and cell area was measured with Image-pro Plus 4.5.1 as previously described (Noto, Zahradka et al. 2007).

5.6. Protein isolation and immunoblotting

Protein was extracted from growing (day -3), confluent (day 0), growth-arrested (day 2) and differentiated 3T3-L1 (day 8) cells by lysing with 2× sample buffer (2×SB) (20% glycerol, 0.05 M Tris pH 6.8 and 10% SDS). Protein was extracted from epididymal adipose tissue using a mortar and pestle and 3× sample buffer (3×SB) (20% glycerol, 0.05 M Tris pH 6.8 and 15% SDS). After sonicating the samples, the

Bicinchoninic Acid (BCA) protein assay (Thermo Fisher Scientific) was used to determine the protein concentration of all cell and tissue lysates to enable equal protein loading onto the SDS-polyacrylamide gels.

Ten µg of lysate protein was separated on SDS-polyacrylamide gels (% depended on the size of the desired protein; proteins smaller than 30 kDa were run on 15% or 12.5% gel; proteins in the 30-100 kDa range were run on 10% gel; proteins greater than 100 kDa were run on a 5% gel) at 20 mA constant current per gel for 70-90 minutes and transferred electrophoretically to polyvinylidene difluoride membranes using 100 volts for 60 minutes for 1.0 mm thick 12.5% and 10% gels, and 90 minutes for 1.5 mm thick and 5% gels. For large proteins (5% gel), the amount of methanol used for the protein transfer was halved. To determine the molecular mass, the Bench Mark™ Prestained Protein Ladder (Bio–Rad) was used. Subsequently, the membranes were immunoblotted and blocked with 3% BSA-TBST (bovine serum albumin in Tris-buffer saline with Tween-20) (50 mM Tris pH 7.4, 150 mM NaCl, 0.05% Tween 20). The membranes were incubated with primary antibody that was diluted in 3% BSA-TBST for 1 hour at room temperature or overnight at 4°C. The antibodies and their dilutions are listed in Table 2. Subsequently, the primary antibody was removed and the membrane washed for a minimum of 20 minutes in 1× TBST, with the TBST refreshed at least four times. The membrane was then incubated with horseradish peroxidase-conjugated secondary antibody for 1 hour and the wash repeated as previously described. All secondary antibodies were used at a dilution of 1:10000 in phosphate-buffered saline (PBS) containing 1% BSA. The membrane was dipped in Luminata™ Crescendo Western HRP Substrate (Millipore) and the relative intensity was captured by exposing the membrane

to CL-XPosure™ film (Thermo Scientific). The band of interest on the film was quantified by densitometry with a model GS-800 Imaging Densitometer (Bio-Rad Laboratories, Hercules, CA) and adjusted to the loading control where applicable. Different loading controls were used throughout this study to account for differences in the percentage of acrylamide used to fomr the gel. eEF2, GAPDH and β-tubulin were used for 5%, 10% and 12.5% gels, respectively, while MAPK (ERK1/2) was used exclusively for samples from the animal study. The utility of these loading controls has been validated previously (DeClercq, Zahradka et al. 2010).

5.7. Immunoprecipitation (IP)

3T3-L1 cells were grown on 100 mm culture dishes, differentiated and treated with 60 μM *c*9-*t*11 or *t*10-*c*12 CLA as described previously (section 5.1). Cells were lysed by adding 1 ml IP buffer (1% NP-40, 20 mmol/L Tris-HCl pH 7.5, 10% glycerol, 137 mmol/L NaCl, 1 mmol/L $MgCl_2$, 1 mmol/L PMSF and 0.4 mmol/L orthovanadate) to each dish. Cells were removed from the dish using a scraper and transferred into a cold 1.5 μl microfuge tube, followed by sonication to reduce viscosity. The BCA (Thermo Fisher Scientific) protein assay was used to determine the protein concentration. Twenty μl of Washed Protein G-Sepharose Beads (Sigma Aldrich) were added per 100 μl sample (1 μg/μl) and rotated at 4°C for 30 minutes. The beads were collected by centrifuging the tubes at 19,300×g for 5 minutes (Eppendorf centrifuge 5804R with rotor # FA-45-30-11). The supernatant was transferred to a new microfuge tube and incubated with 2 μg primary antibody to PPARγ (E-8, Santa Cruz) with rotation for 2.5 hours at 4°C. Then, 50 μl of Washed Protein G-Sepharose Beads were added to each sample and rotated at

4°C for one hour. The beads were washed 4 times with IP buffer. The samples were centrifuged after each wash at 19,300×g for 2 minutes. After the last wash, the pellet was re-suspended in 25 µl of 2×SB and 2.5 µl of 1:1, 5% β-mercaptoethanol: 0.005% bromophenol blue, boiled in a pre-heated water bath for 5 minutes, and centrifuged at 19,300×g for 5 minutes to remove the beads. The supernatants were analyzed by Western blotting using mouse anti-active β-catenin (EMD Millipore) and PPARγ (E-8, Santa Cruz).

5.8 Immunofluorescence

To study the distribution pattern and relative amounts of perilipin-1 and β-catenin, immunofluorescence staining was performed on differentiated 3T3-L1 cells. The 3T3-L1 cells were grown on coverslips in the same growth conditions as those used for the immunoblotting experiments. Immunofluorescence was conducted as previously described by Yeganeh et al. (2012). Briefly, cells were fixed with fresh 4% paraformaldehyde, permeabilized with 0.1% Triton X-100 in PBS and, after blocking with 3% BSA, were incubated overnight at 4°C with primary antibodies. Slides were incubated with fluorescently targeted secondary antibodies diluted in PBS containing 1% BSA, followed by application of the nuclear stain Hoechst 33342 (Sigma) (diluted 1:40000 in PBS). The antibodies and their dilutions are listed in Table 2. Negative controls lacking primary antibody were processed similarly. The cells were viewed and photographed using a Zeiss Axiovert 3.0 microscope and images were processed with Axiovision Rel. 4.7 software.

5.9 Subcellular fractionation

3T3-L1 cells were grown on 100-mm plates, induced to differentiate and treated with *c*9-*t*11 or *t*10-*c*12 CLA for the 8 day differentiation period, as previously described (section 5.1). Subsequently, the plates were washed twice with PBS, and covered with 1 ml of ice-cold HLB containing 1 mM PMSF and 0.5% Tween-20. The plates were on ice for 5 minutes, then scraped and the contents transferred to a 1.5 ml microfuge tube. After 30 minutes on ice, the tubes were centrifuged at 4200×g (Eppendorf centrifuge 5804R with rotor # FA-45-30-11) for 5 minutes at 4°C. The nuclear fraction (pellet) was solubilized in 2×SB and the supernatant was transferred to an ultracentrifuge tube and spun at 630,000×g (Optima ultracentrifuge, rotor # MLA-130) for 45 minutes at 4°C. The cytosolic fraction (supernatant) was transferred to a fresh tube while the membrane fraction (pellet) was solubilized in 2×SB. Phosphatase and protease inhibitors were added to both fractions, which were then analyzed by Western blotting to detect the levels of the proteins of interest (e.g., perilipin-1, PKCα) as well as specific markers of each fraction; IGF-1 receptor β (membrane), Glyceraldehyde 3-phosphate dehydrogenase (GAPDH) (cytosol) and Histone (H3) (nucleus), were used to distinguished the membrane, cytosolic and nuclear fractions, respectively.

5.10 Animal study

5.10.1 Animal and diets

Six-week old male *db/db* (n=36) and C57BL/6 (n=36) mice were obtained from Jackson Laboratory (JAX Mice and Services). The animals were acclimatized for 7 days to the housing conditions (12 hour light and dark cycle with controlled humidity and

temperature) and diet (control diet containing 0% CLA). After acclimation, the mice were randomly assigned to different groups: control (CTL, 0% CLA; 8 *db/db* and 8 C57BL/6 mice), *t*10-*c*12-CLA (0.4% w/w; 10 *db/db* and 20 C57BL/6 mice), *c*9-*t*11-CLA (0.4% w/w; 8 *db/db* and 8 C57BL/6 mice) and pair weight (PW, 0% CLA; 8 *db/db* and 8 C57BL/6 mice). Due to extreme fat loss in C57BL/6 mice fed *t*10-*c*12-CLA, extra mice were included to ensure there was enough adipose tissue for Western blotting. For all other groups, there was enough adipose tissue to complete all analyses on tissue from individual mice. Mice were fed *ad libitum* except the paired weight group, which was fed restricted amounts of CTL diet to maintain a body weight comparable to the *t*10-*c*12 CLA-fed mice. The pair weight group was included in the study design to distinguish between the metabolic effects of fat loss due to CLA consumption and fat loss due to reduced body weight from feed restriction. The diet formulation is shown in Table 4.

The CLA dose in this study was based on a previous animal study in our laboratory (Hunt 2009), which showed weight loss in *db/db* and C57BL/6 mice fed *t*10-*c*12-CLA. However, the duration of the previous study was 6 weeks and significant weight loss was observed at 4 weeks. Therefore, to balance achieving weight loss and having adequate adipose tissue to test our hypothesis, the duration of study was shortened to 4 weeks.

5.10.2 Physiological assessments

Mice were fed daily to control feed intake (PW group) and minimize food spillage. Body weight was measured once a week, except the PW groups that were weighed three times a week. Body temperature was measured at baseline and at the end

of the study (4 weeks) using an Atlas Monitor Series 6200 (Welch Allyn Canada Ltd.) thermometer with a mouse specific rectal probe. At the baseline and at the end of study (week 4) animals were fasted (no feed but access to water) in metabolic cages for 5-6 hours. Urine was collected in 30 ml plastic vials, weighed, aliquoted and stored at -80°C for future analysis. Fasting blood was obtained by pricking the tail with a lancet and the glucose concentration in the blood droplet was determined using an Alpha TRAK Blood Glucose Monitoring System (Cat #32115-01). An overview of the study design and timelines is presented in Figure 1.

(a)

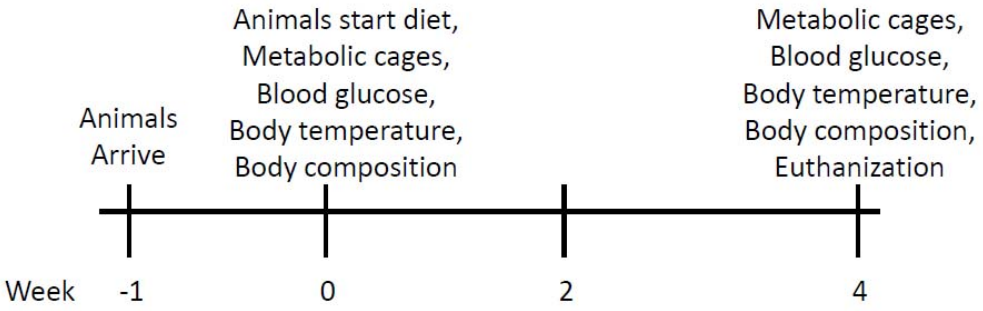

(b)

	*t*10-*c*12 CLA (0.4% w/w CLA)	*c*9-*t*11 CLA (0.4% w/w CLA)	Pair weight (PW) (0% CLA)	Control (CTL) (0% CLA)
db/db	10 mice	8 mice	8 mice	8 mice
C57BL/6	20 mice	8 mice	8 mice	8 mice

Figure 3. Animal study design

(a) Time line. One week after arrival (week -1), fasting blood glucose, body temperature and body composition were measured; animals were then started on the experimental diet (week 0). Animals were fed the experimental diet for 4 weeks. At the end of the study (week 4), fasting blood glucose, body temperature and body composition were measured immediately before termination.

(b) Dietary groups. One week after arrival, the mice were randomly assigned to different groups: *t*10-*c*12-CLA (0.4% w/w; 10 *db/db* and 20 C57BL/6 mice), *c*9-*t*11-CLA (0.4% w/w; 8 *db/db* and 8 C57BL/6 mice), pair weight (PW, 0% CLA; 8 *db/db* and 8 C57BL/6 mice) and control (CTL, 0% CLA; 8 *db/db* and 8 C57BL/6 mice).

5.10.2 Body composition

During Week 4 (prior to termination), body composition was measured using the EchoMRI-700™ whole body Quantitative Magnetic Resonance (QMR) instrument (Echo Medical System). This machine takes *in vivo* measurements using the nuclear magnetic resonance properties of hydrogen atoms to distinguish signals from fat mass, lean mass, free water, and total water (Taicher, Tinsley et al. 2003).

5.10.3 Tissue collection

At the end of the 4 week feeding period, mice were weighed and euthanized using a decapitator. After decapitation, the trunk blood was collected in a 1.5 ml microfuge tube, allowed to coagulate, and serum was obtained by centrifuging the tube at 1000×g for 10 minutes at 4°C (Eppendorf centrifuge 5804R with rotor # FA-45-30-11). Serum was aliquoted and stored at -80°C for future analysis. Various tissues were dissected, weighed, and either flash frozen in liquid nitrogen and stored at -80°C or placed in Cryo-Gel™ (Electron Microscopy Sciences Cat# 62806-01) or OCT (Optimal Cutting Temperature) (Tissue-Tek Cat#4583) embedding medium for histological analysis and then frozen in an ethyl alcohol-dry ice bath and stored at -80°C. The collected tissues included all white adipose pads (epididymal, peri-renal, inguinal and mesenteric), interscapular and associated brown fat, liver, and heart. A large portion of the epididymal adipose tissue (~0.3 g from C57BL/6 mice and ~1.2 g from *db/db* mice) was used immediately for SVF isolation and flow cytometry analysis. For this thesis various analyses were completed on epididymal and inguinal fat pads.

5.10.4 SVF isolation

The epididymal adipose tissue was dissected and thoroughly minced (1-2 mm pieces) using sterile scissors. The minced adipose tissue was placed in a 50 ml conical tube and digested in solution containing 0.8 mg/ml Collagenase A (Roche Cat# 10103586001), 3% BSA and 10% FBS in DMEM, for 60 minutes in a shaking 37°C incubator (200 rpm) (VWR Incubating Mini shaker). After 50 minutes of incubation time, the tubes were shaken vigorously by hand (10-20 seconds) to assist the separation of SVF from adipose tissue. On average, 10 ml of digestion solution was used for each gram of adipose tissue. At the end of the digestion period, the tube's contents were filtered through a 250 μm mesh to remove undigested adipose tissue. The mesh was washed with 4 ml of wash buffer (3% BSA in DMEM). The tube contents (filtered and washed solution) were centrifuged at 300×g for 5 minutes at room temperature. The floating fraction (adipocytes) was separated and stored at -80°C for further analysis. The pellet was resuspended in 2 ml wash buffer and the cells washed and separated thoroughly by gently pipeting (20-30 times), then the mixture was filtered through a sterile 40 μm cell strainer (BD Biosciences (Falcon) Cat #087711) and the filter was washed with 4 ml of wash buffer, followed by centrifugation at 300×g for 5 minutes at room temperature. The supernatant was discarded and the pellet was resuspended in 1 ml DPBS (Dulbecco's PBS; 2.7 mM KCl, 1.5 mM KH_2PO_4, 136.9 mM NaCl, 8.9 mM Na_2 $HPO_4.7H_2O$, PH 7.3) containing 0.5% FBS.

5.10.5 Cell counting and viability

To determine the cell number and viability of the SVF, 10 µl of the cell suspension and 10 µl of 0.4% Trypan Blue solution were mixed, and incubated at room temperature for one minute. Ten µl of stained cells were loaded onto a counting chamber slide and analyzed with the Countess® Cell Counter (Life Technologies). The Countess® Cell Counter measures the average number of live, dead and total cells, with a range from 1×10^4 to 1×10^7 cell/ml.

5.11 Flow cytometry

Identifying adipocyte precursors from the SVF is not achievable by using one single marker. Thus, to identify non-adipogenic endothelial and hematopoietic stem cells from adipocytes precursors in the SVF, multicolor flow cytometry is required, since it allows quantification of various cell populations in the total sample.

Flow cytometry was used to distinguish populations of preadipocyte and adipocyte stem cells in the SVF, as well as quantify the proportions of different immune cells in the SVF. For this purpose the SVF isolated from epididymal adipose tissue was transferred into two 15 mm round bottom staining tubes (1×10^6 cells/tube). Cells in tube #1 were stained with fluorochrome-targeted antibodies for CD45, CD31, CD29, CD34, Sca-1 and CD24. The cells in tube one were gated as $CD45^-CD31^-CD29^-CD34^+Sca\text{-}1^+CD24^-$ and $CD24^+$ (see Figure A1 and A2 for representative flow cytometry plots). Cells in tube #2 were stained with fluorochrome-conjugated antibodies for F4/80, CD11c, MHCII, CD3 and NK1.1 (see Figure A3 and A4 for representative flow cytometry plots). The details regarding the antibodies used in flow cytometry are listed in Table 3.

The procedure for preparing the samples for flow cytometry was as follows: cells from SVF isolated from each animal were transferred into two tubes (tube #1 and tube #2) (1×10^6 cells/tube; 300-500 µl depending on number of isolated cells). In the dark, the fluorochrome-conjugated antibodies were added into each tube as described previously and incubated for 1 hour on ice. The cells were then washed with 1 ml cold 0.5% FBS-DPBS and centrifuged at 300×g at 4°C for 8 minutes. The supernatant was discarded and cell pellet was resuspended in 1 ml 1% paraformaldehyde (made fresh weekly) and stored at 4°C overnight until analyzed on the flow cytometer. Along with the experimental tubes, an unstained cell sample was prepared in separate tube (1×10^6 cells/tube) as a negative control and also fixed overnight in 1% paraformaldehyde.

Due to low cell numbers in the SVF, compensation beads, which are polystyrene particles that have been coupled to an antibody specific for the IgG κ light chain of mouse, were used instead of SVF cells to determine the sensitivity of primary antibody and isotype controls. At the beginning of the flow cytometry experiment, the level of background staining was evaluated using isotype control antibodies which are matched to each primary antibody's host species and isotype. In addition, the sensitivity of the antibodies was evaluated weekly, also using beads; these samples are referred to as negative controls and they were prepared as follows. On the same day as the flow cytometry analyses, a drop of compensation beads (BD Biosciences cat# 01-1111-42) was added into a round bottom staining tube containing 1 ml of 0.5% FBS-DPBS. A similar amount of antibody or isotype control as used in the flow cytometry analyses was added into each negative control and isotype control tubes; as we were using 10 different antibodies, there were 10 different negative controls and 4 different isotype controls. The

tubes were incubated in the dark and on ice for 30 minutes. After incubation, the beads were washed with 2 ml of 0.5% FBS-DPBS and the tubes centrifuged at 200×g at 4°C for 10 minutes. The supernatant was discarded and the pellet was resuspended in 0.5 ml of 0.5% FBS-DPBS.

All the experimental samples and negative controls were taken to the flow cytometer at the same time. Flow cytometry was performed using a BD FACSCanto-II flow cytometry analyzer (BD Biosciences). The voltage was set at 293 for forward scatter and 385 for side-scatter. Five thousand events were collected and data were analyzed using FlowJo software (Version 100SX.Zip).

5.12 Adipose tissue sections

To investigate the presence of macrophages in adipose tissue by immunofluorescence staining, 7 μm sections of inguinal adipose tissue frozen in Cryo-Gel embedding medium were prepared. The working temperature on the Cryostat was set to -35°C. The sections were kept at -80°C until they were used for immunofluorescence staining as described in 5.8.

5.13 Statistical analysis

Data are presented as mean ± SEM (standard error of the mean). One-way Analysis of Variance (ANOVA) followed by post-hoc testing with Tukey's test was performed using SAS (SAS Institute Inc, NC, USA) for the *in vitro* experiments. Chi square testing was also used to assess differences among cell size ranges for the *in vitro* experiments. All the *in vitro* experiments were independently repeated at least 3 times.

For the *in vivo* study (end point data) and some of the *in vitro* experiments (as indicated in the figure legend where applicable) two-way ANOVA was used to determine main effects (*in vivo*: genotype, diet and genotype×diet interaction; *in vitro*: CLA, inhibitor and CLA×inhibitor interaction). Differences between specific groups or treatments were determined by contrast statements for pre-planned comparisons (*in vivo* study) or Tukey's test (*in vitro* experiments). For the time course data in the *in vivo* experiment, two-way repeated measurers ANOVA followed by means testing with least square means with Tukey-Kramer adjustment for multiple comparisons was used. Data that were not normal or homogeneous were log transformed. If data were not normal or homogenous after log transformation, they were analyzed by non-parametric testing using the Kruskal-Wallis test followed by contrast statements for pre-planned comparisons. Differences were considered statistically significant at $P<0.05$.

Table 1. Chemicals and functions

Chemical	Functions	Working Conc.	Vehicle	Catalog #	Company
Bisindolylmaleimide I	PKC α, β_I, β_{II}, γ, δ and ε inhibitor	10^{-5} M	DMSO	203290	Calbiochem
CHIR99021	GSK3-α and -β inhibitor	60×10^{-9}M	DMSO	4423	Tocris Bioscience
*c*9-*t*11 CLA	*Cis*9-*trans*11 CLA isomer	60 μM	Ethanol	90140	Cayman Che Co.
*t*10-*c*12 CLA	*Trans*10-*cis*12 CLA isomer	60 μM	Ethanol	90145	Cayman Che Co.
Dexamethasone	Synthetic glucocorticoid agonist	0.25 μM	Water	D4902	Sigma Aldrich
Gö6976	PKCα inhibitor	10^{-6} M	DMSO	365250	Calbiochem
Insulin	Activates insulin receptor	10^{-6} M	Water	407694	Calbiochem
JW67	Canonical Wnt pathway inhibitor	20×10^{-6} M	DMSO	4651	Tocris Bioscience
LY333531	PKC βI and βII inhibitor	40×10^{-9} M	DMSO	4738	Tocris Bioscience
Methylisobutylxanthine	cAMP phosphodiesterase inhibitor	0.5 mM	DMSO	I5879	Sigma Aldrich
PKC β inhibitor	PKC βI inhibitor	50×10^{-9} M	DMSO	539654	Calbiochem

Table 2. Western blotting, IF and IP antibodies

Antibody	Secondary	Application	Dilution	Size (kDa)	Catalog #	Company	Function
ACRP30 (Adiponectin)	Rabbit	WB	1:1000	27	2789	Cell Signaling	Adipokine
Adipsin	Goat	WB	1:1000	45,28	SC-12402	Santa Cruz	Adipokine
β-catenin	Mouse	WB IF	1:1000 1:300	92	SC-7963	Santa Cruz	Cell-cell adhesion & transcription factor activator
Active β-catenin	Mouse	WB/IP IF	1:1000 1:100	92	05-665	EMD Millipore	Transcription factor activator
Ser-675 β-catenin	Mouse	WB	1:1000	92	9567	Cell Signaling	Stabilize β-catenin
Ser-45/Thr-41 β-catenin	Mouse	WB	1:1000	92	9565	Cell Signaling	Unsatiable β-catenin
CD206	Rat	IF	1:200	175	MCA2235	Bio Rad	M2 Macrophage marker
Caspase-3	Rabbit	WB	1:1000	35	6962	Cell Signaling	Proteolytic cleavages of proteins
Cleaved Caspase-3 (Asp 175)	Rabbit	WB	1:1000	17, 19	9664	Cell Signaling	Active form of Caspase-3
Chemerin	Goat	WB	1:1000	16	AF2325	R&D System	Adipokine
Cyclin D1	Mouse	WB	1:1000	36	2926	Cell Signaling	Cell cycle regulator/ downstream of Wnt
eEF2	Rabbit	WB	1:1000	100	2332	Cell Signaling	Loading control
F4/80	Rabbit	IF	1:100	130	Ab74383	Abcam	Macrophage marker

Table 2. (cont'd)

Antibody	Secondary	Application	Dilution	Size (kDa)	Catalog #	Company	Function
F4/80	Rat	IF	1:200	102-130	Ab6640	Abcam	Macrophage marker
GAPDH	Mouse	WB	1:5000	36	Ab1484	Abcam	Cytosol protein
Histone (H3)	Rabbit	WB	1:1000	17	9717	Cell Signaling	Nuclear protein
HSL	Rabbit	WB	1:1000	81,83	4107	Cell Signaling	Lipase
LC3	Rabbit	WB	1:1000	19, 17	2755	Cell Signaling	Bind to autophagosomes and activate autophagy
LRP5/6	Rabbit	WB	1:1000	180, 210	3395	Cell Signaling	Receptor
Ser-1490-LRP6	Rabbit	WB	1:1000	180, 210	2568	Cell Signaling	Phosphorylated receptor
IGF-1 receptor β	Rabbit	WB	1:1000	95	3027	Cell Signaling	Membrane protein
iNOS	Rabbit	IF	1:400	130	13120	Cell Signaling	M1 Macrophage marker
Perilipin-1	Rabbit	WB IF	1:1000 1:100	62	3467	Cell Signaling	Lipid droplet protein
PKCα-C (H-7)	Mouse	WB	1:1000	80	SC8393	Santa Cruz	Kinase
PPAR γ	Mouse	WB IP	1:1000 1:250	67	SC-7273	Santa Cruz	Adipocyte specific transcription factor
PRDM16	Goat	IF	10µg/ml	170	AF6295	R&D System	Beige adipocyte marker

Table 2. (cont'd)

Antibody	Secondary	Application	Dilution	Size (kDa)	Catalog #	Company	Function
SFRP-5 (SARP-3)	Mouse	WB	1:5000	40	SC-374397	Santa Cruz	Modulator of Wnt signaling
TBX-1	Rabbit	WB IF	1:1000 1:100	43	Ab18530	Abcam	Beige adipocyte marker
β-tubulin	Rabbit	WB	1:1000	55	2146	Cell Signaling	Loading control
Wnt10b	Rabbit	WB	1:1000	43	Ab70816	Abcam	Wnt/ β-catenin agonist

Table 3. Flow cytometry antibodies

Antibody	Fluorochrome	Application	Dilution µl/10^6 cells	Voltage	Catalog #	Company	Function
CD3	APC	FCM	2.5	516	17-0032	eBioscience	Mature T cell marker
CD11c	PE-Cy7	FCM	2.5	500	25-0114	eBioscience	Dendritic cell and M1 macrophage marker
CD24	PE	FCM	1	385	12-0242	eBioscience	Adipocyte progenitor cells marker
CD29	FITC	FCM	2	313	11-0291	eBioscience	Leukocyte, endothelial, smooth muscle and epithelial cell marker
CD31	PE-Cy7	FCM	2.5	544	25-0311	eBioscience	Platelet-endothelial cell adhesion molecule-1 (PECAM-1) marker
CD34	eFluor® 660 (APC)	FCM	2	462	50-0341	eBioscience	Capillary endothelial cell and mesenchymal stem cell marker
CD45	APC-e780	FCM	2	462	47-0451	eBioscience	Hematopoietic cell marker excluding mature erythrocytes and platelets
F4/80	PE	FCM	2	384	12-4801	eBioscience	Macrophage marker
MHC Class II	eFluor® 450 (Pacific Blue)	FCM	2	390	48-5321	eBioscience	Activated dendritic cell marker
NK1.1	eFluor® 450 (Pacific Blue)	FCM	2	390	48-5941	eBioscience	Natural killer cell marker
Sca-1/Ly-6	V450 (Pacific Blue)	FCM	2	276	560653	BD Bioscience	Stem cell marker

Table 4. Isotype controls

Antibody	Flourochrome	Application	Dilution µl/10^6 cells	Voltage	Catalog #	Company	Function
Armenian Hamster IgG	PE-Cyanine7	FCM	2.5	544	25-4888	eBioscience	Isotype Control
Armenian Hamster IgG	FITC	FCM	2	313	11-4888	eBioscience	Isotype Control
Rat IgG2a K	eFluor® 660	FCM	2	462	50-4321	eBioscience	Isotype Control
Rat IgG2b K	PE	FCM	1	385	12-4031	BD Bioscience	Isotype Control

Table 5. Diet formulation

Ingredients (g/kg Diet)	Control Diet	*c*9-*t*12 CLA	*t*10-*c*12 CLA
Cornstarch[1]	363	363	363
Maltodextrin[1]	132	132	132
Sucrose[1]	100	100	100
Egg White[1]	212.5	212.5	212.5
Cellulose[1]	50	50	50
AIN-93G-Mineral Mix[1]	35	35	35
AIN-93VM-Vitamin Mix[1]	10	10	10
Choline[1]	2.5	2.5	2.5
Biotin Mix[1] (200 mg biotin/Kg cornstarch)	10	10	10
Tert-butylhydroquinone[2]	0.014	0.014	0.014
Soy Oil[1]	85	80.57	80.57
*c*9,*t*11 CLA (90% pure)[3] cat #: 10-1823-90 lot #: G438:12	0	4.44	0
*t*10, *c*12 CLA (90% pure)[3] cat #: 10-1826-90 lot #: I-261:8	0	0	4.44

1. Dyets Inc.
2. Sigma Aldrich
3. Larodan

6. Results

6.1 CLA accelerates early lipid droplet formation

To investigate the effects of CLA isomers on the early stages of adipogenesis, 3T3-L1 cells were treated with 60 μM *c*9-*t*11 CLA or 60 μM *t*10-*c*12 CLA at the time differentiation was induced and lipid droplet formation was evaluated after 4 days rather than 8 days when differentiation is complete.

In comparison to untreated controls, cells treated with the CLA isomers contained a higher proportion of cells with lipid droplets (Figure 4a), thus indicating faster maturation. Quantification of the data showed that 78% of cells treated with *c*9-*t*11CLA and 85% of cells treated with *t*10-*c*12 CLA had lipid droplets compared to 48% of cells in the control (Figure 4b), while the total number of cells did not change. These data suggest both CLA isomers accelerate adipocyte differentiation.

To confirm this finding, we also measured the levels of a key lipid droplet protein, perilipin-1, on days 2 and 4 of differentiation. The amount of perilipin-1 was clearly elevated in both *t*10-*c*12 and *c*9-*t*11 CLA treated cells in comparison with control on day 2 of differentiation (Figure 5a, b), thus indicating lipid droplet formation had begun earlier than usual in response to CLA.

Figure 4. Stimulation of adipocyte differentiation by CLA isomers

(a) Representative photographs of 3T3-L1 cells were taken 4 days after addition of adipogenic cocktail without (Null) and with treatment of 60 μM *c*9-*t*11 CLA or 60 μM *t*10-*c*12 CLA beginning on day 0. Arrows indicate the location of lipid droplets. Images were captured using a 10× objective. Bar (*c*9-*t*11 panel) represents 10 μm and is applicable to all panels.

(b) The number of cells with lipid droplets was quantified and used to calculate the percentage of differentiated cells. The data are plotted as means ± SEM for n=3/treatment. Statistical analysis was performed using one-way ANOVA and Tukey's test. Significant differences ($P<0.05$) relative to control are indicated by #.

(a)

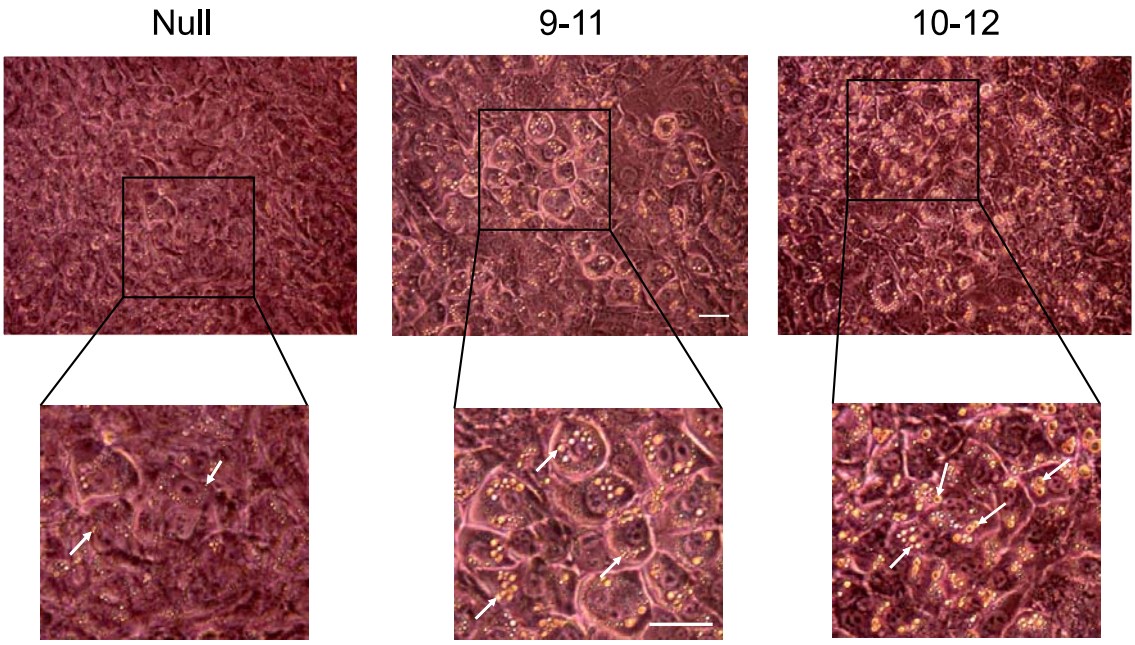
Null
9-11
10-12

(b)

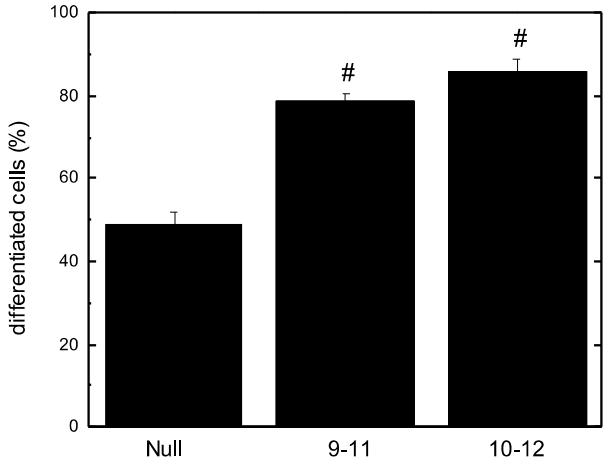
differentiated cells (%)
100
80
60
40
20
0
#
#
Null
9-11
10-12

6.2 CLA alters perilipin-1 phosphorylation but not its localization

A role for perilipin-1 phosphorylation in lipolysis and fat loss is well recognized (Miyoshi, Souza et al. 2006). In addition, Marcinkiewicz et al (2006) reported that phosphorylation of perilipin-1 at Ser 496 by PKA leads to fragmentation and dispersion of lipid droplets and ultimately to the activation of lipolysis. To investigate the role of CLA isomers on perilipin-1 phosphorylation, 3T3-L1 cells were treated with CLA isomers (60 μM) and lysed on days 2, 4 and 8 of differentiation for Western blot analysis using an antibody capable of detecting both unphosphorylated and phosphorylated perilipin-1; an antibody specific for phosphorylated perilipin-1 is not commercially available. It was possible to distinguish both forms of perilipin-1 because phosphorylation slowed the rate of migration of the protein in the gel and thus phosphorylated perilipin-1 could be visualized as a distinct band above the unphosphorylated form. No phosphorylation of perilipin-1 was observed on day 2 of differentiation, but it was detectable on days 4 and 8. While *c*9-*t*11 CLA had no effect on basal levels of phosphorylation, *t*10-*c*12 CLA treated cells showed significantly lower levels (~ 2 -fold) of perilipin-1 phosphorylation (Figure 5a, c).

To confirm the upper band detected with the anti-perilipin-1 antibody in Western blotting was phosphorylated, calf intestinal alkaline phosphatase (CIP) was added to the protein lysate obtained from mature adipocytes, as described in the Methods. Our data showed that addition of alkaline phosphatase leads to a significant reduction of the upper band as a result of perilipin-1 dephosphorylation (Figure 5d). These data support our assertion that the upper band detected by Western blotting data in Figure 5a is the phosphorylated form of perilipin-1.

To investigate changes in perilipin-1 localization relative to lipid droplet morphology, immunofluorescence (IF) was employed to visualize perilipin-1 in differentiated 3T3-L1 cells treated with *c*9-*t*11 CLA and *t*10-*c*12 CLA. Cells were fixed on day 8 of differentiation and perilipin-1 immunostaining was performed. Perilipin-1 is shown in green and the nuclei are blue. The distribution pattern of perilipin-1 in untreated cells and cells treated with *c*9-*t*11 CLA showed it was dispersed throughout the cell, with strong staining also present in the perinuclear region where no lipid droplets were located (Figure 6a). On the other hand, cells treated with *t*10-*c*12 CLA had perilipin-1 restricted to the periphery of the lipid droplets, with no staining present in the perinuclear region. Based on these results, it appears that treatment with *t*10-*c*12 CLA triggers movement of perilipin-1 out of a cellular compartment that is located close to the nucleus. It is presumed this compartment may be the Golgi and/or the ER, as observed with *c*9-*t*11 and null 3T3-L1, but not *t*10-*c*12 treated cells.

Figure 5. Effect of CLA isomers on perilipin-1 levels and phosphorylation state during adipogenesis

(a) Western blot of 3T3-L1 cells lysed at days 2, 4 and 8 of differentiation without (Null) and after treatment with 60 μM *c*9-*t*11 CLA or *t*10-*c*12 CLA beginning on day 0. The blots were probed for perilipin-1 and β-tubulin and are representative of 4 independent experiments.

(b,c) Densitometry was used to quantify the intensity of the bands in panel (a) of total perilipin-1 on days 2, 4 and 8 (b), and phosphorylated perilipin-1 on days 4 and 8 (c). Data were normalized to the loading control (β-tubulin) or perilipin-1. The results are presented as means ± SEM for n=4/treatment. Statistical analysis was performed using one-way ANOVA and Tukey's test. Significant differences ($P<0.05$) relative to the respective Null are indicated by #.

(d) Western blot of 3T3-L1 adipocyte proteins extracted on day 8 of differentiation with hypotonic lysing buffer (HLB) and subsequently treated without (Null) and with Alkaline Phosphatase (ALK phosphatase). The blot was probed for perilipin-1. The arrow indicates the phosphorylated perilipin-1 band. The experiment was done twice.

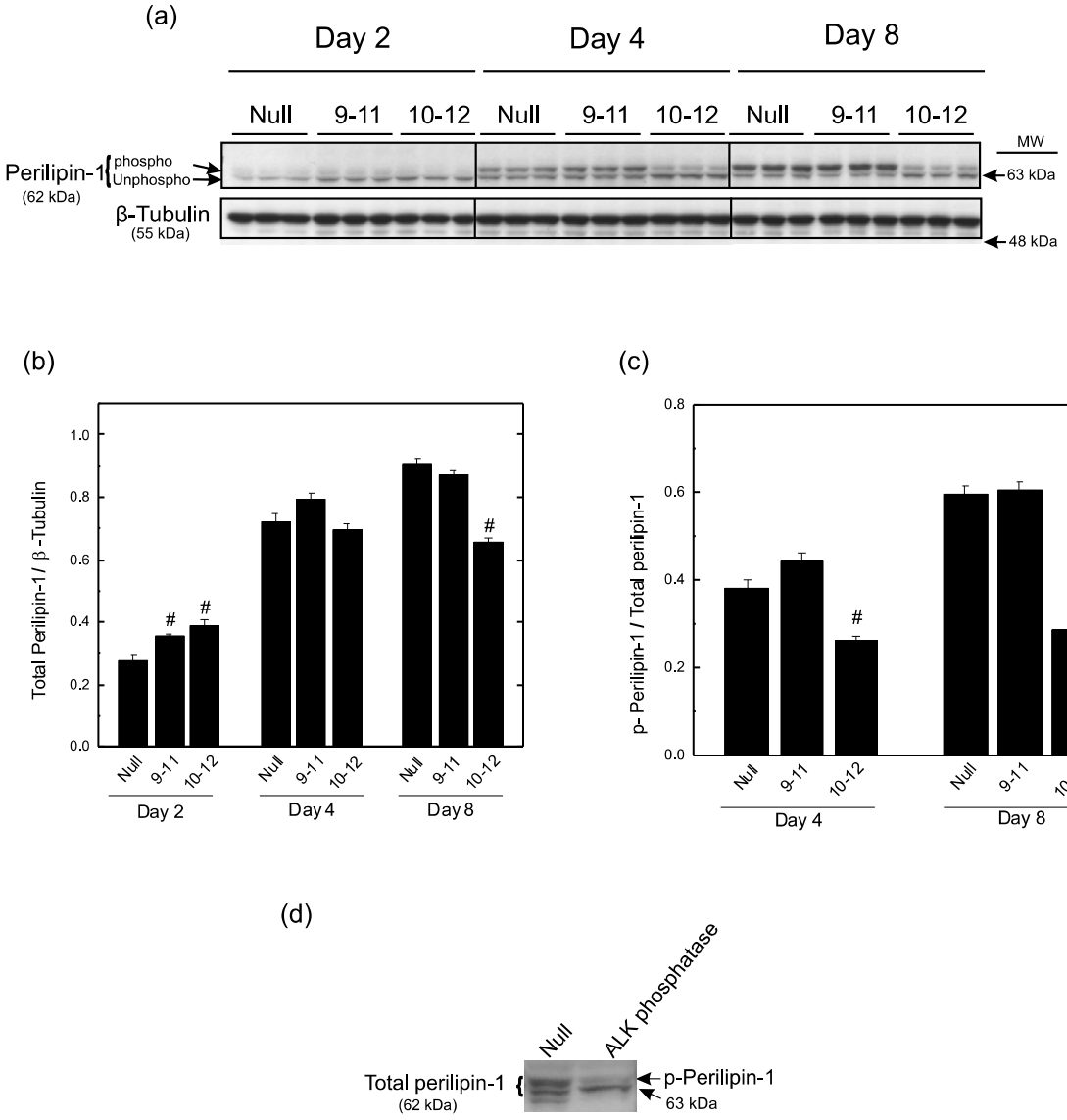
(a)
Day 2
Day 4
Day 8
Null
9-11
10-12
Null
9-11
10-12
Null
9-11
10-12
MW
Perilipin-1
(62 kDa)
phospho
Unphospho
63 kDa
β-Tubulin
(55 kDa)
48 kDa
(b)
Total Perilipin-1 / β -Tubulin
1.0
0.8
0.6
0.4
0.2
0.0
#
#
#
Null
9-11
10-12
Null
9-11
10-12
Null
9-11
10-12
Day 2
Day 4
Day 8
(c)
p- Perilipin-1 / Total perilipin-1
0.8
0.6
0.4
0.2
0.0
#
#
Null
9-11
10-12
Null
9-11
10-12
Day 4
Day 8
(d)
Null
ALK phosphatase
Total perilipin-1
(62 kDa)
p-Perilipin-1
63 kDa

Figure 6. Effect of CLA isomers on perilipin-1 localization during adipogenesis

(a) Immunofluorescence staining was performed on fixed cells prepared on day 8 of differentiation without (Null) and after treatment with 60 μM *c*9-*t*11 CLA or *t*10-*c*12 CLA beginning on day 0. Total perilipin-1 is indicated by green and nuclei are in blue. Scale bar represents 5 μm. The orange arrows show the lipid droplet and the white arrows show the perinuclear region.

(b) Subcellular fractionation was performed with 3T3-L1 adipocytes on day 8 of differentiation without (Null) and after treatment with 60 μM *c*9-*t*11 CLA or *t*10-*c*12 CLA beginning on day 0. Comparisons to cells at day -3 and 0, before differentiation is triggered, and cells maintained for 8 days without differentiation (Undiff) are provided. C: Cytosolic fraction M: membrane fraction. The blot was probed for total perilipin-1.

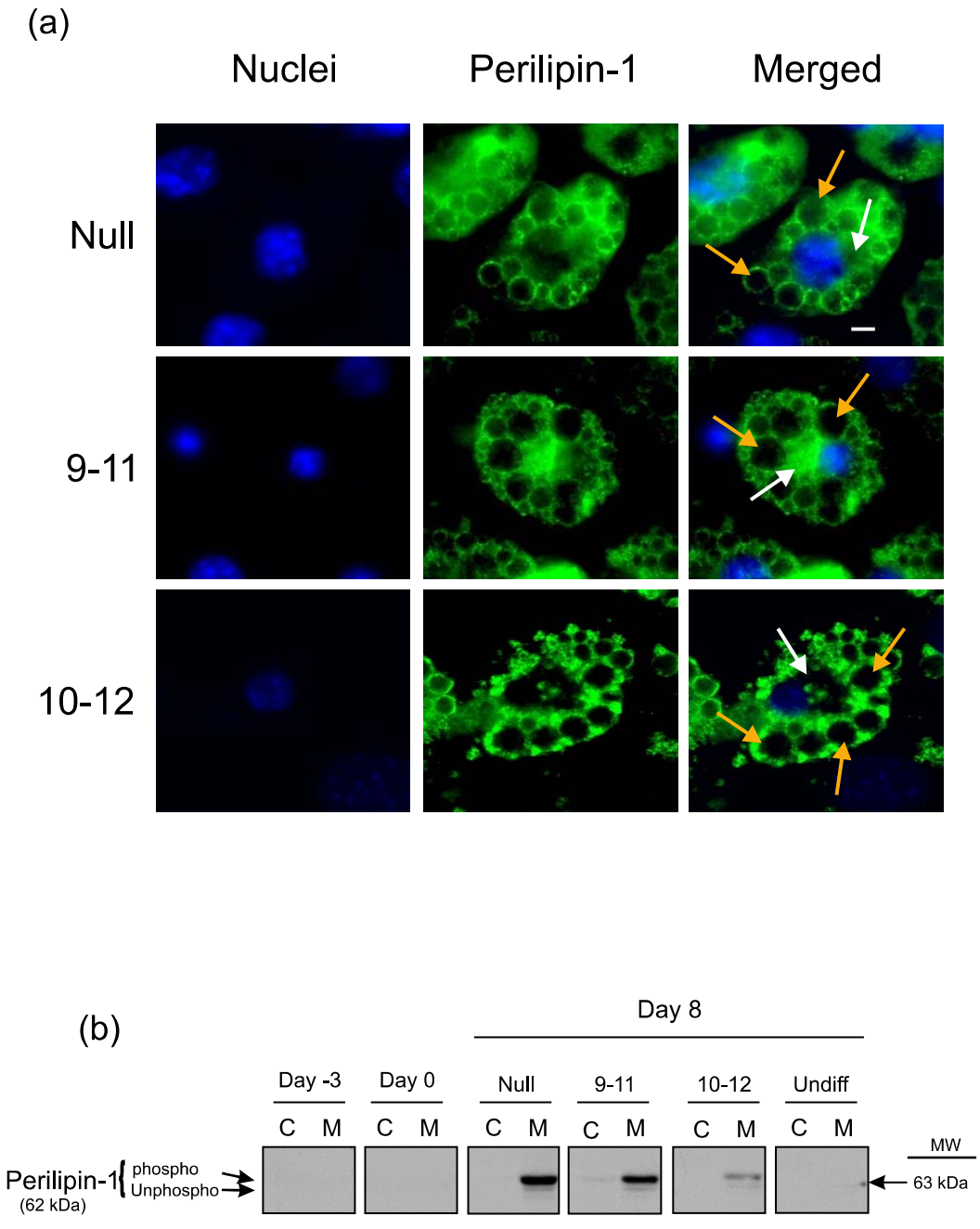
(a)
Nuclei
Perilipin-1
Merged
Null
9-11
10-12
(b)
Day 8
Day -3
Day 0
Null
9-11
10-12
Undiff
C M C M C M C M C M C M
MW
Perilipin-1
(62 kDa)
phospho
Unphospho
63 kDa

6.3 CLA does not alter membrane localization of perilpin-1

To further investigate the effect of CLA isomers on the localization of perilipin-1, subcellular fractionation of preadipocytes (day -3), confluent preadipocytes (day 0) and adipocytes treated without (Null) or with *c*9-*t*11 CLA or *t*10-*c*12 CLA for 8 days during differentiation was employed; cells maintained for 8 days without differentiation were considered undifferentiated controls. Subcellular fractionation 8 days after differentiation showed that there was almost no perilipin-1 associated with the cytosolic fraction and all protein was localized to the membrane fraction (Figure 6b). Interestingly, all of the perilipin-1 was in the phosphorylated form and only a minimal amount of unphosphorylated perilipin-1 was detected (Figure 6b). The remainder of the unphosphorylated perilipin-1 was likely lost with the lipid droplets, since they do not sediment with the membrane fraction. As expected, perilipin-1 was not detectable in either the cytosol or the membrane fraction of day -3 or day 0 preadipocytes (Figure 6b). The enrichment of the membrane and cytosolic fractions was confirmed by the presence of IGF-1 receptor β and GAPDH, respectively (data not shown). In agreement with Skinner et al (2013), and further supported by our IF results, our data suggest that perilipin-1 is localized primarily on organelles, possibly the ER and/or the Golgi apparatus, and that CLA treatment does not affect its localization. Furthermore, the reduced level of perilipin-1 in the membrane fraction from *t*10-*c*12 CLA treated cells is likely explained by the lower amount of perilipin-1 present in day 8 adipocytes (Figure 5a).

6.4 *t*10-*c*12 CLA inhibits lipolysis in 3T3-L1 adipocytes

Phosphorylation of perilipin-1 plays an important role in lipolysis (Miyoshi, Souza et al. 2006), and *t*10-*c*12 CLA reduces perilipin-1 phosphorylation. Consequently, we quantified the rate of lipolysis in CLA treated adipocytes using a colorimetric assay kit that measures glycerol formation to determine if CLA affected this process. The effects of CLA isomers on lipolysis were examined under both acute (24 hours) and long-term (8 days-the entire adipogenic period) conditions. Our data showed that long-term treatment with *t*10-*c*12 CLA as the adipocytes differentiated reduces the production of glycerol to below the basal level of untreated adipocytes (Figure 7a). Unlike *t*10-*c*12 CLA, the release of glycerol was elevated in *c*9-*t*11 CLA treated cells in comparison to null, untreated adipocytes. On the other hand, treatment of mature adipocytes with CLA isomers for 24 hours reduced the lipolysis rate by both isomers in comparison to null (Figure 7b).

Our data indicate that long-term treatment of *t*10-*c*12 CLA blocks lipolysis in adipocytes. We therefore examined the effect of CLA on HSL, another enzyme required for lipolysis in addition to perilipin-1. Western blotting showed that the level of HSL was significantly reduced with *t*10-*c*12 CLA treatment, by 55% and 68% on days 4 and 8 of differentiation, respectively, when compared with untreated adipocytes (Figure 7c, d). In contrast, HSL levels were reduced by 40% on day 4 and unchanged at day 8 in *c*9-*t*11 CLA treated adipocytes compared to untreated adipocytes. These findings suggest the mechanism by which *t*10-*c*12 CLA treatment enhances adipocyte lipid droplet production is mediated by effects on perilipin-1 and HSL.

Figure 7. Effect of CLA isomers on adipocyte lipolysis and HSL levels during adipogenesis

(a) Glycerol production by 3T3-L1 cells, without (Null) and with 60 μM *c*9-*t*11 CLA or 60 μM *t*10-*c*12 CLA treatment beginning on day 0 and continuing for the entire differentiation period, was measured on day 8. For the positive control, null cells were treated with 100 nM isoproterenol on day 7, 24 hours prior to glycerol measurement. The results are presented as means ± SEM for n=3/treatment. Statistical analysis was performed using one-way ANOVA and Tukey's test. Significant differences ($P<0.05$) relative to the respective null are indicated by # and differences between treatments are shown by *.

(b) Glycerol production by mature 3T3-L1 adipocytes, treated on day 8 with 60 μM *c*9-*t*11 CLA or 60 μM *t*10-*c*12 CLA, or untreated (Null), for 24 hours. 100 nM isoproterenol was added to the cells at the same time as CLA, 24 hours prior to glycerol measurement, as a positive control. The results are presented as means ± SEM for n=3/treatment. Statistical analysis was performed using one-way ANOVA and Tukey's test. Significant differences ($P<0.05$) relative to the respective null are indicated by # and differences between treatments are shown by *.

(c) Western blot of 3T3-L1 cells lysed at days 0, 2, 4 and 8 of differentiation without (Null) or with 60 μM *c*9-*t*11 CLA or *t*10-*c*12 CLA treatment beginning on day 0. The blots were probed for HSL and β-tubulin and are representative of 3 independent experiments.

(d) Densitometry was used to quantify HSL band intensity shown in panel (c) on days 0, 2, 4 and 8. Data were normalized to the loading control (β-tubulin). The results are

presented as means ± SEM for n=3/treatment. Statistical analysis was performed using one-way ANOVA and Tukey's test. Significant differences ($P<0.05$) relative to the respective null are indicated by #.

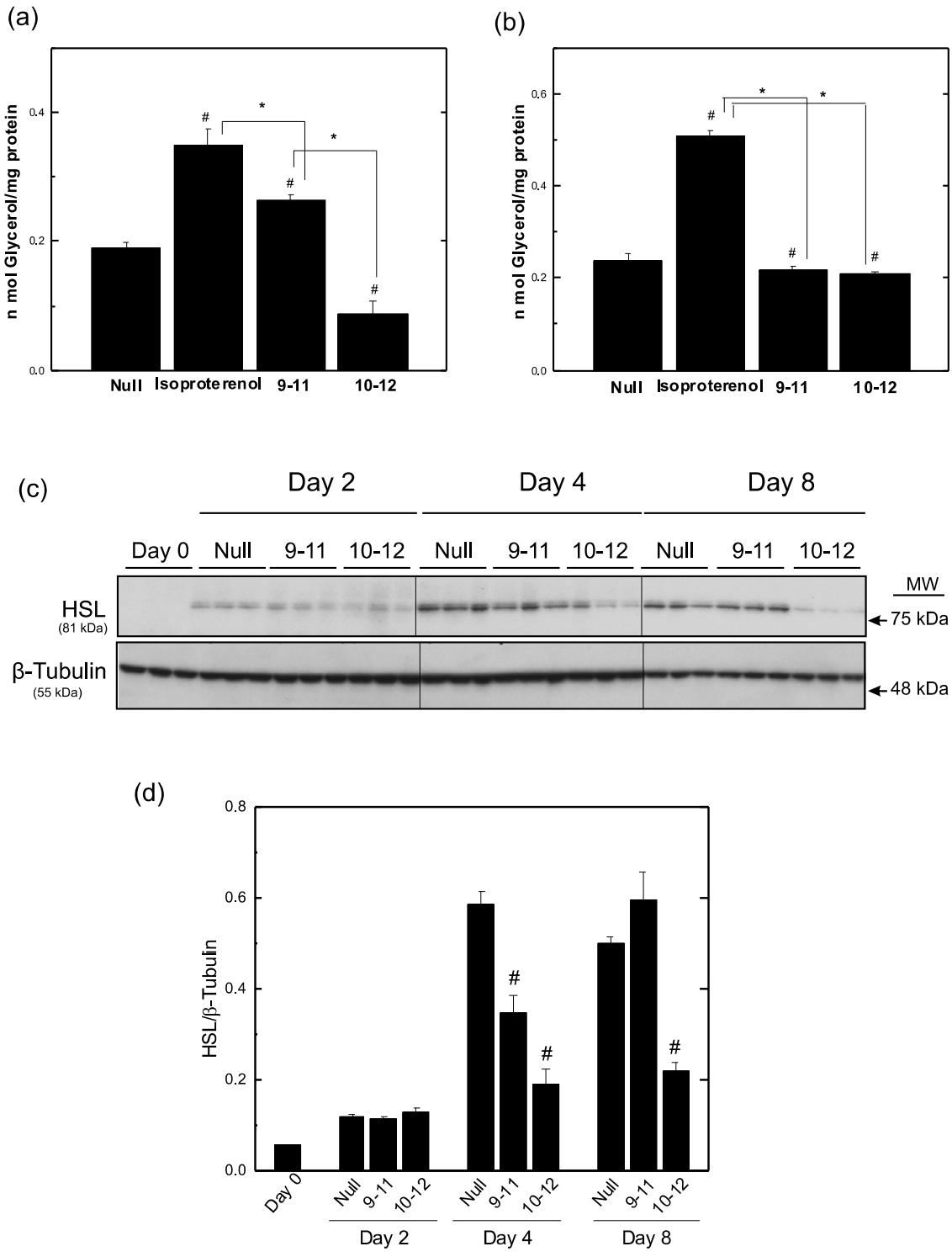
(a)
n mol Glycerol/mg protein
0.0
0.2
0.4
#
*
*
#
#
Null
Isoproterenol
9-11
10-12
(b)
n mol Glycerol/mg protein
0.0
0.2
0.4
0.6
#
*
*
#
#
Null
Isoproterenol
9-11
10-12
(c)
Day 2
Day 4
Day 8
Day 0
Null
9-11
10-12
Null
9-11
10-12
Null
9-11
10-12
MW
HSL
(81 kDa)
75 kDa
β-Tubulin
(55 kDa)
48 kDa
(d)
HSL/β-Tubulin
0.0
0.2
0.4
0.6
0.8
#
#
#
Day 0
Null
9-11
10-12
Null
9-11
10-12
Null
9-11
10-12
Day 2
Day 4
Day 8

6.5 CLA alters adipokine production and lipid droplet formation in mature adipocytes

To investigate the role of CLA on adipokine production, two-day post-confluent (day 0) 3T3-L1 cells were treated with 60 μM of *c*9-*t*11 CLA or 60 μM *t*10-*c*12 CLA. Cells were lysed on day 8 (differentiated) and markers for lipid droplet formation and adipokine generation were examined by Western blotting. Adiponectin levels increased during 3T3-L1 differentiation as expected (data not shown) and, in agreement with previous studies (Brown, Boysen et al. 2004), we found that adiponectin levels were lower on day 8 in cells treated with *t*10-*c*12 CLA but not *c*9-*t*11 CLA compared to untreated control cells (Figure 8a).

We extended the adipokine analyses to include chemerin and adipsin because of their important roles in obesity (Harada, Shen et al. 2003; Bozaoglu, Bolton et al. 2007). Chemerin, a recently recognized pro-inflammatory adipokine, was detectable by day 4 (data not shown). On day 8, chemerin levels were lower in both *t*10-*c*12 CLA and *c*9-*t*11 CLA treated cells compared to control (Figure 8b), with this effect being more pronounced in *t*10-*c*12 CLA treated cells suggesting that chemerin's synthesis or clearance is affected by CLA. Both glycosylated (44-37 kDa) and non-glycosylated (26 kDa) forms of adipsin were detectable only on day 8, and *t*10-*c*12 CLA treated cells had lower levels of both forms compared to the control and *c*9-*t*11 CLA treated cells on day 8 (Figure 8c, d). No difference was observed between *c*9-*t*11 CLA and control cells for adipsin.

To further investigate the effects of CLA isomers on adipogenesis, 3T3-L1 cell maturation was examined following treatment with CLA isomers for 8 days in

comparison with untreated cells (Null) by quantifying the number of cells containing lipid droplets compared to cells with no lipid droplets. There were fewer cells with lipid droplets following treatment with *t*10-*c*12 CLA compared to treatment with *c*9-*t*11 CLA or no treatment (Figure 9a). In addition, in null and *c*9-*t*11 CLA treated adipocytes the cellular periphery is clearly defined and observed, however in *t*10-*c*12 CLA treated adipocyte the cellular periphery is not clear and adipocytes are becoming smaller possibly due to loosing lipid droplets. Quantification of the data showed that 88% of cells treated with *c*9-*t*11 CLA and 89% of the control cells had lipid droplets compared to only 32% of cells treated with *t*10-*c*12 CLA (Figure 9b).

Figure 8. Effect of CLA isomers on production of adipokines by mature adipocytes

(a) Western blot of 3T3-L1 cells lysed on day 8 of differentiation after treatment without (Null) or with 60 μM *c*9-*t*11 CLA or *t*10-*c*12 CLA beginning on day 0. The blots were probed for adiponectin, chemerin, glycosylated and non-glycosylate adipsin and GAPDH (loading control) and are representative of 4 independent experiments.

(b-e) Densitometry was used to quantify the intensity of the bands in panel (a): adiponectin (b), chemerin (c), glycosylated adipsin (d) and non-glycosylated adipsin (e). Data were normalized to the loading control (GAPDH). The data are plotted as means ± SEM for n=4/treatment. Statistical analysis was performed using one-way ANOVA and Tukey's test. Significant differences ($P<0.05$) relative to Null are indicated by #.

(a)

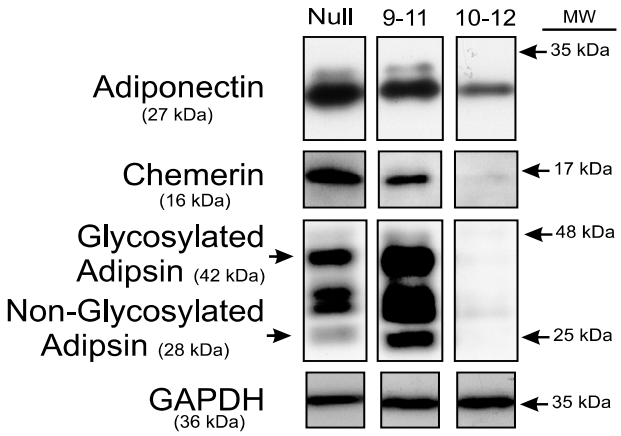
Null
9-11
10-12
MW
35 kDa
Adiponectin
(27 kDa)
Chemerin
(16 kDa)
17 kDa
Glycosylated
Adipsin (42 kDa)
48 kDa
Non-Glycosylated
Adipsin (28 kDa)
25 kDa
GAPDH
(36 kDa)
35 kDa

(b)

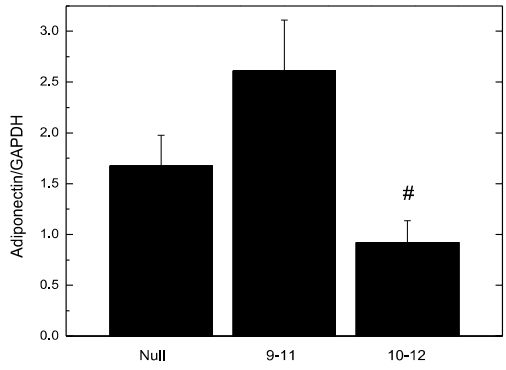
Adiponectin/GAPDH
3.0
2.5
2.0
1.5
1.0
0.5
0.0
#
Null
9-11
10-12

(c)

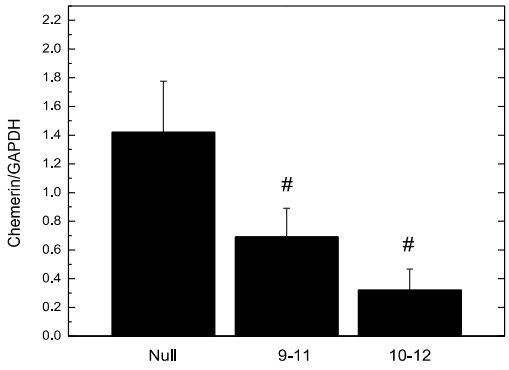
Chemerin/GAPDH
2.2
2.0
1.8
1.6
1.4
1.2
1.0
0.8
0.6
0.4
0.2
0.0
#
#
Null
9-11
10-12

(d)

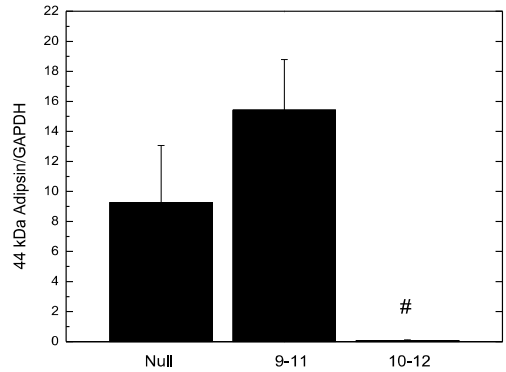
44 kDa Adipsin/GAPDH
22
20
18
16
14
12
10
8
6
4
2
0
#
Null
9-11
10-12

(e)

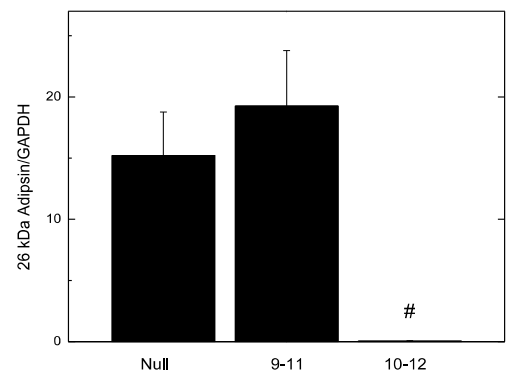
26 kDa Adipsin/GAPDH
20
10
0
#
Null
9-11
10-12

Figure 9. Stimulation of adipocyte differentiation by CLA isomers

(a) Photographs of 3T3-L1 cells were taken 8 days after addition of adipogenic cocktail without (Null) and with treatment of 60 μM *c*9-*t*11 CLA or 60 μM *t*10-*c*12 CLA beginning on day 0. Arrows indicate the location of lipid droplets. Images were captured using a 20× objective. Bar (Null panel) represents 5 μm and is applicable to all panels. The colour of the images reflects the colour of the culture medium; differences are due to differences in cell metabolism on the pH of the medium.

(b) The number of cells with lipid droplets was quantified and used to calculate the percentage of differentiated cells. The data are plotted as means ± SEM for n=3/treatment. Statistical analysis was performed using one-way ANOVA and Tukey's test. Significant differences ($P<0.05$) relative to control are indicated by #.

(a)

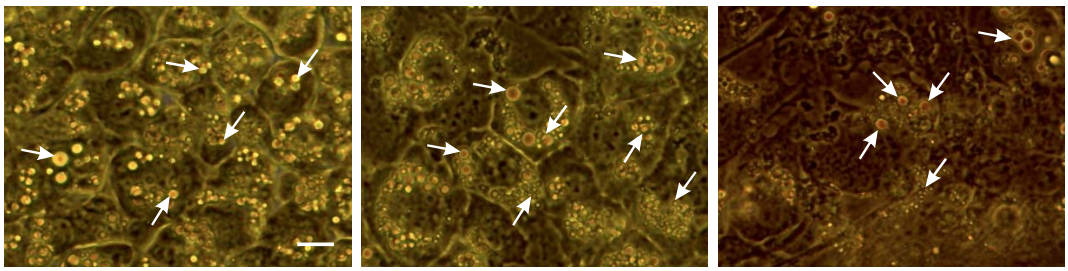
Null
9-11
10-12

(b)

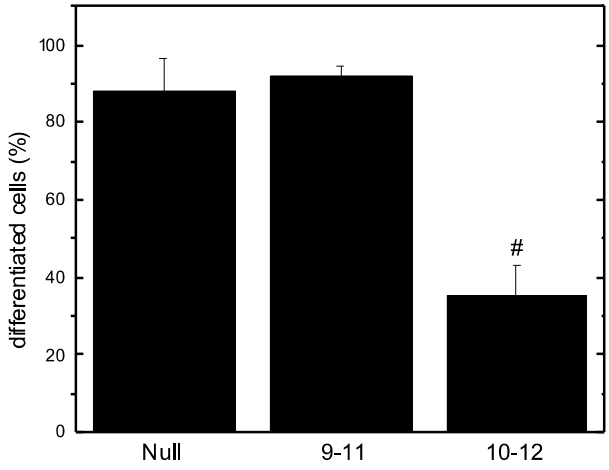
differentiated cells (%)
100
80
60
40
20
0
#
Null
9-11
10-12

6.6 *c*9-*t*11 CLA alters adipocyte cell size after 8 days of treatment

The size of CLA treated adipocytes was measured on day 8 of differentiation. Our data showed that *c*9-*t*11 CLA treatment results in a higher percentage of large cells in the 400-600 and 600-800 size range and fewer cells in the 200-400 size range relative to control untreated cells. In contrast, cells treated with *t*10-*c*12 CLA were typically smaller in area, with 83% of *t*10-*c*12 CLA cells in the 200-400 size range compared to 60% and 39% for the control and *c*9-*t*11 CLA treated cells, respectively (Figure 10). This finding is in agreement with other observations from our group performed *in vivo*, which showed that adipocyte cell size was reduced in *t*10-*c*12 CLA fed rats (DeClercq, Zahradka et al. 2010).

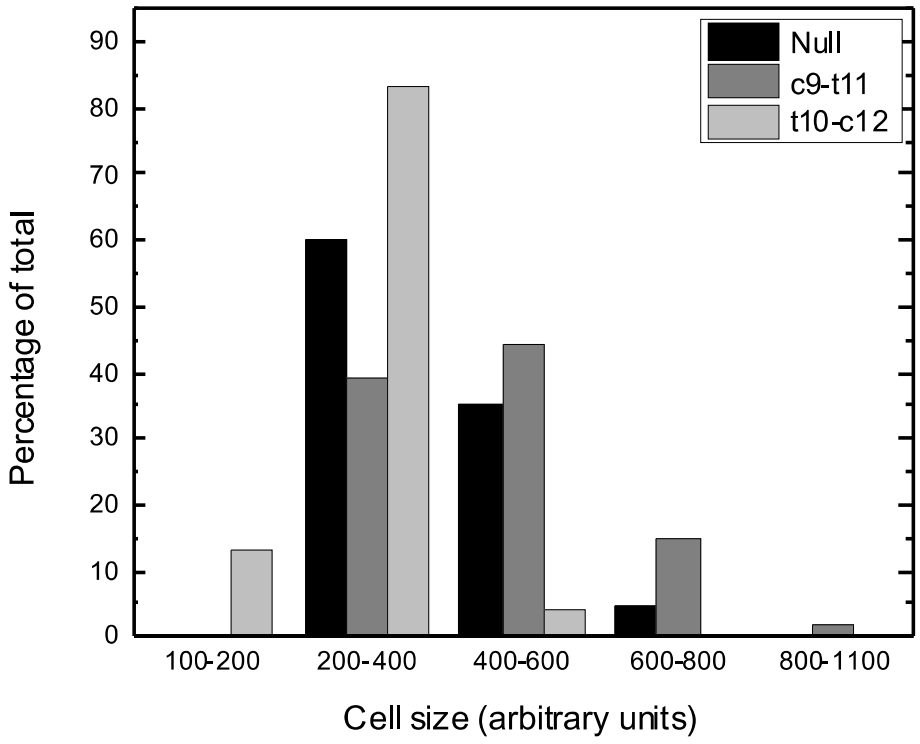

Figure 10. Effect of CLA isomers on 3T3-L1 cell size on day 8 of differentiation

Cell size distribution of 3T3-L1 adipocytes on day 8 after treatment without (Null) or with 60 μM c9-t11 CLA or t10-c12 CLA isomers beginning on day 0. The data were derived as described in Methods by analysis of at least 490 cells for each treatment; data are presented as means for n=4/treatment. Chi square testing revealed that there were significant differences among the treatments for all cell size ranges except the 800-1100 size range.

6.7 *t*10-*c*12 CLA activates PKCα

There is evidence that the anti-adipogenic effects of *t*10-*c*12 CLA may operate through PKA (Ashwell, Ceddia et al. 2010; Zhai, Liu et al. 2010). On the other hand, a role for members of the PKC family in the actions of CLA is also possible (Song, Sneddon et al. 2004; Shah, Mahmud et al. 2006). To investigate the contribution of PKC to the actions of CLA isomers on adipocytes, Bisindolylmaleimide I (BIS, general PKC inhibitor), PKCβ inhibitor (selective for PKCβI), LY333531 (PKCβI and βII inhibitor) and Gö6976 (PKCα inhibitor) were added to the cells in parallel with adipogenic induction (day 0), and concurrent with *c*9-*t*11 CLA and *t*10-*c*12 CLA. These agents were replenished along with the CLA isomers at the time of each media change. Cells were lysed on day 8, when the morphologic features of differentiation were established.

Western blotting showed that concurrent treatment with CLA isomers and either PKCβ inhibitor or LY333531 did not prevent the reduction of adiponectin levels by *t*10-*c*12 CLA treatment (data not shown). In contrast, Gö6976 treatment blocked the reduction of adiponectin levels by *t*10-*c*12 CLA (Figure 11a, b). Treating 3T3-L1 cells with BIS also diminished adipocyte differentiation as determined by the level of adiponectin (Figure 11a, b). Additionally, BIS and Gö6976 treatments blocked perilipin-1 phosphorylation (Figure 11a, c, e); however the levels of total perilipin-1 were increased by Gö6976, but they were not affected by BIS treatment relative to untreated control cells (Figure 11a, d). Since the same effect was observed with *t*10-*c*12 CLA treatment, it was considered plausible that *t*10-*c*12 CLA may act through PKCα.

To further test the possible role of PKCα in mediating the effect of *t*10-*c*12 CLA on adipocytes, we investigated PKCα localization in CLA treated cells. Subcellular

fractionation of 3T3-L1 adipocytes on day 8 of differentiation showed that PKCα was distributed between the cytosol and membrane fractions in the null and *c*9-*t*11 CLA treated cells (Figure 12). In contrast, no cytosolic PKCα was present with *t*10-*c*12 CLA treatment. Rather PKCα was solely localized to the membrane fraction. Since association with the membrane is indicative of PKC activation, this finding suggests treatment with *t*10-*c*12 CLA leads to activation of PKCα in 3T3-L1 adipocytes.

Figure 11. Effect of PKC inhibitors on production of adipocyte proteins.

(a) Western blot of 3T3-L1 cells lysed on day 8 of differentiation after treatment without (Null) or with 60 μM *c*9-*t*11 CLA or *t*10-*c*12 CLA beginning on day 0. BIS (10 μM; inhibits PKCα, βI, βII, γ, δ, ε) and Gö6976 (10 μM; inhibits PKCα) were added to the cells at the time of stimulation (day 0) and every 48 h with the media change, concurrent with *c*9-*t*11 CLA and *t*10-*c*12 CLA treatment. The blots were probed for total adiponectin, perilipin-1 and β-tubulin (loading control) and are representative of 3 independent experiments.

(b-e) Densitometry was used to quantify the intensities of the adiponectin and perilipin-1 bands shown in panel (a). Data were normalized to the loading control (β-tubulin) and un-phosphorylated perilipin-1 as indicated. The results are presented as means ± SEM for n=3/treatment. Statistical analysis was performed using two-way ANOVA and Tukey's test. Columns not sharing the same letter are significantly different ($P<0.05$).

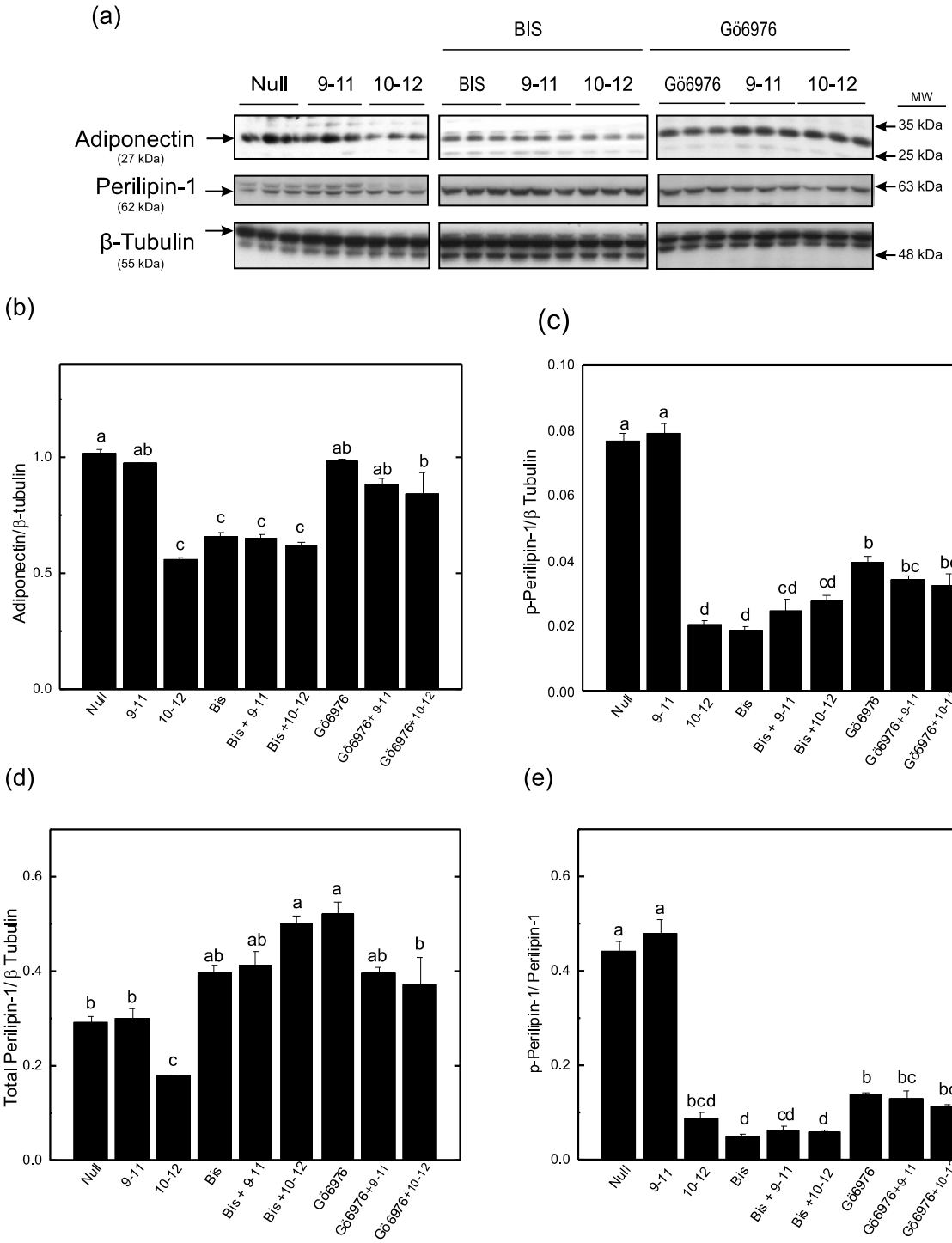
(a)
BIS
Gö6976
Null
9-11
10-12
BIS
9-11
10-12
Gö6976
9-11
10-12
MW
Adiponectin
(27 kDa)
Perilipin-1
(62 kDa)
β-Tubulin
(55 kDa)
35 kDa
25 kDa
63 kDa
48 kDa
(b)
Adiponectin/β-tubulin
(c)
p-Perilipin-1/β Tubulin
(d)
Total Perilipin-1/β Tubulin
(e)
p-Perilipin-1/ Perilipin-1
Null
9-11
10-12
Bis
Bis + 9-11
Bis +10-12
Gö6976
Gö6976+9-11
Gö6976+10-12

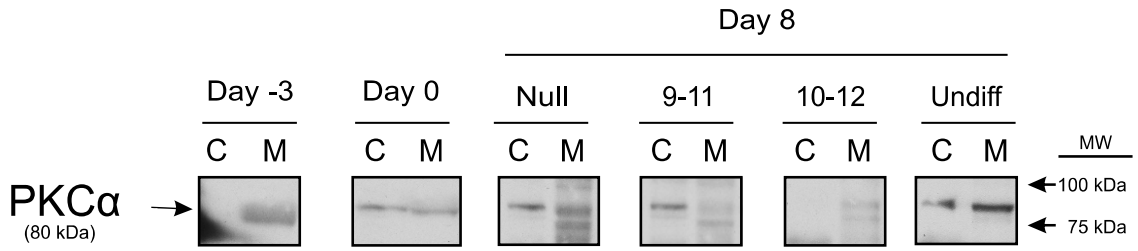

Figure 12. Effect of CLA isomers on PKCα localization on day 8 of differentiation

Subcellular fractionation of 3T3-L1 adipocytes was used to determine PKCα localization in response to CLA. Cells were treated without (Null) or with 60 μM *c*9-*t*11 CLA or *t*10-*c*12 CLA beginning at day 0 and membrane (M) and cytosol (C) fractions were prepared on day 8. Comparisons are provided to subconfluent (day -3) and confluent (day 0) cells before induction of differentiation cells and to cells maintained for 8 days without differentiation (Undiff). The samples were analyzed for PKCα by Western blotting. Undiff: undifferentiated cells. There is an artifact, which obscures part of the C lane in D-3.

6.8 Summary of CLA effects on adipogenesis and lipid droplets

To this point, the effects of CLA isomers on adipokines, lipid droplet proteins and TG hydrolysis in lipid droplets during adipogenesis were examined using 3T3-L1 adipocytes. We showed that *t*10-*c*12 CLA and *c*9-*t*11 CLA reduce the perilipin-1 levels early in adipocyte differentiation, while in mature adipocytes, only *t*10-*c*12 CLA reduces both perilipin-1 levels and its phosphorylation. In mature adipocytes, *t*10-*c*12 CLA reduces the levels of adipokines such as adiponectin and chemerin. We also showed that *t*10-*c*12 CLA decreases perilipin-1 membrane localization. Furthermore, *t*10-*c*12 CLA reduces HSL, possibly via PKCα, and decreases TG hydrolysis in mature adipocytes in parallel with a decrease in cell size.

Next we investigated the effect of CLA isomers on the Wnt/β-catenin pathway and its contribution to adipogenesis in 3T3-L1 adipocytes.

6.9 *t*10-*c*12 CLA increases β-catenin and its phosphorylation

To investigate the effects of CLA isomers on the Wnt/β-catenin signaling pathway, 3T3-L1 cells were treated with CLA isomers (60 μM) and lysed on day 2 (adipocytes at mitotic clonal expansion), day 4 (mid-differentiation) and day 8 (mature adipocytes) of differentiation.

Western blotting showed that *t*10-*c*12 CLA treatment increased β-catenin on days 2, 4 and 8 and its phosphorylated form (Ser 675) on day 8 compared to null (Figure 13a, c, d). In contrast, *c*9-*t*11 CLA decreased β-catenin and its phosphorylation at Ser 675 on day 8 compared to null. To investigate the effect of *t*10-*c*12 CLA on upstream signaling effectors of Wnt/β-catenin signaling, we looked at the levels of Wnt10b and SFRP-5. Our data showed no changes in Wnt10b levels following CLA isomer treatments when compared to null (Figure 13a); the same result was obtained with SFRP-3 (data not shown). We also measured cyclin D1 levels, since this protein is regulated by β-catenin. Surprisingly, despite an increase in the levels of β-catenin by *t*10-*c*12 CLA, the levels of cyclin D1 on day 8 were reduced by treatment with *t*10-*c*12 CLA (Figure 13a, e). Perilipin-1, a lipid droplet coating protein, and adiponectin, an adipokine secreted by adipocytes, were measured as characteristic markers of mature adipocytes. *t*10-*c*12 CLA treatment reduced total perilipin-1 on day 8, and adiponectin on days 4 and 8 (Figure 13a, f, g), indicating less adipocyte differentiation compared to both untreated and *c*9-*t*11 CLA treated cells. We also looked at LRP6 phosphorylation as a marker for active Wnt/β-catenin signaling. Our data showed no significant changes in LRP6 phosphorylation with CLA isomer treatments (Figure 13b).

Figure 13. Effect of CLA isomers on Wnt/β-catenin pathways and adipogenesis

(a) Western blot of 3T3-L1 cells lysed on days 2, 4 and 8 of differentiation after treatment without (Null) or with 60 μM *c*9-*t*11 CLA or *t*10-*c*12 CLA beginning on day 0. SDS PAGE was performed with a 10% gel. The blots were probed for total β-catenin, p-Ser 675-β-catenin, active β-catenin, Wnt10b, cyclin D1, total perilipin-1 and adiponectin, with β-tubulin as the loading control. Data are representative of 4 independent experiments.

(b) Western blot of 3T3-L1 cells lysed at days 2, 4 and 8 of differentiation after treatment without (Null) or with 60 μM *c*9-*t*11 CLA or *t*10-*c*12 CLA beginning on day 0. SDS PAGE was performed with a 5% gel. The blots were probed for p-Ser-1490-LRP6 and LRP6 with eEF2 as the loading control.

(c-g) Densitometry was used to quantify the intensity of the bands in panel (a) of total β-catenin (c), p-Ser 675-β-catenin (d), cyclin D1 (e), total perilpin-1 (f) and adiponectin (g) on days 2, 4 and 8. Data were normalized to the loading control (β-tubulin). The results are presented as means ± SEM for n=3/treatment. Statistical analysis was performed using one-way ANOVA and Tukey's test. Significant differences ($P<0.05$) relative to the respective Null control are indicated by *.

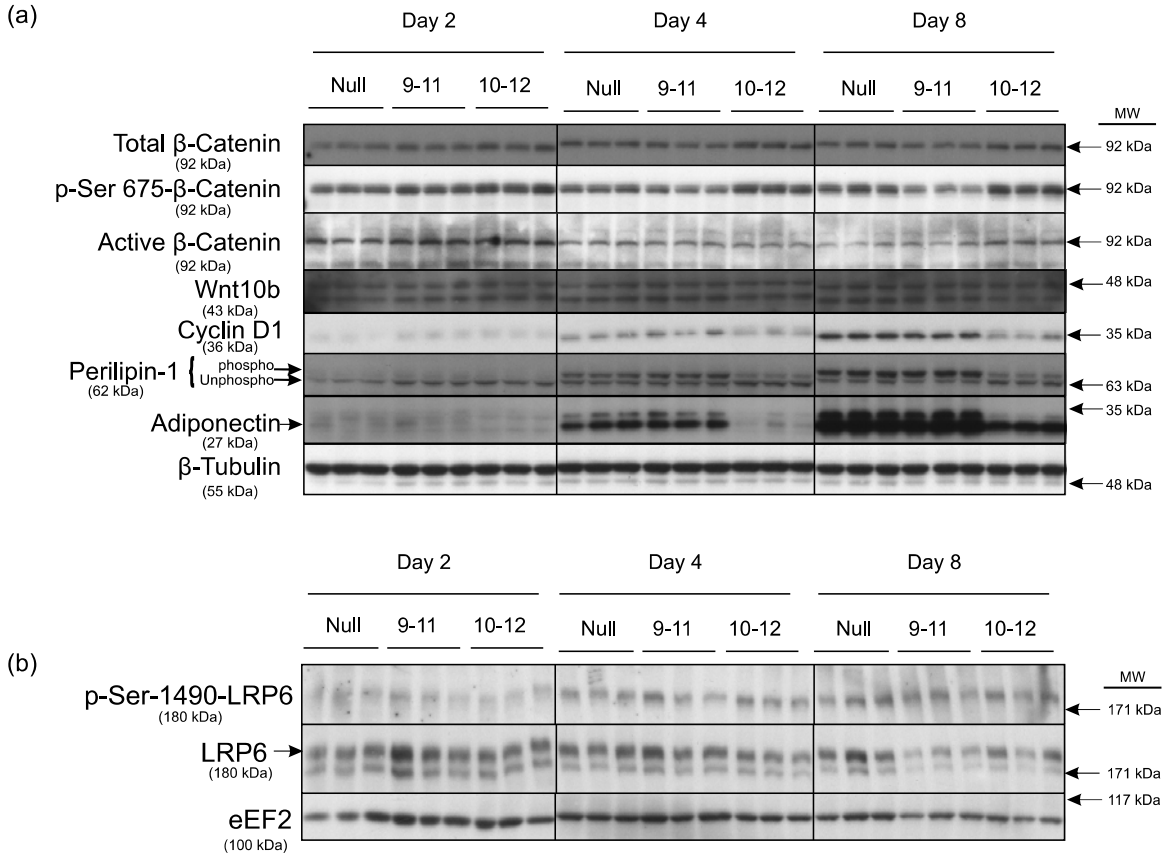
(a)
Day 2
Day 4
Day 8
Null
9-11
10-12
MW
Total β-Catenin
(92 kDa)
p-Ser 675-β-Catenin
(92 kDa)
Active β-Catenin
(92 kDa)
Wnt10b
(43 kDa)
Cyclin D1
(36 kDa)
Perilipin-1
(62 kDa)
phospho
Unphospho
Adiponectin
(27 kDa)
β-Tubulin
(55 kDa)
92 kDa
92 kDa
92 kDa
48 kDa
35 kDa
63 kDa
35 kDa
48 kDa
(b)
p-Ser-1490-LRP6
(180 kDa)
LRP6
(180 kDa)
eEF2
(100 kDa)
171 kDa
171 kDa
117 kDa

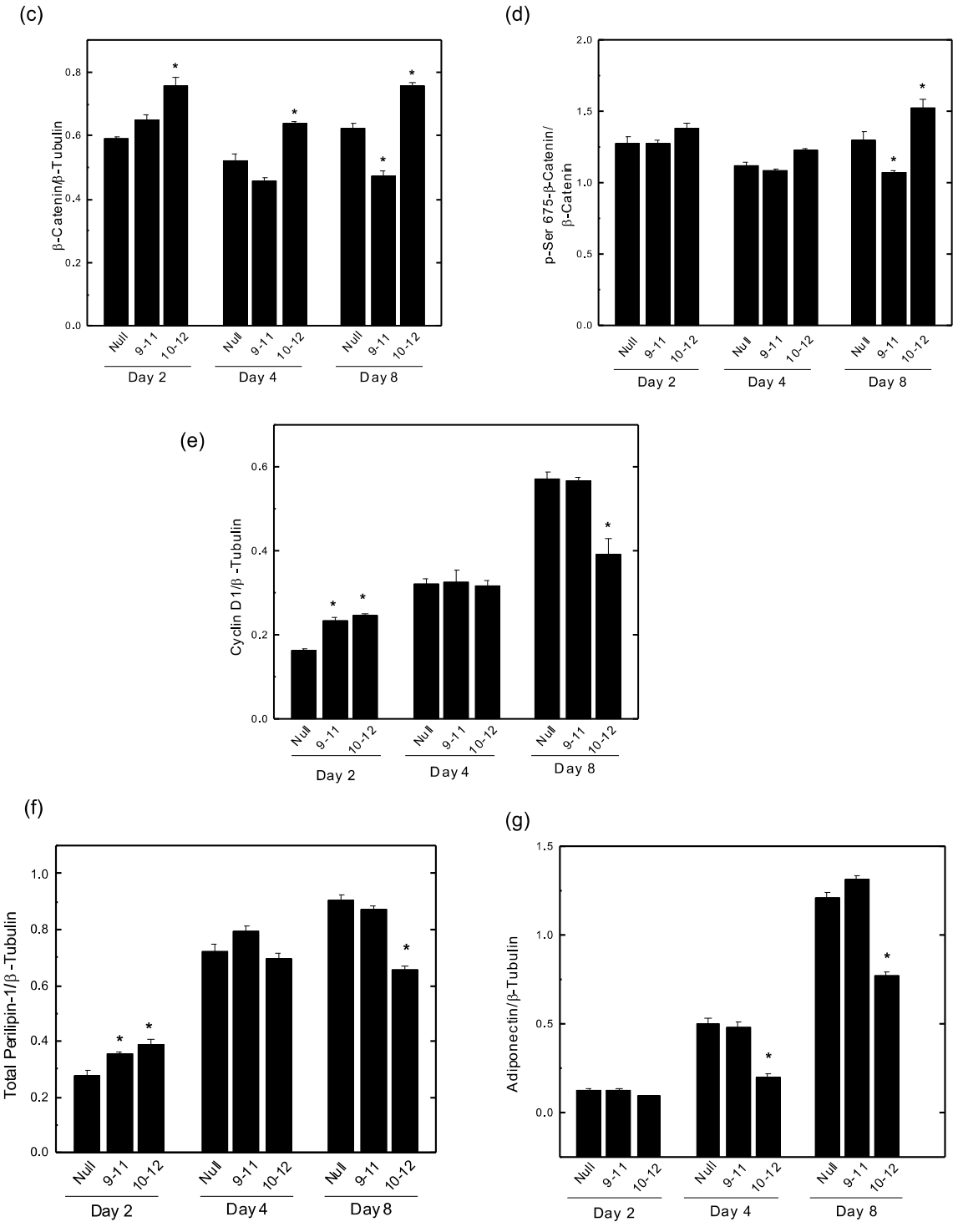
(c)
β-Catenin/β-Tubulin
0.0
0.2
0.4
0.6
0.8
Null
9-11
10-12
Day 2
Day 4
Day 8
(d)
p-Ser 675-β-Catenin/
β-Catenin
0.0
0.5
1.0
1.5
2.0
(e)
Cyclin D1/β -Tubulin
0.0
0.2
0.4
0.6
(f)
Total Perilipin-1/β -Tubulin
0.0
0.2
0.4
0.6
0.8
1.0
(g)
Adiponectin/β-Tubulin
0.0
0.5
1.0
1.5

6.10 *t*10-*c*12 CLA does not alter β-catenin localization in mature adipocytes

To investigate β-catenin localization in *c*9-*t*11 CLA and *t*10-*c*12 CLA treated 3T3-L1 adipocytes, immunofluorescence and subcellular fractionation were performed with an antibody that recognizes the active form of β-catenin, which is dephosphorylated on Ser-37 or Thr-41. Co-staining of total β-catenin (green), active β-catenin (red) and nuclei (blue) showed that CLA isomer treatment does not alter active β-catenin localization, as it was observed in the nucleus in both CLA treated and untreated mature adipocytes (Figure 14a).

To further investigate the effect of CLA isomers on the localization of β-catenin, subcellular fractionation of preadipocytes (day -3), confluent preadipocytes (day 0) and adipocytes treated without (Null) or with *c*9-*t*11 CLA and *t*10-*c*12 CLA for 8 days during differentiation was employed; cells that were not differentiated and maintained in 10% FBS for 8 days were considered undifferentiated controls. Subcellular fractionation showed that 3T3-L1 cells treated with *t*10-*c*12 CLA for 8 days had nearly no active β-catenin associated with the cytosolic fraction, and all of the protein was located in the membrane and nuclear fractions (Figure 14b). This pattern was also observed with undifferentiated 3T3-L1 cells. Unlike the *t*10-*c*12 CLA treated adipocytes, the null and *c*9-*t*11 CLA treated adipocytes had β-catenin in the cytosol, membrane and nuclear fractions. Interestingly, preadipocytes (day 3) and confluent adipocytes (day 0) showed very low levels of β-catenin in the membrane fraction (Figure 14b).

Figure 14. Effect of CLA isomers on total β-catenin and active β-catenin localization during adipogenesis

(a) Immunofluorescence staining was performed on fixed cells prepared on day 8 of differentiation without any treatment (Null) and after treatment with 60 μM *c*9-*t*11 CLA or *t*10-*c*12 CLA beginning on day 0. Total β-catenin is indicated by green, active β-catenin is indicated by red and nuclei are blue. Scale bar represents 20 μm.

(b) Subcellular fractionation was performed with 3T3-L1 adipocytes on day -3 (preadipocytes), day 0 (confluent preadipocytes) and day 8 (mature adipocytes) of differentiation after treatment without (Null) or with 60 μM *c*9-*t*11 CLA or *t*10-*c*12 CLA beginning on day 0. Comparisons to cells at day -3 and 0, before differentiation is triggered, and cells maintained for 8 days without differentiation (Undiff) are provided. C: Cytosolic fraction M: membrane fraction. N: Nuclear fraction. The blot was probed for active β-catenin.

(a)

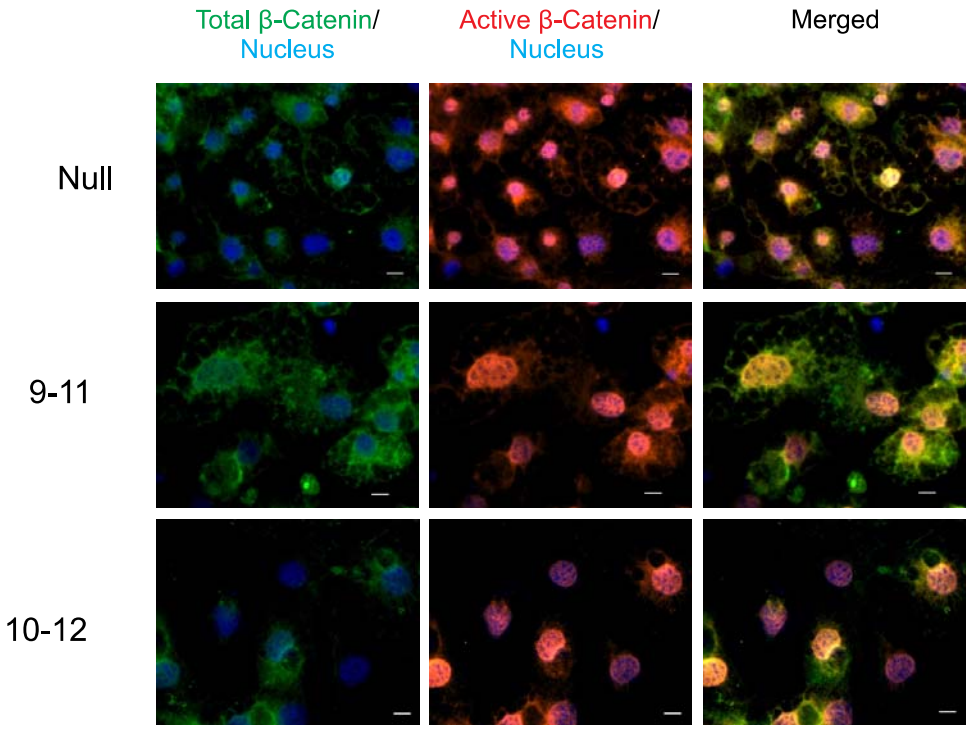
Total β-Catenin/
Nucleus
Active β-Catenin/
Nucleus
Merged
Null
9-11
10-12

(b)

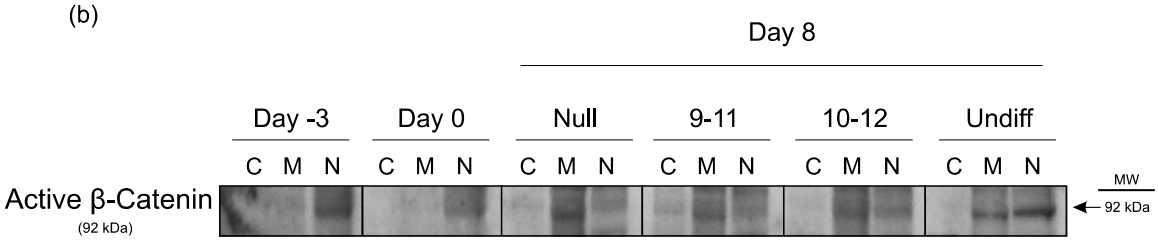
Day 8
Day -3
Day 0
Null
9-11
10-12
Undiff
C M N C M N C M N C M N C M N C M N
Active β-Catenin
(92 kDa)
MW
92 kDa

6.11 *t*10-*c*12 CLA increases β-catenin and PPARγ protein-protein interaction

One of the ways that β-catenin prevents adipocyte differentiation is by binding to PPARγ and inhibiting its activity. Thus, conditions where more β-catenin is complexed with PPARγ have less β-catenin available to bind to the TCF/LEF transcription factor and promote gene expression (Liu, Wang et al. 2006). Since our data showed no changes in β-catenin localization with CLA isomer treatment, we investigated the protein-protein interaction of β-catenin and PPARγ using immunoprecipitation. Treatment of 3T3-L1 cells for 8 days with *t*10-*c*12 CLA during differentiation increased the association of β-catenin and PPARγ when compared with *c*9-*t*11 CLA treated and untreated differentiated adipocytes (Figure 15). This finding likely explains the decrease in cyclin D1 levels with *t*10-*c*12 CLA treatment, since binding of β-catenin to PPARγ decreases the availability of β-catenin to activate the TCF/LEF transcription factor.

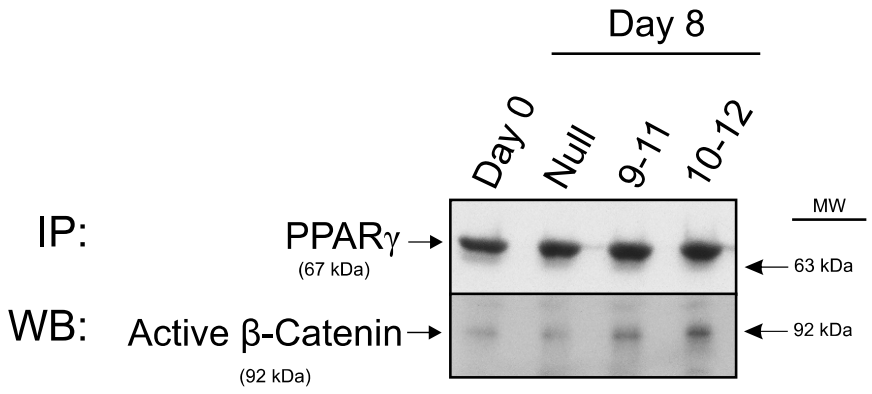

Figure 15. Effect of CLA isomers on β-catenin and PPARγ protein-protein interaction

Immunoprecipitation was performed with 3T3-L1 adipocytes on day 0 (confluent preadipocytes) and day 8 (mature adipocytes) after treatment without (Null) or with 60 μM *c*9-*t*11 CLA or *t*10-*c*12 CLA beginning on day 0. Anti-PPARγ antibody was used for precipitation and Western blotting was used to detect both PPARγ and active β-catenin. Data are representative of 3 independent experiments.

6.12 β-catenin is responsible for *t*10-*c*12 CLA action

To further investigate the ability of β-catenin to mediate the actions of *t*10-*c*12 CLA, JW67 (canonical Wnt pathway inhibitor) or CHIR99021 (GSK3-α and GSK3-β inhibitor) were added to the 3T3-L1 cells at the time that differentiation was induced and included during the entire differentiation period concurrent with CLA isomer treatments. Triggering β-catenin degradation with JW67 stimulated adipogenesis as indicated by an increase in the level of adiponectin (Figure 16a, b). In contrast, inhibition of GSK3-β with CHIR99021 had no effect on adiponectin levels (Figure 16a, b). However, when JW67 and CHIR99021 were applied concurrent with the CLA isomers, CHIR99021 blocked the ability of *t*10-*c*12 CLA to reduce adiponectin levels, while JW67 had no effect (Figure 16a, b).

Similarly, treatment with JW67 or CHIR99021 did not alter perilipin-1 levels, but concurrent treatment of CHIR99021 with *t*10-*c*12 blocked the decrease in perilipin-1 obtained with *t*10-*c*12 CLA, while JW67 had no effect (Figure 16a, c). Likewise, JW67 partially prevented the increase in active β-catenin induced by *t*10-*c*12 treatment alone, whereas the combination of CHIR99021 and *t*10-*c*12 further increased active β-catenin levels (Figure 16a, d). Although the levels of active β-catenin were higher after *t*10-*c*12 CLA treatment, there was no comparable increase in cyclin D1 levels; rather, levels of cyclin D1 were decreased with *t*10-*c*12 CLA treatment compared to untreated cells (Figure 16a, e). The effect of *t*10-*c*12 CLA treatment on cyclin D1 levels was not changed by treatment with either CHIR99021 or JW67 (Figure 16a, e).

Live cell microscopy of adipocytes 8 days after induction of adipogenesis was used to examine the effect of treatment with CLA isomers alone or in combination with

the CHIR99021 or JW67 inhibitors on differentiation. *t*10-*c*12 CLA treatment decreased the numbers of cells containing lipid droplets, indicating a marked decline in the formation of mature adipocytes (Figure 16f). Treatment with JW67 or CHIR99021 in combination with *t*10-*c*12 CLA increased the number of cells with lipid droplets. These results indicate that treatment with either JW67 or CHIR99021 can prevent *t*10-*c*12 CLA from inhibiting lipid droplet formation.

Figure 16. Effect of GSK3β and Wnt/β-catenin inhibitors on adipocyte proteins and Wnt/β-catenin pathway markers

(a) Western blot of 3T3-L1 cells lysed on day 8 of differentiation without (Null) or with 60 μM *c*9-*t*11 CLA or *t*10-*c*12 CLA treatment beginning on day 0. JW67 (20 μM; inhibits canonical Wnt pathway by inducing β-catenin degradation) and CHIR99021 (60 nM; GSK3-α inhibitor and GSK3-β) were added to the cells at the time of stimulation (day 0) and every 48 h with the media change, concurrent with the *c*9-*t*11 CLA and *t*10-*c*12 CLA treatments. The blots were probed for adiponectin, total perilipin-1, cyclin D1, active β-catenin and β-tubulin (loading control) and are representative of 3 independent experiments.

(b-e) Densitometry was used to quantify adiponectin (b), total perilipin-1 (c), active β-catenin (d) and cyclin D1 (e) band intensities shown in panel (a). Data were normalized to the loading control (β-tubulin) as indicated. The results are presented as means ± SEM for n=3/treatment. Statistical analysis was performed using two-way ANOVA and Tukey's test. Columns not sharing the same letter are significantly different ($P<0.05$).

(f) Photographs of 3T3-L1 cells were taken 8 days after addition of adipogenic cocktail without (Null) and with treatment of 60 μM *c*9-*t*11 CLA or 60 μM *t*10-*c*12 CLA and concurrent with JW67 or CHIR99021 beginning on day 0. Images were captured using a 20× objective. Bar (Null panel) represents 10 μm and is applicable to all panels. The null images are identical to those shown in figure 9a.

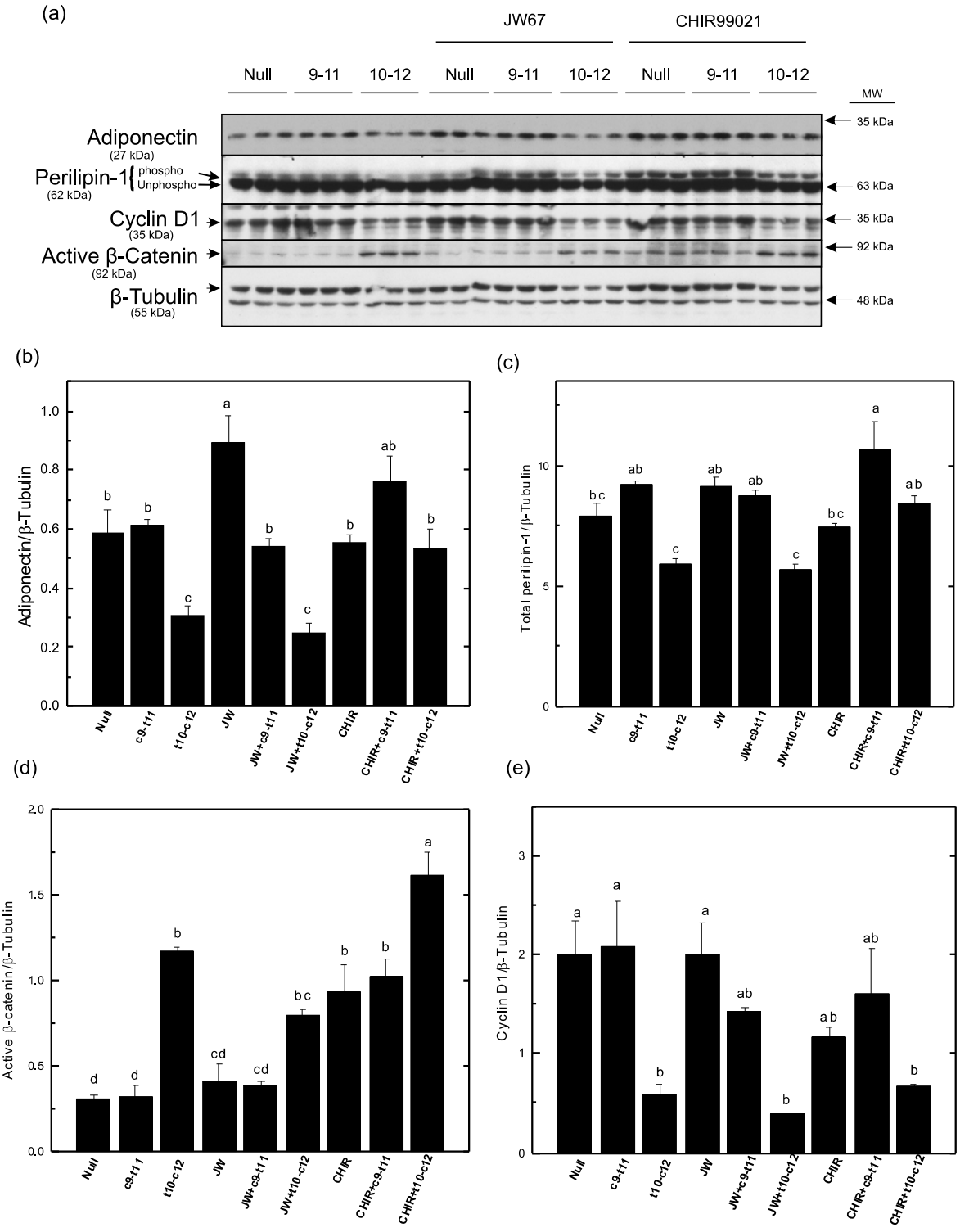
(a)
JW67
CHIR99021
Null
9-11
10-12
Null
9-11
10-12
Null
9-11
10-12
MW
Adiponectin
(27 kDa)
Perilipin-1
(62 kDa)
phospho
Unphospho
Cyclin D1
(35 kDa)
Active β-Catenin
(92 kDa)
β-Tubulin
(55 kDa)
35 kDa
63 kDa
35 kDa
92 kDa
48 kDa
(b)
Adiponectin/β-Tubulin
(c)
Total perilipin-1/β-Tubulin
(d)
Active β-catenin/β-Tubulin
(e)
Cyclin D1/β-Tubulin
Null
c9-t11
t10-c12
JW
JW+c9-t11
JW+t10-c12
CHIR
CHIR+c9-t11
CHIR+t10-c12

(f)

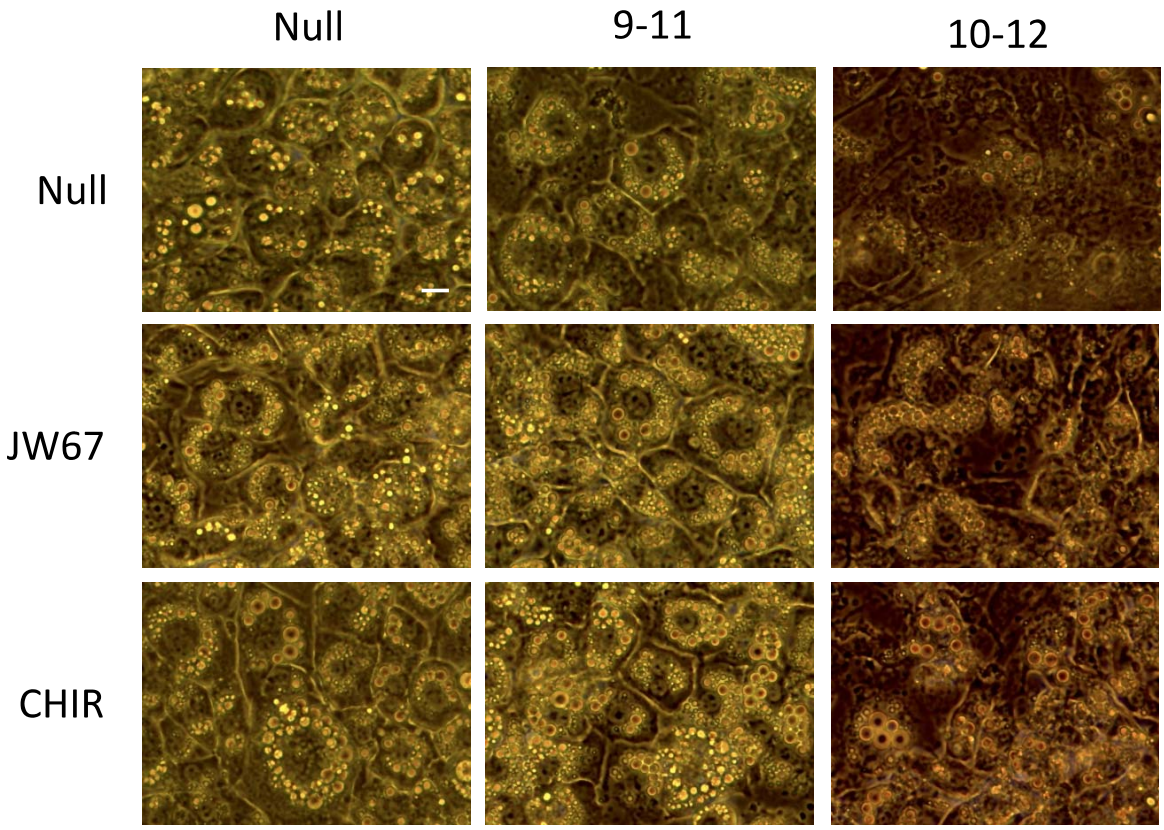

6.13 Summary of CLA isomers and Wnt/β-catenin pathway in 3T3-L1 adipocytes

We observed that *t*10-*c*12 CLA treatment leads to increased levels of β-catenin and its phosphorylation on Ser-675, which stabilizes cytosolic β-catenin. The increase in β-catenin levels was not due to increases in the Wnt/β-catenin agonist, Wnt10b, or other upstream effectors such as SFRP-5, and it did not elevate cyclin D1 levels. Subcellular fractionation suggested β-catenin was undetectable in the cytosol of *t*10-*c*12 CLA treated cells. IP showed that *t*10-*c*12 CLA increased the amount of β-catenin bound to PPARγ.

Our data suggest that reduction of adiponectin and perilipin-1 with *t*10-*c*12 CLA is not dependent upon β-catenin and is not regulated by GSK3-β. In addition the increase in active β-catenin levels and subsequent inhibition of adipogenesis is independent of GSK3-β activity and may indicate either a direct effect of *t*10-*c*12 CLA on β-catenin or the existence of an alternative pathway.

Next we investigated the effect of CLA isomers in wild type (C57BL/6) and leptin receptor deficient (*db/db*) mice in relation to Wnt/β-catenin signaling and adiposity.

6.14 *t*10-*c*12 CLA reduces body weight but not feed intake in *db/db* mice

The *db/db* mice had higher body weights (average 10 g) at 6-weeks of age (Day 0) when compared to C57BL/6 mice (Figure 17). During the first 7 days of feeding, animals grew similarly within their genotype. This rate of growth stayed constant in C57BL/6 mice up to 21 days of feeding, at which time the C57BL/6 CTL animals were 9% heavier than the C57BL/6 *t*10-*c*12 CLA, C57BL/6 *c*9-*t*11 CLA and C57BL/6 PW groups. In the *db/db* groups, animals fed *t*10-*c*12 CLA weighed less after 14 days and for the remainder of the study than the *db/db c*9-*t*11 CLA and *db/db* CTL groups. The body weight of the *db/db* CTL and *c*9-*t*11 groups increased by 24% from day 0 to day 28 while the body weight of the *db/db t*10-*c*12 group was decreased by 8% and the *db/db* PW maintained a body weight similar to baseline (Day 0). Although the *db/db* PW group was provided a restricted amount of diet to maintain a weight close to the *db/db t*10-*c*12 CLA group, the *db/db* PW group had a 18% higher body weight compared to the *db/db t*10-*c*12 CLA group at the end of the feeding period (Figure 17).

With respect to feed intake, after 7 days, the *db/db c*9-*t*11 CLA, *db/db* CTL and C57BL/6 PW groups had a higher average daily feed intake compared to the rest of the groups (Figure 18). Intentionally, the *db/db* PW group was fed less in order to maintain a body weight similar to *db/db t*10-*c*12 CLA. Interestingly, average daily feed intake by the *db/db t*10-*c*12 CLA group remained constant throughout the study, even though their body weight was less. During the third and fourth weeks, there was no difference in feed intake between the *db/db t*10-*c*12 CLA group and other groups, except the *db/db* PW group which consumed a lower amount of feed compared to all other groups.

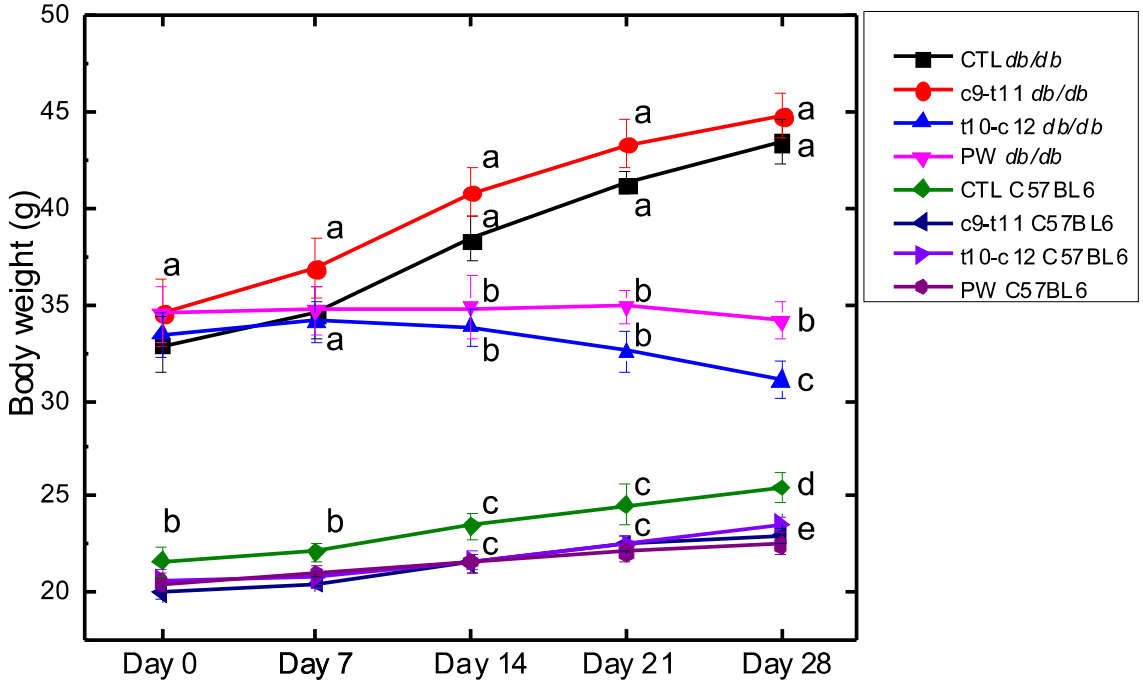

Figure 17. Effect of CLA isomers and feed restriction on weekly body weights

Body weights are presented as means ± SEM; n=10 for *t*10-*c*12 groups and n=8 for the other groups. Statistical analysis was performed using two-way repeated measures ANOVA and SAS software; least square means with Tukey-Kramer adjustment for multiple comparisons was used for means testing. There were significant main effects of time, time×genotype, time×diet and time×genotype×diet. At the same time point, statistical differences ($P \leq 0.05$) among means are indicated by different lower case letters.

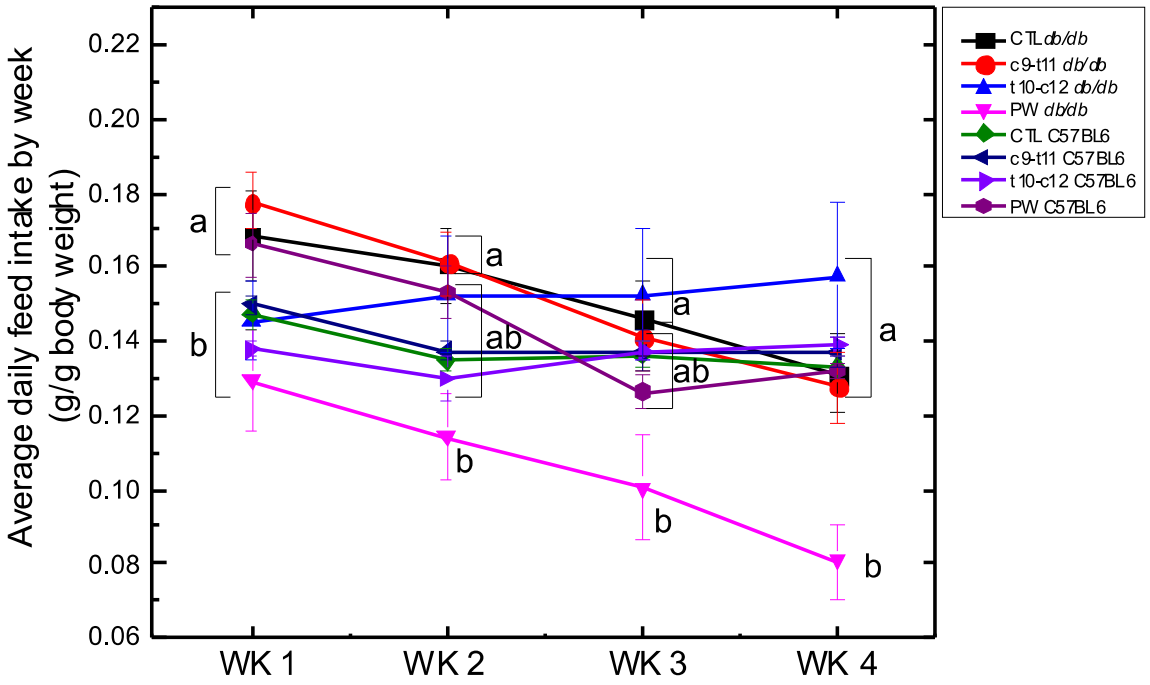

Figure 18. Effect of CLA isomers and feed restriction on average daily feed intake by week

Average daily feed intake is presented as means ± SEM; and for each week n=10 for *t*10-*c*12 groups and n=8 for the other groups. Statistical analysis was performed using two-way repeated measures ANOVA and SAS software; least square means with Tukey-Kramer adjustment for multiple comparisons was used for means testing. There were significant main effects of time, time×genotype, time×diet and time×genotype×diet. At the same time point, statistical differences ($P \leq 0.05$) among means are indicated by different lower case letters.

6.15 *t*10-*c*12 CLA reduces adiposity in both obese *db/db* and lean C57BL/6 mice

Visceral adipose depots, which include epididymal, peri-renal, mesenteric, and subcutaneous fat, which includes inguinal, were dissected and weighed at the time of termination. As expected, the *db/db* mice had higher visceral and subcutaneus adipose mass compared to C57BL/6 mice (Figure 19a). The *t*10-*c*12 CLA groups had smaller size visceral and subcutaneous adipose depots in both the *db/db* and C57BL/6 mice compared to the rest of the groups. The peri-renal adipose depots were smaller in the *db/db c*9-*t*11 CLA and *db/db* PW groups compared to the *db/db* CTL group, an effect that was not observed in the C57BL/6 mice. Epididymal and inguinal fat pads were not different among the *db/db c*9-*t*11 CLA, *db/db* PW and *db/db* CTL groups. There were no depot-specific differences among the C57BL/6 mice. The mesenteric adipose depots were equally distributed among the groups in *db/db* mice, while in C57BL/6 mice, the *t*10-*c*12 CLA group had lower mesenteric adipose mass than the CTL, *c*9-*t*11 CLA and PW groups.

In addition to WAT, the BAT and interscapular adipose depots were also dissected and weighed at termination. The *db/db* mice had higher BAT and interscapular adipose mass compared to C57BL/6 mice (Figure 19b). In both *db/db* and C57BL/6 mice, the *t*10-*c*12 CLA groups had lower BAT adipose mass compared to the PW group. In addition, the *db/db t*10-*c*12 CLA group had less interscapular adipose mass compared to the rest of the *db/db* mice. However, no significant differences were observed in the interscapular adipose among the C57BL/6 mice.

Figure 19. Effect of CLA isomers and feed restriction on visceral and subcutaneous WAT and BAT

The amounts of (a) visceral (mesenteric (Mes), peri-renal (Peri) and epididymal (Epi)) and (b) subcutaneous (inguinal) adipose depots, and (c) brown adipose tissue (BAT) and interscapular (Int-Scap) adipose depots are presented as means ± SEM; n=10 for *t*10-*c*12 groups and n=8 for all other groups. The adipose tissue weights are expressed relative to total body weight. Statistical analysis was performed using two-way ANOVA and SAS software; contrast statements for pre-planned comparisons were used for means testing. Statistical differences ($P \leq 0.05$) among means are indicated by different letters within each genotype or an * for diet effects across both genotypes. In (a) statistical differences ($P \leq 0.05$) among means for the visceral fat are indicated by different upper case letters within each genotype, and statistical differences ($P \leq 0.05$) among means for Mes, Peri and Epi are indicated by different lower case letters. There were no statistical differences for the mesenteric fat in the *db/db* groups, and for C57BL/6 mice, the changes in all 3 fat depots were identical as indicated by the single set of lower case letters.

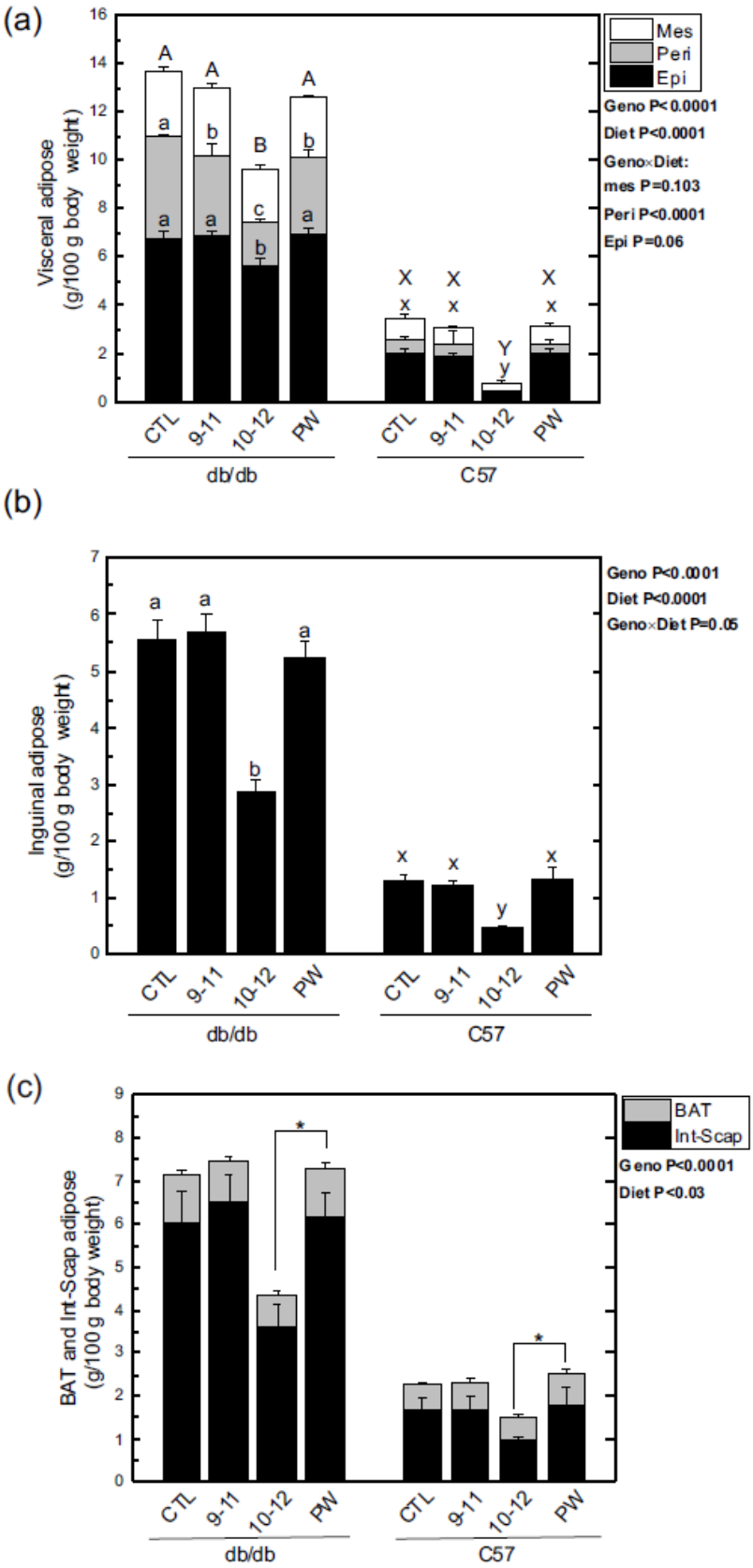
(a)
Visceral adipose (g/100 g body weight)
Mes
Peri
Epi
Geno P< 0.0001
Diet P<0.0001
Geno×Diet:
mes P=0.103
Peri P<0.0001
Epi P=0.06
CTL
9-11
10-12
PW
db/db
C57
(b)
Inguinal adipose (g/100 g body weight)
Geno P<0.0001
Diet P<0.0001
Geno×Diet P=0.05
(c)
BAT and Int-Scap adipose (g/100 g body weight)
BAT
Int-Scap
Geno P<0.0001
Diet P<0.03

6.16 *t*10-*c*12 CLA reduces adipose but not lean tissue mass in both obese *db/db* and lean C57BL/6 mice

To further investigate the effect of CLA isomers on adiposity and lean mass, body composition was examined by QMR *in vivo*. Our data confirmed that the *db/db* mice had higher fat mass compared to C57BL/6 mice (Figure 20a). The *t*10-*c*12 CLA diet reduced fat mass in *db/db* and C57BL/6 mice by 54% and 75%, respectively, compared to their respective CTL group. The *db/db* PW group also exhibited significant fat loss when compared to the *db/db c*9-*t*11 CLA and *db/db* CTL, however, fat loss was more pronounced in the *db/db t*10-*c*12 CLA group. The C57BL/6 PW and C57BL/6 CTL groups had similar fat mass.

Interestingly, despite the extreme reduction in body weight and fat mass in the *db/db t*10-*c*12 group, lean mass was unaffected, and the *db/db t*10-*c*12 CLA group had similar lean mass as the *db/db c*9-*t*11 CLA and *db/db* CTL groups (Figure 20a). The lean body mass was reduced in the *db/db* PW group, possibly due to the restriction in calorie intake. Similar to *db/db* mice, the C57BL/6 *t*10-*c*12 CLA mice had the same lean mass as the C57BL/6 CTL, while the C57BL/6 *c*9-*t*11 CLA and C57BL/6 PW groups had reductions in lean body mass compared to C57BL/6 CTL mice.

Body composition analysis revealed that there was a genotype difference in free water, as the *db/db* mice had a higher percentage of free water compared to C57BL/6 mice (Figure 20b). There were no significant diet differences among the *db/db* mice, however, a trend was observed for less free water in *db/db t*10-*c*12 CLA compared to the *db/db* CTL and the *db/db c*9-*t*11 CLA groups (P=0.076 and P=0.082, respectively). In

C57BL/6 mice, the *t*10-*c*12 CLA group had a lower amount of free water compared to the *c*9-*t*11 CLA group.

The QMR also measured the amount of total water in the body. Among the *db/db* mice, the PW group had the lowest amount of total water followed by the *t*10-*c*12 CLA group (Figure 20c). The amount of total water in these groups was significantly different from each other and from the *db/db* CTL and *c*9-*t*11 CLA groups. In contrast, the C57BL/6 CTL and *t*10-*c*12 CLA groups had a higher total water than the C57BL/6 *c*9-*t*11 CLA and PW groups.

Figure 20. Effect of CLA isomers and feed restriction on *in vivo* body composition at 4 weeks

Body composition ((a) fat mass, lean mass, (b) free water and (c) total water) was measured with an EchoMRI-700™ whole body Quantitative Magnetic Resonance (QMR) instrument. Data are presented as means ± SEM; n=12 for C57BL/6 *t*10-*c*12 CLA, n=11 for *db/db t*10-*c*12 CLA, n=7 for *db/db* PW and n=8 for all other groups. Statistical analysis was performed using two-way ANOVA and SAS software; contrast statements for pre-planned comparisons were used for means testing. Statistical differences ($P \leq 0.05$) among means are indicated by different lower case letters within each genotype. The ‡ in (b) indicates a trend (P=0.076 and P=0.082, respectively) for the *db/db* CTL and the *db/db c*9-*t*11 CLA versus the *db/db t*10-*c*12 group.

(a)

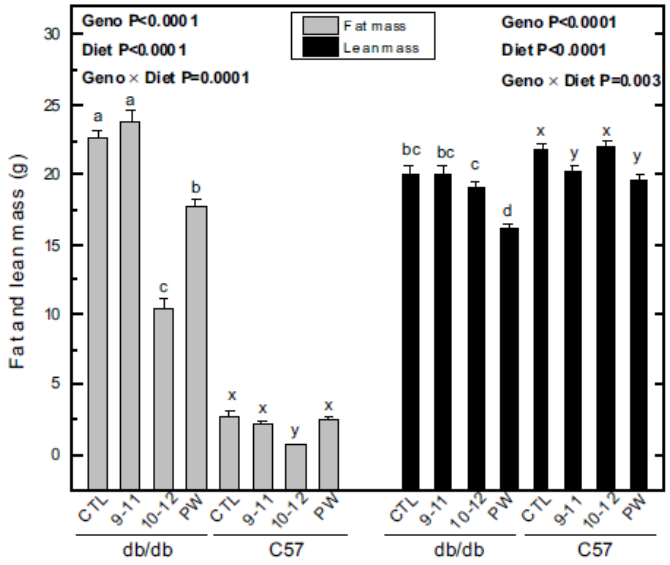
Geno P<0.0001
Diet P<0.0001
Geno × Diet P=0.0001
Fat mass
Lean mass
Geno P<0.0001
Diet P<0.0001
Geno × Diet P=0.003
Fat and lean mass (g)
CTL
9-11
10-12
PW
db/db
C57

(b)

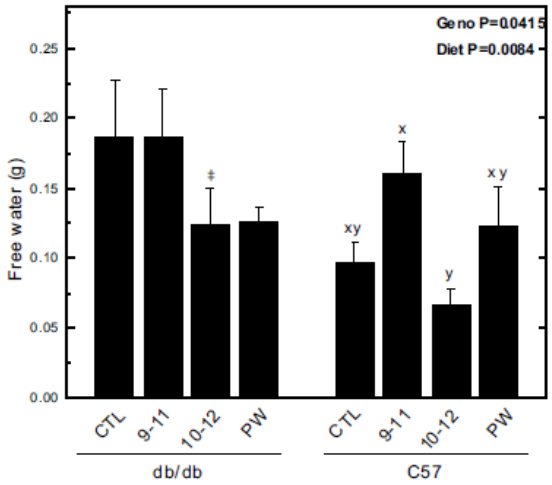
Geno P=0.0415
Diet P=0.0084
Free water (g)
CTL
9-11
10-12
PW
db/db
C57

(c)

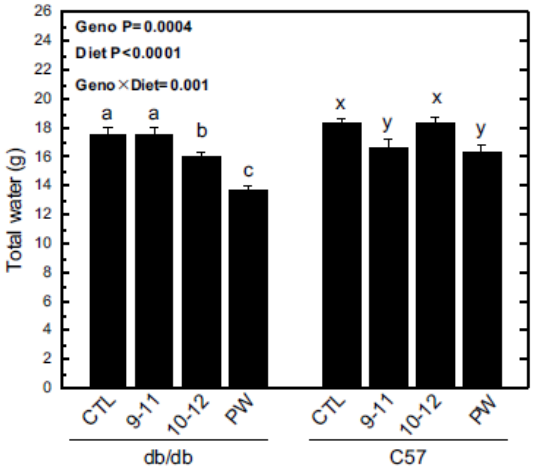
Geno P=0.0004
Diet P<0.0001
Geno×Diet=0.001
Total water (g)
CTL
9-11
10-12
PW
db/db
C57

6.17 *t*10-*c*12 CLA increases fasting blood glucose levels in both obese *db/db* and lean C57BL/6 mice

To investigate the effect of CLA isomers on diabetes and blood glucose levels, fasting blood glucose was measured at baseline (week 0) and end (week 4) of study. Blood glucose levels were higher in *db/db* mice at baseline compared to the C57BL/6 lean mice (genotype means: 19.2 ± 2.9 and 9.0 ± 0.8, respectively). At the end of 4 weeks of feeding, the *db/db* mice still had 2-fold higher fasting blood glucose compared to lean C57BL/6 mice (Figure 21a). The *t*10-*c*12 CLA group in both *db/db* and C57BL/6 mice had higher blood glucose compared to the CTL and PW groups. There were no differences between the *t*10-*c*12 CLA and *c*9-*t*11 CLA groups. Calorie restriction in the PW groups did not decrease fasting blood glucose compared to their respective genotype CTL groups.

Adipsin is an adipokine that is associated with blood glucose (Lo, Ljubicic et al. 2014). Thus, we measured the glycosylated and non-glycosylated forms of adipsin in epididymal adipose tissue of obese *db/db* and lean C57BL/6 mice. Levels of glycosylated and non-glycosylated adipsin were significantly lower in *db/db* mice compared to lean C57BL/6 mice (Figure 21b, c, d). The *db/db t*10-*c*12 CLA mice had elevated non-glycosylated adipsin (relative to the MAPK (ERK1/2) loading control) compared to the CTL, *c*9-*t*11 CLA and PW groups, and reduced adipsin glycosylation (ratio of glycosylated to non-glycosylated adipsin) compared to *db/db* CTL mice (Figure 21b, c, d). In C57BL/6 mice, the *t*10-*c*12 CLA diet increased non-glycosylated adipsin and reduced adipsin glycosylation compared to both CTL and PW groups. However, the *c*9-*t*11 CLA group also had increased non-glycosylated adipsin compared to CTL and PW

C57BL/6 groups when adjusted to the loading control, but adipsin glycosylation was similar to the C57BL/6 CTL mice (Figure 21b, c, d).

Figure 21. Effect of CLA isomers and feed restriction on fasting blood glucose and adipsin levels

(a) Fasting blood glucose was measured at the end of study (week 4) using a glucometer to determine glucose concentrations in a tail prick blood droplet. Data are presented as means ± SEM; n=12 for C57BL/6 *t*10-*c*12 CLA, n=11 for *db/db t*10-*c*12 CLA, n=7 for *db/db* PW and n=8 for all other groups. Statistical differences ($P \leq 0.05$) among means are indicated by an * for diet effects across both genotypes.

(b) Glycosylated and non-glycosylated adipsin were measured in epididymal adipose tissue by Western blotting. Representative bands are shown. Individual bands were arranged to present the data in the same order as the figures. The blot was overexposed to visualize the glycosylated adipsin in the *db/db* mouse samples. The bands shown are from the same blot and exposure.

(c-d) Densitometry was used to quantify the adipsin band intensities shown in panel (b). Data were normalized to the loading control (MAPK) or non-glycosylated adipsin. Data are presented as means ± SEM; n=9 for *db/db t*10-*c*12, n=8 for *db/db* CTL and *db/db c*9-*t*11, n=7 for *db/db* PW, n=6 for C57BL/6 *t*10-*c*12, and n=4 for C57BL/6 CTL, C57BL/6 *c*9-*t*11 and C57BL/6 PW groups. Statistical analysis was performed using two-way ANOVA and SAS software; contrast statements for pre-planned comparisons were used for means testing. Statistical differences ($P \leq 0.05$) among means are indicated by different lower case letters within a genotype. An absence of letters indicates no significant differences among individual means.

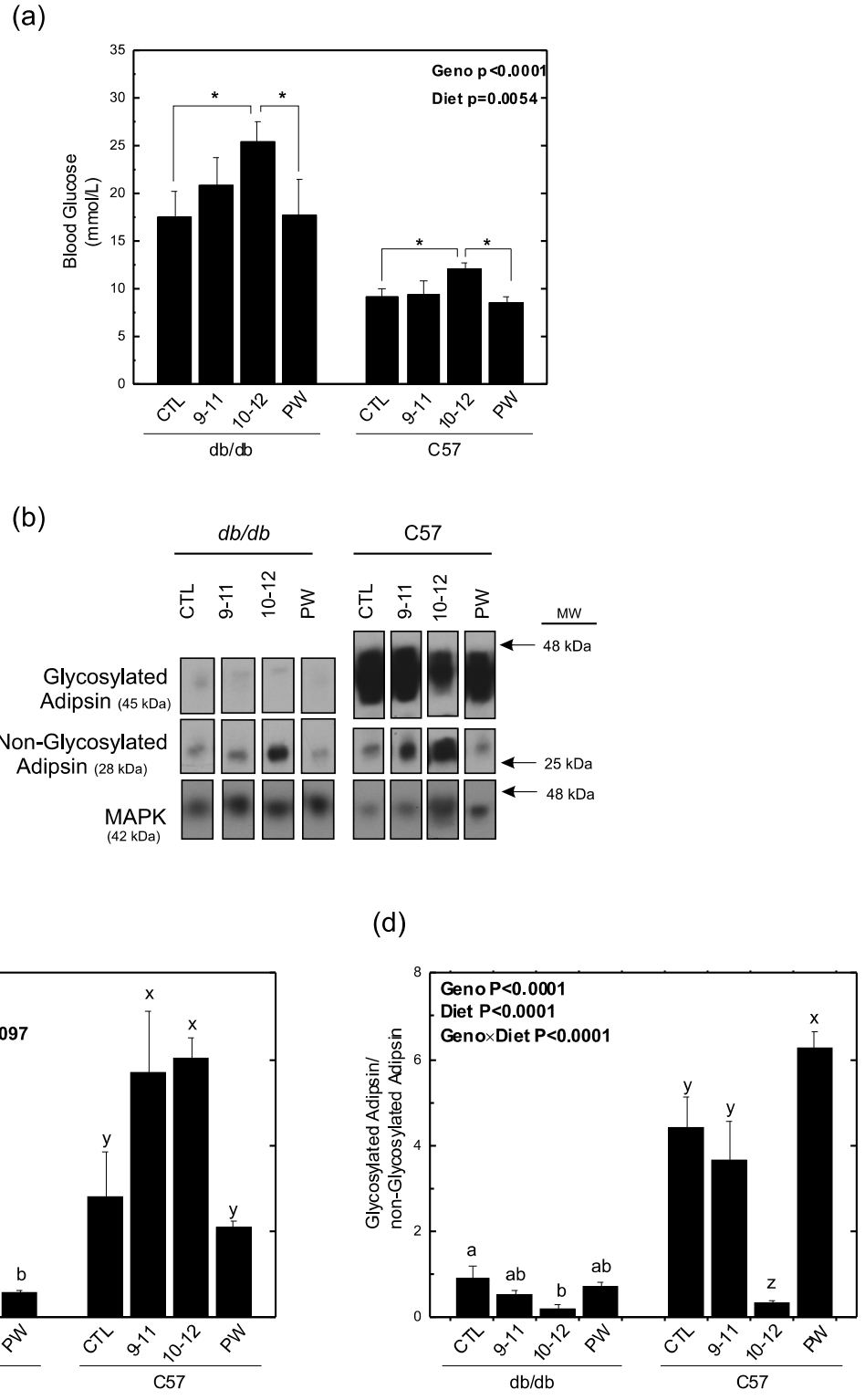
(a)
Geno p<0.0001
Diet p=0.0054
Blood Glucose (mmol/L)
CTL
9-11
10-12
PW
db/db
C57
(b)
db/db
C57
MW
48 kDa
Glycosylated Adipsin (45 kDa)
Non-Glycosylated Adipsin (28 kDa)
25 kDa
MAPK (42 kDa)
(c)
Geno P<0.0001
Diet P<0.0001
Geno×Diet P=0.0097
Non Glycosylated Adipsin/ MAPK
(d)
Geno P<0.0001
Diet P<0.0001
Geno×Diet P<0.0001
Glycosylated Adipsin/ non-Glycosylated Adipsin

6.18 *t*10-*c*12 CLA does not alter body temperature but increases browning in inguinal adipose tissue

One of the proposed mechanisms for reducing adiposity with *t*10-*c*12 CLA is through higher energy expenditure by increasing thermogenesis. To investigate the effect of CLA isomers on total body thermogenesis, body temperature was measured at baseline (week 0) and at the end (week 4) of the study. There were no significant differences in body temperature, either between the *db/db* and C57BL/6 mice at baseline (data not shown) or week 4 or among the dietary groups at week 4 (Figure 22).

Another way that CLA could influence thermogenesis at the cellular level is by an increase in beige adipocytes (browning of WAT). To investigate the possibility of higher metabolic rates through beige adipocytes, the levels of TBX-1, a marker of beige adipocytes, were measured in inguinal adipose tissue, a subcutaneous fat pad which is more susceptible to "browning" than visceral fat. Western blotting for TBX-1 showed no differences due to genotype as the *db/db* mice and C57BL/6 mice had similar levels of TBX-1 (genotype means: *db/db,* 1.38 ± 0.09; C57BL/6, 1.24 ± 0.13). Among the *db/db* mice, the CTL had lower levels of TBX-1 compared to the rest of the *db/db* groups. Among the C57BL/6 mice, the CTL had higher levels of TBX-1 compared to the *t*10-*c*12 CLA and the PW groups. Our data suggest that there is an association between diet and genotype for the beige cell marker, TBX-1, in WAT (Figure 23a, b).

The localization of TBX-1 in inguinal adipose tissue was studied using immunofluorescence. Immunofluorescence showed a strong TBX-1 localization in the nucleus of the inguinal adipose tissue of the *db/db t*10-*c*12 CLA and the *db/db* PW

groups, while the nuclear localization of TBX-1 was not observed in the CTL or *c*9-*t*11 CLA mice of both *db/db* and C57BL/6 genotypes or in the C57BL/6 PW group.

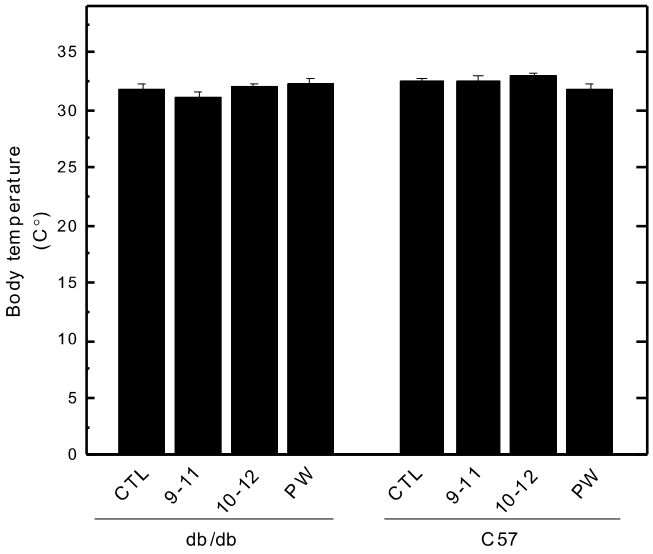

Figure 22. Effect of CLA isomers and feed restriction on body temperature.

Body temperature was measured at the end of the study (week 4) using a rectal thermometer. Data are presented as means ± SEM; n=10 for *t*10-*c*12 groups and n=8 for all other groups. There were no significant differences.

Figure 23. Effect of CLA isomers and feed restriction on beige adipocytes in inguinal adipose tissue of obese *db/db* mice and lean C57BL/6

(a) Western blotting used to measure the levels of TBX-1 in the inguinal adipose tissue of obese *db/db* mice and lean C57BL/6. MAPK was used as the loading control. Representative bands are shown in the panel. Individual bands were arranged to present the data in the same order as the figures. All bands were taken from the same blot and exposure without any other manipulation.

(b) Densitometry was used to quantify the intensity of the bands in panel (a). Data were normalized to the loading control (MAPK), which showed the same intensity pattern as seen after Ponceau S staining of the blot. Data are presented as means ± SEM; n=5 for the *db/db* CTL, *db/db c*9-*t*11, *db/db t*10-*c*12, *db/db* PW, C57BL/6 *c*9-*t*11 and C57BL/6 PW groups and n=4 for the C57BL/6 CTL and C57BL/6 *t*10-*c*12 groups. Statistical analysis was performed using two-way ANOVA and SAS software; contrast statements for pre-planned comparisons were used for means testing. Statistical differences among means ($P \leq 0.05$) are indicated by different lower case letters within each genotype.

(c) Immunofluorescence staining was performed on sections of inguinal adipose tissue of of *db/db* and C57BL/6 mice. TBX-1 is indicated by red and nuclei are in blue. White arrows show TBX-1 located in the nucleus. Scale bar (*db/db* CTL) represents 10 μm and is applicable to all panels.

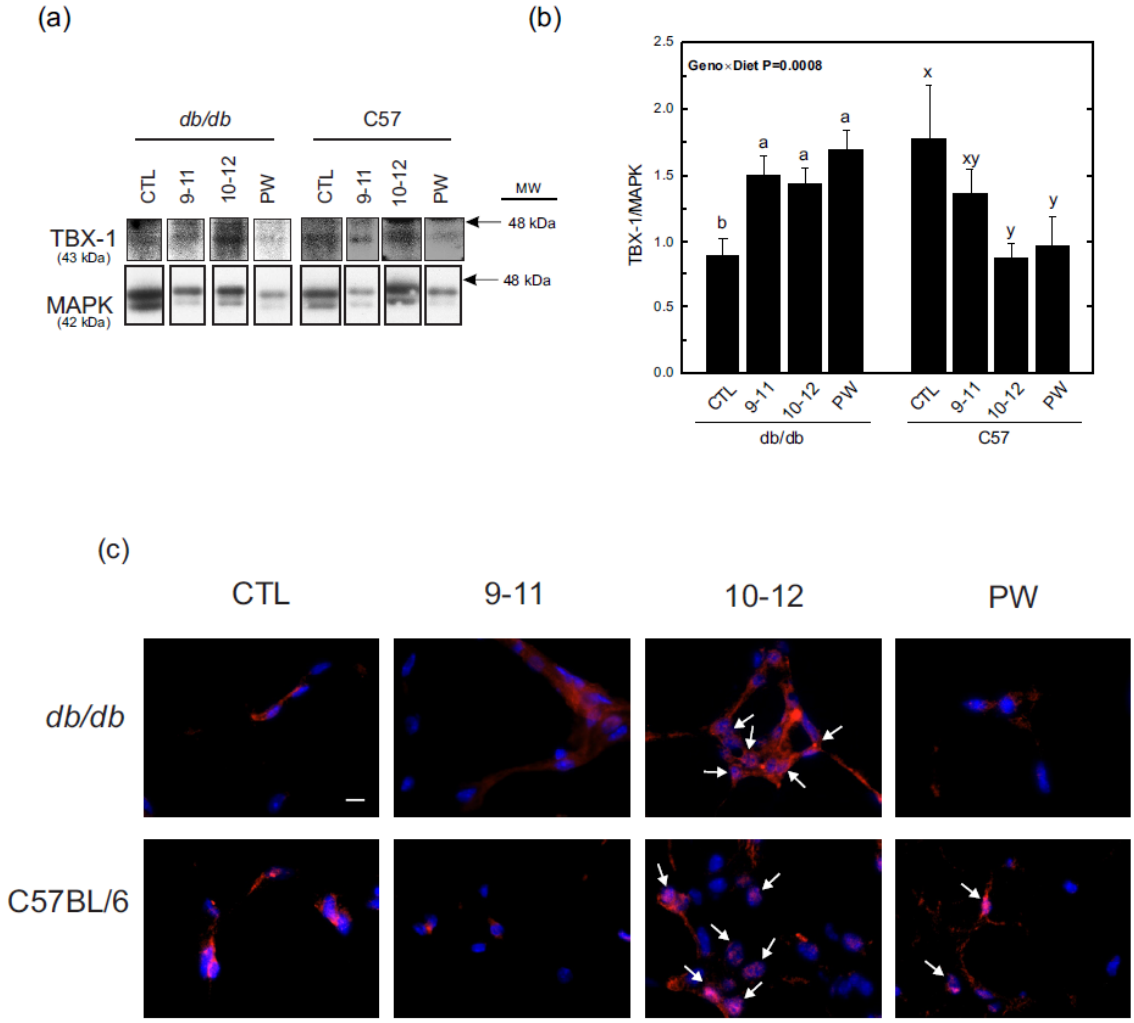
(a)
db/db
C57
CTL
9-11
10-12
PW
CTL
9-11
10-12
PW
MW
TBX-1
(43 kDa)
48 kDa
MAPK
(42 kDa)
48 kDa
(b)
Geno×Diet P=0.0008
TBX-1/MAPK
2.5
2.0
1.5
1.0
0.5
0.0
b
a
a
a
x
xy
y
y
CTL
9-11
10-12
PW
CTL
9-11
10-12
PW
db/db
C57
(c)
CTL
9-11
10-12
PW
db/db
C57BL/6

6.19 *t*10-*c*12 CLA reduces β-catenin activity in epididymal adipose tissue of obese *db/db* mice and lean C57BL/6 mice

We showed that *t*10-*c*12 CLA increases β-catenin levels and its phosphorylation at Ser 675 in 3T3-L1 adipocytes, resulting in activation of β-catenin. Here we investigated the effects of CLA isomers on β-catenin in epididymal adipose tissue of obese *db/db* mice and lean C57BL/6 mice. Western blotting showed that the *db/db* mice had lower total β-catenin levels compared to the C57BL/6 mice and the levels of β-catenin were higher in the *db/db* *t*10-*c*12 CLA and *db/db* PW groups compared to the *db/db* CTL group (Figure 24a, b). In C57BL/6 mice, the *c*9-*t*11 CLA group had increased levels of β-catenin compared to the *t*10-*c*12 CLA and CTL groups (Figure 24a, b). The levels of β-catenin phosphorylation (Ser 675) were decreased in both *db/db* and C57BL/6 mice fed *t*10-*c*12 CLA compared to the CTL and PW groups (Figure 24a, c). The c9-*t*11 CLA fed C57BL/6 mice also had reduced β-catenin phosphorylation (Ser 675) compared to the C57BL/6 CTL and C57PW groups. The levels of Wnt10b were not changed in either *db/db* or C57BL/6 mice and it was not affected by the CLA isomers or feed restriction (Figure 24a).

The levels of cyclin D1, a representative Wnt/β-catenin downstream target, were also measured. The *db/db* mice had lower cyclin D1 levels compared to C57BL/6 mice (Figure 24a, d). Among the *db/db* mice, the *t*10-*c*12 CLA group had significantly higher levels of cyclin D1 compared to the rest of the groups, while in the C57BL/6 mice the *c*9-*t*11 CLA group showed a robust increase in cyclin D1 levels compared to the other groups (Figure 24a, e). Also, there was a trend (P=0.06) for lower cyclin D1 levels in C57BL/6 PW compared to the C57BL/6 *t*10-*c*12 CLA group.

Figure 24. Effect of CLA isomers and feed restriction on β-catenin and its phosphorylation in epididymal adipose tissue of *db/db* and C57BL/6 mice

(a) Western blotting was used to measure the levels of different proteins involved in Wnt/ β-catenin signalling, including total β-catenin, p-Ser 675-β-catenin, Wnt10b and cyclin D1 relative to MAPK (loading control) in the epididymal adipose tissue of obese *db/db* mice and lean C57BL/6. Representative bands are shown. Individual bands were arranged to present the data in the same order as the figures. All bands were taken from the same blot and exposure without any other manipulation.

(b-d) Densitometry was used to quantify the intensity of the bands in panel (a) of total β-catenin (b), p-Ser 675-β-catenin (c) and cyclin D1 (d). Data were normalized to the loading control (MAPK). Data are presented as means ± SEM; n=9 for *db/db t*10-*c*12, n=8 for *db/db* CTL and *db/db c*9-*t*11, n=7 for *db/db* PW, n=6 for C57BL/6 *t*10-*c*12, and n=4 for C57BL/6 CTL, C57BL/6 *c*9-*t*11 and C57BL/6 PW groups. Statistical analysis was performed using two-way ANOVA and SAS software; contrast statements for pre-planned comparisons were used for means testing. Statistical differences ($P \leq 0.05$) among means are indicated by different lower case letters. The ‡ indicates there was a trend ($P = 0.06$) for less cyclin D1 in C57BL/6 PW compared to the C57BL/6 *t*10-*c*12 group.

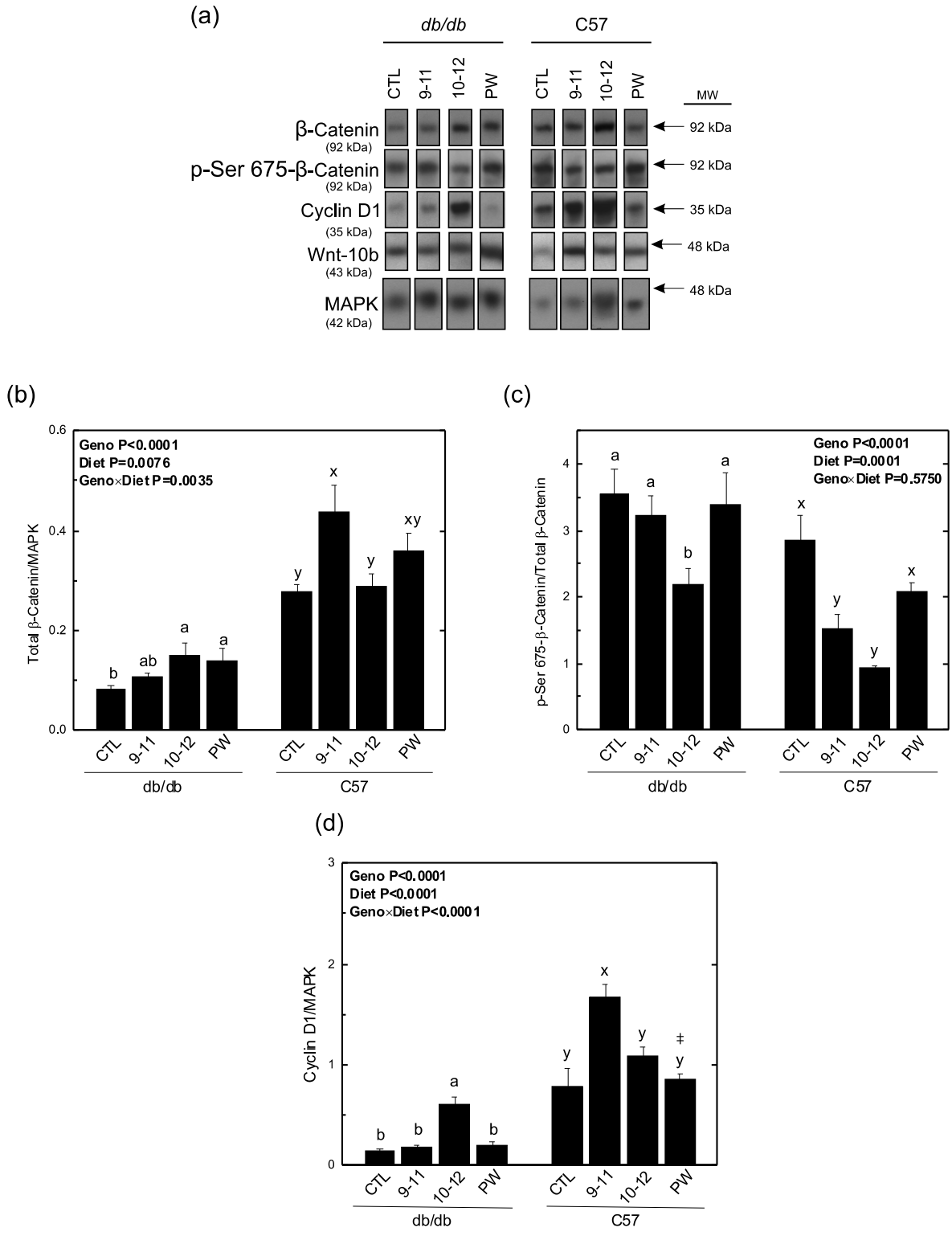
(a)
db/db
C57
CTL
9-11
10-12
PW
MW
β-Catenin
(92 kDa)
p-Ser 675-β-Catenin
(92 kDa)
Cyclin D1
(35 kDa)
Wnt-10b
(43 kDa)
MAPK
(42 kDa)
92 kDa
35 kDa
48 kDa
(b)
Geno P<0.0001
Diet P=0.0076
Geno×Diet P=0.0035
Total β-Catenin/MAPK
(c)
Geno P<0.0001
Diet P=0.0001
Geno×Diet P=0.5750
p-Ser 675-β-Catenin/Total β-Catenin
(d)
Geno P<0.0001
Diet P<0.0001
Geno×Diet P<0.0001
Cyclin D1/MAPK

6.20 *t*10-*c*12 does not alter differentiation of stem cells to preadipocytes but it alters adipocyte clearance

To investigate the role of CLA isomers on adipocyte turnover, the relative proportions of preadipocytes ($Sca1^{+}CD24^{-}$) and stem cells ($Sca1^{+}CD24^{+}$) in the SVF of epididymal adipose tissue of *db/db* and C57BL/6 mice were determined using flow cytometry. The flow cytometry data revealed that the *db/db* mice had a higher percentage of preadipocytes compared to the C57BL/6 mice. However, there were no differences among the treatment groups either in *db/db* or C57BL6 mice except for a reduction in the preadipocyte population of the *db/db* PW group compared to the other *db/db* groups (Figure 25a and Appendix A2). Our data also showed a genotype effect on the percentage of stem cells, as the *db/db* mice had higher levels of stem cells compared to the C57BL6 mice (genotype means: *db/db,* 6.7 ± 2.4%; C57BL/6, 5.2 ± 2.2%), with no differences among the dietary groups (Figure 25b and Appendix A1).

Flow cytometry also allowed us to investigate the preadipocytes ($Sca1^{-}CD24^{-}$) that had begun to differentiate but still had not become mature adipocytes. There was a genotype difference in this cell population as the *db/db* mice had a lower proportion of this cell population than the C57BL/6 mice (Figure 25c and Appendix A1). In addition, in the *db/db* mice, the *t*10-*c*12 CLA group had fewer immature adipocytes than the CTL group, and there was no significant difference between *t*10-*c*12 CLA and the *c*9-*t*11 CLA groups. Interestingly, the *db/db* PW group showed a 2.5-fold increase in the immature adipocyte population compared to the *db/db* CTL, *db/db c*9-*t*11 CLA and *db/db t*10-*c*12 CLA groups (Figure 25c and Appendix A2). No significant differences were observed in

C57BL/6 mice with respect to the immature adipocyte population and the dietary treatments.

To further investigate the effect of CLA isomers on adipocyte turnover, we measured markers of programmed cell death, apoptosis, and autophagy, in the epididymal adipose tissue of *db/db* and the C57BL/6 mice. Our data showed that there was a genotype effect, as the *db/db* mice had less caspase-3 compared to C57BL/6 mice (genotype means: *db/db*, 0.49 ± 0.03; C57BL/6, 0.57 ± 0.04) (Figure 26a, b). Western blotting also showed that the *db/db t*10-*c*12 CLA group had 2-fold higher levels of caspase-3 compared to the *db/db* CTL, *db/db c*9-*t*11 CLA and *db/db* PW groups The *db/db* PW group had lower caspase-3 levels compared to the rest of the groups. Among the C57BL/6 mice, the *t*10-*c*12 CLA group also had ~1.5-fold higher levels of caspase-3 when compared to other groups (Figure 26a, b). There was a trend (P=0.06) for lower caspase-3 levels in the C57BL/6 PW group compared to the C57BL/6 *c*9-*t*11 CLA group.

The ratio of cleaved caspase-3 to caspase-3 was calculated and our data showed that there was a genotype difference, as the *db/db* mice had 80% less activated caspase-3 compared to the C57BL/6 mice (Figure 26a, c). No significant differences in activation of caspase-3 (ratio of cleaved caspase-3 to caspase-3) were observed among the groups in the *db/db* mice, however, there was a trend (P=0.07) for less caspase-3 activation in *db/db t*10-*c*12 CLA mice compared to *db/db* PW mice. In the C57BL/6 mice, the *t*10-*c*12 CLA group had the lowest ratio of cleaved caspase-3 to caspase-3 compared to the rest of the groups. The *c*9-*t*11 CLA and the PW groups also had lower levels of cleaved caspase-3 to caspase-3 compared to the CTL group (Figure 26a, c).

LC3I levels and the LC3II/LC3I ratio were measured in epididymal adipose tissue samples from *db/db* and the C57BL/6 mice as indicators of autophagy. Our data showed a genotype difference as the *db/db* mice had less LC3I than C57BL/6 mice (Figure 27a, b). In the *db/db* mice, the *db/db* PW group had higher LC3I levels compared to *db/db* CTL group. No significant changes were detected between CLA isomer groups in *db/db* mice, while in C57BL/6 mice *t*10-*c*12 CLA reduced the levels of LC3I compared to the CTL, *c*9-*t*11 CLA and PW groups. However, when the ratio of LC3II/LC3I calculated, no significant effects of genotype and/or diet were observed (Figure 27a, c), indicating no changes in these autophagy-associated proteins occurred in response to the the dietary interventions.

Figure 25. Effect of CLA isomers and feed restriction on the stem cell and preadipocyte populations in the SVF of epididymal adipose tissue from *db/db* and C57BL/6 mice

The percentage of preadipocytes (a), stem cells (b) and immature adipocytes (c) in the SVF of epididymal adipose tissue was determined by flow cytometry. Data are presented as means ± SEM as a percentage of mesenchymal stem cells ($CD45^{-}CD31^{-}CD34^{+}CD29^{+}$); n=7 for *db/db t*10-*c*12, n=6 for *db/db* CTL, *db/db c*9-*t*11, C57BL/6 CTL and C57BL/6 *c*9-*t*11, n=5 for *db/db* and C57BL/6 PW, and n=4 for C57BL/6 *t*10-*c*12 groups. Statistical analysis was performed using two-way ANOVA and SAS software; contrast statements for pre-planned comparisons were used for means testing. Statistical differences ($P \leq 0.05$) among means are indicated by different lower case letters within a genotype. An absence of letters indicates no significant differences among individual means. Sc = Stem cells.

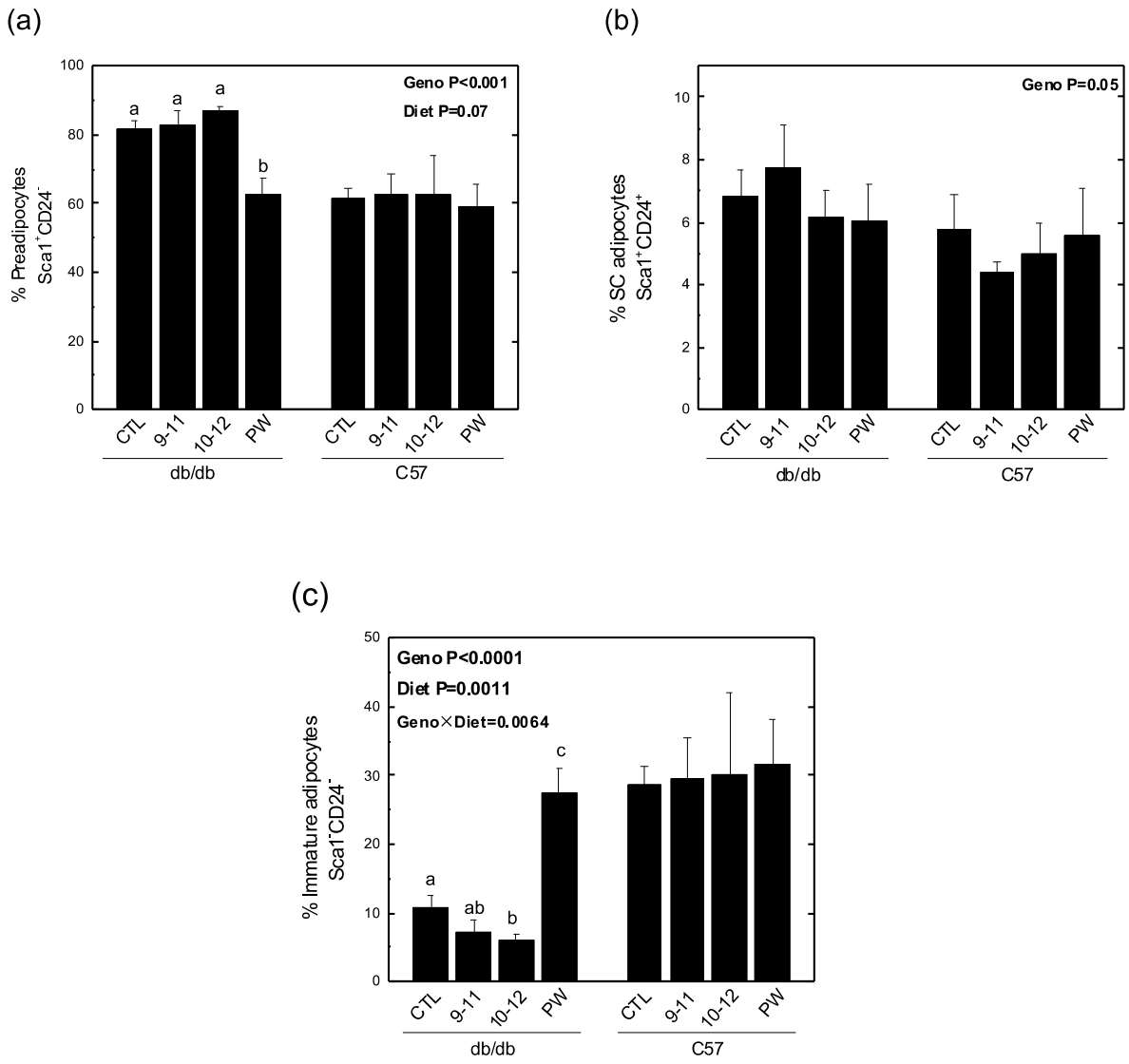
(a)
Geno P<0.001
Diet P=0.07
% Preadipocytes
Sca1+CD24-
a
a
a
b
CTL
9-11
10-12
PW
db/db
C57
(b)
Geno P=0.05
% SC adipocytes
Sca1+CD24+
(c)
Geno P<0.0001
Diet P=0.0011
Geno×Diet=0.0064
% Immature adipocytes
Sca1-CD24-
a
ab
b
c

Figure 26. Effect of CLA isomers and feed restriction on apoptosis in epididymal adipose tissue of obese *db/db* mice and lean C57BL/6 mice

(a) The levels of caspase-3 and cleaved caspase-3 were measured in the epididymal adipose tissue of the *db/db* and the C57BL/6 mice using Western blotting. MAPK was used as loading control. Individual bands were arranged to present the data as organized in the figures. All bands were taken from the same blot and exposure without any other manipulation.

(b-c) Densitometry was used to quantify the intensity of the bands in panel (a). Data were normalized to the loading control (MAPK) or caspase-3. The results are presented as means ± SEM; n=9 for *db/db t*10-*c*12, n=8 for *db/db* CTL and *db/db c*9-*t*11, n=7 for *db/db* PW, n=6 for C57BL/6 *t*10-*c*12, and n=4 for C57BL/6 CTL, C57BL/6 *c*9-*t*11 and C57BL/6 PW groups. Statistical analysis was performed using two-way ANOVA and SAS software; contrast statements for pre-planned comparisons were used for means testing. Statistical differences ($P \leq 0.05$) among means are indicated by different lower case letters. The ‡ indicates a trend ($P=0.06$) for lower caspase-3 levels in the C57BL/6 PW group compared to the C57BL/6 *c*9-*t*11 CLA group and a trend ($P=0.07$) for less activation of caspase-3 in *db/db t*10-*c*12 CLA compared to *db/db* PW mice.

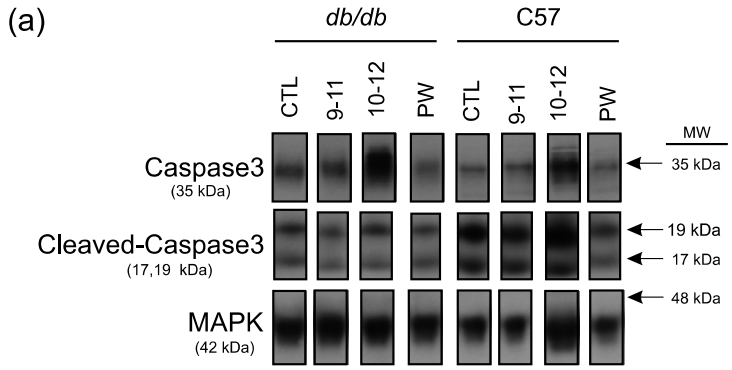
(a)
db/db
C57
CTL
9-11
10-12
PW
CTL
9-11
10-12
PW
MW
Caspase3
(35 kDa)
35 kDa
Cleaved-Caspase3
(17,19 kDa)
19 kDa
17 kDa
MAPK
(42 kDa)
48 kDa

(b)

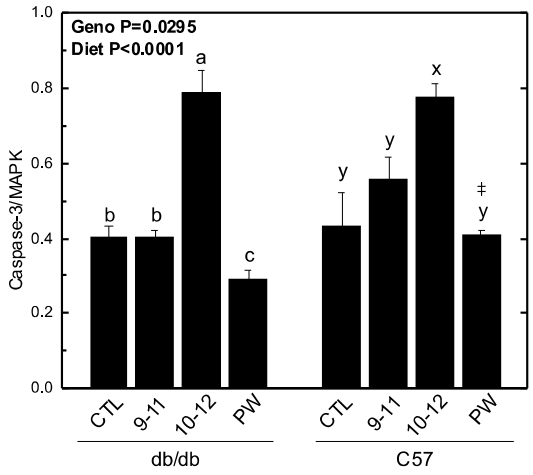
Geno P=0.0295
Diet P<0.0001
Caspase-3/MAPK
1.0
0.8
0.6
0.4
0.2
0.0
a
b
b
c
x
y
y
‡
y
CTL
9-11
10-12
PW
CTL
9-11
10-12
PW
db/db
C57

(c)

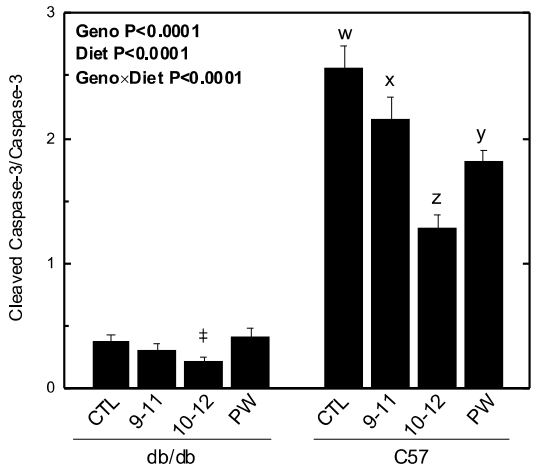
Geno P<0.0001
Diet P<0.0001
Geno×Diet P<0.0001
Cleaved Caspase-3/Caspase-3
3
2
1
0
w
x
z
y
‡
CTL
9-11
10-12
PW
CTL
9-11
10-12
PW
db/db
C57

Figure 27. Effect of CLA isomers and feed restriction on autophagy-associated proteins in epididymal adipose tissue of obese *db/db* mice and lean C57BL/6

(a) The relative levels of LC3I and LC3II in epididymal adipose tissue of *db/db* and C57BL/6 mice were obtained using Western blotting. MAPK was used as the loading control. Individual bands were arranged to present the data as organized in the figures. All bands were taken from the same blot and exposure without any other manipulation.

(b) Densitometry was used to quantify the intensity of the bands in panel (a). Data were normalized to the loading control (MAPK). The ratio of LC3II to LC3I was also calculated as an indication of autophagy. The results are presented as means ± SEM; n=9 for *db/db t*10-*c*12, n=8 for *db/db* CTL and *db/db c*9-*t*11, n=7 for *db/db* PW, n=6 for C57BL/6 *t*10-*c*12, and n=4 for C57BL/6 CTL, C57BL/6 *c*9-*t*11 and C57BL/6 PW groups. Statistical analysis was performed using two-way ANOVA and SAS software; contrast statements for pre-planned comparisons were used for means testing. Statistical differences ($P \leq 0.05$) among means are indicated by different lower case letters within a genotype. An absence of letter indicates no significant differences.

(a)

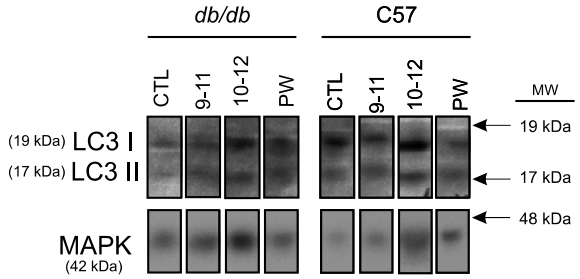
db/db
C57
CTL
9-11
10-12
PW
CTL
9-11
10-12
PW
MW
(19 kDa) LC3 I
(17 kDa) LC3 II
19 kDa
17 kDa
48 kDa
MAPK
(42 kDa)

(b)

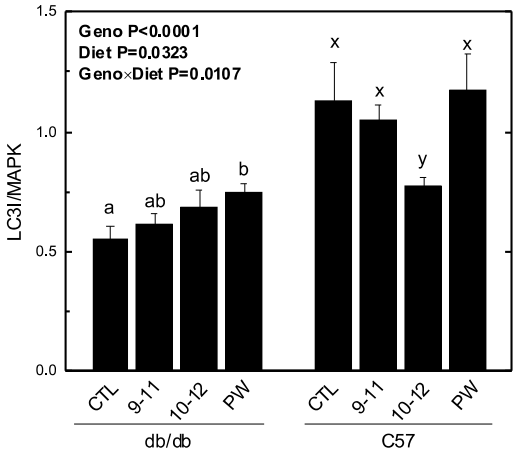
Geno P<0.0001
Diet P=0.0323
Geno×Diet P=0.0107
LC3I/MAPK
1.5
1.0
0.5
0.0
a
ab
ab
b
x
x
y
x
CTL
9-11
10-12
PW
CTL
9-11
10-12
PW
db/db
C57

(c)

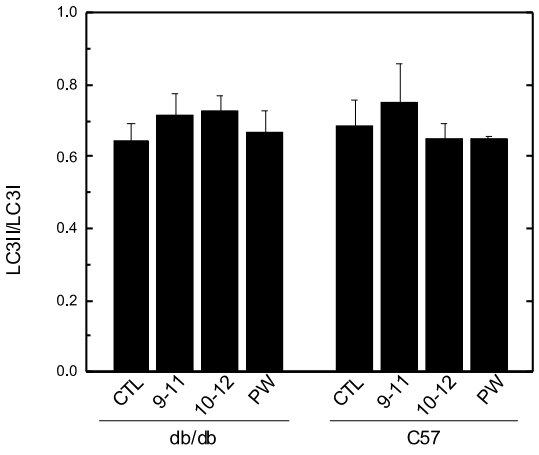
LC3II/LC3I
1.0
0.8
0.6
0.4
0.2
0.0
CTL
9-11
10-12
PW
CTL
9-11
10-12
PW
db/db
C57

6.21 CLA isomers do not alter macrophages but increase the total DC percentage in SVF from epididymal adipose tissue of lean C57BL/6

To investigate the effect of CLA isomers on different populations of immune cells, macrophages, T cells, DC and natural killer T cells (NKT) in the SVF of epididymal adipose tissue of *db/db* and C57BL/6 mice were measured using flow cytometry. Flow cytometry showed no genotype-specific effect on macrophage percentages (genotype means: *db/db*, 6.8 ± 0.7%; C57BL6, 4.9 ± 0.4%) (Figure 28a and Appendices A3, A4). However, among the *db/db* mice, the percentage of macrophages was 3-fold lower in the PW group compared to *db/db* CTL, *db/db c*9-*t*11 CLA and *db/db t*10-*c*12 CLA groups (Figure 28a and Appendix A4). No significant differences were observed among the groups of C57BL/6 mice.

A genotype difference was observed in the T cell population. The *db/db* mice had fewer T cells compared to C57BL/6 mice (genotype means: *db/db*, 3.4 ± 0.3%; C57BL6, 4.6 ± 0.2%). No significant differences were detected among the groups in C57BL/6 mice, however, *t*10-*c*12 CLA and PW group had lower T cells compared to the rest of the *db/db* mice (Figure 28b and Appendix A3, A4).

DCs were detected using antibodies for CD11c and MHCII, to distinguish between mature ($CD11C^+MHCII^+$) and immature ($CD11C^+MHCII^-$) DCs. Flow cytometry showed a trend (P=0.07) for a genotype effect for the proportion of total DC ($CD11C^+$) (genotype means: *db/db,* 3.36 ± 0.37; C57BL/6, 3.67 ± 0.35) (Figure 28c). The *db/db* PW group had a lower percentage of total DC compared to the *db/db* CTL and *db/db c*9-*t*11 CLA groups. Among the C57BL/6 mice, the *t*10-*c*12 group had a 2-fold higher percentage of total DC compared to the CTL, *c*9-*t*11 CLA and PW groups. Only a

genotype effect was detected for mature and immature DC, as the *db/db* mice had fewer mature DC and more immature DC compared to C57BL/6 mice (Figure 28d, e and Appendix A3, A4).

We also looked at the population of NKT cells in the SVF of epididymal adipose tissue of the *db/db* and the C57BL/6 mice, but NKT cells were not detectable in either (data not shown).

Figure 28. Effect of CLA isomers and feed restriction on immune cell markers in epididymal adipose tissue

The percentage of macrophages (a), T cells (b), total DC (c), mature DC (d) and immature DC (e) in the SVF of epididymal adipose tissue was determined by flow cytometry. Data are presented as means ± SEM as a percentage of total gated cells; n=7 for *db/db t*10-*c*12, n=6 for *db/db* CTL, *db/db c*9-*t*11, C57BL/6 CTL and C57BL/6 *c*9-*t*11, n=5 for *db/db* and C57BL/6 PW, and n=4 for C57BL/6 *t*10-*c*12 groups. Statistical analysis was performed using two-way ANOVA and SAS software; contrast statements for pre-planned comparisons were used for means testing. Statistical differences ($P \leq 0.05$) among means are indicated by different lower case letters within a genotype. An absence of letters indicates no significant differences among individual means.

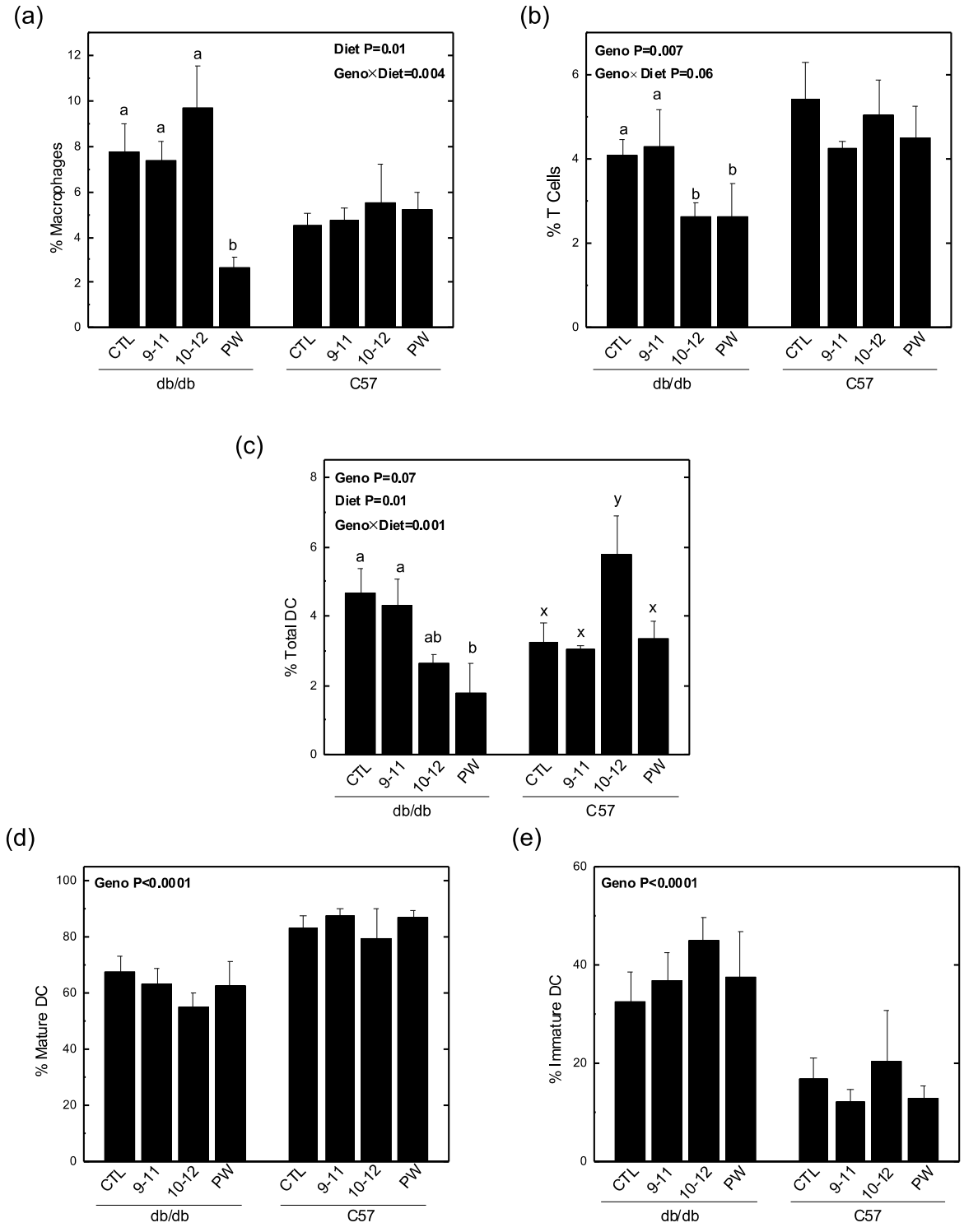
(a)
Diet P=0.01
Geno×Diet=0.004
% Macrophages
a
a
a
b
CTL
9-11
10-12
PW
db/db
C57
(b)
Geno P=0.007
Geno× Diet P=0.06
% T Cells
(c)
Geno P=0.07
Diet P=0.01
Geno×Diet=0.001
% Total DC
ab
x
y
(d)
Geno P<0.0001
% Mature DC
(e)
Geno P<0.0001
% Immature DC

6.22 CLA isomers alter the macrophage presence in WAT

To investigate the effect of CLA isomers on macrophage infiltration and activation, the proportions of classically activated M1 ($F4/80^{+}CD11C^{+}$) and alternatively activated M2 ($F4/80^{+}CD11C^{-}$) macrophages in the SVF of epididymal adipose tissue of *db/db* and C57BL/6 mice were determined using flow cytometry. Our data showed that there was a genotype difference (genotype means: *db/db,* 14.46 ± 1.34; C57BL/6, 4.40 ± 0.8) as the *db/db* mice had a higher percentage of M1 macrophages compared to C57BL/6 mice (Figure 29a). Among the *db/db* mice, the *db/db* PW group had 40% fewer M1 macrophages than the *t*10-*c*12 CLA group. Among the C57BL/6 mice, the *t*10-*c*12 CLA group had a 2-fold higher proportion of M1 macrophages compared to the rest of the C57BL/6 groups (Figure 29a).

With respect to the alternatively activated M2 macrophages, there was no genotype effect based on the absence of a significant difference between *db/db* and C57BL/6 mice. However, there was a trend (P=0.09) for a diet effect, with the *db/db* PW group having ~2-fold fewer M2 macrophages compared to the rest of the *db/db* groups (Figure 29 b).

To investigate the effect of CLA on macrophage infiltration in inguinal adipose tissue, the levels of F4/80, a macrophage marker, were measured using Western blotting. Our data showed that the *db/db t*10-*c*12 CLA group had ~2-fold higher levels of F4/80 among the *db/db* mice. However, in C57BL/6 mice, the *t*10-*c*12 CLA and PW groups had ~4-fold higher levels of F4/80 compared to the *c*9-*t*11 CLA and CTL groups (Figure 29c, d). In agreement with our Western blot data, IF shows a strong F4/80 localization among adipocytes in the *t*10-*c*12 CLA groups compared to the rest of the animals. The

macrophages in the *t*10-*c*12 CLA and C57BL/6 PW groups were primarily distributed in crown-like structures, which are characteristic of necrosis in adipose tissue (Figure 29e). The crown-like structures were observed in all *db/db* mice except the PW group.

To investigate the localization of activated M1 and M2 macrophages in inguinal adipose tissue, immunofluorescence microscopy was used to detect iNOS (M1 macrophage marker) and CD206 (M2 macrophage marker). IF showed the presence of M1 and M2 macrophages in all the groups, however, *t*10-*c*12 CLA groups of both *db/db* and C57BL/6 mice had fewer distinct M2 macrophages compared to the rest of the groups (Figure 29f).

Figure 29. Effect of CLA isomers on macrophages

(a-b) The percentage of M1 macrophages (a) and M2 macrophages (b) in the SVF of epididymal adipose tissue were determined by flow cytometry. The data are presented as means ± SEM as a percentage of total gated cells; n=7 for *db/db t*10-*c*12, n=6 for *db/db* CTL, *db/db c*9-*t*11, C57BL/6 CTL and C57BL/6 *c*9-*t*11, n=5 for *db/db* and C57BL/6 PW, and n=4 for C57BL/6 *t*10-*c*12 groups. Statistical analysis was performed using two-way ANOVA and SAS software; contrast statements for pre-planned comparisons were used for means testing. Statistical differences ($P \leq 0.05$) among means are indicated by an * for diet effects across both genotypes.

(c) The levels of F4/80 were measured in inguinal adipose tissue of *db/db* and the C57BL/6 mice using Western blotting. eEF2 was used as the loading control. Individual bands were arranged to present the data in an organized fashion in the same order as the figures. All bands were taken from the same blot and exposure without any other manipulation.

(d) Densitometry was used to quantify the intensity of the bands in panel (c). Data were normalized to the loading control (eEF2). The results are presented as means ± SEM; n=5 for all groups except n=4 for the C57BL/6 CTL and C57BL/6 *t*10-*c*12 groups. Statistical analysis was performed using two-way ANOVA and SAS software; contrast statements for pre-planned comparisons were used for means testing. Statistical differences ($P \leq 0.05$) among means are indicated by different lower case letters within genotype.

(e) Immunofluorescence staining was performed on sections of inguinal adipose tissue of *db/db* and C57BL/6 mice. F4/80 (macrophage marker) is indicated by green, and

nuclei are in blue. Scale bar (*db/db* CTL) represents 10 μm and is applicable to all panels. White arrows indicate the crown-like structures.

(f) Immunofluorescence staining was performed on sections of inguinal adipose tissue of *db/db* and C57BL/6 mice. iNOS (M1 polarization) is indicated by red, CD206 (M2 polarization) by green, and nuclei are in blue. Scale bar (*db/db* CTL) represents 10 μm and is applicable to all panels

(a)

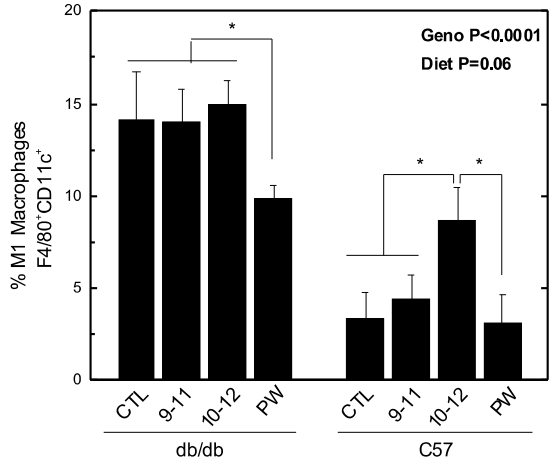
Geno P<0.0001
Diet P=0.06
% M1 Macrophages
F4/80+CD11c+
20
15
10
5
0
*
*
*
CTL
9-11
10-12
PW
CTL
9-11
10-12
PW
db/db
C57

(b)

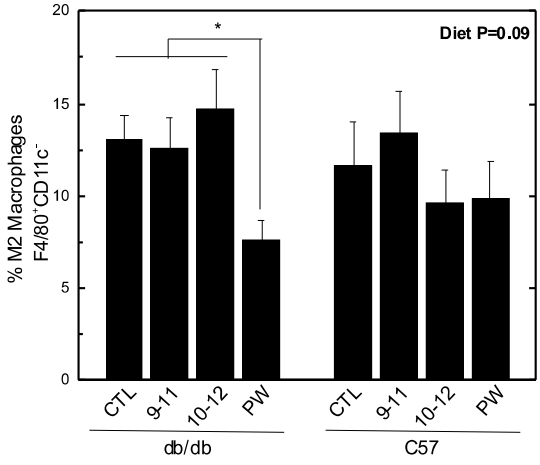
Diet P=0.09
% M2 Macrophages
F4/80+CD11c-
20
15
10
5
0
*
CTL
9-11
10-12
PW
CTL
9-11
10-12
PW
db/db
C57

(c)

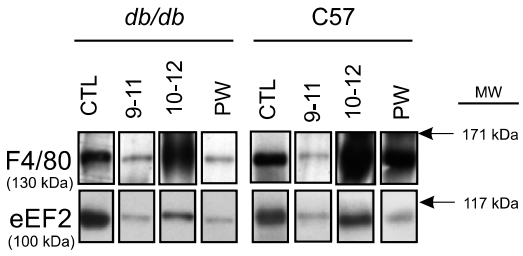
db/db
C57
CTL
9-11
10-12
PW
CTL
9-11
10-12
PW
MW
171 kDa
117 kDa
F4/80
(130 kDa)
eEF2
(100 kDa)

(d)

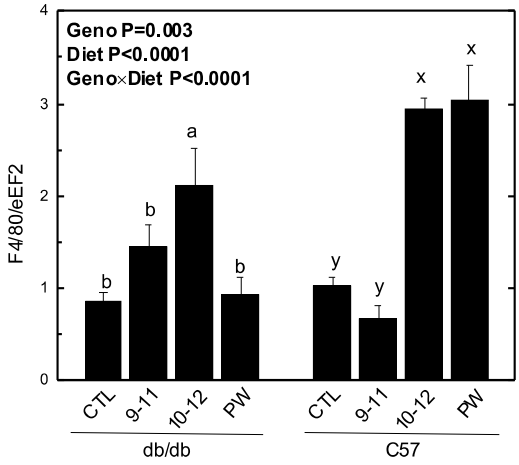
Geno P=0.003
Diet P<0.0001
Geno×Diet P<0.0001
F4/80/eEF2
4
3
2
1
0
b
b
a
b
y
y
x
x
CTL
9-11
10-12
PW
CTL
9-11
10-12
PW
db/db
C57

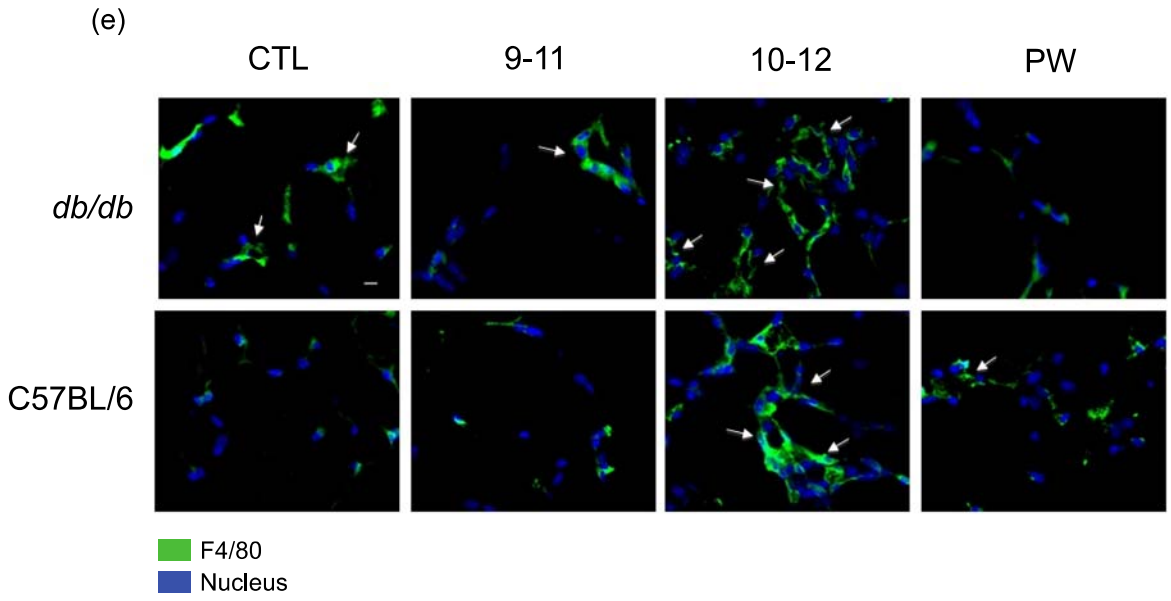
(e)
CTL
9-11
10-12
PW
db/db
C57BL/6
F4/80
Nucleus

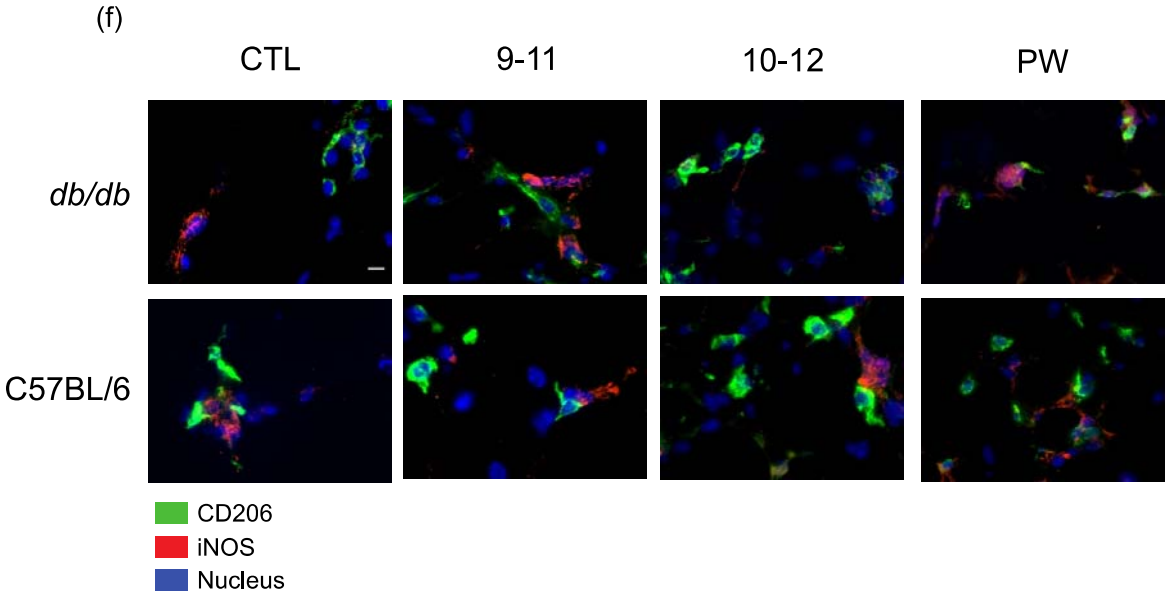
(f)
CTL
9-11
10-12
PW
db/db
C57BL/6
CD206
iNOS
Nucleus

6.23 Summary of CLA isomers and feed restriction in obese *db/db* and lean C57BL/6 mice

We showed that *t*10-*c*12 CLA leads to reduced body weight in both obese *db/db* and lean C57BL/6 mice due to a reduction in fat mass (both white and brown adipose tissue), without changing lean body mass. Weight loss in *t*10-*c*12 CLA groups occurred despite no change in feed intake or metabolic rate as indicated by body temperature during the course of the study. However, the presence of TBX-1 in the nucleus of *t*10-*c*12 CLA fed animals and C57BL/6 PW mice suggests an increase in beige adipocytes. The Wnt/βcatenin pathway was not affected by *t*10-*c*12 CLA in the adipose tissue of obese and/or lean mice. In addition, *t*10-*c*12 CLA-induced weight loss worsened hyperglycemia in *db/db* mice even though there was considerable weight loss. The reduction in adiposity observed in the *t*10-*c*12 CLA group was likely not due to a decline in adipogenesis or an increase in adipocyte clearance. We also showed that *t*10-*c*12 CLA effect on macrophage infiltration varies in subcutaneous versus visceral adipose depots.

7. Discussion and conclusions

7.1 Summary of Findings

The research in this thesis supports the view that CLA, specifically the *t*10-*c*12 CLA isomer, has an anti-obesity effect and suggests several novel routes by which it achieves this outcome, such as altering lipid droplet properties and β-catenin signaling. Both *in vitro* and *in vivo* approaches were used to examine the contribution of these potential mechanisms to the inhibition of adipogenesis by *t*10-*c*12 CLA treatment in 3T3-L1 adipocytes, and for the weight loss due to *t*10-*c*12 CLA feeding in obese and lean mice.

A consequence of this study was discovering that CLA isomers affect adipocytes differently during the early and late stages of differentiation *in vitro*. Both the *c*9-*t*11 and *t*10-*c*12 CLA isomers stimulate lipid droplet formation in early differentiation. However, as the cells mature, *c*9-*t*11 CLA tends to have no effect, while *t*10-*c*12 CLA inhibits lipid droplet accumulation and adipokine production, likely by preventing adipocyte maturation. The lipid droplet profile and adipokine secretion were not affected by *c*9-*t*11 CLA; however, *c*9-*t*11 CLA treatment increased mature adipocyte cell size, which is a phenotype associated with obesity. Our data show the *t*10-*c*12 CLA isomer inhibits perilipin-1 phosphorylation, a process that is makes lipid droplets available to lipases. The *t*10-*c*12 CLA isomer also reduces the level of HSL and inhibits lipolysis through a PKCα-dependent pathway. *t*10-*c*12 CLA increases and stabilizes β-catenin in 3T3-L1 adipocyte, and the resultant elevation of β-catenin levels increases its interaction with

PPARγ and in this way leads to inhibition of 3T3-L1 adipocyte differentiation. However, this β-catenin-dependent effect of *t*10-*c*12 CLA was not observed in mouse epididymal adipose tissue, possibly due to the fact that adipose tissue is an organ containing various cell types and adipocytes, each contributing just a fraction of the total cells present in this multicellular organ. Thus, *t*10-*c*12 inhibits adipogenesis in 3T3-L1 adipocytes by altering lipid droplet properties, reducing HSL and increasing β-catenin levels.

The *in vivo* study demonstrated that a reduction in body weight can be achieved in mice via calorie restriction or by *t*10-*c*12 CLA consumption, however, these weight loss outcomes were attained by distinct mechanisms. Weight loss via *t*10-*c*12 CLA is fat mass specific, while weight loss as a result of calorie restriction affects both fat and lean mass. The *t*10-*c*12 CLA isomer elevates blood glucose in obese mice, and a similar effect is observed in lean mice. Weight loss as a result of calorie restriction did not lower the obesity-induced elevation of blood glucose in *db/db* mice or alter blood glucose concentrations in the lean mice. These data suggest that either further fat loss in obese *db/db* mice is required before hyperglycemia can decrease, or there is another factor responsible for the diabetic state in *db/db* mice that it is not affected by fat loss. In lean C57BL/6 mice, calorie restriction did not lead to fat loss as measured by body composition, thus a reduction in blood glucose concentration was not expected in lean animals. *t*10-*c*12 CLA reduced adiposity without either lowering the recruitment of new adipocytes or increasing adipocyte clearance. In contrast, adipose tissue had a reduced number of preadipocytes under conditions of calorie restriction due to enhanced recruitment of new adipocytes. Based on the *in vivo* study, weight loss due to *t*10-*c*12 CLA consumption could occur through the induction of more metabolically active beige

adipocytes within WAT, as evidenced by presence of TBX-1 in the nucleus. However, TBX-1 is also present in the nuclei of adipocytes of the lean C57BL/6 calorie restricted group. Furthermore, *t*10-*c*12 CLA increases macrophages in inguinal adipose tissue, which have been shown to contribute to the higher numbers of beige adipocytes (Qiu, Nguyen et al. 2014); this effect is observed in calorie restriction as well. In addition, *t*10-*c*12 CLA and calorie restriction reduces T cell and DC infiltration in the epididymal adipose tissue of obese *db/db* mice. Finally, *t*10-*c*12 CLA increases DCs in the epididymal adipose tissue of lean C57BL/6 mice, which may lead to greater inflammation.

7.2 Discussion

The prevalence of obesity is increasing worldwide and this is having a significant impact on human health. The research presented in this thesis is important because CLA supplements are found in every health store, and these products claim CLA provides weight loss benefits with no side effects. However, there is a considerable controversy regarding both the safety and efficacy of using CLA as a loss agent, and further study to address the possible side effects of CLA is still required. In addition, investigating the underlying biological mechanisms by which CLA regulates adipocyte lipid metabolism and differentiation are necessary to obtain the evidence needed to establish whether it can or cannot be employed for successful long-term weight loss. This thesis describes the effect of CLA isomers in the regulation of lipid droplets, adipokines and lipolysis in the context of adipocyte maturation. In addition, the pathways and mechanisms contributing to fat loss by CLA isomers and calorie restriction were examined. Our data describe for

the first time the effect of CLA isomers on Wnt/β-catenin, a key mediator of adipocyte determination and differentiation, using *in vitro* and *in vivo* models. In addition, the contribution of adipocyte turnover to adipose tissue in the context of weight gain and loss was investigated. One of the important aspects of the current study was determining the effect of CLA isomers and calorie restriction, side-by-side and comparing the beneficial and detrimental effects of weight loss by these two different methods.

7.2.1 Effect of CLA isomers in 3T3-L1 preadipocyte differentiation

Our *in vitro* data show that both *t*10-*c*12 and *c*9-*t*11 CLA have a transient effect on adipocyte development, stimulating early adipocyte differentiation as indicated by lipid droplet accumulation. As adipogenesis proceeds, however, *t*10-*c*12 CLA inhibits adipocyte maturation as indicated by a decrease in the production of adipokines such as adiponectin, chemerin and adipsin, and a reduction in lipid droplet accumulation. Production of adipokines and formation of lipid droplets are two important characteristics of mature adipocytes, and in this study we showed that both of these processes are altered by CLA treatment. The effects of CLA on the production of well-known adipokines (adiponectin, leptin) are clear (Kang and Pariza 2001; Nagao, Inoue et al. 2003), but its effect on more recently identified adipokines (adipsin, chemerin) had not been previously investigated. The reduction of adiponectin, adipsin and chemerin implies that the preadipocytes do not differentiate into mature adipocytes in the presence of *t*10-*c*12 CLA. Likewise, the inhibition of late-stage adipogenesis by *t*10-*c*12 CLA is supported by the lower numbers of lipid droplets in 3T3-L1 cells treated with this isomer. Various reports have shown that *t*10-*c*12 CLA is capable of reducing adiposity (Evans, Park et al. 2001;

Brown, Boysen et al. 2003). The results of this study indicate the decrease in adipocyte number in response to *t*10-*c*12 CLA treatment is achieved by a mechanism that involves the inhibition of adipogenesis. Furthermore, *t*10-*c*12 CLA reduces 3T3-L1 adipocyte size, in agreement with previous findings *in vivo* (DeClercq, Zahradka et al. 2010) showing that adipocyte size is smaller in *t*10-*c*12 CLA-fed obese rats. Consequently, it is possible that *t*10-*c*12 CLA is capable of preventing both adipocyte hypertrophy and hyperplasia, thus impacting on obesity development. Further information related to this controversial issue of weight loss through consumption of CLA was provided in section 1.5.1 above.

7.2.2 Effect of CLA isomers on lipid droplets and lipolysis in 3T3-L1 preadipocytes

We also examined the effects of *t*10-*c*12 CLA on lipid droplet coat proteins and their cellular localization. Perilipin-1 is a critical lipid droplet protein that plays an essential role in protecting lipid droplets from lipases (Blanchette-Mackie, Dwyer et al. 1995). We found that *t*10-*c*12 CLA reduces the levels of both phosphorylated and total perilipin-1 in 3T3-L1 adipocytes treated for 8 days relative to untreated control cells. The reduction in perilipin-1 levels are in agreement with the observation that with *t*10-*c*12 CLA treatment there are fewer lipid droplets requiring lipid droplet coat proteins. As well, the decrease in perilipin-1 phosphorylation due to *t*10-*c*12 CLA treatment likely explains the absence of perilipin-1 in the perinuclear region of the cells, since perilipin-1 moves between the lipid droplet and the ER during lipid synthesis (Skinner, Shew et al. 2009). The presence of staining both in the lipid droplet periphery and surrounding the nucleus of untreated and *c*9-*t*11 CLA treated cells suggests there may be two pools of perilipin-1 in the cell with different states of phosphorylation. In contrast,

phosphorylation of perilipin-1 was suppressed with *t*10-*c*12 CLA treatment, and the majority of the protein was tightly associated with the lipid droplets and thus not in the perinuclear pool. Resolution of this concept would be possible if an antibody selective for the phosphorylated perilipin-1 was available.

The decline in perilipin-1 phosphorylation likely stabilizes the lipid droplets and leads to a reduction in lipolysis. In contrast, two studies have concluded that *t*10-*c*12 CLA increases lipolysis in adipocytes, but their experiments used different doses of CLA, different treatment times, and different cell types. Specifically, den Hartigh et al. (2013) treated differentiated 3T3-L1 (mature adipocytes) for 7 days with 250 μM *t*10-*c*12 CLA, while Chung et al. (2005) examined the acute effect (3 hours) of 30 μM *t*10-*c*12 CLA on adipocyte lipolysis, using newly differentiated human adipocytes generated from the stromal vascular fraction. However, contrary to these reports (Chung, Brown et al. 2005; den Hartigh, Han et al. 2013), we found that *t*10-*c*12 CLA did not stimulate lipolysis in 3T3-L1 adipocytes based on an assay for glycerol release. Instead, lipolysis was inhibited by this CLA isomer. In support of this observation, *t*10-*c*12 CLA treated cells had decreased levels of HSL, which catalyzes the second step of triglyceride breakdown in lipid droplets through removal of the acyl group from diacylglycerol. HSL is also required for the activation of ATGL, which removes the first acyl group from triglycerides, the first step of lipolysis. Thus, we report for the first time that *t*10-*c*12 CLA blocks lipolysis in adipocytes by inhibiting perilipin-1 phosphorylation and by reducing the level of HSL, both key mediators of lipolysis. These findings also support the view that the decrease in lipid droplets caused by *t*10-*c*12 CLA treatment is likely the

result of an inhibition of lipid droplet production during adipogenesis rather than a stimulation of lipolysis.

We did not pursue whether the inhibition of HSL by *t*10-*c*12 CLA is a primary effect or if it is due to inhibition of adipogenesis. However, it has been shown that HSL acts as a ligand or pro-ligand for PPARγ (Shen, Yu et al. 2011), which suggests the presence of HSL is important for induction of adipogenesis.

The effect of PKA on induction of lipolysis in relation to HSL and perilipin-1 is well recognized. PKA is responsible for phosphorylation of HSL at Ser-653, which stimulates lipolysis (Anthonsen, Ronnstrand et al. 1998). But the role of PKC on lipid droplet formation and lipolysis is not clear. Therefore, we investigated the contribution of PKC on perilipin-1 phosphorylation and evaluated the possibility that *t*10-*c*12 CLA may act through this kinase. Our data show that general PKC inhibition via BIS prevents adiponectin production and blocks perilipin-1 phosphorylation. Similarly, selective inhibition with the PKCα inhibitor Gö6976 also prevented perilipin-1 phosphorylation, while PKCβ inhibition did not. This finding suggests that PKCα has a critical role in the phosphorylation of perilipin-1. PKCγ was not considered based on previous findings that it has no significant role in adipocyte differentiation (Fleming, MacKenzie et al. 1998). Since perilipin-1 phosphorylation was reduced by treatment with *t*10-*c*12 CLA and subcellular fractionation showed that *t*10-*c*12 CLA treatment activates PKCα, it was concluded that the effects of *t*10-*c*12 CLA on lipid droplets are mediated by PKCα. Interestingly, Unal et al. (2008) have reported that activation of PKA is mediated by PKCα depletion in adipocytes. Our data suggest that *t*10-*c*12 CLA inhibits lipolysis in

adipocytes by activating PKCα, which in turn could inhibit PKA activity and thus decrease perilipin-1 and HSL phosphorylation.

Figure 30 depicts a possible mechanism by which *t*10-*c*12 CLA regulates lipolysis in 3T3-L1 adipocytes. One of the important aspects of our findings is that PKCα inhibition blocks the reduction of both adiponectin and perilipin-1 levels by *t*10-*c*12 CLA. This observation suggests that PKCα is required for the actions of *t*10-*c*12 CLA on adipokine and lipid droplet protein production. Similarly, *t*10-*c*12 CLA regulates perilipin-1 activity through PKCα, since PKCα inhibition blocked perilipin-1 phosphorylation, equivalent to what is observed with *t*10-*c*12 CLA treatment. These data indicate that production of lipid droplet proteins and adipokines, as well as the activation of lipolysis by PKA, are controlled by two divergent signaling pathways, both regulated by PKCα and sensitive to *t*10-*c*12 CLA.

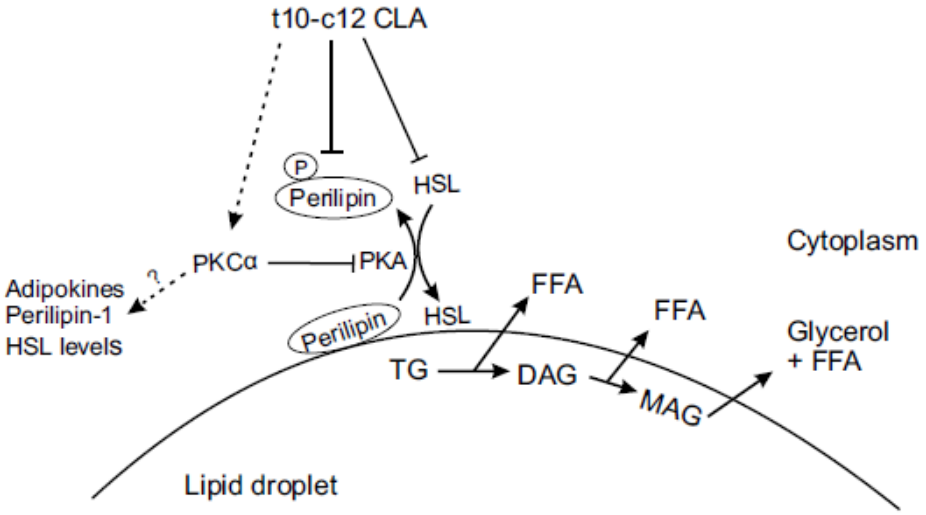

Figure 30. Proposed mechanism by which t10-c12 CLA regulates lipolysis in 3T3-L1 adipocytes

7.2.3 Effect of CLA on Wnt/β-catenin signaling in *in vitro* and *in vivo* models

One explanation for the weight loss effect of *t*10-*c*12 CLA could be its ability to regulate pathways that control both adipocyte commitment and differentiation (Christodoulides, Lagathu et al. 2009; Laudes 2011). Fat loss in both WAT and BAT with dietary *t*10-*c*12 CLA in *db/db* mice suggests that *t*10-*c*12 CLA possibly affects a pathway that has a dual effect on both WAT and BAT production. The Wnt/β-catenin pathway is the best candidate, since it is involved in the commitment of mesenchyme stem cells to either the adipocyte or the *myf*-5 positive myocyte (the origin of BAT) lineage (Timmons, Wennmalm et al. 2007). In the current study, we first investigated the

action of CLA in relation to the Wnt/β-catenin pathway *in vitro*, using 3T3-L1 preadipocytes, and followed this by testing the effects of CLA isomers *in vivo* using obese and lean mice. *t*10-*c*12 CLA affected β-catenin directly and increased β-catenin levels and phosphorylation in 3T3-L1 adipocytes. Additionally, there was an increase in β-catenin-PPARγ complexes, which inhibits adipocyte differentiation *in vitro* through sequestration of PPARγ. In the animal study, the increase in β-catenin levels in the *db/db* *t*10-*c*12 CLA treated group was associated with an increase in cyclin D1 levels, but these results were not seen in *t*10-*c*12 CLA treated C57BL/6 mice.

We investigated the effect of CLA on the Wnt/β-catenin pathway during adipogenesis, from early differentiation (day 2) to late differentiation (day 8). *t*10-*c*12 CLA treatment resulted in an increase in β-catenin levels in both early and late adipocyte differentiation; however, the elevation of β-catenin led to different outcomes regarding cyclin D1, a downstream target of β-catenin at the different time points. Specifically, the increase in β-catenin levels due to *t*10-*c*12 CLA resulted in an increase in cyclin D1 levels in early differentiation, and a reduction in late differentiation. Although an explanation of this paradox is not possible on the basis of the experimental data, it is plausible that cyclin D1 is regulated by different mechanisms during adipocyte differentiation. During early differentiation and at the time of clonal expansion, when the adipocytes go through several cycles of mitosis, and PPARγ is not highly expressed, the increase in β-catenin levels caused by *t*10-*c*12 CLA treatment activates TCF/LEF and subsequently increases cyclin D1. However, during late differentiation, when PPARγ is present, β-catenin activity is blocked through sequestration by PPARγ. As a result, cyclin D1 is not transcribed and adipocyte proliferation ceases.

In particular, factors other than β-catenin may be involved in regulating cyclin D1, such as cell cycle regulators including $p21^{cip1}$ or $p27^{kip1}$ (Maddika, Ande et al. 2007). The ability of *t*10-*c*12 CLA to elevate β-catenin levels while decreasing cyclin D1 levels on day 8 of differentiation suggests that β-catenin either does not get transported into the nucleus, thus remaining in the cytosol where it is inactive, or it does not activate the cyclin D1 gene upon entering the nucleus. Since subcellular fractionation and IF both showed β-catenin is present in the nucleus of CLA treated and untreated cells, it can be concluded that β-catenin gets transported into the nucleus but is not active or its effects are antagonized. This effect could be explained by high levels of PPARγ in mature adipocytes (day 8 of differentiation), which may hold β-catenin in an inactive complex, thus preventing β-catenin from binding to the promoter elements TCF/LEF. In agreement with the Liu et al. (2006) findings, our data showed that *t*10-*c*12 CLA treatment increases the relative amount of β-catenin bound to PPARγ. These data thus explain the increase in β-catenin levels and reduction in cyclin D1 levels on day 8 of differentiation, since β-catenin is not able to bind to TCF/LEF transcription factor and, therefore, the cyclin D1 gene is not transcribed and the levels of cyclin D1 are decreased. On the other hand, binding of β-catenin to PPARγ could inhibit the ability of PPARγ to induce adipogenesis (Liu, Wang et al. 2006), which would explain why adipogenesis is blocked, as indicated by a reduction in adiponectin and perilipin-1 levels with t10-c12 CLA treatment on day 8 of differentiation but not on day 2. To our surprise, and in contrast with literature (Fox, Colton et al. 2008), the levels of cyclin D1 did not decline during adipogenesis, remaining constant through preadipocyte differentiation from day 0 to day 8. However, the localization of cyclin D1, which is an important factor for regulating cell cycle, is not

clear during adipogenesis. Animal data show that there is a genotype effect with respect to β-catenin, Ser675 phosphorylation of β-catenin and cyclin D1, as the *db/db* mice have lower levels of β-catenin and cyclin D1 compared to the C57BL/6. These data suggest that the Wnt/β-catenin pathway is less active in the *db/db* mice compared to C57BL/6 mice, which could possibly lead to an increase in adipogenesis and induction of obesity. However, unlike the results obtained *in vitro*, the *in vivo* data produced some divergent results with respect to the CLA isomers and calorie restriction. In our animal models, Ser675 phosphorylation of β-catenin was decreased in *t*10-*c*12 CLA isomer fed mice of both genotypes, which indicates that the *t*10-*c*12 CLA isomer did not activate β-catenin in epididymal adipose tissue in either *db/db* or C57BL/6 mice. Unexpectedly, the cyclin D1 levels in the *db/db* mice fed *t*10-*c*12 CLA isomer were increased, potentially through other factors that regulate cyclin D1 levels in the adipocyte, such as the cell cycle regulators $p27^{kip1}$ and $p21^{cip1}$. However, neither $p27^{kip1}$ nor $p21^{cip1}$ was detected in the epididymal adipose tissue of *db/db* and C57BL/6 mice (data not shown). This finding is not surprising, since mature adipocytes, particularly those in epididymal adipose tissue, pass slowly through the cell cycle due to their decreased rate of adipogenesis. This could also explain the elevated levels of activated β-catenin (Ser 675-phosphorylated β-catenin) in 3T3-L1 adipocytes, as they have a higher rate of cell division than epididymal adipose tissue. Therefore, we speculate that the effects of the *t*10-*c*12 CLA isomer in activating β-catenin are possibly dependent upon the rate of cell cycling in adipose tissue. To verify this concept, the effects of CLA isomers on β-catenin activation in inguinal adipose tissue, a depot that is known to have higher rate of adipogenesis, should be determined. On the other hand, even though the *db/db* PW and *db/db* *t*10-*c*12 CLA groups both

underwent significant fat loss, the responses involving cyclin D1 were quite distinct, which suggests that fat loss in the PW and *t*10-*c*12 CLA groups occurs through different mechanisms with respect to the Wnt/β-catenin pathway.

The Wnt/β-catenin pathway is also involved in regulating cancer and tumorigenesis (Sherwood 2015). Specifically, *c*9-*t*10 CLA has exhibited an anti-carcinogenic effect, which is mediated through inhibition of NF-κB and blocking of PI3K-AKT signaling in the skin of hairless mice (Hwang, Kundu et al. 2007; Igal 2011). Here we investigated the effect of *c*9-*t*10 CLA on Wnt/β-catenin signaling in 3T3 L1 adipocytes and adipose tissue. Our data showed that *c*9-*t*10 CLA affected β-catenin and cyclin D1 differently at early and late stages of adipocyte differentiation through different mechanisms. The levels of cyclin D1 were elevated by *c*9-*t*10 CLA on day 2 of differentiation, but since the β-catenin levels were not affected, this increase in cyclin D1 is likely not β-catenin dependent. On day 8 of differentiation, *c*9-*t*10 CLA reduced the levels of total and activated β-catenin, but cyclin D1 was not affected. In the *db/db* mouse, *c*9-*t*10 CLA did not affect either β-catenin or cyclin D1, while in C57BL/6 mice it increased the levels of both β-catenin and cyclin D1 despite a reduction in activated β-catenin. These results suggest that the effect of *c*9-*t*10 CLA on β-catenin and cyclin D1 may be dependent on functional leptin receptors and leptin signaling. The discrepancy between the data obtained from 3T3-L1 and the lean C57BL/6 mice could be explained by the fact that, in the cell line, the CLA effect is obtained from one cell type cell, whereas more than one cell type contributes to the results from adipose tissue.

Next we investigated the factors that are responsible for the increased β-catenin levels in response to *t*10-*c*12 CLA treatment. The levels of Wnt10b, SFRP3 and LRP6/5

phosphorylation were measured as upstream effectors of Wnt/β-catenin signaling. However, Wnt10b, SFRP3 and LRP6/5 phosphorylation was not altered by *t*10-*c*12 CLA in either the 3T3-L1 cell line or the mice. These data suggest that there is a factor downstream of these regulators that is responsible for the actions of *t*10-*c*12 CLA.

GSK3-β is an important regulator of β-catenin degradation (Cook, Fry et al. 1996), since GSK3-β phosphorylation of β-catenin leads to β-catenin ubiquitination. Thus, we examined the effect of CHIR99021 (a GSK3-α and -β inhibitor) and JW67 (a stimulator of β-catenin degradation) on 3T3-L1 adipocyte differentiation and active β-catenin levels. Our data showed that enhancing β-catenin degradation with JW67 did not interfere with the reduction of adiponectin and perilipin-1 by *t*10-*c*12 CLA. However, inhibition of GSK3 with CHIR99021 blocked these actions of *t*10-*c*12 CLA, which suggests that modulation of adiponectin and perilipin-1 by *t*10-*c*12 CLA is not β-catenin dependent, but is regulated by GSK3-β or GSK3-α. On the other hand, increasing β-catenin degradation did not lower the level of active β-catenin resulting from *t*10-*c*12 CLA treatment, while inhibiting GSK3 resulted in even higher levels of β-catenin. These findings indicate that the increase in active β-catenin and subsequent inhibition of adipogenesis caused by *t*10-*c*12 CLA are independent of GSK3-β activity. Thus, we propose that the elevation of β-catenin levels by *t*10-*c*12 CLA occurs independent of the Wnt pathway. This conclusion is supported by the fact that the upstream effectors of the Wnt/β-catenin pathway, such as Wnt10b or SFRP3, which regulate GSK3-β, were not affected by CLA either. Furthermore, the reduction in cyclin D1 levels caused by *t*10-*c*12 CLA was independent of either β-catenin or GSK3, thus suggesting that an unknown factor(s) may be responsible for regulating cyclin D1 levels in adipocytes.

As previously discussed in section 1.2.1.4, it can be speculated that CLA acts as an activator of PKC by mimicking diacylglycerol (Steinberg 2008; Newton 2010; Pearce, Komander et al. 2010; Lipp and Reither 2011; Hui, Kaestner et al. 2014). Alternatively, CLA may operate by bind to a specific G protein-coupled receptor (Hsu, Meng et al. 2010; Schmidt, Liebscher et al. 2011) that in turn activates PKC (Chuang, Iacovelli et al. 1996). PKC could also be involved in the phosphorylation of both β-catenin (Ishitani, Ninomiya-Tsuji et al. 1999; Gwak, Cho et al. 2006; Gwak, Jung et al. 2009) and GSK3β (Rovedo, Krett et al. 2011; Moore, van den Bosch et al. 2013), the two major regulators of the Wnt/β-catenin pathway. These possible mechanisms for CLA action on β-catenin function were not addressed in this study and would need further investigations.

In light of the above evidence, it appears that *t*10-*c*12 CLA affects adiponectin and perilipin-1 through pathways that are independent of β-catenin and cyclin D1, while at the same time *t*10-*c*12 CLA has a direct effect on β-catenin. At this time it is not possible to reconcile these observations, and thus further investigation is required. However, it is worth noting that the differential regulation of cyclin D1 levels at different time points during adipocyte differentiation means cyclin D1 may not be the best marker for β-catenin activity. Our findings are in agreement with others who showed that leptin can modulate cyclin D1 levels (Xu, Ye et al. 2010; Zheng, Hursting et al. 2012), and this could explain why cyclin D1 levels were reduced by 2 fold in the *db/db* mice compared to C57BL/6 mice. A summary of the effects of the CLA isomers on β-catenin signaling can be found in Tables 6 and 7and Figure 31.

Table 6. A summary of the effects of the CLA isomers on β-catenin signaling and perilipin-1 and adiponectin, markers of mature adipocytes.[1]

	3T3-L1 mature adipocytes				
	Total β-Catenin	P-Ser675 β-Catenin[2]	Cyclin D1	Perilipin-1	Adiponectin
***c*9-*t*11 CLA**	↓	↓	↔	↔	↔
***t*10-*c*12 CLA**	↑	↑	↓	↓	↓

[1]Comparisons are relative to the respective null. ↑: increased, ↓: decreased, ↔: unchanged

[2]Phosphorylation of β-Catenin on Ser675 leads to β-Catenin stabilization.

Table 7. A summary of the effects of CLA isomers and calorie restriction on β-catenin signaling.[1]

	db/db			**C57BL/6**		
	Total β-Catenin	P-Ser675 β-Catenin	Cyclin D1	Total β-Catenin	P-Ser675 β-Catenin	Cyclin D1
***c*9-*t*11 CLA**	↔	↔	↔	↑	↓	↑
***t*10-*c*12 CLA**	↑	↓	↑	↔	↓	↔
PW	↑	↔	↔	↔	↔	↔

[1]Comparisons are relative to the respective control group of the same genotype; PW = pair-weight (calorie restricted) group.

↑: increased, ↓: decreased, ↔: unchanged

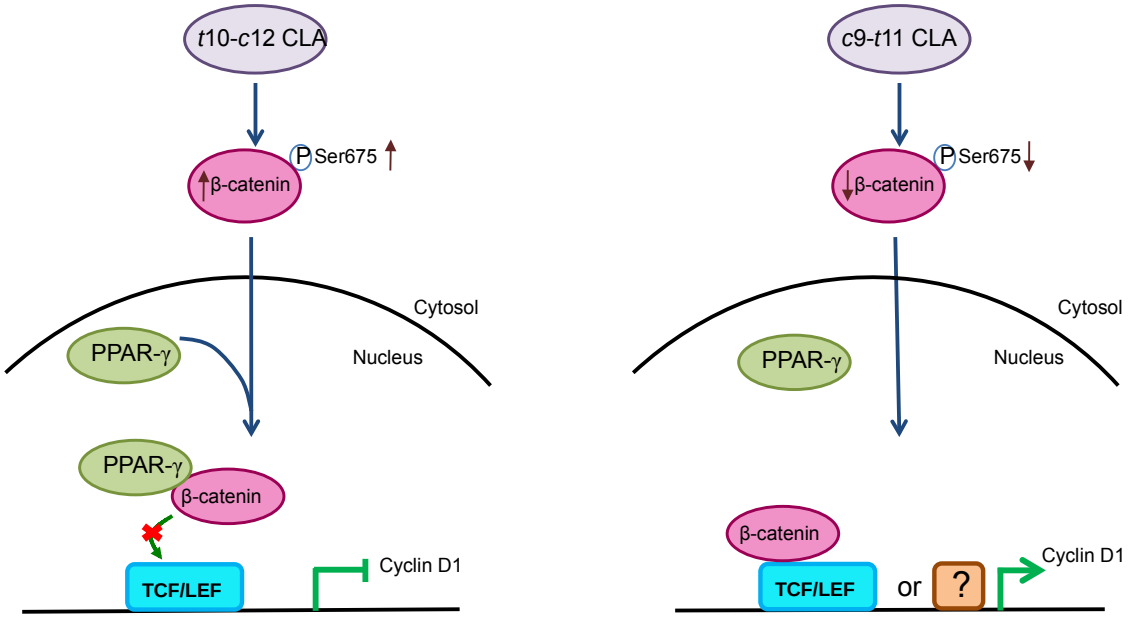

Figure 31. A summary of the effects of the CLA isomers on β-catenin signaling

The diagram provides a potential mechanism to explain why *t*10-*c*12 CLA inhibits adipogenesis in 3T3-L1 adipocytes while *c*9-*t*10 CLA does not. *t*10-*c*12 CLA treatment of 3T3-L1 adipocytes leads to an increase in β-catenin levels and Ser 675 phosphorylation, which increases its stability in the cytosol. Consequently, β-catenin is translocated into the nucleus, where it binds to PPARγ. Formation of this complex prevents the activation of genes responsive to both β-catenin and PPARγ. On the other hand, *c*9-*t*10 CLA treatment of adipocytes leads reduces both β-catenin levels and Ser 675 phosphorylation. Despite this reduction in β-catenin, *c*9-*t*10 CLA treatment leads to β-catenin translocation into the nucleus and responsive genes such as cyclin D1 are transcribed, either via β-catenin or an unknown factor(s). Further investigation is required to elucidate the exact mechanism of CLA action.

7.2.4 Effect of CLA isomers and calorie restriction in healthy and obese mice

One of the best strategies for reducing obesity and related complications such as CVD and type 2 diabetes is weight control. However, since pharmacological approaches have had limited success, lifestyle modification via decreased energy intake and/or increased energy expenditure has become the most common approach to weight control. In this thesis, the physiological effects of CLA isomers and calorie restriction were compared in parallel in obese and lean models. Furthermore, two distinct approaches for fat loss, increased metabolic rate and adipocyte turnover, were studied.

Our group has shown that *t*10-*c*12 CLA reduces insulin resistance and hepatic steatosis despite no changes in adiposity in the obese *fa/fa* Zucker rat, which has a leptin receptor defect (Noto, Zahradka et al. 2007). In addition, the effects of CLA isomers have been examined in both the leptin deficient *ob/ob* and wild type mice, and it was reported that *t*10-*c*12 CLA reduces adiposity but does not improve insulin resistance (Wendel, Purushotham et al. 2008). However, the effects of CLA in obese *db/db* mice, which have a genetic defect in the leptin receptor similar to that of *fa/fa* Zucker rats, have not been investigated. Therefore, to determine whether the responses of these different animal models to CLA were comparable, CLA isomers were fed to obese *db/db* mice and we investigated the effect of these isomers on fat loss and insulin sensitivity, and surveyed the possible underlying mechanisms.

7.2.4.1 Effects of CLA isomers and calorie restriction on body weight and fat mass in healthy and obese mice

Our data showed *db/db* mice fed *t*10-*c*12 CLA had a reduction of 34% in body weight compared to the *db/db* CTL group at the end of the 4 week study. However, a lower body weight was not observed in C57BL/6 mice fed *t*10-*c*12 CLA compared to CTL. These data suggest that *db/db* mice are more sensitive to the actions of CLA compared to C57BL/6 mice. The effect of the *t*10-*c*12 CLA isomer on body weight was seen despite the fact that they consumed the same amount of feed as the other groups, with the exception of the PW groups.

This effect of *t*10-*c*12 CLA is in agreement with other findings that showed AKR/J mice (another obesity-prone inbred strain like C57B/L6 mice) fed 0.5% w/w CLA for 6 weeks had a 10% reduction in body weight and 40% reduction in adipose mass (West, Delany et al. 1998). The fact we had less overall fat loss in our study compared to the results of West et al (1998) could be due to the shorter study length (4 weeks), the smaller dose of CLA (0.4% w/w) or the different mouse strain used in the current study. Similar weight loss was observed in genetically obese mice, as the *ob/ob* mice fed a 1.5% w/w mixture of CLA isomers for 4 weeks had a 30% body weight reduction compared with the control diet (Wendel, Purushotham et al. 2008). The smaller weight loss in this study compared to the current one could be due to the use of a mixture of CLA isomers and the possible contribution of the *c*9-*t*11 CLA isomer. The effect of *c*9-*t*11 CLA on body weight was different in the *db/db* and C57BL/6 mice. The *c*9-*t*11 CLA maintained the body weight equivalent to the respective CTL group in the *db/db* mice; however, in C57BL/6 mice, the body weight of the *c*9-*t*11 CLA group was similar to the *t*10-*c*12 CLA

group, but these were different from the respective CTL group, with no apparent changes in fat or lean mass.

In contrast to other findings that showed less feed intake in mice fed a 0.5% mixture of CLA isomers (Park, Albright et al. 1997) or 0.5% *t*10-*c*12 CLA isomer (So, Tse et al. 2009) for 4 weeks, our data show no significant changes in feed intake with the CLA isomers in either obese or lean mice. It is important to note that intercerebroventricular injection of 150 nM of a CLA mixture suppressed feed intake by decreasing expression of neuropeptide Y (NPY) and agouti-related protein (AgRP) and increasing the circulating leptin levels in rat (Cao, Wang et al. 2007). Thus, the defective leptin receptor in the *db/db* mice could be responsible for the lack of a change in the feed intake of these animals; however, similar to *db/db* mice, no changes in feed intake were observed in C57BL/6 mice.

One of the important aspects of our study design was the ability to compare dietary intervention with CLA isomers with restricted feed intake, which more closely resembles a change in lifestyle. These two weight loss approaches operate by distinct mechanisms, as the *t*10-*c*12 CLA has a fat-specific effect, while restricting feed intake in PW groups lead to a reduction in both fat and lean body mass. The *db/db t*10-*c*12 CLA and PW groups maintained their body weight equivalent to that of week 0 through the course of the study just by losing fat mass in *t*10-*c*12 CLA groups and losing a combination of fat and lean mass in PW groups. In the long term, the loss of lean body mass by calorie restriction reduces basal metabolic rate because muscle is one of the most metabolically active tissues in the body. However, as our data show, the effect of *t*10-*c*12 CLA is not fat type specific, as we observed changes in two different visceral adipose depots

(epididymal and peri-renal) as well as subcutaneous (inguinal) adipose tissue and BAT. Despite the fundamental differences among the fat depots, *t*10-*c*12 CLA affects every major fat depot in the body. This effect could be explained in two ways. First, *t*10-*c*12 CLA does not selectively alter processes such as adipocyte hypertrophy and adipogenesis that are depot-specific. Second, *t*10-*c*12 CLA affects a common signaling pathway active in all the fat depots, but is involved in distinct depot-specific processes. In this way, *t*10-*c*12 CLA feeding could have different outcomes in the various fat depots.

7.2.4.2 Effect of CLA isomers and calorie restriction in adipocyte turnover

One factor that could promote extreme loss of adiposity as observed in *t*10-*c*12 CLA isomer fed mice is a change in the adipocyte turnover rate. Adipocyte turnover is a function of adipogenesis and adipocyte clearance. We investigated the rate of adipogenesis by looking at the proportions of preadipocytes ($Sca1^{+}CD24^{-}$) and stem cell adipocytes ($Sca1^{+}CD24^{+}$) in the SVF of epididymal adipose tissue of the *db/db* and the C57BL/6 mice. Despite the obesity in *db/db* mice, the higher percentages of preadipocytes and stem cell adipocytes suggest that the adipose tissue of *db/db* mice is in an active state. However, these data could be interpreted in another way: the increased percentages of preadipocytes ($Sca1^{+}CD24^{-}$) and stem cell adipocytes ($Sca1^{+}CD24^{+}$) in the SVF of epididymal adipose tissue in the *db/db* mice could be due to a decrease in adipogenesis. As a result, stem cells and preadipocytes would not differentiate into preadipocytes and adipocytes, respectively, and instead remain in the tissue in an undifferentiated state. This assumption could be tested by double staining adipose tissue from the *db/db* mice with Sca-1 and CD24, which can distinguished between stem cells

and preadipocytes. In contrast, the proportions of these cell types remain low in C57BL/6 mice, since these cells are constantly differentiating into preadipocytes and adipocytes. This is the first time that the effect of CLA or any other diet intervention has been examined with respect to preadipocytes and stem cells adipocytes and their contribution to overall adipose tissue dynamics.

Another remarkable finding of this study is the effect of calorie restriction (PW groups) on adipocyte turnover. Unlike weight loss with *t*10-*c*12 CLA, the weight loss resulting from calorie restriction reduced preadipocyte numbers. These data suggest that either the rate of stem cell to preadipocyte differentiation decreased, although no changes in the proportion of stem cells were observed in this group, or preadipocyte differentiation was accelerated. The genetic defect in *db/db* mice leads to obesity via hyperphagy, and when this was controlled by calorie restriction the proportion of preadipocytes ($Sca1^{+}CD24^{-}$) in the SVF of epididymal adipose tissue was reduced to levels that were similar to the C57BL/6 CTL group. Our method for isolating the SVF utilized centrifugation, during which lighter cells with lipid droplets (i.e. mature adipocytes) do not pellet and are therefore lost. As a result, the $Sca1^{-}CD24^{-}$ population consists of immature adipocytes that are intermediate (in both size and the process of maturation) between preadipocytes and adipocytes that are dense enough to remain with the SVF. The higher percentages of immature adipocytes ($Sca1^{-}CD24^{-}$) in obese *db/db* mice compared to the lean C57B/L6 mice suggests that the majority of preadipocytes in the *db/db* mice did not fully differentiate These data suggest that in *db/db* mice there are immature adipocytes ready to differentiate and store more TG. The presence of a population of not fully differentiated adipocytes or very small adipocytes in obese

animals under calorie restriction could possibly indicate that fat mass loss in these animals is due to reduced adipocyte size not fewer adipocyte numbers. This speculation agrees with evidence that an increase in input (over eating) after calorie restriction leads to rapid weight gain. Thus our findings suggest that CLA isomers do not alter adipocyte commitment in lean and obese mice, however, calorie restriction of obese mice could alter adipocyte commitment as they had lower numbers of preadipocytes compared to the rest of the groups.

Another way that CLA isomers could affect adipocyte turnover is by increasing the rate of adipocyte clearance. In this study, we investigated the two major forms of programmed cell death, apoptosis and autophagy. Others have shown that mice fed a 1% w/w mixture of CLA isomers had increased levels of TNFα in the adipose tissue, a factor that is known to induce apoptosis (Tsuboyama-Kasaoka, Takahashi et al. 2000). However, in the current study, the *t*10-*c*12 CLA isomer did not appear to stimulate apoptosis in lean and obese mice as suggested by the reduced caspase-3 activity (cleaved caspase 3/caspase 3 ratio) in extracts from *t*10-*c*12 CLA treated mice compared to CTL. To further investigate the apoptotic effect of CLA isomers on adipocytes, additional analyses such as TUNEL assay, chromatin condensation and DNA fragmentation should be applied in conjunction with measuring apoptotic regulators such as TNFα and cytochrome c. In addition, immunostaining of adipose tissue could identify which cell types in adipose tissue have active caspase 3. Interestingly, the lean C57BL/6 mice had higher levels of both caspase-3 and its active form; these findings suggest there is a higher turnover of adipocytes in lean animals compared to obese.

Autophagy is another form of programmed cell death. Our data show that the LC3II to LC3I ratio (suggestive of autophagy) is not changed by either diet or genotype, and therefore the extreme fat loss obtained with the *t*10-*c*12 CLA isomer may not be due to dysregulated autophagy. Interestingly, the high levels of LC3I in lean C57BL/6 mice suggest an elevation in the recycling of intracellular material by autophagy is occurring, possibly due to a higher rate of adipogenesis, since autophagy is a requirement for adipogenesis (Singh, Xiang et al. 2009). Note that among the lean C57BL/6 mice, the *t*10-*c*12 CLA group had the lowest levels of LC3 levels, which possibly could suggest less recycling of intracellular material and a lower rate of adipogenesis in the lean animals fed *t*10-*c*12 CLA. Contrary to our expectation, extreme calorie restriction in obese mice may not induce autophagy. Since there were no significant changes among the groups in the LC3II to LC3I ratio, a hallmark of autophagy, we did not investigate the autophagy pathway any further.

7.2.4.3 Effect of CLA isomers and calorie restriction on induction of beige adipocytes

One of the proposed mechanisms for weight loss with CLA isomers involves the disruption of energy balance by either decreasing energy intake or increasing energy expenditure. The levels of energy intake (feed intake) were not changed as a result of CLA consumption in our animal models. With respect to energy expenditure, increases in basal metabolic rate, thermogenesis and/or physical activity could increase energy expenditure. We did not observe any unusual change in activity in either of the genotypes fed CLA isomers. There were also no differences in body temperature with CLA isomers

or between the genotypes. However, according to others, thermoregulation in the *db/db* mice is altered and these animals have a body temperature 1-2°C degrees less than wild type mice (Trayhurn 1979). Since the greatest loss of mass was observed in adipose tissue, we investigated the capacity for greater metabolic activity by comparing the relative amount of beige adipocytes in the WAT of the different groups, since these cells are known to have higher metabolic activity compared to white adipocytes. We specifically analyzed inguinal adipose tissue because it is more susceptible to browning than visceral fat.

Western blotting showed that all three experimental groups (*c*9-*t*11 CLA, *t*10-*c*12 CLA and PW) in the *db/db* mice had increased TBX-1 levels, a beige adipocyte transcription factor, compared to the *db/db* CTL group. While unexpected in the lean C57BL/6 mice, the *t*10-*c*12 CLA and PW groups had reduced the levels of TBX-1.

Since the levels of TBX-1 in the *db/db* mice were not differentially affected by *t*10-*c*12 CLA or the other interventions and there were no genotype differences, we speculate that TBX-1 levels are not regulated by leptin but they might be affected by the degree of adiposity. On the other hand, in support of the Western blot data, immunofluorescence microscopy showed that TBX-1 was expressed in all groups, however, only in the *t*10-*c*12 CLA fed animals and C57BL/6 PW group was TBX-1 located in the nucleus. Thus, under these conditions would TBX-1 be able to stimulate gene transcription. While it may be concluded that the presence of elevated levels of TBX-1 in the other groups likely has no link to its activity, it is nonetheless possible to conclude that *t*10-*c*12 CLA does stimulate the browning in WAT, but may not result in an increase in energy expenditure. Knowing the TBX-1 target gene(s) would be needed to address this question, however,

since the beige adipocytes biology is a new area of research the exact target genes of TBX-1 have not yet been determined. Interestingly nuclear localization of TBX-1 was not observed in obese calorie restricted (PW) groups, which further suggests that these two models of weight loss act through distinct mechanisms.

7.2.4.4 Effect of CLA isomers and calorie restriction on macrophages and other immune cells

Since obesity leads to increased macrophage infiltration (Weisberg, McCann et al. 2003), we investigated the role of CLA isomers on the infiltration of macrophages and other immune cells into WAT. Our data showed that the epididymal adipose tissue of the *db/db* CTL group had a higher proportion of macrophages by flow cytometry compared to C57B/L6 mice, and consumption of either CLA isomer did not change this result. This is contrary to other published findings showing that a *t*10-*c*12 CLA–rich diet for just one week induced the expression of genes for inflammatory mediators such as TNFα and IL-6 in WAT from female C57BL/6 mice and also promoted macrophage proliferation and infiltration as indicated by an increase in the levels of F4/80 and MCP-1 in WAT (Poirier, Shapiro et al. 2006). However, in agreement with Cancello et al. (2005), who showed that weight loss in morbidly obese subjects reduced macrophage infiltration, the *db/db* PW group had ~2-fold fewer macrophages than the *db/db* CTL group. This shows another difference between the two weight loss mechanisms induced by *t*10-*c*12 CLA and calorie restriction.

In addition to their role in innate immunity, macrophages may also be involved in the induction of beige adipocytes in subcutaneous WAT via the secretion of

catecholamines and other cytokines (Nguyen, Qiu et al. 2011; Qiu, Nguyen et al. 2014). In support of macrophages inducing beige adipocytes, Western blotting showed that F4/80 levels were elevated in inguinal adipose tissue of *t*10-*c*12 CLA groups and C57BL/6 PW, along with nuclear localized TBX-1. However, further investigation is required to confirm this observation.

In contrast with our flow cytometry results in SVF from epididymal fat, the inguinal fat of *t*10-*c*12 CLA isomer-fed mice had higher levels of F4/80 in both genotypes. It is important to note that in the inguinal depot the level of F4/80 in the *db/db* CTL group was similar to the C57B/L6 CTL group, which suggests macrophage infiltration in inguinal adipose tissue, unlike visceral adipose tissue, is not affected by obesity and therefore it may not contribute to obesity-induced inflammation. This hypothesis is in agreement with other findings that show subcutaneous fat has less inflammation than visceral fat (Bremer, Devaraj et al. 2011). Therefore, increased levels of F4/80 in inguinal adipose tissue of *t*10-*c*12 CLA isomer-fed mice, and not their epididymal adipose tissue, could be explained by the fact that cytokines secreted by the F4/80 positive classically activated macrophages stimulate the induction of beige adipocytes (Qiu, Nguyen et al. 2014). Thus macrophages could have dual roles based on the specific adipose depot; increased metabolism in inguinal adipose tissue and induction of inflammation in visceral adipose tissue.

Similar to *t*10-*c*12 CLA fed mice, the lean mice under calorie restriction also had higher levels of macrophage markers in their inguinal adipose tissue. These data could be explained in two different ways. First, similar to *t*10-*c*12 CLA-fed lean animals, the increase in macrophages in the calorie restricted lean group could lead to the induction of

beige adipocytes. The presence of TBX-1 in the nucleus of inguinal adipocytes of calorie restricted lean animals supports this theory. A second explanation for this observation is that the calorie restricted C57BL/6 group had a small number of adipocytes containing nuclear TBX-1, but very high levels of F4/80 in their inguinal adipose tissue. This leads us to suggest that high levels of F4/80 in the lean calorie restricted group are indicative of an increase in inflammation and not induction of beige adipocytes. However, to confirm this speculation, inflammatory cytokines such as TNFα and IL-6 should be measured in inguinal adipose tissue as well. It should be noted that the differences in macrophage content in Figures 28a and 29c, d could be attributed to differences in the adipose depots, the techniques (flow cytometry and Western blotting) or the antibodies employed (monoclonal versus polyclonal). It is most likely that the differences are characteristic of the two adipose depots that were examined, epididymal and inguinal.

Given the importance of macrophages to adipose tissue, we also investigated the effect of CLA isomers on classically activated M1 macrophages and alternatively activated M2 macrophages in epididymal and inguinal adipose tissue by flow cytometry and IF, respectively. The flow cytometry data suggest that the lean C57BL/6 mice had higher ratio of M2/M1 macrophages, while the M1 and M2 macrophages were equally distributed in obese *db/db* mice. As expected, the proportion of M1 macrophages was higher in epididymal adipose tissue of *db/db* mice compared to C57B/L6 mice, and these percentages were not altered in the CLA isomer groups, but they were reduced with calorie restriction and thus may improve obesity-induced inflammation.

To investigate the number and localization of the two forms of macrophages, M1 and M2, flow cytometry and IF were employed. Although both of these methods are

based on immune detection, different antibodies were used to detect M1 and M2 macrophages. For flow cytometry, the M1 versus M2 ratio was determined with $F4/80^{+}CD11c^{-}$ and $F4/80^{+}CD11c^{+}$, respectively, however, in IF, iNOS and CD206 were used to distinguished M1 and M2 macrophages, respectively. This inconsistency was due to the fact that CD11c is present in DCs as well, and in IF, both M2 and DCs would stain CD11c+ and distinguishing them would be impossible. Therefore, results from these distinct methods may not completely support each other.

Adipose tissue is an immune organ since it is involved in anti-microbial defense and inflammation. In addition to macrophages, which are the most abundant leukocyte in WAT, other immune cells such as T cells and DCs are also present. The role of macrophage infiltration during obesity was studied previously; however, the potential role of other immune cells such as T cells and DCs is less clear. Here we investigated the effect of CLA isomers on T cells and DCs in epididymal adipose tissue of obese *db/db* and lean C57BL/6 mice. Our data show that the *db/db* mice have a lower proportion of T cells compared to C57/BL6 mice. This finding is in agreement with the findings of others showing that T cells are decreased in the adipose tissue of obese *ob/ob*, *db/db* and DIO mice compared to their respective lean controls (Huh, Park et al. 2014). However, this controversy could be explained by the fact that *db/db* and *ob/ob* mice are known to have thymic and lymph node atrophy and impaired cell-mediated immune responses (Mandel and Mahmoud 1978; Chandra 1980; Howard, Lord et al. 1999; Matarese 2000). Since T cells develop in the thymus, fewer numbers of T cells in the *db/db* mice is not unexpected. Interestingly, the *db/db t*10-*c*12 CLA isomer and PW groups had even lower numbers of T cells, which further suggests a reduction in adiposity could decrease

inflammation in WAT. However, the *t*10-*c*12 CLA isomer did not have a similar effect in C57BL/6 mice, as the T cells numbers were unchanged. This effect could be due to the degree of fat loss in the *db/db* mice compare to C57BL/6 mice.

DCs are innate immune cells that are involved in promoting inflammation in the obese state (Bertola, Ciucci et al. 2012). However, in contrast with this statement, our data show a trend (P=0.07) for lower DCs in the obese *db/db* compared to lean C57BL/6 mice. A similar effect was observed with mature DCs as the obese *db/db* mice had fewer mature DCs compared to lean C57BL/6 mice, while the proportion of immature DCs were higher in the obese *db/db* mice. These opposing results could be due to the age of our animals, which were 11 weeks old at the end of the study, compared to Bertola et al. (2012), whose mice were about 25 weeks old. We also showed that reduced adiposity through calorie restriction but not *t*10-*c*12 CLA isomer consumption could reduce the numbers of DCs in the obese state (i.e. *db/db* mice). This finding could be explained through the effects of macrophages on DCs. It is known that DCs promote macrophage infiltration in WAT (Stefanovic-Racic, Yang et al. 2012). If we assume there is a similar effect by macrophages on DCs, then we can conclude that lower numbers of macrophages in *db/db* PW group are responsible for the lower number of DCs in this group compared to the rest of the *db/db* mice. Interestingly, the *t*10-*c*12 CLA isomer had a completely opposite effect on DCs in C57BL/6 mice as the proportion of DCs was increased. A recent study reported that feeding C57BL/6 mice 1% w/w *c*9-*t*11 CLA for 5 weeks suppressed DCs in the spleen and bone marrow, however, our data show no changes in the *c*9-*t*11 CLA isomer group compared to the rest of the groups. This difference could be explained by the different doses of the CLA. Our data also suggest

that dendritic cell maturation, which leads to activation of T cells, is a leptin dependent process, since a genotype effect was observed in both mature and immature DCs populations.

7.2.4.5 Effect of CLA isomers and calorie restriction in blood glucose

One of the important effects of CLA isomers, specifically the *t*10-*c*12 CLA isomer, observed in the *fa/fa* Zucker rat was a reduction in impaired glucose tolerance caused by obesity (Noto, Zahradka et al. 2007). It was of interest to investigate if the reduced adiposity in our animals was accompanied by an improvement of hyperglycemia in the obese *db/db* mice. Unlike the *fa/fa* Zucker, the *db/db* mice are a model of diabetes and they develop hyperglycemia. The *t*10-*c*12 CLA isomer elevated blood glucose in both hyperglycemic *db/db* and normoglycemic lean C57BL/6 mice compared to their respective CTL. To investigate the possible contribution of adipose tissue, we analyzed adipsin, an adipokine that has been shown improve β-cell function in diabetes (Lo, Ljubicic et al. 2014). Adipsin is found in two forms, glycosylated and non-glycosylated. In healthy adipose tissue, adipsin is mostly found in the glycosylated form. Since adipsin levels are decreased in many animal models of obesity and diabetes (Flier, Cook et al. 1987), the low levels of adipsin in the *db/db* mice were expected. However, in the *t*10-*c*12 CLA-fed groups, adipsin glycosylation was decreased in WAT in both genotypes. These data suggest consuming *t*10-*c*12 CLA results in adipsin inactivation and therefore worsens the effect of obesity on hyperglycemia. In addition, since adipsin assists with proper insulin secretion by pancreatic β-cells (Lo, Ljubicic et al. 2014), the low levels of adipsin may drive diabetes to the next level. One of the controversies in the field of CLA

is the observation that the *t*10-*c*12 CLA isomer has an anti-diabetic effect in rats, while this effect is not observed in mice (Nagao, Inoue et al. 2003; LaRosa, Miner et al. 2006). Thus, the levels of adipsin and its glycosylated form in rat models fed the *t*10-*c*12 CLA isomer could prove valuable information, however, this has not been investigated.

7.3 Conclusions and implications

The current study was designed to investigate the anti-obesity effect of CLA isomers with respect to lipid droplet modulation, Wnt/β-catenin pathway activity and the modulation of adipogenesis by either decreasing adipocyte production or increasing adipocyte death. We also investigated the effects of CLA isomers on immune cell populations in obese and lean mice.

The current study suggests that in the 3T3-L1 cell line, *t*10-*c*12 and *c*9-*t*11 CLA affect early and late adipocyte differentiation by different mechanisms. Specifically, *t*10-*c*12 CLA inhibits adipocyte differentiation by inhibiting perilipin-1 phosphorylation, reducing HSL levels, and inhibiting lipolysis via PKCα, a mechanism that has not been previously suggested. In contrast, *c*9-*t*11 CLA treatment of 3T3-L1 adipocytes increases adipocyte cell size, a characteristic that is observed during obesity, although no changes in the adipokine profile were detected with *c*9-*t*11 CLA.

*t*10-*c*12 CLA also inhibits adipocyte differentiation by directly affecting β-catenin stability in 3T3-L1 adipocytes, resulting in the sequestration of PPARγ in an inactive complex, which thus prevents progression of adipogenesis. On the other hand, *c*9-*t*11 CLA inhibits β-catenin and does not stimulate adipocyte differentiation. In animals, CLA isomers act differently in the *db/db* and C57BL/6 mice. Elevation of β-catenin levels was observed only in the *db/db* mice, while β-catenin phosphorylation at Ser675 was decreased in both *db/db* and C57BL/6 mice. Finally the *t*10-*c*12 CLA increases cyclin D1 levels in the *db/db* mice, and a similar effect was observed in *c*9-*t*11 CLA treated mice despite lower levels of β-catenin. This finding leads to speculation that there are other factors involved in regulating cyclin D1 in addition to β-catenin. The direct effect of *t*10-

*c*12 CLA on β-catenin was confirmed in animals, although the consequence of this effect is unclear. Wnt/β-catenin activation and a subsequent increase in cyclin D1 were not the cause of fat loss in the *t*10-*c*12 CLA and PW groups. Figure 32 depicts a possible mechanism of action for *t*10-*c*12 CLA on Wnt/β-catenin signaling.

This study confirmed that of the two most metabolically active isomers of CLA, the *t*10-*c*12 CLA is the isomer responsible for weight loss and its effect was independent of feed intake. Fat loss was achieved successfully with both *t*10-*c*12 CLA and calorie restriction, however, they operate through distinct mechanisms. Weight loss in the *t*10-*c*12 CLA-fed animals was fat mass–specific, while reduced body weight as a result of calorie restriction was due to decreases in both fat and lean mass. The ability of *t*10-*c*12 CLA to reduce fat mass was observed in both lean and obese animals. The *t*10-*c*12 CLA isomer has no effect on the recruitment of new adipocytes, although it lowered adipocyte cell death compared to CTL as determined by caspase-3 activity. In contrast, weight loss as a result of calorie restriction leads to a decrease in the proportions of preadipocytes, either by preventing their differentiation from stem cells or by triggering their differentiation into adipocytes. Similar to *t*10-*c*12 CLA, calorie restriction also reduced adipocyte death but to a lesser extent. However, the presence of crown like structures in the *t*10-*c*12 CLA fed mice indicates remodeling is occurring. As has been shown in several studies, crown-like structures are a site of adipocyte death. In the absence of apoptosis and autophagy as shown in this study it is most likely that loss of adipocytes due to treatment of *t*10-*c*12 CLA occurs through necrosis, further investigation is required to confirm this possibility.

The effects of *t*10-*c*12 CLA on macrophages were fat depot dependent. *t*10-*c*12 CLA does not alter macrophage levels in epididymal fat, but it increases macrophages in inguinal adipose based on higher protein levels of F4/80. In contrast, weight loss as a result of calorie restriction reduced macrophage infiltration in epididymal adipose tissue and possibly reduced obesity–induced inflammation; however, calorie restriction increased levels of the macrophage marker, F4/80, in the inguinal fat of lean mice. Calorie restriction also reduced the proportions of DCs in the WAT of obese *db/db* mice, while *t*10-*c*12 CLA increased DCs in epididymal adipose tissue of C57BL/6, which could exacerbate inflammation. Despite the apparent positive effects of weight loss, *t*10-*c*12 CLA consumption elevated blood glucose levels. Weight loss via calorie restriction also did not improve blood glucose in obese mice nor did it contribute to a worsening of this condition. A summary of the effects of the *t*10-*c*12 CLA isomer and calorie restriction in obese *db/db* and lean mice is shown in Table 8.

Although CLA is considered a nutraceutical, and *t*10-*c*12 CLA has been thoroughly studied as an anti-obesity agent, this isomer is not naturally found at high levels in food. In contrast, the *c*9-*t*11 isomer is naturally abundant in foods such as cheese, milk and ruminant meat (Kepler, Hirons et al. 1966). Therefore, the dose of *t*10-*c*12 CLA used in the experimental models is not achievable by consuming natural food products. Furthermore, since the current study examined the effect of CLA isomers and feed restriction in 11-week old male mice, which are considered fully mature and adult, the findings of this study may not be applicable to children and female subjects. The major contribution of this study to the field of physiology has been the establishment of a link between a naturally derived component, such as CLA, and an anti-obesity effect that is

manifested through alterations in adipocyte metabolism and phenotype. The outcomes of *t*10-*c*12 CLA consumption are similar to those obtained through calorie restriction, which represents the most common and successful approach to weight control today, although they act through different mechanisms. Nevertheless, the fact that *t*10-*c*12 CLA treatment increases blood glucose argues against this CLA isomer being a useful nutraceutical for promoting weight loss. Rather calorie restriction, which does not lead to an increase in blood glucose, would be the prefered approach for losing weight.

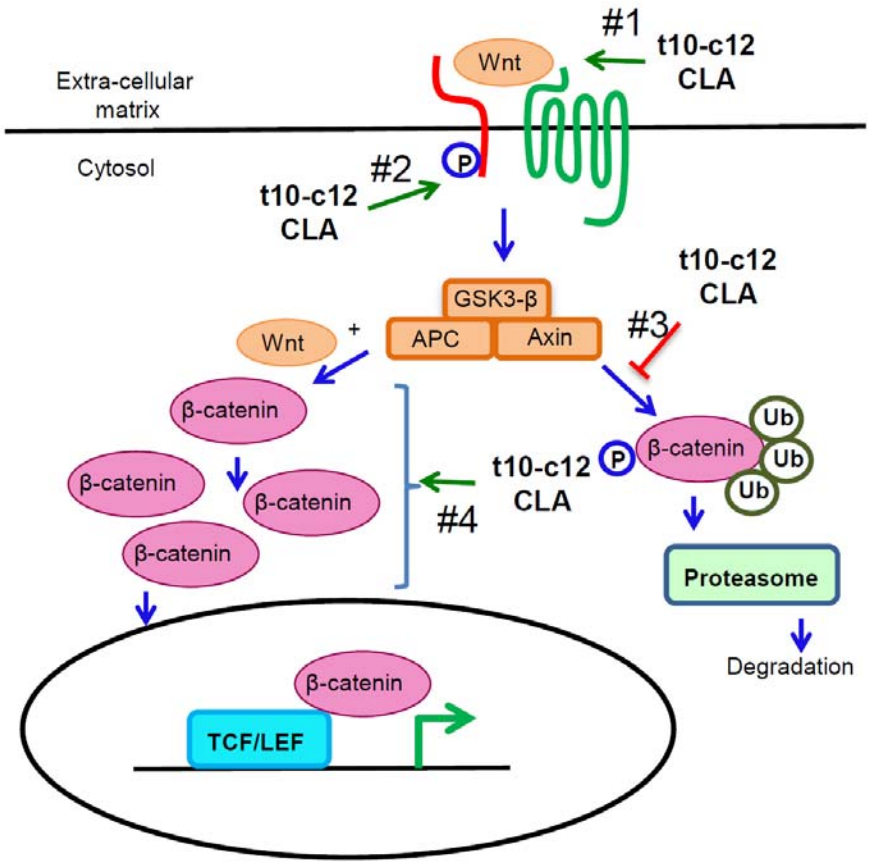

Figure 32: A summary of the effects of the CLA isomers on Wnt/β-catenin signaling

The mechanism of action of *t*10-*c*12 CLA at four different sites was investigated. #1) *t*10-*c*12 CLA does not alter Wnt10b and SFRP-5, the extracellular regulators of Wnt signaling; #2) *t*10-*c*12 CLA does not affect LRP5/6 levels or its phosphorylation, one of the intracellular regulators of the Wnt signaling; #3) *t*10-*c*12 CLA does not affect β-catenin degradation; #4) A direct effect of *t*10-*c*12 CLA on β-catenin is the likely mechanism by which *t*10-*c*12 CLA affects Wnt/ β-catenin signaling

.

Table 8. A summary of the effects of the CLA isomers and calorie restriction (PW groups) in obese and lean mice.[1]

	db/db									**C57BL/6**								
	Adipocyte turnover				**Macrophage**		**TBX-1**		**Blood glucose**	**Adipocyte turnover**				**Macrophage**		**TBX-1**		**Blood glucose**
	Stem cell adipocyte	Preadipocyte	Autophagy	Apoptosis	Inguinal depot	Epididymal depot	Levels	Localization		Stem cell adipocyte	Preadipocyte	Autophagy	Apoptosis	Inguinal depot	Epididymal depot	Levels	Localization	
***c*9-*t*11 CLA**	↔	↔	↔	↔	↔	↔	↑	C	↔	↔	↔	↔	↓	↔	↔	↔	C	↔
***t*10-*c*12 CLA**	↔	↔	↔	↓	↑	↔	↑	N	↑	↔	↔	↔	↓	↑	↔	↓	N	↑
PW	↔	↓	↔	↔	↔	↓	↑	C	↔	↔	↔	↔	↓	↑	↔	↓	C & N	↔

[1]Comparisons are relative to the respective control group of the same genotype.

↑: increased, ↓: decreased, ↔: unchanged, C: cytosol, N: nucleus

8. Strengths and limitations

8.1 Strengths

- CLA isomers: the availability of high purity single isomers allowed the examination of isomer-specific effects of CLA.
- Complementary experimental designs: use of both *in vitro* and *in vivo* approaches to compare and contrast the mechanism of action and physiological actions of the CLA isomers on adipocytes as single cells and as a component of adipose tissue.
- 3T3-L1 cell line: these cells allowed the study of both early and late adipocyte differentiation.
- Animal model: *db/db* mice are a physiologically relevant model of obesity that were appropriate for the study of weight loss by CLA, with comparison to weight loss by calorie restriction (pair weight group) and to healthy lean C57BL/6 mice.
- Primary SVF: isolation of primary cells allowed characterization of key cell types in adipose tissue, including stem cells, preadipocytes and immune cells, by flow cytometry.
- Study length: based on a previous study with the *t*10-*c*12 CLA and *db/db* mice, the 4 week timeframe was appropriate for significant weight loss but still provided sufficient adipose tissue for the analyses.
- Methodological approaches: several complementary techniques were used in parallel to validate the results.

- ## 8.2 Limitations

  - Adipocyte differentiation: 3T3-L1 preadipocytes are already committed to the adipocyte lineage; therefore, investigating the effect of CLA isomers on the commitment phase of adipocyte differentiation was not possible.
  - Specificity of chemical inhibitors: chemical inhibitors can have unknown effects on other signaling pathways.
  - Monogenic obesity model: a leptin receptor mutation is very rare in humans, and the mutation may affect physiological processes other than those associated with obesity.
  - Dose of CLA: the amount of CLA used in this study can not attained through food consumption by humans or through commercially available supplements
  - Sex: the effects of CLA isomers and feed restriction were studied in male mice, thus the data may not be relevant to females.
  - Beige adipocytes: one of the suggested mechanisms in this thesis for anti-obesity action of *t*10-*c*12 CLA isomers and feed restriction was an increase in metabolically active beige adipocytes in inguinal adipose tissue.

9. Future directions

- Confirm the role of PKCα in mediating the effects of the *t*10-*c*12 CLA isomer on perilipin phosphorylation and adipokine secretion by transfection of dominant negative PKCα into 3T3-L1 adipocytes.
- Investigate the role of of PKCα in mediating the effects of the *t*10-*c*12 CLA isomer in an *in vivo* model
- Investigate the mechanism by which the *t*10-*c*12 CLA isomer regulates the size of 3T3-L1 adipocytes.
- Determine whether there is a direct effect of *t*10-*c*12 CLA on the ability of HSL to activate PPARγ gene expression.
- Determine the contribution of β-catenin to the actions of *t*10-*c*12 CLA by transfecting 3T3-L1 adipocytes on day 4 of differentiation with β-catenin siRNA.
- Investigate the effect of CLA isomers in females since they have higher amounts of subcutaneous adipose relative to visceral adipose; CLA might have a more pronounced browning effect in females than in males.
- Investigate the effect of CLA isomers on β-catenin and cell cycle regulators in the inguinal fat pad as it has a higher rate of adipogenesis than the epididymal fat pad.
- Investigate the effect of CLA isomers in pancreatic islets and on β-cell function.
- Investigate the effect of CLA isomers on fatty liver.
- Investigate the effect of CLA isomers and calorie restriction on autophagy in greater detail

- Compare inflammation markers in subcutaneous versus visceral fat depots in response to CLA isomers.
- Examine the effect of the *t*10-*c*12 CLA isomer and calorie restriction in a diet-induced model of obesity.
- Determine the number and activity of mitochondria in inguinal adipose tissue of *t*10-*c*12 CLA fed mice compared to the CTL group and establish whether this CLA isomer affects thermogenesis.
- Examine the relationship between macrophage polarization and adipocyte clearance by necrosis.

10. References

Aguilera, C.M., J. Olza, and A. Gil. 2013. Genetic susceptibility to obesity and metabolic syndrome in childhood. *Nutricion hospitalaria*. 28 Suppl 5:44-55.

Ahn, J., H. Lee, S. Kim, and T. Ha. 2010. Curcumin-induced suppression of adipogenic differentiation is accompanied by activation of Wnt/beta-catenin signaling. *American journal of physiology. Cell physiology*. 298:C1510-1516.

Anderson, P.D., N.N. Mehta, M.L. Wolfe, C.C. Hinkle, L. Pruscino, L.L. Comiskey, J. Tabita-Martinez, K.F. Sellers, M.R. Rickels, R.S. Ahima, and M.P. Reilly. 2007. Innate immunity modulates adipokines in humans. *The Journal of clinical endocrinology and metabolism*. 92:2272-2279.

Anthonsen, M.W., L. Ronnstrand, C. Wernstedt, E. Degerman, and C. Holm. 1998. Identification of novel phosphorylation sites in hormone-sensitive lipase that are phosphorylated in response to isoproterenol and govern activation properties in vitro. *The Journal of biological chemistry*. 273:215-221.

Aranda, A., and A. Pascual. 2001. Nuclear hormone receptors and gene expression. *Physiological reviews*. 81:1269-1304.

Arita, Y., S. Kihara, N. Ouchi, M. Takahashi, K. Maeda, J. Miyagawa, K. Hotta, I. Shimomura, T. Nakamura, K. Miyaoka, H. Kuriyama, M. Nishida, S. Yamashita, K. Okubo, K. Matsubara, M. Muraguchi, Y. Ohmoto, T. Funahashi, and Y. Matsuzawa. 1999. Paradoxical decrease of an adipose-specific protein, adiponectin, in obesity. *Biochem Biophys Res Commun*. 257:79-83.

Ashwell, M.S., R.P. Ceddia, R.L. House, J.P. Cassady, E.J. Eisen, T.E. Eling, J.B. Collins, S.F. Grissom, and J. Odle. 2010. Trans-10, cis-12-conjugated linoleic acid alters hepatic gene expression in a polygenic obese line of mice displaying hepatic lipidosis. *The Journal of nutritional biochemistry*. 21:848-855.

Ayer, J., M. Charakida, J.E. Deanfield, and D.S. Celermajer. 2015. Lifetime risk: childhood obesity and cardiovascular risk. *European heart journal*.

Ayers, S.D., K.L. Nedrow, R.E. Gillilan, and N. Noy. 2007. Continuous nucleocytoplasmic shuttling underlies transcriptional activation of PPARgamma by FABP4. *Biochemistry*. 46:6744-6752.

Baar, R.A., C.S. Dingfelder, L.A. Smith, D.A. Bernlohr, C. Wu, A.J. Lange, and E.J. Parks. 2005. Investigation of in vivo fatty acid metabolism in AFABP/aP2(-/-) mice. *American journal of physiology. Endocrinology and metabolism*. 288:E187-193.

Baerga, R., Y. Zhang, P.H. Chen, S. Goldman, and S. Jin. 2009. Targeted deletion of autophagy-related 5 (atg5) impairs adipogenesis in a cellular model and in mice. *Autophagy*. 5:1118-1130.

Barbatelli, G., I. Murano, L. Madsen, Q. Hao, M. Jimenez, K. Kristiansen, J.P. Giacobino, R. De Matteis, and S. Cinti. 2010. The emergence of cold-induced brown adipocytes in mouse white fat depots is determined predominantly by white to brown adipocyte transdifferentiation. *American journal of physiology. Endocrinology and metabolism*. 298:E1244-1253.

Barnea, G., W. Strapps, G. Herrada, Y. Berman, J. Ong, B. Kloss, R. Axel, and K.J. Lee. 2008. The genetic design of signaling cascades to record receptor activation. *Proceedings of the National Academy of Sciences of the United States of America*. 105:64-69.

Bates, S.H., R.N. Kulkarni, M. Seifert, and M.G. Myers, Jr. 2005. Roles for leptin receptor/STAT3-dependent and -independent signals in the regulation of glucose homeostasis. *Cell metabolism*. 1:169-178.

Baxa, C.A., R.S. Sha, M.K. Buelt, A.J. Smith, V. Matarese, L.L. Chinander, K.L. Boundy, and D.A. Bernlohr. 1989. Human adipocyte lipid-binding protein: purification of the protein and cloning of its complementary DNA. *Biochemistry*. 28:8683-8690.

Belda, B.J., J.T. Thompson, P.O. Eser, and J.P. Vanden Heuvel. 2012. 10e12z CLA alters adipocyte differentiation and adipocyte cytokine expression and induces macrophage proliferation. *The Journal of nutritional biochemistry*. 23:510-518.

Belfrage, P., G. Fredrikson, N.O. Nilsson, and P. Stralfors. 1981. Regulation of adipose-tissue lipolysis by phosphorylation of hormone-sensitive lipase. *International journal of obesity*. 5:635-641.

Beller, M., D. Riedel, L. Jansch, G. Dieterich, J. Wehland, H. Jackle, and R.P. Kuhnlein. 2006. Characterization of the Drosophila lipid droplet subproteome. *Molecular & cellular proteomics : MCP*. 5:1082-1094.

Bennett, C.N., S.E. Ross, K.A. Longo, L. Bajnok, N. Hemati, K.W. Johnson, S.D. Harrison, and O.A. MacDougald. 2002. Regulation of Wnt signaling during adipogenesis. *The Journal of biological chemistry*. 277:30998-31004.

Bernlohr, D.A., C.W. Angus, M.D. Lane, M.A. Bolanowski, and T.J. Kelly, Jr. 1984. Expression of specific mRNAs during adipose differentiation: identification of an mRNA encoding a homologue of myelin P2 protein. *Proceedings of the National Academy of Sciences of the United States of America*. 81:5468-5472.

Bernlohr, D.A., M.A. Bolanowski, T.J. Kelly, Jr., and M.D. Lane. 1985. Evidence for an increase in transcription of specific mRNAs during differentiation of 3T3-L1 preadipocytes. *The Journal of biological chemistry*. 260:5563-5567.

Berry, R., and M.S. Rodeheffer. 2013. Characterization of the adipocyte cellular lineage in vivo. *Nature cell biology*. 15:302-308.

Bertola, A., T. Ciucci, D. Rousseau, V. Bourlier, C. Duffaut, S. Bonnafous, C. Blin-Wakkach, R. Anty, A. Iannelli, J. Gugenheim, A. Tran, A. Bouloumie, P. Gual, and A. Wakkach. 2012. Identification of adipose tissue dendritic cells correlated with obesity-associated insulin-resistance and inducing Th17 responses in mice and patients. *Diabetes*. 61:2238-2247.

Bickel, P.E., J.T. Tansey, and M.A. Welte. 2009. PAT proteins, an ancient family of lipid droplet proteins that regulate cellular lipid stores. *Biochimica et biophysica acta*. 1791:419-440.

Billon, N., and C. Dani. 2012. Developmental origins of the adipocyte lineage: new insights from genetics and genomics studies. *Stem cell reviews*. 8:55-66.

Blanchette-Mackie, E.J., N.K. Dwyer, T. Barber, R.A. Coxey, T. Takeda, C.M. Rondinone, J.L. Theodorakis, A.S. Greenberg, and C. Londos. 1995. Perilipin is located on the surface layer of intracellular lipid droplets in adipocytes. *Journal of lipid research*. 36:1211-1226.

Blankson, H., J.A. Stakkestad, H. Fagertun, E. Thom, J. Wadstein, and O. Gudmundsen. 2000. Conjugated linoleic acid reduces body fat mass in overweight and obese humans. *The Journal of nutrition*. 130:2943-2948.

Blogowski, W., M. Budkowska, D. Salata, K. Serwin, B. Dolegowska, M. Lokaj, P. Prowans, and T. Starzynska. 2013. Clinical analysis of selected complement-derived molecules in human adipose tissue. *Journal of translational medicine*. 11:11.

Bluher, M., N. Kloting, S. Wueest, E.J. Schoenle, M.R. Schon, A. Dietrich, M. Fasshauer, M. Stumvoll, and D. Konrad. 2014. Fas and FasL expression in human adipose tissue is related to obesity, insulin resistance, and type 2 diabetes. *The Journal of clinical endocrinology and metabolism*. 99:E36-44.

Bocking, C., H. Harb, M.J. Ege, N. Zehethofer, K. Fischer, J. Krauss, O. Holst, R.M. Nusing, B. Lindner, E. von Mutius, H. Renz, H. Garn, and P.I. Pfefferle. 2014. Bioavailability and allergoprotective capacity of milk-associated conjugated linoleic acid in a murine model

of allergic airway inflammation. *International archives of allergy and immunology*. 163:234-242.

Bornstein, S.R., M. Abu-Asab, A. Glasow, G. Path, H. Hauner, M. Tsokos, G.P. Chrousos, and W.A. Scherbaum. 2000. Immunohistochemical and ultrastructural localization of leptin and leptin receptor in human white adipose tissue and differentiating human adipose cells in primary culture. *Diabetes*. 49:532-538.

Bosello, O., and M. Zamboni. 2000. Visceral obesity and metabolic syndrome. *Obesity reviews : an official journal of the International Association for the Study of Obesity*. 1:47-56.

Boss, O., S. Samec, A. Paoloni-Giacobino, C. Rossier, A. Dulloo, J. Seydoux, P. Muzzin, and J.P. Giacobino. 1997. Uncoupling protein-3: a new member of the mitochondrial carrier family with tissue-specific expression. *FEBS letters*. 408:39-42.

Bottcher, Y., H. Unbehauen, N. Kloting, K. Ruschke, A. Korner, D. Schleinitz, A. Tonjes, B. Enigk, S. Wolf, K. Dietrich, M. Koriath, G.H. Scholz, Y.H. Tseng, A. Dietrich, M.R. Schon, W. Kiess, M. Stumvoll, M. Bluher, and P. Kovacs. 2009. Adipose tissue expression and genetic variants of the bone morphogenetic protein receptor 1A gene (BMPR1A) are associated with human obesity. *Diabetes*. 58:2119-2128.

Bouchoux, J., F. Beilstein, T. Pauquai, I.C. Guerrera, D. Chateau, N. Ly, M. Alqub, C. Klein, J. Chambaz, M. Rousset, J.M. Lacorte, E. Morel, and S. Demignot. 2011. The proteome of cytosolic lipid droplets isolated from differentiated Caco-2/TC7 enterocytes reveals cell-specific characteristics. *Biology of the cell / under the auspices of the European Cell Biology Organization*. 103:499-517.

Bowers, R.R., and M.D. Lane. 2008. Wnt signaling and adipocyte lineage commitment. *Cell cycle*. 7:1191-1196.

Bozaoglu, K., K. Bolton, J. McMillan, P. Zimmet, J. Jowett, G. Collier, K. Walder, and D. Segal. 2007. Chemerin is a novel adipokine associated with obesity and metabolic syndrome. *Endocrinology*. 148:4687-4694.

Bozaoglu, K., D. Segal, K.A. Shields, N. Cummings, J.E. Curran, A.G. Comuzzie, M.C. Mahaney, D.L. Rainwater, J.L. VandeBerg, J.W. MacCluer, G. Collier, J. Blangero, K. Walder, and J.B. Jowett. 2009. Chemerin is associated with metabolic syndrome phenotypes in a Mexican-American population. *The Journal of clinical endocrinology and metabolism*. 94:3085-3088.

Brasaemle, D.L., B. Rubin, I.A. Harten, J. Gruia-Gray, A.R. Kimmel, and C. Londos. 2000. Perilipin A increases triacylglycerol storage by decreasing the rate of triacylglycerol hydrolysis. *The Journal of biological chemistry*. 275:38486-38493.

Bray, G.A. 1977. The Zucker-fatty rat: a review. *Federation proceedings*. 36:148-153.

Bremer, A.A., S. Devaraj, A. Afify, and I. Jialal. 2011. Adipose tissue dysregulation in patients with metabolic syndrome. *The Journal of clinical endocrinology and metabolism*. 96:E1782-1788.

Brown, J.M., M.S. Boysen, S. Chung, O. Fabiyi, R.F. Morrison, S. Mandrup, and M.K. McIntosh. 2004. Conjugated linoleic acid induces human adipocyte delipidation: autocrine/paracrine regulation of MEK/ERK signaling by adipocytokines. *The Journal of biological chemistry*. 279:26735-26747.

Brown, J.M., M.S. Boysen, S.S. Jensen, R.F. Morrison, J. Storkson, R. Lea-Currie, M. Pariza, S. Mandrup, and M.K. McIntosh. 2003. Isomer-specific regulation of metabolism and PPARgamma signaling by CLA in human preadipocytes. *Journal of lipid research*. 44:1287-1300.

C.D.A. 2006. The prevalence and costs of diabetes. Retrieved January 5, 2006 from the World Wide *Web:* http://www.diabetes.ca/Section_About/prevalence.asp.

Cai, D., H. Li, B. Zhou, L. Han, X. Zhang, G. Yang, and G. Yang. 2012. Conjugated linoleic acid supplementation caused reduction of perilipin1 and aberrant lipolysis in epididymal adipose tissue. *Biochemical and biophysical research communications*. 422:621-626.

Cancello, R., C. Henegar, N. Viguerie, S. Taleb, C. Poitou, C. Rouault, M. Coupaye, V. Pelloux, D. Hugol, J.L. Bouillot, A. Bouloumie, G. Barbatelli, S. Cinti, P.A. Svensson, G.S. Barsh, J.D. Zucker, A. Basdevant, D. Langin, and K. Clement. 2005. Reduction of macrophage infiltration and chemoattractant gene expression changes in white adipose tissue of morbidly obese subjects after surgery-induced weight loss. *Diabetes*. 54:2277-2286.

Cannon, B., and J. Nedergaard. 2004. Brown adipose tissue: function and physiological significance. *Physiological reviews*. 84:277-359.

Cao, Z.P., F. Wang, X.S. Xiang, R. Cao, W.B. Zhang, and S.B. Gao. 2007. Intracerebroventricular administration of conjugated linoleic acid (CLA) inhibits food intake by decreasing gene expression of NPY and AgRP. *Neuroscience letters*. 418:217-221.

Capeau, J., J. Magre, O. Lascols, M. Caron, V. Bereziat, C. Vigouroux, and J.P. Bastard. 2005. Diseases of adipose tissue: genetic and acquired lipodystrophies. *Biochemical Society transactions*. 33:1073-1077.

Cefalu, W.T. 2001. Insulin resistance: cellular and clinical concepts. *Experimental biology and medicine*. 226:13-26.

Chandra, R.K. 1980. Cell-mediated immunity in genetically obese C57BL/6J ob/ob) mice. *The American journal of clinical nutrition*. 33:13-16.

Chang, B.H., L. Li, A. Paul, S. Taniguchi, V. Nannegari, W.C. Heird, and L. Chan. 2006. Protection against fatty liver but normal adipogenesis in mice lacking adipose differentiation-related protein. *Molecular and cellular biology*. 26:1063-1076.

Chang, S., B. Graham, F. Yakubu, D. Lin, J.C. Peters, and J.O. Hill. 1990. Metabolic differences between obesity-prone and obesity-resistant rats. *The American journal of physiology*. 259:R1103-1110.

Chatzigeorgiou, A., A. Halapas, K. Kalafatakis, and E. Kamper. 2009. The use of animal models in the study of diabetes mellitus. *In vivo*. 23:245-258.

Chawla, A., K.D. Nguyen, and Y.P. Goh. 2011. Macrophage-mediated inflammation in metabolic disease. *Nature reviews. Immunology*. 11:738-749.

Chen, H., O. Charlat, L.A. Tartaglia, E.A. Woolf, X. Weng, S.J. Ellis, N.D. Lakey, J. Culpepper, K.J. Moore, R.E. Breitbart, G.M. Duyk, R.I. Tepper, and J.P. Morgenstern. 1996. Evidence that the diabetes gene encodes the leptin receptor: identification of a mutation in the leptin receptor gene in db/db mice. *Cell*. 84:491-495.

Chen, W., B. Chang, X. Wu, L. Li, M. Sleeman, and L. Chan. 2013. Inactivation of Plin4 downregulates Plin5 and reduces cardiac lipid accumulation in mice. *American journal of physiology. Endocrinology and metabolism*. 304:E770-779.

Childhoodobesityfoundation. 2014. http://www.childhoodobesityfoundation.ca/.

Chmurzynska, A. 2006. The multigene family of fatty acid-binding proteins (FABPs): function, structure and polymorphism. *Journal of applied genetics*. 47:39-48.

Cho, M., S. Park, J. Gwak, D.E. Kim, S.S. Yea, J.G. Shin, and S. Oh. 2008. Bisindoylmaleimide I suppresses adipocyte differentiation through stabilization of intracellular beta-catenin protein. *Biochemical and biophysical research communications*. 367:195-200.

Chobanian, A.V., G.L. Bakris, H.R. Black, W.C. Cushman, L.A. Green, J.L. Izzo, Jr., D.W. Jones, B.J. Materson, S. Oparil, J.T. Wright, Jr., E.J. Roccella, D.E. Joint National Committee on Prevention, L. Treatment of High Blood Pressure. National Heart, I. Blood, and C. National High Blood Pressure Education Program Coordinating. 2003. Seventh report of the Joint National Committee on Prevention, Detection, Evaluation, and Treatment of High Blood Pressure. *Hypertension*. 42:1206-1252.

Choi, J.H., A.S. Banks, J.L. Estall, S. Kajimura, P. Bostrom, D. Laznik, J.L. Ruas, M.J. Chalmers, T.M. Kamenecka, M. Bluher, P.R. Griffin, and B.M. Spiegelman. 2010. Anti-

diabetic drugs inhibit obesity-linked phosphorylation of PPARgamma by Cdk5. *Nature*. 466:451-456.

Choi, Y., Y. Park, J.M. Storkson, M.W. Pariza, and J.M. Ntambi. 2002. Inhibition of stearoyl-CoA desaturase activity by the cis-9,trans-11 isomer and the trans-10,cis-12 isomer of conjugated linoleic acid in MDA-MB-231 and MCF-7 human breast cancer cells. *Biochemical and biophysical research communications*. 294:785-790.

Choy, L., and R. Derynck. 2003. Transforming growth factor-beta inhibits adipocyte differentiation by Smad3 interacting with CCAAT/enhancer-binding protein (C/EBP) and repressing C/EBP transactivation function. *The Journal of biological chemistry*. 278:9609-9619.

Choy, L., J. Skillington, and R. Derynck. 2000. Roles of autocrine TGF-beta receptor and Smad signaling in adipocyte differentiation. *The Journal of cell biology*. 149:667-682.

Christodoulides, C., C. Lagathu, J.K. Sethi, and A. Vidal-Puig. 2009. Adipogenesis and WNT signalling. *Trends in endocrinology and metabolism: TEM*. 20:16-24.

Christy, R.J., K.H. Kaestner, D.E. Geiman, and M.D. Lane. 1991. CCAAT/enhancer binding protein gene promoter: binding of nuclear factors during differentiation of 3T3-L1 preadipocytes. *Proceedings of the National Academy of Sciences of the United States of America*. 88:2593-2597.

Chuang, T. T., L. Iacovelli, et al. (1996). "G protein-coupled receptors: heterologous regulation of homologous desensitization and its implications." Trends Pharmacol Sci 17(11): 416-421.

Christy, R.J., V.W. Yang, J.M. Ntambi, D.E. Geiman, W.H. Landschulz, A.D. Friedman, Y. Nakabeppu, T.J. Kelly, and M.D. Lane. 1989. Differentiation-induced gene expression in 3T3-L1 preadipocytes: CCAAT/enhancer binding protein interacts with and activates the promoters of two adipocyte-specific genes. *Genes & development*. 3:1323-1335.

Chung, S., J.M. Brown, M.B. Sandberg, and M. McIntosh. 2005. Trans-10,cis-12 CLA increases adipocyte lipolysis and alters lipid droplet-associated proteins: role of mTOR and ERK signaling. *Journal of lipid research*. 46:885-895.

Cinti, S., G. Mitchell, G. Barbatelli, I. Murano, E. Ceresi, E. Faloia, S. Wang, M. Fortier, A.S. Greenberg, and M.S. Obin. 2005. Adipocyte death defines macrophage localization and function in adipose tissue of obese mice and humans. *Journal of lipid research*. 46:2347-2355.

Clement, L., H. Poirier, I. Niot, V. Bocher, M. Guerre-Millo, S. Krief, B. Staels, and P. Besnard. 2002. Dietary trans-10,cis-12 conjugated linoleic acid induces hyperinsulinemia and fatty liver in the mouse. *Journal of lipid research*. 43:1400-1409.

Clouthier, D.E., S.A. Comerford, and R.E. Hammer. 1997. Hepatic fibrosis, glomerulosclerosis, and a lipodystrophy-like syndrome in PEPCK-TGF-beta1 transgenic mice. *The Journal of clinical investigation*. 100:2697-2713.

Coe, N.R., and D.A. Bernlohr. 1998. Physiological properties and functions of intracellular fatty acid-binding proteins. *Biochimica et biophysica acta*. 1391:287-306.

Cohen, M.M., Jr. 2003. The hedgehog signaling network. *American journal of medical genetics. Part A*. 123A:5-28.

Colaianni, G., G. Brunetti, M.F. Faienza, S. Colucci, and M. Grano. 2014. Osteoporosis and obesity: Role of Wnt pathway in human and murine models. *World journal of orthopedics*. 5:242-246.

Collins, S., T.L. Martin, R.S. Surwit, and J. Robidoux. 2004. Genetic vulnerability to diet-induced obesity in the C57BL/6J mouse: physiological and molecular characteristics. *Physiology & behavior*. 81:243-248.

Combs, T.P., A.H. Berg, M.W. Rajala, S. Klebanov, P. Iyengar, J.C. Jimenez-Chillaron, M.E. Patti, S.L. Klein, R.S. Weinstein, and P.E. Scherer. 2003. Sexual differentiation, pregnancy, calorie restriction, and aging affect the adipocyte-specific secretory protein adiponectin. *Diabetes*. 52:268-276.

Combs, T.P., J.A. Wagner, J. Berger, T. Doebber, W.J. Wang, B.B. Zhang, M. Tanen, A.H. Berg, S. O'Rahilly, D.B. Savage, K. Chatterjee, S. Weiss, P.J. Larson, K.M. Gottesdiener, B.J. Gertz, M.J. Charron, P.E. Scherer, and D.E. Moller. 2002. Induction of adipocyte complement-related protein of 30 kilodaltons by PPARgamma agonists: a potential mechanism of insulin sensitization. *Endocrinology*. 143:998-1007.

Cook, D., M.J. Fry, K. Hughes, R. Sumathipala, J.R. Woodgett, and T.C. Dale. 1996. Wingless inactivates glycogen synthase kinase-3 via an intracellular signalling pathway which involves a protein kinase C. *EMBO J*. 15:4526-4536.

Cook, K.S., D.L. Groves, H.Y. Min, and B.M. Spiegelman. 1985. A developmentally regulated mRNA from 3T3 adipocytes encodes a novel serine protease homologue. *Proceedings of the National Academy of Sciences of the United States of America*. 82:6480-6484.

Cook, K.S., H.Y. Min, D. Johnson, R.J. Chaplinsky, J.S. Flier, C.R. Hunt, and B.M. Spiegelman. 1987. Adipsin: a circulating serine protease homolog secreted by adipose tissue and sciatic nerve. *Science*. 237:402-405.

Cornelius, P., O.A. MacDougald, and M.D. Lane. 1994. Regulation of adipocyte development. *Annual review of nutrition*. 14:99-129.

Corsetti, J.P., J.D. Sparks, R.G. Peterson, R.L. Smith, and C.E. Sparks. 2000. Effect of dietary fat on the development of non-insulin dependent diabetes mellitus in obese Zucker diabetic fatty male and female rats. *Atherosclerosis*. 148:231-241.

Curat, C.A., A. Miranville, C. Sengenes, M. Diehl, C. Tonus, R. Busse, and A. Bouloumie. 2004. From blood monocytes to adipose tissue-resident macrophages: induction of diapedesis by human mature adipocytes. *Diabetes*. 53:1285-1292.

da Silva, B.A., C. Bjorbaek, S. Uotani, and J.S. Flier. 1998. Functional properties of leptin receptor isoforms containing the gln-->pro extracellular domain mutation of the fatty rat. *Endocrinology*. 139:3681-3690.

Dalen, K.T., K. Schoonjans, S.M. Ulven, M.S. Weedon-Fekjaer, T.G. Bentzen, H. Koutnikova, J. Auwerx, and H.I. Nebb. 2004. Adipose tissue expression of the lipid droplet-associating proteins S3-12 and perilipin is controlled by peroxisome proliferator-activated receptor-gamma. *Diabetes*. 53:1243-1252.

Dandona, P., R. Weinstock, K. Thusu, E. Abdel-Rahman, A. Aljada, and T. Wadden. 1998. Tumor necrosis factor-alpha in sera of obese patients: fall with weight loss. *The Journal of clinical endocrinology and metabolism*. 83:2907-2910.

Darlington, G.J., S.E. Ross, and O.A. MacDougald. 1998. The role of C/EBP genes in adipocyte differentiation. *The Journal of biological chemistry*. 273:30057-30060.

Dawson, K., M. Aflaki, and S. Nattel. 2013. Role of the Wnt-Frizzled system in cardiac pathophysiology: a rapidly developing, poorly understood area with enormous potential. *The Journal of physiology*. 591:1409-1432.

de Luis, D.A., M. Gonzalez Sagrado, R. Conde, R. Aller, O. Izaola, and D. Primo. 2011. Lack of association of serum resistin levels with metabolic syndrome criteria in obese female patients. *Clinical biochemistry*. 44:1280-1283.

De Rosa, V., C. Procaccini, G. Cali, G. Pirozzi, S. Fontana, S. Zappacosta, A. La Cava, and G. Matarese. 2007. A key role of leptin in the control of regulatory T cell proliferation. *Immunity*. 26:241-255.

De Ugarte, D.A., Z. Alfonso, P.A. Zuk, A. Elbarbary, M. Zhu, P. Ashjian, P. Benhaim, M.H. Hedrick, and J.K. Fraser. 2003. Differential expression of stem cell mobilization-associated molecules on multi-lineage cells from adipose tissue and bone marrow. *Immunology letters*. 89:267-270.

DeClercq, V., J.E. Enns, A. Yeganeh, C.G. Taylor, and P. Zahradka. 2013. Modulation of cardiovascular function by adipokines. *Cardiovascular & hematological disorders drug targets*. 13:59-72.

DeClercq, V., P. Zahradka, and C.G. Taylor. 2010. Dietary t10,c12-CLA but not c9,t11 CLA reduces adipocyte size in the absence of changes in the adipose renin-angiotensin system in fa/fa Zucker rats. *Lipids*. 45:1025-1033.

Della-Fera, M.A., H. Qian, and C.A. Baile. 2001. Adipocyte apoptosis in the regulation of body fat mass by leptin. *Diabetes, obesity & metabolism*. 3:299-310.

den Hartigh, L.J., C.Y. Han, S. Wang, M. Omer, and A. Chait. 2013. 10E,12Z-conjugated linoleic acid impairs adipocyte triglyceride storage by enhancing fatty acid oxidation, lipolysis, and mitochondrial reactive oxygen species. *Journal of lipid research*. 54:2964-2978.

Derynck, R., and Y.E. Zhang. 2003. Smad-dependent and Smad-independent pathways in TGF-beta family signalling. *Nature*. 425:577-584.

Dhiman, T.R., S.H. Nam, and A.L. Ure. 2005. Factors affecting conjugated linoleic acid content in milk and meat. *Critical reviews in food science and nutrition*. 45:463-482.

Dilzer, A., and Y. Park. 2012. Implication of conjugated linoleic acid (CLA) in human health. *Critical reviews in food science and nutrition*. 52:488-513.

Ding, Y., Y. Wu, R. Zeng, and K. Liao. 2012. Proteomic profiling of lipid droplet-associated proteins in primary adipocytes of normal and obese mouse. *Acta biochimica et biophysica Sinica*. 44:394-406.

Drummond, E.M., and E.R. Gibney. 2013. Epigenetic regulation in obesity. *Current opinion in clinical nutrition and metabolic care*. 16:392-397.

Ealey, K.N., A. El-Sohemy, and M.C. Archer. 2002. Effects of dietary conjugated linoleic acid on the expression of uncoupling proteins in mice and rats. *Lipids*. 37:853-861.

Elberg, G., J.M. Gimble, and S.Y. Tsai. 2000. Modulation of the murine peroxisome proliferator-activated receptor gamma 2 promoter activity by CCAAT/enhancer-binding proteins. *The Journal of biological chemistry*. 275:27815-27822.

Elmasri, H., C. Karaaslan, Y. Teper, E. Ghelfi, M. Weng, T.A. Ince, H. Kozakewich, J. Bischoff, and S. Cataltepe. 2009. Fatty acid binding protein 4 is a target of VEGF and a regulator of cell proliferation in endothelial cells. *FASEB journal : official publication of the Federation of American Societies for Experimental Biology*. 23:3865-3873.

Enns, J.E., C.G. Taylor, and P. Zahradka. 2011. Variations in Adipokine Genes AdipoQ, Lep, and LepR are Associated with Risk for Obesity-Related Metabolic Disease: The Modulatory Role of Gene-Nutrient Interactions. *Journal of obesity*. 2011:168659.

Eto, H., H. Suga, D. Matsumoto, K. Inoue, N. Aoi, H. Kato, J. Araki, and K. Yoshimura. 2009. Characterization of structure and cellular components of aspirated and excised adipose tissue. *Plastic and reconstructive surgery*. 124:1087-1097.

Evans, M., C. Geigerman, J. Cook, L. Curtis, B. Kuebler, and M. McIntosh. 2000. Conjugated linoleic acid suppresses triglyceride accumulation and induces apoptosis in 3T3-L1 preadipocytes. *Lipids*. 35:899-910.

Evans, M., X. Lin, J. Odle, and M. McIntosh. 2002. Trans-10, cis-12 conjugated linoleic acid increases fatty acid oxidation in 3T3-L1 preadipocytes. *The Journal of nutrition*. 132:450-455.

Evans, M., Y. Park, M. Pariza, L. Curtis, B. Kuebler, and M. McIntosh. 2001. Trans-10,cis-12 conjugated linoleic acid reduces triglyceride content while differentially affecting peroxisome proliferator activated receptor gamma2 and aP2 expression in 3T3-L1 preadipocytes. *Lipids*. 36:1223-1232.

Fain, J.N., P.S. Cheema, S.W. Bahouth, and M. Lloyd Hiler. 2003. Resistin release by human adipose tissue explants in primary culture. *Biochemical and biophysical research communications*. 300:674-678.

Fan, W., T. Imamura, N. Sonoda, D.D. Sears, D. Patsouris, J.J. Kim, and J.M. Olefsky. 2009. FOXO1 transrepresses peroxisome proliferator-activated receptor gamma transactivation, coordinating an insulin-induced feed-forward response in adipocytes. *The Journal of biological chemistry*. 284:12188-12197.

Faust, I.M., P.R. Johnson, J.S. Stern, and J. Hirsch. 1978. Diet-induced adipocyte number increase in adult rats: a new model of obesity. *The American journal of physiology*. 235:E279-286.

Faust, I.M., W.H. Miller, Jr., A. Sclafani, P.F. Aravich, J. Triscari, and A.C. Sullivan. 1984. Diet-dependent hyperplastic growth of adipose tissue in hypothalamic obese rats. *The American journal of physiology*. 247:R1038-1046.

Feng, D., Y. Tang, H. Kwon, H. Zong, M. Hawkins, R.N. Kitsis, and J.E. Pessin. 2011. High-fat diet-induced adipocyte cell death occurs through a cyclophilin D intrinsic signaling pathway independent of adipose tissue inflammation. *Diabetes*. 60:2134-2143.

Fischer-Posovszky, P., V. Kukulus, M.A. Zulet, K.M. Debatin, and M. Wabitsch. 2007. Conjugated linoleic acids promote human fat cell apoptosis. *Hormone and metabolic research = Hormon- und Stoffwechselforschung = Hormones et metabolisme*. 39:186-191.

Fisher, R.M., P. Eriksson, J. Hoffstedt, G.S. Hotamisligil, A. Thorne, M. Ryden, A. Hamsten, and P. Arner. 2001. Fatty acid binding protein expression in different adipose tissue depots from lean and obese individuals. *Diabetologia*. 44:1268-1273.

Fitzgibbons, T.P., S. Kogan, M. Aouadi, G.M. Hendricks, J. Straubhaar, and M.P. Czech. 2011. Similarity of mouse perivascular and brown adipose tissues and their resistance to diet-induced inflammation. *American journal of physiology. Heart and circulatory physiology*. 301:H1425-1437.

Flegal, K.M., M.D. Carroll, B.K. Kit, and C.L. Ogden. 2012. Prevalence of obesity and trends in the distribution of body mass index among US adults, 1999-2010. *Jama*. 307:491-497.

Fleming, I., S.J. MacKenzie, R.G. Vernon, N.G. Anderson, M.D. Houslay, and E. Kilgour. 1998. Protein kinase C isoforms play differential roles in the regulation of adipocyte differentiation. *The Biochemical journal*. 333 (Pt 3):719-727.

Fleury, C., M. Neverova, S. Collins, S. Raimbault, O. Champigny, C. Levi-Meyrueis, F. Bouillaud, M.F. Seldin, R.S. Surwit, D. Ricquier, and C.H. Warden. 1997. Uncoupling protein-2: a novel gene linked to obesity and hyperinsulinemia. *Nature genetics*. 15:269-272.

Flier, J.S., K.S. Cook, P. Usher, and B.M. Spiegelman. 1987. Severely impaired adipsin expression in genetic and acquired obesity. *Science*. 237:405-408.

Flodby, P., C. Barlow, H. Kylefjord, L. Ahrlund-Richter, and K.G. Xanthopoulos. 1996. Increased hepatic cell proliferation and lung abnormalities in mice deficient in CCAAT/enhancer binding protein alpha. *The Journal of biological chemistry*. 271:24753-24760.

Fontaine, C., W. Cousin, M. Plaisant, C. Dani, and P. Peraldi. 2008. Hedgehog signaling alters adipocyte maturation of human mesenchymal stem cells. *Stem cells*. 26:1037-1046.

Fox, K.E., L.A. Colton, P.F. Erickson, J.E. Friedman, H.C. Cha, P. Keller, O.A. MacDougald, and D.J. Klemm. 2008. Regulation of cyclin D1 and Wnt10b gene expression by cAMP-responsive element-binding protein during early adipogenesis involves differential promoter methylation. *The Journal of biological chemistry*. 283:35096-35105.

Freytag, S.O., and T.J. Geddes. 1992. Reciprocal regulation of adipogenesis by Myc and C/EBP alpha. *Science*. 256:379-382.

Freytag, S.O., D.L. Paielli, and J.D. Gilbert. 1994. Ectopic expression of the CCAAT/enhancer-binding protein alpha promotes the adipogenic program in a variety of mouse fibroblastic cells. *Genes & development*. 8:1654-1663.

Fricke, K., A. Heitland, and E. Maronde. 2004. Cooperative activation of lipolysis by protein kinase A and protein kinase C pathways in 3T3-L1 adipocytes. *Endocrinology*. 145:4940-4947.

Friedman, A.D. 2007. Transcriptional control of granulocyte and monocyte development. *Oncogene*. 26:6816-6828.

Friedman, J.M., and J.L. Halaas. 1998. Leptin and the regulation of body weight in mammals. *Nature*. 395:763-770.

Fruebis, J., T.S. Tsao, S. Javorschi, D. Ebbets-Reed, M.R. Erickson, F.T. Yen, B.E. Bihain, and H.F. Lodish. 2001. Proteolytic cleavage product of 30-kDa adipocyte complement-related protein increases fatty acid oxidation in muscle and causes weight loss in mice. *Proceedings of the National Academy of Sciences of the United States of America*. 98:2005-2010.

Fu, Y., N. Luo, M.F. Lopes-Virella, and W.T. Garvey. 2002. The adipocyte lipid binding protein (ALBP/aP2) gene facilitates foam cell formation in human THP-1 macrophages. *Atherosclerosis*. 165:259-269.

Fuchs, Y., and H. Steller. 2011. Programmed cell death in animal development and disease. *Cell*. 147:742-758.

Fukuhara, A., M. Matsuda, M. Nishizawa, K. Segawa, M. Tanaka, K. Kishimoto, Y. Matsuki, M. Murakami, T. Ichisaka, H. Murakami, E. Watanabe, T. Takagi, M. Akiyoshi, T. Ohtsubo, S. Kihara, S. Yamashita, M. Makishima, T. Funahashi, S. Yamanaka, R. Hiramatsu, Y. Matsuzawa, and I. Shimomura. 2005. Visfatin: a protein secreted by visceral fat that mimics the effects of insulin. *Science*. 307:426-430.

Gainsford, T., T.A. Willson, D. Metcalf, E. Handman, C. McFarlane, A. Ng, N.A. Nicola, W.S. Alexander, and D.J. Hilton. 1996. Leptin can induce proliferation, differentiation, and functional activation of hemopoietic cells. *Proceedings of the National Academy of Sciences of the United States of America*. 93:14564-14568.

Gallagher, D., M. Visser, D. Sepulveda, R.N. Pierson, T. Harris, and S.B. Heymsfield. 1996. How useful is body mass index for comparison of body fatness across age, sex, and ethnic groups? *American journal of epidemiology*. 143:228-239.

Garofalo, R.S., S.J. Orena, K. Rafidi, A.J. Torchia, J.L. Stock, A.L. Hildebrandt, T. Coskran, S.C. Black, D.J. Brees, J.R. Wicks, J.D. McNeish, and K.G. Coleman. 2003. Severe diabetes, age-dependent loss of adipose tissue, and mild growth deficiency in mice lacking Akt2/PKB beta. *The Journal of clinical investigation*. 112:197-208.

Garrison, R.J., W.B. Kannel, J. Stokes, 3rd, and W.P. Castelli. 1987. Incidence and precursors of hypertension in young adults: the Framingham Offspring Study. *Preventive medicine*. 16:235-251.

Ge, Q., L. Ryken, L. Noel, E. Maury, and S.M. Brichard. 2011. Adipokines identified as new downstream targets for adiponectin: lessons from adiponectin-overexpressing or -deficient mice. *Am J Physiol Endocrinol Metab*. 301:E326-335.

Gebauer, S.K., J.M. Chardigny, M.U. Jakobsen, B. Lamarche, A.L. Lock, S.D. Proctor, and D.J. Baer. 2011. Effects of ruminant trans fatty acids on cardiovascular disease and cancer: a comprehensive review of epidemiological, clinical, and mechanistic studies. *Advances in nutrition*. 2:332-354.

Gerber, M., A. Boettner, B. Seidel, A. Lammert, J. Bar, E. Schuster, J. Thiery, W. Kiess, and J. Kratzsch. 2005. Serum resistin levels of obese and lean children and adolescents: biochemical analysis and clinical relevance. *The Journal of clinical endocrinology and metabolism*. 90:4503-4509.

Gerin, I., G.T. Bommer, M.E. Lidell, A. Cederberg, S. Enerback, and O.A. Macdougald. 2009. On the role of FOX transcription factors in adipocyte differentiation and insulin-stimulated glucose uptake. *The Journal of biological chemistry*. 284:10755-10763.

Germinario, R., A.D. Sniderman, S. Manuel, S.P. Lefebvre, A. Baldo, and K. Cianflone. 1993. Coordinate regulation of triacylglycerol synthesis and glucose transport by acylation-stimulating protein. *Metabolism: clinical and experimental*. 42:574-580.

Gesta, S., M. Bluher, Y. Yamamoto, A.W. Norris, J. Berndt, S. Kralisch, J. Boucher, C. Lewis, and C.R. Kahn. 2006. Evidence for a role of developmental genes in the origin of obesity

and body fat distribution. *Proceedings of the National Academy of Sciences of the United States of America*. 103:6676-6681.

Gimble, J.M., A.J. Katz, and B.A. Bunnell. 2007. Adipose-derived stem cells for regenerative medicine. *Circulation research*. 100:1249-1260.

Glinka, A., W. Wu, H. Delius, A.P. Monaghan, C. Blumenstock, and C. Niehrs. 1998. Dickkopf-1 is a member of a new family of secreted proteins and functions in head induction. *Nature*. 391:357-362.

Golozoubova, V., B. Cannon, and J. Nedergaard. 2006. UCP1 is essential for adaptive adrenergic nonshivering thermogenesis. *American journal of physiology. Endocrinology and metabolism*. 291:E350-357.

Golozoubova, V., E. Hohtola, A. Matthias, A. Jacobsson, B. Cannon, and J. Nedergaard. 2001. Only UCP1 can mediate adaptive nonshivering thermogenesis in the cold. *FASEB journal : official publication of the Federation of American Societies for Experimental Biology*. 15:2048-2050.

Gong, J., Z. Sun, and P. Li. 2009. CIDE proteins and metabolic disorders. *Current opinion in lipidology*. 20:121-126.

Gong, J., Z. Sun, L. Wu, W. Xu, N. Schieber, D. Xu, G. Shui, H. Yang, R.G. Parton, and P. Li. 2011. Fsp27 promotes lipid droplet growth by lipid exchange and transfer at lipid droplet contact sites. *The Journal of cell biology*. 195:953-963.

Goralski, K.B., T.C. McCarthy, E.A. Hanniman, B.A. Zabel, E.C. Butcher, S.D. Parlee, S. Muruganandan, and C.J. Sinal. 2007. Chemerin, a novel adipokine that regulates adipogenesis and adipocyte metabolism. *The Journal of biological chemistry*. 282:28175-28188.

Gordon, M.D., and R. Nusse. 2006. Wnt signaling: multiple pathways, multiple receptors, and multiple transcription factors. *The Journal of biological chemistry*. 281:22429-22433.

Gouranton, E., B. Romier, J. Marcotorchino, F. Tourniaire, J. Astier, F. Peiretti, and J.F. Landrier. 2014. Visfatin is involved in TNFalpha-mediated insulin resistance via an NAD(+)/Sirt1/PTP1B pathway in 3T3-L1 adipocytes. *Adipocyte*. 3:180-189.

Granlund, L., L.K. Juvet, J.I. Pedersen, and H.I. Nebb. 2003. Trans10, cis12-conjugated linoleic acid prevents triacylglycerol accumulation in adipocytes by acting as a PPARgamma modulator. *Journal of lipid research*. 44:1441-1452.

Granneman, J.G., H.P. Moore, R.L. Granneman, A.S. Greenberg, M.S. Obin, and Z. Zhu. 2007. Analysis of lipolytic protein trafficking and interactions in adipocytes. *The Journal of biological chemistry*. 282:5726-5735.

Green, H., and O. Kehinde. 1975. An established preadipose cell line and its differentiation in culture. II. Factors affecting the adipose conversion. *Cell*. 5:19-27.

Green, H., and M. Meuth. 1974. An established pre-adipose cell line and its differentiation in culture. *Cell*. 3:127-133.

Greenberg, A.S., J.J. Egan, S.A. Wek, N.B. Garty, E.J. Blanchette-Mackie, and C. Londos. 1991. Perilipin, a major hormonally regulated adipocyte-specific phosphoprotein associated with the periphery of lipid storage droplets. *The Journal of biological chemistry*. 266:11341-11346.

Greenberg, A.S., J.J. Egan, S.A. Wek, M.C. Moos, Jr., C. Londos, and A.R. Kimmel. 1993. Isolation of cDNAs for perilipins A and B: sequence and expression of lipid droplet-associated proteins of adipocytes. *Proceedings of the National Academy of Sciences of the United States of America*. 90:12035-12039.

Greenwood, M.R., and J. Hirsch. 1974. Postnatal development of adipocyte cellularity in the normal rat. *Journal of lipid research*. 15:474-483.

Gronthos, S., D.M. Franklin, H.A. Leddy, P.G. Robey, R.W. Storms, and J.M. Gimble. 2001. Surface protein characterization of human adipose tissue-derived stromal cells. *Journal of cellular physiology*. 189:54-63.

Gruen, M.L., M. Hao, D.W. Piston, and A.H. Hasty. 2007. Leptin requires canonical migratory signaling pathways for induction of monocyte and macrophage chemotaxis. *American journal of physiology. Cell physiology*. 293:C1481-1488.

Gudbrandsen, O.A., E. Rodriguez, H. Wergedahl, S. Mork, J.E. Reseland, J. Skorve, A. Palou, and R.K. Berge. 2009. Trans-10, cis-12-conjugated linoleic acid reduces the hepatic triacylglycerol content and the leptin mRNA level in adipose tissue in obese Zucker fa/fa rats. *The British journal of nutrition*. 102:803-815.

Guilak, F., K.E. Lott, H.A. Awad, Q. Cao, K.C. Hicok, B. Fermor, and J.M. Gimble. 2006. Clonal analysis of the differentiation potential of human adipose-derived adult stem cells. *Journal of cellular physiology*. 206:229-237.

Gumperz, J.E. 2006. The ins and outs of CD1 molecules: bringing lipids under immunological surveillance. *Traffic*. 7:2-13.

Guo, L., X. Li, and Q.Q. Tang. 2015. Transcriptional regulation of adipocyte differentiation: a central role for CCAAT/enhancer-binding protein (C/EBP) beta. *The Journal of biological chemistry*. 290:755-761.

Gustafson, B., S. Gogg, S. Hedjazifar, L. Jenndahl, A. Hammarstedt, and U. Smith. 2009. Inflammation and impaired adipogenesis in hypertrophic obesity in man. *American journal of physiology. Endocrinology and metabolism*. 297:E999-E1003.

Gwak, J., M. Cho, S.J. Gong, J. Won, D.E. Kim, E.Y. Kim, S.S. Lee, M. Kim, T.K. Kim, J.G. Shin, and S. Oh. 2006. Protein-kinase-C-mediated beta-catenin phosphorylation negatively regulates the Wnt/beta-catenin pathway. *Journal of cell science*. 119:4702-4709.

Gwak, J., S.J. Jung, D.I. Kang, E.Y. Kim, D.E. Kim, Y.H. Chung, J.G. Shin, and S. Oh. 2009. Stimulation of protein kinase C-alpha suppresses colon cancer cell proliferation by down-regulation of beta-catenin. *Journal of cellular and molecular medicine*. 13:2171-2180.

Hackstein, H., and A.W. Thomson. 2004. Dendritic cells: emerging pharmacological targets of immunosuppressive drugs. *Nature reviews. Immunology*. 4:24-34.

Han, J., R. Murthy, B. Wood, B. Song, S. Wang, B. Sun, H. Malhi, and R.J. Kaufman. 2013. ER stress signalling through eIF2alpha and CHOP, but not IRE1alpha, attenuates adipogenesis in mice. *Diabetologia*. 56:911-924.

Hanada, T., N.N. Noda, Y. Satomi, Y. Ichimura, Y. Fujioka, T. Takao, F. Inagaki, and Y. Ohsumi. 2007. The Atg12-Atg5 conjugate has a novel E3-like activity for protein lipidation in autophagy. *The Journal of biological chemistry*. 282:37298-37302.

Hansen, I.R., K.M. Jansson, B. Cannon, and J. Nedergaard. 2014. Contrasting effects of cold acclimation versus obesogenic diets on chemerin gene expression in brown and brite adipose tissues. *Biochimica et biophysica acta*. 1841:1691-1699.

Hao, R., L. Yuan, N. Zhang, C. Li, and J. Yang. 2012. Brown adipose tissue: distribution and influencing factors on FDG PET/CT scan. *Journal of pediatric endocrinology & metabolism : JPEM*. 25:233-237.

Harada, K., W.J. Shen, S. Patel, V. Natu, J. Wang, J. Osuga, S. Ishibashi, and F.B. Kraemer. 2003. Resistance to high-fat diet-induced obesity and altered expression of adipose-specific genes in HSL-deficient mice. *American journal of physiology. Endocrinology and metabolism*. 285:E1182-1195.

Harland, R., and J. Gerhart. 1997. Formation and function of Spemann's organizer. *Annual review of cell and developmental biology*. 13:611-667.

Hata, K., R. Nishimura, F. Ikeda, K. Yamashita, T. Matsubara, T. Nokubi, and T. Yoneda. 2003. Differential roles of Smad1 and p38 kinase in regulation of peroxisome proliferator-activating receptor gamma during bone morphogenetic protein 2-induced adipogenesis. *Molecular biology of the cell*. 14:545-555.

Hatsell, S., T. Rowlands, M. Hiremath, and P. Cowin. 2003. Beta-catenin and Tcfs in mammary development and cancer. *Journal of mammary gland biology and neoplasia*. 8:145-158.

Hauner, H. 2005. Secretory factors from human adipose tissue and their functional role. *The Proceedings of the Nutrition Society*. 64:163-169.

Haunerland, N.H., and F. Spener. 2004. Fatty acid-binding proteins--insights from genetic manipulations. *Progress in lipid research*. 43:328-349.

Hausman, D.B., M. DiGirolamo, T.J. Bartness, G.J. Hausman, and R.J. Martin. 2001. The biology of white adipocyte proliferation. *Obesity reviews : an official journal of the International Association for the Study of Obesity*. 2:239-254.

Hausman, G.J., D.R. Campion, and R.J. Martin. 1980. Search for the adipocyte precursor cell and factors that promote its differentiation. *Journal of lipid research*. 21:657-670.

He, X., M. Semenov, K. Tamai, and X. Zeng. 2004. LDL receptor-related proteins 5 and 6 in Wnt/beta-catenin signaling: arrows point the way. *Development*. 131:1663-1677.

Herzig, S., and C. Wolfrum. 2013. Brown and white fat: from signaling to disease. *Biochimica et biophysica acta*. 1831:895.

Himms-Hagen, J., A. Melnyk, M.C. Zingaretti, E. Ceresi, G. Barbatelli, and S. Cinti. 2000. Multilocular fat cells in WAT of CL-316243-treated rats derive directly from white adipocytes. *American journal of physiology. Cell physiology*. 279:C670-681.

Hinney, A., C.I. Vogel, and J. Hebebrand. 2010. From monogenic to polygenic obesity: recent advances. *European child & adolescent psychiatry*. 19:297-310.

Hoang, B.H., J.T. Thomas, F.W. Abdul-Karim, K.M. Correia, R.A. Conlon, F.P. Luyten, and R.T. Ballock. 1998. Expression pattern of two Frizzled-related genes, Frzb-1 and Sfrp-1, during mouse embryogenesis suggests a role for modulating action of Wnt family members. *Developmental dynamics : an official publication of the American Association of Anatomists*. 212:364-372.

Holcomb, I.N., R.C. Kabakoff, B. Chan, T.W. Baker, A. Gurney, W. Henzel, C. Nelson, H.B. Lowman, B.D. Wright, N.J. Skelton, G.D. Frantz, D.B. Tumas, F.V. Peale, Jr., D.L. Shelton, and C.C. Hebert. 2000. FIZZ1, a novel cysteine-rich secreted protein associated with pulmonary inflammation, defines a new gene family. *The EMBO journal*. 19:4046-4055.

Hotamisligil, G.S., R.S. Johnson, R.J. Distel, R. Ellis, V.E. Papaioannou, and B.M. Spiegelman. 1996. Uncoupling of obesity from insulin resistance through a targeted mutation in aP2, the adipocyte fatty acid binding protein. *Science*. 274:1377-1379.

Hotamisligil, G.S., and B.M. Spiegelman. 1994. Tumor necrosis factor alpha: a key component of the obesity-diabetes link. *Diabetes*. 43:1271-1278.

Hotta, K., T. Funahashi, Y. Arita, M. Takahashi, M. Matsuda, Y. Okamoto, H. Iwahashi, H. Kuriyama, N. Ouchi, K. Maeda, M. Nishida, S. Kihara, N. Sakai, T. Nakajima, K. Hasegawa, M. Muraguchi, Y. Ohmoto, T. Nakamura, S. Yamashita, T. Hanafusa, and Y. Matsuzawa. 2000. Plasma concentrations of a novel, adipose-specific protein, adiponectin, in type 2 diabetic patients. *Arteriosclerosis, thrombosis, and vascular biology*. 20:1595-1599.

Houseknecht, K.L., J.P. Vanden Heuvel, S.Y. Moya-Camarena, C.P. Portocarrero, L.W. Peck, K.P. Nickel, and M.A. Belury. 1998. Dietary conjugated linoleic acid normalizes impaired glucose tolerance in the Zucker diabetic fatty fa/fa rat. *Biochemical and biophysical research communications*. 244:678-682.

Howard, J.K., and J.S. Flier. 2006. Attenuation of leptin and insulin signaling by SOCS proteins. *Trends in endocrinology and metabolism: TEM*. 17:365-371.

Howard, J.K., G.M. Lord, G. Matarese, S. Vendetti, M.A. Ghatei, M.A. Ritter, R.I. Lechler, and S.R. Bloom. 1999. Leptin protects mice from starvation-induced lymphoid atrophy and increases thymic cellularity in ob/ob mice. *The Journal of clinical investigation*. 104:1051-1059.

Hrabak, A., L. Derzbach, I. Csuka, T. Bajor, and A. Korner. 2011. Role of nitric oxide (NO) metabolism and inflammatory mediators in childhood obesity. *Inflammation research : official journal of the European Histamine Research Society ... [et al.]*. 60:1061-1070.

Hsieh, J.C., L. Kodjabachian, M.L. Rebbert, A. Rattner, P.M. Smallwood, C.H. Samos, R. Nusse, I.B. Dawid, and J. Nathans. 1999. A new secreted protein that binds to Wnt proteins and inhibits their activities. *Nature*. 398:431-436.

Hsu, Y. C., X. Meng, et al. (2010). "Activation of the AMP-activated protein kinase-p38 MAP kinase pathway mediates apoptosis induced by conjugated linoleic acid in p53-mutant mouse mammary tumor cells." Cell Signal 22(4): 590-599.

Hu, E., P. Liang, and B.M. Spiegelman. 1996. AdipoQ is a novel adipose-specific gene dysregulated in obesity. *J Biol Chem*. 271:10697-10703.

Huang, H., T.J. Song, X. Li, L. Hu, Q. He, M. Liu, M.D. Lane, and Q.Q. Tang. 2009. BMP signaling pathway is required for commitment of C3H10T1/2 pluripotent stem cells to the adipocyte lineage. *Proceedings of the National Academy of Sciences of the United States of America*. 106:12670-12675.

Huang, H.C., and P.S. Klein. 2004. The Frizzled family: receptors for multiple signal transduction pathways. *Genome biology*. 5:234.

Huh, J.Y., Y.J. Park, M. Ham, and J.B. Kim. 2014. Crosstalk between adipocytes and immune cells in adipose tissue inflammation and metabolic dysregulation in obesity. *Molecules and cells*. 37:365-371.

Hui, X., L. Kaestner, and P. Lipp. 2014. Differential targeting of cPKC and nPKC decodes and regulates Ca(2)(+) and lipid signalling. *Biochemical Society transactions*. 42:1538-1542.

Hunt, C.R., J.H. Ro, D.E. Dobson, H.Y. Min, and B.M. Spiegelman. 1986. Adipocyte P2 gene: developmental expression and homology of 5'-flanking sequences among fat cell-specific genes. *Proceedings of the National Academy of Sciences of the United States of America*. 83:3786-3790.

Hunt, R. 2009. *In* Department of Human Nutritional Sciences-. Vol. Master of scienses. University of Manitoba.

Hunt, W.R. 2009. Investigating the isomer-specific effects of conjugated linoleic acid on adiposity and insulin resistance in db/db mice.

Hutley, L., W. Shurety, F. Newell, R. McGeary, N. Pelton, J. Grant, A. Herington, D. Cameron, J. Whitehead, and J. Prins. 2004. Fibroblast growth factor 1: a key regulator of human adipogenesis. *Diabetes*. 53:3097-3106.

Hwang, D.M., J.K. Kundu, J.W. Shin, J.C. Lee, H.J. Lee, and Y.J. Surh. 2007. cis-9,trans-11-conjugated linoleic acid down-regulates phorbol ester-induced NF-kappaB activation and subsequent COX-2 expression in hairless mouse skin by targeting IkappaB kinase and PI3K-Akt. *Carcinogenesis*. 28:363-371.

Igal, R.A. 2011. Roles of StearoylCoA Desaturase-1 in the Regulation of Cancer Cell Growth, Survival and Tumorigenesis. *Cancers*. 3:2462-2477.

Ikejima, S., S. Sasaki, H. Sashinami, F. Mori, Y. Ogawa, T. Nakamura, Y. Abe, K. Wakabayashi, T. Suda, and A. Nakane. 2005. Impairment of host resistance to Listeria monocytogenes infection in liver of db/db and ob/ob mice. *Diabetes*. 54:182-189.

Ingalls, A.M., M.M. Dickie, and G.D. Snell. 1950. Obese, a new mutation in the house mouse. *The Journal of heredity*. 41:317-318.

Inouye, K.E., H. Shi, J.K. Howard, C.H. Daly, G.M. Lord, B.J. Rollins, and J.S. Flier. 2007. Absence of CC chemokine ligand 2 does not limit obesity-associated infiltration of macrophages into adipose tissue. *Diabetes*. 56:2242-2250.

Ip, M.M., P.A. Masso-Welch, S.F. Shoemaker, W.K. Shea-Eaton, and C. Ip. 1999. Conjugated linoleic acid inhibits proliferation and induces apoptosis of normal rat mammary epithelial cells in primary culture. *Experimental cell research*. 250:22-34.

Ishitani, T., J. Ninomiya-Tsuji, S. Nagai, M. Nishita, M. Meneghini, N. Barker, M. Waterman, B. Bowerman, H. Clevers, H. Shibuya, and K. Matsumoto. 1999. The TAK1-NLK-MAPK-related pathway antagonizes signalling between beta-catenin and transcription factor TCF. *Nature*. 399:798-802.

Jackson, A.S., P.R. Stanforth, J. Gagnon, T. Rankinen, A.S. Leon, D.C. Rao, J.S. Skinner, C. Bouchard, and J.H. Wilmore. 2002. The effect of sex, age and race on estimating percentage body fat from body mass index: The Heritage Family Study. *International journal of obesity and related metabolic disorders : journal of the International Association for the Study of Obesity*. 26:789-796.

Jackson Laboratories. 2015. Strain: B6.Cg-*Lep*^{ob}/J. Retrived on June 26, 2015, from Jax mice database http://jaxmice.jax.org/strain/000632.html.

Jain, M.V., A.M. Paczulla, T. Klonisch, F.N. Dimgba, S.B. Rao, K. Roberg, F. Schweizer, C. Lengerke, P. Davoodpour, V.R. Palicharla, S. Maddika, and M. Los. 2013. Interconnections between apoptotic, autophagic and necrotic pathways: implications for cancer therapy development. *Journal of cellular and molecular medicine*. 17:12-29.

James, A.W. 2013. Review of Signaling Pathways Governing MSC Osteogenic and Adipogenic Differentiation. *Scientifica*. 2013:684736.

James, A.W., P. Leucht, B. Levi, A.L. Carre, Y. Xu, J.A. Helms, and M.T. Longaker. 2010. Sonic Hedgehog influences the balance of osteogenesis and adipogenesis in mouse adipose-derived stromal cells. *Tissue engineering. Part A*. 16:2605-2616.

Jia, S.H., Y. Li, J. Parodo, A. Kapus, L. Fan, O.D. Rotstein, and J.C. Marshall. 2004. Pre-B cell colony-enhancing factor inhibits neutrophil apoptosis in experimental inflammation and clinical sepsis. *The Journal of clinical investigation*. 113:1318-1327.

Joe, A.W., L. Yi, Y. Even, A.W. Vogl, and F.M. Rossi. 2009. Depot-specific differences in adipogenic progenitor abundance and proliferative response to high-fat diet. *Stem cells*. 27:2563-2570.

Kaestner, K.H., R.J. Christy, and M.D. Lane. 1990. Mouse insulin-responsive glucose transporter gene: characterization of the gene and trans-activation by the CCAAT/enhancer binding protein. *Proceedings of the National Academy of Sciences of the United States of America*. 87:251-255.

Kang, E.S., F. Magkos, E. Sienkiewicz, and C.S. Mantzoros. 2011. Circulating vaspin and visfatin are not affected by acute or chronic energy deficiency or leptin administration in humans. *European journal of endocrinology / European Federation of Endocrine Societies*. 164:911-917.

Kang, K., W. Liu, K.J. Albright, Y. Park, and M.W. Pariza. 2003. trans-10,cis-12 CLA inhibits differentiation of 3T3-L1 adipocytes and decreases PPAR gamma expression. *Biochemical and biophysical research communications*. 303:795-799.

Kang, K., and M.W. Pariza. 2001. trans-10,cis-12-Conjugated linoleic acid reduces leptin secretion from 3T3-L1 adipocytes. *Biochemical and biophysical research communications*. 287:377-382.

Kang, S., L. Bajnok, K.A. Longo, R.K. Petersen, J.B. Hansen, K. Kristiansen, and O.A. MacDougald. 2005. Effects of Wnt signaling on brown adipocyte differentiation and metabolism mediated by PGC-1alpha. *Molecular and cellular biology*. 25:1272-1282.

Kang, S., C.N. Bennett, I. Gerin, L.A. Rapp, K.D. Hankenson, and O.A. Macdougald. 2007. Wnt signaling stimulates osteoblastogenesis of mesenchymal precursors by suppressing CCAAT/enhancer-binding protein alpha and peroxisome proliferator-activated receptor gamma. *The Journal of biological chemistry*. 282:14515-14524.

Kappes, A., and G. Loffler. 2000. Influences of ionomycin, dibutyryl-cycloAMP and tumour necrosis factor-alpha on intracellular amount and secretion of apM1 in differentiating primary human preadipocytes. *Horm Metab Res*. 32:548-554.

Kaushik, S., and A.M. Cuervo. 2012. Chaperone-mediated autophagy: a unique way to enter the lysosome world. *Trends in cell biology*. 22:407-417.

Kawaguchi, N., K. Toriyama, E. Nicodemou-Lena, K. Inou, S. Torii, and Y. Kitagawa. 1998. De novo adipogenesis in mice at the site of injection of basement membrane and basic fibroblast growth factor. *Proceedings of the National Academy of Sciences of the United States of America*. 95:1062-1066.

Kawai, M., S. Mushiake, K. Bessho, M. Murakami, N. Namba, C. Kokubu, T. Michigami, and K. Ozono. 2007. Wnt/Lrp/beta-catenin signaling suppresses adipogenesis by inhibiting mutual activation of PPARgamma and C/EBPalpha. *Biochemical and biophysical research communications*. 363:276-282.

Kazanskaya, O., A. Glinka, I. del Barco Barrantes, P. Stannek, C. Niehrs, and W. Wu. 2004. R-Spondin2 is a secreted activator of Wnt/beta-catenin signaling and is required for Xenopus myogenesis. *Developmental cell*. 7:525-534.

Kennedy, A., S. Chung, K. LaPoint, O. Fabiyi, and M.K. McIntosh. 2008. Trans-10, cis-12 conjugated linoleic acid antagonizes ligand-dependent PPARgamma activity in primary cultures of human adipocytes. *The Journal of nutrition*. 138:455-461.

Kepler, C.R., K.P. Hirons, J.J. McNeill, and S.B. Tove. 1966. Intermediates and products of the biohydrogenation of linoleic acid by Butyrinvibrio fibrisolvens. *The Journal of biological chemistry*. 241:1350-1354.

Kern, P.A., S. Ranganathan, C. Li, L. Wood, and G. Ranganathan. 2001. Adipose tissue tumor necrosis factor and interleukin-6 expression in human obesity and insulin resistance. *American journal of physiology. Endocrinology and metabolism*. 280:E745-751.

Keuper, M., M. Bluher, M.R. Schon, P. Moller, A. Dzyakanchuk, K. Amrein, K.M. Debatin, M. Wabitsch, and P. Fischer-Posovszky. 2011. An inflammatory micro-environment promotes human adipocyte apoptosis. *Molecular and cellular endocrinology*. 339:105-113.

Kim, J.E., and J. Chen. 2004. regulation of peroxisome proliferator-activated receptor-gamma activity by mammalian target of rapamycin and amino acids in adipogenesis. *Diabetes*. 53:2748-2756.

Kim, K.H., K. Lee, Y.S. Moon, and H.S. Sul. 2001. A cysteine-rich adipose tissue-specific secretory factor inhibits adipocyte differentiation. *The Journal of biological chemistry*. 276:11252-11256.

Kitagawa, K., B.S. Rosen, B.M. Spiegelman, G.E. Lienhard, and L.I. Tanner. 1989. Insulin stimulates the acute release of adipsin from 3T3-L1 adipocytes. *Biochimica et biophysica acta*. 1014:83-89.

Klionsky, D.J., F.C. Abdalla, H. Abeliovich, R.T. Abraham, A. Acevedo-Arozena, K. Adeli, L. Agholme, M. Agnello, P. Agostinis, J.A. Aguirre-Ghiso, H.J. Ahn, O. Ait-Mohamed, S. Ait-Si-Ali, T. Akematsu, S. Akira, H.M. Al-Younes, M.A. Al-Zeer, M.L. Albert, R.L. Albin, J. Alegre-Abarrategui, M.F. Aleo, M. Alirezaei, A. Almasan, M. Almonte-Becerril, A. Amano, R. Amaravadi, S. Amarnath, A.O. Amer, N. Andrieu-Abadie, V. Anantharam, D.K. Ann, S. Anoopkumar-Dukie, H. Aoki, N. Apostolova, G. Arancia, J.P. Aris, K. Asanuma, N.Y. Asare, H. Ashida, V. Askanas, D.S. Askew, P. Auberger, M. Baba, S.K. Backues, E.H. Baehrecke, B.A. Bahr, X.Y. Bai, Y. Bailly, R. Baiocchi, G. Baldini, W. Balduini, A. Ballabio, B.A. Bamber, E.T. Bampton, G. Banhegyi, C.R. Bartholomew, D.C. Bassham, R.C. Bast, Jr., H. Batoko, B.H. Bay, I. Beau, D.M. Bechet, T.J. Begley, C. Behl, C. Behrends, S. Bekri, B. Bellaire, L.J. Bendall, L. Benetti, L. Berliocchi, H. Bernardi, F. Bernassola, S. Besteiro, I. Bhatia-Kissova, X. Bi, M. Biard-Piechaczyk, J.S. Blum, L.H. Boise, P. Bonaldo, D.L. Boone, B.C. Bornhauser, K.R. Bortoluci, I. Bossis, F. Bost, J.P. Bourquin, P. Boya, M. Boyer-Guittaut, P.V. Bozhkov, N.R. Brady, C. Brancolini, A. Brech, J.E. Brenman, A. Brennand, E.H. Bresnick, P. Brest, D. Bridges, M.L. Bristol, P.S. Brookes, E.J. Brown, J.H. Brumell, et al. 2012.

Guidelines for the use and interpretation of assays for monitoring autophagy. *Autophagy*. 8:445-544.

Komiya, Y., and R. Habas. 2008. Wnt signal transduction pathways. *Organogenesis*. 4:68-75.

Konishi, M., T. Mikami, M. Yamasaki, A. Miyake, and N. Itoh. 2000. Fibroblast growth factor-16 is a growth factor for embryonic brown adipocytes. *The Journal of biological chemistry*. 275:12119-12122.

Korah, T.E., H.H. Ibrahim, E.A. Badr, and M.K. ElShafie. 2011. Serum resistin in acute myocardial infarction patients with and without diabetes mellitus. *Postgraduate medical journal*. 87:463-467.

Krahmer, N., M. Hilger, N. Kory, F. Wilfling, G. Stoehr, M. Mann, R.V. Farese, Jr., and T.C. Walther. 2013. Protein correlation profiles identify lipid droplet proteins with high confidence. *Molecular & cellular proteomics : MCP*. 12:1115-1126.

Krecki, R., M. Krzeminska-Pakula, J.Z. Peruga, P. Szczesniak, P. Lipiec, K. Wierzbowska-Drabik, D. Orszulak-Michalak, and J.D. Kasprzak. 2011. Elevated resistin opposed to adiponectin or angiogenin plasma levels as a strong, independent predictive factor for the occurrence of major adverse cardiac and cerebrovascular events in patients with stable multivessel coronary artery disease over 1-year follow-up. *Medical science monitor : international medical journal of experimental and clinical research*. 17:CR26-32.

Kretschmer, B.D., P. Schelling, N. Beier, C. Liebscher, S. Treutel, N. Kruger, H.P. Scholz, and A. Haus. 2005. Modulatory role of food, feeding regime and physical exercise on body weight and insulin resistance. *Life sciences*. 76:1553-1573.

Kroemer, G., G. Marino, and B. Levine. 2010. Autophagy and the integrated stress response. *Molecular cell*. 40:280-293.

Kumada, M., S. Kihara, S. Sumitsuji, T. Kawamoto, S. Matsumoto, N. Ouchi, Y. Arita, Y. Okamoto, I. Shimomura, H. Hiraoka, T. Nakamura, T. Funahashi, Y. Matsuzawa, and C.A.D.S.G.C.a.d. Osaka. 2003. Association of hypoadiponectinemia with coronary artery disease in men. *Arteriosclerosis, thrombosis, and vascular biology*. 23:85-89.

Lafontan, M., and D. Langin. 2009. Lipolysis and lipid mobilization in human adipose tissue. *Progress in lipid research*. 48:275-297.

Lagathu, C., L. Yvan-Charvet, J.P. Bastard, M. Maachi, A. Quignard-Boulange, J. Capeau, and M. Caron. 2006. Long-term treatment with interleukin-1beta induces insulin resistance in murine and human adipocytes. *Diabetologia*. 49:2162-2173.

Lambert, E.V., J.H. Goedecke, K. Bluett, K. Heggie, A. Claassen, D.E. Rae, S. West, J. Dugas, L. Dugas, S. Meltzeri, K. Charlton, and I. Mohede. 2007. Conjugated linoleic acid versus high-oleic acid sunflower oil: effects on energy metabolism, glucose tolerance, blood lipids, appetite and body composition in regularly exercising individuals. *The British journal of nutrition*. 97:1001-1011.

Lan, J., X. Chen, X. Chen, S. Wang, X. Zhang, K. Wu, S. He, Y. Peng, L. Jiang, L. Li, and L. Wan. 2011. The relationship between visfatin and HOMA-IR in hypertensive patients, and the effect of antihypertensive drugs on visfatin and HOMA-IR in hypertensive patients with insulin resistance. *Diabetes research and clinical practice*. 94:71-76.

Landschulz, W.H., P.F. Johnson, and S.L. McKnight. 1989. The DNA binding domain of the rat liver nuclear protein C/EBP is bipartite. *Science*. 243:1681-1688.

LaRosa, P.C., J. Miner, Y. Xia, Y. Zhou, S. Kachman, and M.E. Fromm. 2006. Trans-10, cis-12 conjugated linoleic acid causes inflammation and delipidation of white adipose tissue in mice: a microarray and histological analysis. *Physiological genomics*. 27:282-294.

Laudes, M. 2011. Role of WNT signalling in the determination of human mesenchymal stem cells into preadipocytes. *Journal of molecular endocrinology*. 46:R65-72.

Laviola, L., S. Perrini, A. Cignarelli, A. Natalicchio, A. Leonardini, F. De Stefano, M. Cuscito, M. De Fazio, V. Memeo, V. Neri, M. Cignarelli, R. Giorgino, and F. Giorgino. 2006.

Insulin signaling in human visceral and subcutaneous adipose tissue in vivo. *Diabetes*. 55:952-961.

Le Lay, S., J. Boucher, A. Rey, I. Castan-Laurell, S. Krief, P. Ferre, P. Valet, and I. Dugail. 2001. Decreased resistin expression in mice with different sensitivities to a high-fat diet. *Biochemical and biophysical research communications*. 289:564-567.

Lee, G.H., R. Proenca, J.M. Montez, K.M. Carroll, J.G. Darvishzadeh, J.I. Lee, and J.M. Friedman. 1996. Abnormal splicing of the leptin receptor in diabetic mice. *Nature*. 379:632-635.

Lehmann, J.M., L.B. Moore, T.A. Smith-Oliver, W.O. Wilkison, T.M. Willson, and S.A. Kliewer. 1995. An antidiabetic thiazolidinedione is a high affinity ligand for peroxisome proliferator-activated receptor gamma (PPAR gamma). *The Journal of biological chemistry*. 270:12953-12956.

Lehrke, M., M.P. Reilly, S.C. Millington, N. Iqbal, D.J. Rader, and M.A. Lazar. 2004. An inflammatory cascade leading to hyperresistinemia in humans. *PLoS medicine*. 1:e45.

LeRoith, D., H. Werner, D. Beitner-Johnson, and C.T. Roberts, Jr. 1995. Molecular and cellular aspects of the insulin-like growth factor I receptor. *Endocrine reviews*. 16:143-163.

Li, J.Z., J. Ye, B. Xue, J. Qi, J. Zhang, Z. Zhou, Q. Li, Z. Wen, and P. Li. 2007. Cideb regulates diet-induced obesity, liver steatosis, and insulin sensitivity by controlling lipogenesis and fatty acid oxidation. *Diabetes*. 56:2523-2532.

Lin, F.T., and M.D. Lane. 1992. Antisense CCAAT/enhancer-binding protein RNA suppresses coordinate gene expression and triglyceride accumulation during differentiation of 3T3-L1 preadipocytes. *Genes & development*. 6:533-544.

Lin, F.T., and M.D. Lane. 1994. CCAAT/enhancer binding protein alpha is sufficient to initiate the 3T3-L1 adipocyte differentiation program. *Proceedings of the National Academy of Sciences of the United States of America*. 91:8757-8761.

Lipp, P., and G. Reither. 2011. Protein kinase C: the "masters" of calcium and lipid. *Cold Spring Harbor perspectives in biology*. 3.

Listenberger, L.L., A.G. Ostermeyer-Fay, E.B. Goldberg, W.J. Brown, and D.A. Brown. 2007. Adipocyte differentiation-related protein reduces the lipid droplet association of adipose triglyceride lipase and slows triacylglycerol turnover. *Journal of lipid research*. 48:2751-2761.

Liu, J., H. Wang, Y. Zuo, and S.R. Farmer. 2006. Functional interaction between peroxisome proliferator-activated receptor gamma and beta-catenin. *Molecular and cellular biology*. 26:5827-5837.

Liu, L.F., A. Purushotham, A.A. Wendel, and M.A. Belury. 2007. Combined effects of rosiglitazone and conjugated linoleic acid on adiposity, insulin sensitivity, and hepatic steatosis in high-fat-fed mice. *American journal of physiology. Gastrointestinal and liver physiology*. 292:G1671-1682.

Liu, M., L. Qi, Y. Zeng, Y. Yang, Y. Bi, X. Shi, H. Zhu, Z. Zhou, and J. Sha. 2012. Transient scrotal hyperthermia induces lipid droplet accumulation and reveals a different ADFP expression pattern between the testes and liver in mice. *PloS one*. 7:e45694.

Lo, J.C., S. Ljubicic, B. Leibiger, M. Kern, I.B. Leibiger, T. Moede, M.E. Kelly, D. Chatterjee Bhowmick, I. Murano, P. Cohen, A.S. Banks, M.J. Khandekar, A. Dietrich, J.S. Flier, S. Cinti, M. Bluher, N.N. Danial, P.O. Berggren, and B.M. Spiegelman. 2014. Adipsin is an adipokine that improves beta cell function in diabetes. *Cell*. 158:41-53.

Lobstein, T., R. Jackson-Leach, M.L. Moodie, K.D. Hall, S.L. Gortmaker, B.A. Swinburn, W.P. James, Y. Wang, and K. McPherson. 2015. Child and adolescent obesity: part of a bigger picture. *Lancet*.

Loftus, T.M., F.P. Kuhajda, and M.D. Lane. 1998. Insulin depletion leads to adipose-specific cell death in obese but not lean mice. *Proceedings of the National Academy of Sciences of the United States of America*. 95:14168-14172.

Londos, C., C. Sztalryd, J.T. Tansey, and A.R. Kimmel. 2005. Role of PAT proteins in lipid metabolism. *Biochimie*. 87:45-49.

Longo, K.A., J.A. Kennell, M.J. Ochocinska, S.E. Ross, W.S. Wright, and O.A. MacDougald. 2002. Wnt signaling protects 3T3-L1 preadipocytes from apoptosis through induction of insulin-like growth factors. *The Journal of biological chemistry*. 277:38239-38244.

Longo, K.A., W.S. Wright, S. Kang, I. Gerin, S.H. Chiang, P.C. Lucas, M.R. Opp, and O.A. MacDougald. 2004. Wnt10b inhibits development of white and brown adipose tissues. *The Journal of biological chemistry*. 279:35503-35509.

Lu, X., J. Gruia-Gray, N.G. Copeland, D.J. Gilbert, N.A. Jenkins, C. Londos, and A.R. Kimmel. 2001. The murine perilipin gene: the lipid droplet-associated perilipins derive from tissue-specific, mRNA splice variants and define a gene family of ancient origin. *Mammalian genome : official journal of the International Mammalian Genome Society*. 12:741-749.

Luk, T., Z. Malam, and J.C. Marshall. 2008. Pre-B cell colony-enhancing factor (PBEF)/visfatin: a novel mediator of innate immunity. *Journal of leukocyte biology*. 83:804-816.

Lumeng, C.N., J.L. Bodzin, and A.R. Saltiel. 2007. Obesity induces a phenotypic switch in adipose tissue macrophage polarization. *The Journal of clinical investigation*. 117:175-184.

Lutz, T.A., and S.C. Woods. 2012. Overview of animal models of obesity. *Current protocols in pharmacology / editorial board, S.J. Enna*. Chapter 5:Unit5 61.

Ma, D., S. Panda, and J.D. Lin. 2011. Temporal orchestration of circadian autophagy rhythm by C/EBPbeta. *The EMBO journal*. 30:4642-4651.

Maas, A.H., and Y.E. Appelman. 2010. Gender differences in coronary heart disease. *Netherlands heart journal : monthly journal of the Netherlands Society of Cardiology and the Netherlands Heart Foundation*. 18:598-603.

Maddika, S., S.R. Ande, S. Panigrahi, T. Paranjothy, K. Weglarczyk, A. Zuse, M. Eshraghi, K.D. Manda, E. Wiechec, and M. Los. 2007. Cell survival, cell death and cell cycle pathways are interconnected: implications for cancer therapy. *Drug resistance updates : reviews and commentaries in antimicrobial and anticancer chemotherapy*. 10:13-29.

Maeda, K., H. Cao, K. Kono, C.Z. Gorgun, M. Furuhashi, K.T. Uysal, Q. Cao, G. Atsumi, H. Malone, B. Krishnan, Y. Minokoshi, B.B. Kahn, R.A. Parker, and G.S. Hotamisligil. 2005. Adipocyte/macrophage fatty acid binding proteins control integrated metabolic responses in obesity and diabetes. *Cell metabolism*. 1:107-119.

Maeda, K., K. Okubo, I. Shimomura, T. Funahashi, Y. Matsuzawa, and K. Matsubara. 1996. cDNA cloning and expression of a novel adipose specific collagen-like factor, apM1 (AdiPose Most abundant Gene transcript 1). *Biochem Biophys Res Commun*. 221:286-289.

Maeda, N., M. Takahashi, T. Funahashi, S. Kihara, H. Nishizawa, K. Kishida, H. Nagaretani, M. Matsuda, R. Komuro, N. Ouchi, H. Kuriyama, K. Hotta, T. Nakamura, I. Shimomura, and Y. Matsuzawa. 2001. PPARgamma ligands increase expression and plasma concentrations of adiponectin, an adipose-derived protein. *Diabetes*. 50:2094-2099.

Maffei, M., J. Halaas, E. Ravussin, R.E. Pratley, G.H. Lee, Y. Zhang, H. Fei, S. Kim, R. Lallone, S. Ranganathan, and et al. 1995. Leptin levels in human and rodent: measurement of plasma leptin and ob RNA in obese and weight-reduced subjects. *Nat Med*. 1:1155-1161.

Magrone, T., and E. Jirillo. 2015. Childhood obesity: immune response and nutritional approaches. *Frontiers in immunology*. 6:76.

Makowski, L., and G.S. Hotamisligil. 2005. The role of fatty acid binding proteins in metabolic syndrome and atherosclerosis. *Current opinion in lipidology*. 16:543-548.

Malo, E., O. Ukkola, M. Jokela, L. Moilanen, M. Kahonen, M.S. Nieminen, V. Salomaa, A. Jula, and Y.A. Kesaniemi. 2011. Resistin is an indicator of the metabolic syndrome according

to five different definitions in the Finnish Health 2000 survey. *Metabolic syndrome and related disorders*. 9:203-210.

Mandel, M.A., and A.A. Mahmoud. 1978. Impairment of cell-mediated immunity in mutation diabetic mice (db/db). *Journal of immunology*. 120:1375-1377.

Mantell, B.S., M. Stefanovic-Racic, X. Yang, N. Dedousis, I.J. Sipula, and R.M. O'Doherty. 2011. Mice lacking NKT cells but with a complete complement of CD8+ T-cells are not protected against the metabolic abnormalities of diet-induced obesity. *PloS one*. 6:e19831.

Marcinkiewicz, A., D. Gauthier, A. Garcia, and D.L. Brasaemle. 2006. The phosphorylation of serine 492 of perilipin a directs lipid droplet fragmentation and dispersion. *The Journal of biological chemistry*. 281:11901-11909.

Martinez-Botas, J., J.B. Anderson, D. Tessier, A. Lapillonne, B.H. Chang, M.J. Quast, D. Gorenstein, K.H. Chen, and L. Chan. 2000. Absence of perilipin results in leanness and reverses obesity in Lepr(db/db) mice. *Nature genetics*. 26:474-479.

Masaki, T., S. Chiba, H. Tatsukawa, T. Yasuda, H. Noguchi, M. Seike, and H. Yoshimatsu. 2004. Adiponectin protects LPS-induced liver injury through modulation of TNF-alpha in KK-Ay obese mice. *Hepatology*. 40:177-184.

Massague, J., J. Seoane, and D. Wotton. 2005. Smad transcription factors. *Genes & development*. 19:2783-2810.

Matarese, G. 2000. Leptin and the immune system: how nutritional status influences the immune response. *European cytokine network*. 11:7-14.

Matarese, G., A. La Cava, V. Sanna, G.M. Lord, R.I. Lechler, S. Fontana, and S. Zappacosta. 2002. Balancing susceptibility to infection and autoimmunity: a role for leptin? *Trends in immunology*. 23:182-187.

McCrorie, T.A., E.M. Keaveney, J.M. Wallace, N. Binns, and M.B. Livingstone. 2011. Human health effects of conjugated linoleic acid from milk and supplements. *Nutrition research reviews*. 24:206-227.

McManaman, J.L., E.S. Bales, D.J. Orlicky, M. Jackman, P.S. MacLean, S. Cain, A.E. Crunk, A. Mansur, C.E. Graham, T.A. Bowman, and A.S. Greenberg. 2013. Perilipin-2-null mice are protected against diet-induced obesity, adipose inflammation, and fatty liver disease. *Journal of lipid research*. 54:1346-1359.

McTernan, C.L., P.G. McTernan, A.L. Harte, P.L. Levick, A.H. Barnett, and S. Kumar. 2002. Resistin, central obesity, and type 2 diabetes. *Lancet*. 359:46-47.

McTernan, P.G., C.L. McTernan, R. Chetty, K. Jenner, F.M. Fisher, M.N. Lauer, J. Crocker, A.H. Barnett, and S. Kumar. 2002. Increased resistin gene and protein expression in human abdominal adipose tissue. *The Journal of clinical endocrinology and metabolism*. 87:2407.

Medina-Bravo, P., R. Meza-Santibanez, P. Rosas-Fernandez, R. Galvan-Duarte, R. Saucedo-Garcia, L. Velazquez-Lopez, and M. Torres-Tamayo. 2011. Decrease in serum adiponectin levels associated with visceral fat accumulation independent of pubertal stage in children and adolescents. *Archives of medical research*. 42:115-121.

Miller, J.R., P. Siripurkpong, J. Hawes, A. Majdalawieh, H.S. Ro, and R.S. McLeod. 2008. The trans-10, cis-12 isomer of conjugated linoleic acid decreases adiponectin assembly by PPARgamma-dependent and PPARgamma-independent mechanisms. *Journal of lipid research*. 49:550-562.

Miller, R.E., R. Hackenberg, and H. Gershman. 1978. Regulation of glutamine synthetase in cultured 3T3-L1 cells by insulin, hydrocortisone, and dibutyryl cyclic AMP. *Proceedings of the National Academy of Sciences of the United States of America*. 75:1418-1422.

Miller, W.H., Jr., I.M. Faust, and J. Hirsch. 1984. Demonstration of de novo production of adipocytes in adult rats by biochemical and radioautographic techniques. *Journal of lipid research*. 25:336-347.

Mitchell, J.B., K. McIntosh, S. Zvonic, S. Garrett, Z.E. Floyd, A. Kloster, Y. Di Halvorsen, R.W. Storms, B. Goh, G. Kilroy, X. Wu, and J.M. Gimble. 2006. Immunophenotype of human adipose-derived cells: temporal changes in stromal-associated and stem cell-associated markers. *Stem cells*. 24:376-385.

Miura, S., J.W. Gan, J. Brzostowski, M.J. Parisi, C.J. Schultz, C. Londos, B. Oliver, and A.R. Kimmel. 2002. Functional conservation for lipid storage droplet association among Perilipin, ADRP, and TIP47 (PAT)-related proteins in mammals, Drosophila, and Dictyostelium. *The Journal of biological chemistry*. 277:32253-32257.

Miyanari, Y., K. Atsuzawa, N. Usuda, K. Watashi, T. Hishiki, M. Zayas, R. Bartenschlager, T. Wakita, M. Hijikata, and K. Shimotohno. 2007. The lipid droplet is an important organelle for hepatitis C virus production. *Nature cell biology*. 9:1089-1097.

Miyoshi, H., J.W. Perfield, 2nd, S.C. Souza, W.J. Shen, H.H. Zhang, Z.S. Stancheva, F.B. Kraemer, M.S. Obin, and A.S. Greenberg. 2007. Control of adipose triglyceride lipase action by serine 517 of perilipin A globally regulates protein kinase A-stimulated lipolysis in adipocytes. *The Journal of biological chemistry*. 282:996-1002.

Miyoshi, H., S.C. Souza, H.H. Zhang, K.J. Strissel, M.A. Christoffolete, J. Kovsan, A. Rudich, F.B. Kraemer, A.C. Bianco, M.S. Obin, and A.S. Greenberg. 2006. Perilipin promotes hormone-sensitive lipase-mediated adipocyte lipolysis via phosphorylation-dependent and -independent mechanisms. *The Journal of biological chemistry*. 281:15837-15844.

Mizushima, N., and B. Levine. 2010. Autophagy in mammalian development and differentiation. *Nature cell biology*. 12:823-830.

Mizushima, N., T. Noda, T. Yoshimori, Y. Tanaka, T. Ishii, M.D. George, D.J. Klionsky, M. Ohsumi, and Y. Ohsumi. 1998. A protein conjugation system essential for autophagy. *Nature*. 395:395-398.

Molica, F., S. Morel, B.R. Kwak, F. Rohner-Jeanrenaud, and S. Steffens. 2014. Adipokines at the crossroad between obesity and cardiovascular disease. *Thrombosis and haemostasis*. 113.

Moloney, F., S. Toomey, E. Noone, A. Nugent, B. Allan, C.E. Loscher, and H.M. Roche. 2007. Antidiabetic effects of cis-9, trans-11-conjugated linoleic acid may be mediated via anti-inflammatory effects in white adipose tissue. *Diabetes*. 56:574-582.

Moloney, F., T.P. Yeow, A. Mullen, J.J. Nolan, and H.M. Roche. 2004. Conjugated linoleic acid supplementation, insulin sensitivity, and lipoprotein metabolism in patients with type 2 diabetes mellitus. *The American journal of clinical nutrition*. 80:887-895.

Moore, S. F., M. T. van den Bosch, et al. (2013). "Dual regulation of glycogen synthase kinase 3 (GSK3)alpha/beta by protein kinase C (PKC)alpha and Akt promotes thrombin-mediated integrin alphaIIbbeta3 activation and granule secretion in platelets." J Biol Chem 288(6): 3918-3928.

Morrish, N.J., S.L. Wang, L.K. Stevens, J.H. Fuller, and H. Keen. 2001. Mortality and causes of death in the WHO Multinational Study of Vascular Disease in Diabetes. *Diabetologia*. 44 Suppl 2:S14-21.

Moschen, A.R., A. Kaser, B. Enrich, B. Mosheimer, M. Theurl, H. Niederegger, and H. Tilg. 2007. Visfatin, an adipocytokine with proinflammatory and immunomodulating properties. *Journal of immunology*. 178:1748-1758.

Motojima, K. 2000. Differential effects of PPARalpha activators on induction of ectopic expression of tissue-specific fatty acid binding protein genes in the mouse liver. *The international journal of biochemistry & cell biology*. 32:1085-1092.

Mueller, E. 2014. Understanding the variegation of fat: novel regulators of adipocyte differentiation and fat tissue biology. *Biochimica et biophysica acta*. 1842:352-357.

Mukherjee, R., P.J. Davies, D.L. Crombie, E.D. Bischoff, R.M. Cesario, L. Jow, L.G. Hamann, M.F. Boehm, C.E. Mondon, A.M. Nadzan, J.R. Paterniti, Jr., and R.A. Heyman. 1997. Sensitization of diabetic and obese mice to insulin by retinoid X receptor agonists. *Nature*. 386:407-410.

Muruganandan, S., A.A. Roman, and C.J. Sinal. 2010. Role of chemerin/CMKLR1 signaling in adipogenesis and osteoblastogenesis of bone marrow stem cells. *Journal of bone and mineral research : the official journal of the American Society for Bone and Mineral Research*. 25:222-234.

Nagao, K., N. Inoue, Y.M. Wang, and T. Yanagita. 2003. Conjugated linoleic acid enhances plasma adiponectin level and alleviates hyperinsulinemia and hypertension in Zucker diabetic fatty (fa/fa) rats. *Biochemical and biophysical research communications*. 310:562-566.

Naghshineh, S., M. Noguchi, K.P. Huang, and C. Londos. 1986. Activation of adipocyte adenylate cyclase by protein kinase C. *The Journal of biological chemistry*. 261:14534-14538.

Nagpal, S., S. Patel, H. Jacobe, D. DiSepio, C. Ghosn, M. Malhotra, M. Teng, M. Duvic, and R.A. Chandraratna. 1997. Tazarotene-induced gene 2 (TIG2), a novel retinoid-responsive gene in skin. *The Journal of investigative dermatology*. 109:91-95.

Nakano, Y., T. Tobe, N.H. Choi-Miura, T. Mazda, and M. Tomita. 1996. Isolation and characterization of GBP28, a novel gelatin-binding protein purified from human plasma. *Journal of biochemistry*. 120:803-812.

Nall, J.L., G. Wu, K.H. Kim, C.W. Choi, and S.B. Smith. 2009. Dietary supplementation of L-arginine and conjugated linoleic acid reduces retroperitoneal fat mass and increases lean body mass in rats. *The Journal of nutrition*. 139:1279-1285.

National Task Force on the, P., and O. Treatment of. 2000. Overweight, obesity, and health risk. *Archives of internal medicine*. 160:898-904.

Nazare, J.A., A.B. de la Perriere, F. Bonnet, M. Desage, J. Peyrat, C. Maitrepierre, C. Louche-Pelissier, J. Bruzeau, J. Goudable, T. Lassel, H. Vidal, and M. Laville. 2007. Daily intake of conjugated linoleic acid-enriched yoghurts: effects on energy metabolism and adipose tissue gene expression in healthy subjects. *The British journal of nutrition*. 97:273-280.

Nedergaard, J., V. Golozoubova, A. Matthias, A. Asadi, A. Jacobsson, and B. Cannon. 2001. UCP1: the only protein able to mediate adaptive non-shivering thermogenesis and metabolic inefficiency. *Biochimica et biophysica acta*. 1504:82-106.

Newton, A.C. 2010. Protein kinase C: poised to signal. *American journal of physiology. Endocrinology and metabolism*. 298:E395-402.

Ng, C.W., W.J. Poznanski, M. Borowiecki, and G. Reimer. 1971. Differences in growth in vitro of adipose cells from normal and obese patients. *Nature*. 231:445.

Ng, M., T. Fleming, M. Robinson, B. Thomson, N. Graetz, C. Margono, E.C. Mullany, S. Biryukov, C. Abbafati, S.F. Abera, J.P. Abraham, N.M. Abu-Rmeileh, T. Achoki, F.S. AlBuhairan, Z.A. Alemu, R. Alfonso, M.K. Ali, R. Ali, N.A. Guzman, W. Ammar, P. Anwari, A. Banerjee, S. Barquera, S. Basu, D.A. Bennett, Z. Bhutta, J. Blore, N. Cabral, I.C. Nonato, J.C. Chang, R. Chowdhury, K.J. Courville, M.H. Criqui, D.K. Cundiff, K.C. Dabhadkar, L. Dandona, A. Davis, A. Dayama, S.D. Dharmaratne, E.L. Ding, A.M. Durrani, A. Esteghamati, F. Farzadfar, D.F. Fay, V.L. Feigin, A. Flaxman, M.H. Forouzanfar, A. Goto, M.A. Green, R. Gupta, N. Hafezi-Nejad, G.J. Hankey, H.C. Harewood, R. Havmoeller, S. Hay, L. Hernandez, A. Husseini, B.T. Idrisov, N. Ikeda, F. Islami, E. Jahangir, S.K. Jassal, S.H. Jee, M. Jeffreys, J.B. Jonas, E.K. Kabagambe, S.E. Khalifa, A.P. Kengne, Y.S. Khader, Y.H. Khang, D. Kim, R.W. Kimokoti, J.M. Kinge, Y. Kokubo, S. Kosen, G. Kwan, T. Lai, M. Leinsalu, Y. Li, X. Liang, S. Liu, G. Logroscino, P.A. Lotufo, Y. Lu, J. Ma, N.K. Mainoo, G.A. Mensah, T.R. Merriman, A.H. Mokdad, J. Moschandreas, M. Naghavi, A. Naheed, D. Nand, K.M. Narayan, E.L. Nelson, M.L. Neuhouser, M.I. Nisar, T. Ohkubo, S.O. Oti, A. Pedroza, et al. 2014. Global, regional, and national prevalence of overweight and obesity in children and adults during 1980-2013: a systematic analysis for the Global Burden of Disease Study 2013. *Lancet*. 384:766-781.

Nguyen, K.D., Y. Qiu, X. Cui, Y.P. Goh, J. Mwangi, T. David, L. Mukundan, F. Brombacher, R.M. Locksley, and A. Chawla. 2011. Alternatively activated macrophages produce catecholamines to sustain adaptive thermogenesis. *Nature*. 480:104-108.

Nicklas, T.A., T. Baranowski, K.W. Cullen, and G. Berenson. 2001. Eating patterns, dietary quality and obesity. *Journal of the American College of Nutrition*. 20:599-608.

Nilsson, C., K. Raun, F.F. Yan, M.O. Larsen, and M. Tang-Christensen. 2012. Laboratory animals as surrogate models of human obesity. *Acta pharmacologica Sinica*. 33:173-181.

Nishimura, S., I. Manabe, M. Nagasaki, K. Seo, H. Yamashita, Y. Hosoya, M. Ohsugi, K. Tobe, T. Kadowaki, R. Nagai, and S. Sugiura. 2008. In vivo imaging in mice reveals local cell dynamics and inflammation in obese adipose tissue. *The Journal of clinical investigation*. 118:710-721.

Nishino, N., Y. Tamori, S. Tateya, T. Kawaguchi, T. Shibakusa, W. Mizunoya, K. Inoue, R. Kitazawa, S. Kitazawa, Y. Matsuki, R. Hiramatsu, S. Masubuchi, A. Omachi, K. Kimura, M. Saito, T. Amo, S. Ohta, T. Yamaguchi, T. Osumi, J. Cheng, T. Fujimoto, H. Nakao, K. Nakao, A. Aiba, H. Okamura, T. Fushiki, and M. Kasuga. 2008. FSP27 contributes to efficient energy storage in murine white adipocytes by promoting the formation of unilocular lipid droplets. *The Journal of clinical investigation*. 118:2808-2821.

Nolte, R.T., G.B. Wisely, S. Westin, J.E. Cobb, M.H. Lambert, R. Kurokawa, M.G. Rosenfeld, T.M. Willson, C.K. Glass, and M.V. Milburn. 1998. Ligand binding and co-activator assembly of the peroxisome proliferator-activated receptor-gamma. *Nature*. 395:137-143.

Northcott, J.M., A. Yeganeh, C.G. Taylor, P. Zahradka, and J.T. Wigle. 2012. Adipokines and the cardiovascular system: mechanisms mediating health and disease. *Canadian journal of physiology and pharmacology*. 90:1029-1059.

Noto, A., P. Zahradka, N.R. Ryz, N. Yurkova, X. Xie, and C.G. Taylor. 2007. Dietary conjugated linoleic acid preserves pancreatic function and reduces inflammatory markers in obese, insulin-resistant rats. *Metabolism: clinical and experimental*. 56:142-151.

Noto, A., P. Zahradka, N. Yurkova, X. Xie, H. Truong, E. Nitschmann, M.R. Ogborn, and C.G. Taylor. 2007. Dietary conjugated linoleic acid decreases adipocyte size and favorably modifies adipokine status and insulin sensitivity in obese, insulin-resistant rats. *Metabolism: clinical and experimental*. 56:1601-1611.

Nowell, M.A., P.J. Richards, C.A. Fielding, S. Ognjanovic, N. Topley, A.S. Williams, G. Bryant-Greenwood, and S.A. Jones. 2006. Regulation of pre-B cell colony-enhancing factor by STAT-3-dependent interleukin-6 trans-signaling: implications in the pathogenesis of rheumatoid arthritis. *Arthritis and rheumatism*. 54:2084-2095.

Ntambi, J.M., Y. Choi, Y. Park, J.M. Peters, and M.W. Pariza. 2002. Effects of conjugated linoleic acid (CLA) on immune responses, body composition and stearoyl-CoA desaturase. *Canadian journal of applied physiology = Revue canadienne de physiologie appliquee*. 27:617-628.

Nusslein-Volhard, C., and E. Wieschaus. 1980. Mutations affecting segment number and polarity in Drosophila. *Nature*. 287:795-801.

Obesity., I.A.f.t.S.o. 2013. Obesity the Global Epidemic. *Available from:* http://www.iaso.org/iotg/obesitytheglobalepidemic.

Ogawa, H., T. Damrongrungruang, S. Hori, K. Nouno, K. Minagawa, M. Sato, and H. Miyazaki. 2014. Effect of periodontal treatment on adipokines in type 2 diabetes. *World journal of diabetes*. 5:924-931.

Ohno, H., K. Shinoda, B.M. Spiegelman, and S. Kajimura. 2012. PPARgamma agonists induce a white-to-brown fat conversion through stabilization of PRDM16 protein. *Cell metabolism*. 15:395-404.

Ornitz, D.M., and N. Itoh. 2001. Fibroblast growth factors. *Genome biology*. 2:REVIEWS3005.

Ouchi, N., M. Ohishi, S. Kihara, T. Funahashi, T. Nakamura, H. Nagaretani, M. Kumada, K. Ohashi, Y. Okamoto, H. Nishizawa, K. Kishida, N. Maeda, A. Nagasawa, H. Kobayashi,

H. Hiraoka, N. Komai, M. Kaibe, H. Rakugi, T. Ogihara, and Y. Matsuzawa. 2003. Association of hypoadiponectinemia with impaired vasoreactivity. *Hypertension*. 42:231-234.

Pagano, C., C. Pilon, M. Olivieri, P. Mason, R. Fabris, R. Serra, G. Milan, M. Rossato, G. Federspil, and R. Vettor. 2006. Reduced plasma visfatin/pre-B cell colony-enhancing factor in obesity is not related to insulin resistance in humans. *The Journal of clinical endocrinology and metabolism*. 91:3165-3170.

Pariza, M.W., and W.A. Hargraves. 1985. A beef-derived mutagenesis modulator inhibits initiation of mouse epidermal tumors by 7,12-dimethylbenz[a]anthracene. *Carcinogenesis*. 6:591-593.

Pariza, M.W., Y. Park, and M.E. Cook. 2001. The biologically active isomers of conjugated linoleic acid. *Progress in lipid research*. 40:283-298.

Park, A., W.K. Kim, and K.H. Bae. 2014. Distinction of white, beige and brown adipocytes derived from mesenchymal stem cells. *World journal of stem cells*. 6:33-42.

Park, E.A., A.L. Gurney, S.E. Nizielski, P. Hakimi, Z. Cao, A. Moorman, and R.W. Hanson. 1993. Relative roles of CCAAT/enhancer-binding protein beta and cAMP regulatory element-binding protein in controlling transcription of the gene for phosphoenolpyruvate carboxykinase (GTP). *The Journal of biological chemistry*. 268:613-619.

Park, E.A., S. Song, C. Vinson, and W.J. Roesler. 1999. Role of CCAAT enhancer-binding protein beta in the thyroid hormone and cAMP induction of phosphoenolpyruvate carboxykinase gene transcription. *The Journal of biological chemistry*. 274:211-217.

Park, Y., K.J. Albright, W. Liu, J.M. Storkson, M.E. Cook, and M.W. Pariza. 1997. Effect of conjugated linoleic acid on body composition in mice. *Lipids*. 32:853-858.

Park, Y., J.M. Storkson, K.J. Albright, W. Liu, and M.W. Pariza. 1999. Evidence that the trans-10,cis-12 isomer of conjugated linoleic acid induces body composition changes in mice. *Lipids*. 34:235-241.

Parsons, T.J., C. Power, S. Logan, and C.D. Summerbell. 1999. Childhood predictors of adult obesity: a systematic review. *International journal of obesity and related metabolic disorders : journal of the International Association for the Study of Obesity*. 23 Suppl 8:S1-107.

Patel, L., A.C. Buckels, I.J. Kinghorn, P.R. Murdock, J.D. Holbrook, C. Plumpton, C.H. Macphee, and S.A. Smith. 2003. Resistin is expressed in human macrophages and directly regulated by PPAR gamma activators. *Biochemical and biophysical research communications*. 300:472-476.

Pearce, L.R., D. Komander, and D.R. Alessi. 2010. The nuts and bolts of AGC protein kinases. *Nature reviews. Molecular cell biology*. 11:9-22.

Pedersen, S.D. 2013. Metabolic complications of obesity. *Best practice & research. Clinical endocrinology & metabolism*. 27:179-193.

Perez Rodrigo, C. 2013. Current mapping of obesity. *Nutricion hospitalaria*. 28 Suppl 5:21-31.

Petelin, A., M. Bizjak, M. Cernelic-Bizjak, M. Jurdana, T. Jakus, and Z. Jenko-Praznikar. 2014. Low-grade inflammation in overweight and obese adults is affected by weight loss program. *Journal of endocrinological investigation*. 37:745-755.

Petersen, R.K., L. Madsen, L.M. Pedersen, P. Hallenborg, H. Hagland, K. Viste, S.O. Doskeland, and K. Kristiansen. 2008. Cyclic AMP (cAMP)-mediated stimulation of adipocyte differentiation requires the synergistic action of Epac- and cAMP-dependent protein kinase-dependent processes. *Molecular and cellular biology*. 28:3804-3816.

Phillips, M.S., Q. Liu, H.A. Hammond, V. Dugan, P.J. Hey, C.J. Caskey, and J.F. Hess. 1996. Leptin receptor missense mutation in the fatty Zucker rat. *Nature genetics*. 13:18-19.

Pittenger, M.F., A.M. Mackay, S.C. Beck, R.K. Jaiswal, R. Douglas, J.D. Mosca, M.A. Moorman, D.W. Simonetti, S. Craig, and D.R. Marshak. 1999. Multilineage potential of adult human mesenchymal stem cells. *Science*. 284:143-147.

Poirier, H., J.S. Shapiro, R.J. Kim, and M.A. Lazar. 2006. Nutritional supplementation with trans-10, cis-12-conjugated linoleic acid induces inflammation of white adipose tissue. *Diabetes*. 55:1634-1641.

Porreca, E., C. Di Febbo, V. Moretta, A. Angelini, M.D. Guglielmi, M. Di Nisio, and F. Cuccurullo. 2004. Circulating leptin is associated with oxidized LDL in postmenopausal women. *Atherosclerosis*. 175:139-143.

Pradhan, A.D., J.E. Manson, N. Rifai, J.E. Buring, and P.M. Ridker. 2001. C-reactive protein, interleukin 6, and risk of developing type 2 diabetes mellitus. *Jama*. 286:327-334.

Prieur, X., C.Y. Mok, V.R. Velagapudi, V. Nunez, L. Fuentes, D. Montaner, K. Ishikawa, A. Camacho, N. Barbarroja, S. O'Rahilly, J.K. Sethi, J. Dopazo, M. Oresic, M. Ricote, and A. Vidal-Puig. 2011. Differential lipid partitioning between adipocytes and tissue macrophages modulates macrophage lipotoxicity and M2/M1 polarization in obese mice. *Diabetes*. 60:797-809.

Proskuryakov, S.Y., A.G. Konoplyannikov, and V.L. Gabai. 2003. Necrosis: a specific form of programmed cell death? *Experimental cell research*. 283:1-16.

Qi, J., J. Gong, T. Zhao, J. Zhao, P. Lam, J. Ye, J.Z. Li, J. Wu, H.M. Zhou, and P. Li. 2008. Downregulation of AMP-activated protein kinase by Cidea-mediated ubiquitination and degradation in brown adipose tissue. *The EMBO journal*. 27:1537-1548.

Qi, R., F. Yang, J. Huang, H. Peng, Y. Liu, and Z. Liu. 2014. Supplementation with conjugated linoeic acid decreases pig back fat deposition by inducing adipocyte apoptosis. *BMC veterinary research*. 10:141.

Qian, H., G.J. Hausman, M.M. Compton, M.J. Azain, D.L. Hartzell, and C.A. Baile. 1998. Down-regulation of CCAAT/enhancer binding proteins alpha, beta and delta in adipose tissue by intracerebroventricular leptin in rats. *Biochimica et biophysica acta*. 1442:245-251.

Qian, S.W., Y. Tang, X. Li, Y. Liu, Y.Y. Zhang, H.Y. Huang, R.D. Xue, H.Y. Yu, L. Guo, H.D. Gao, Y. Liu, X. Sun, Y.M. Li, W.P. Jia, and Q.Q. Tang. 2013. BMP4-mediated brown fat-like changes in white adipose tissue alter glucose and energy homeostasis. *Proceedings of the National Academy of Sciences of the United States of America*. 110:E798-807.

Qiu, Y., K.D. Nguyen, J.I. Odegaard, X. Cui, X. Tian, R.M. Locksley, R.D. Palmiter, and A. Chawla. 2014. Eosinophils and type 2 cytokine signaling in macrophages orchestrate development of functional beige fat. *Cell*. 157:1292-1308.

Rangwala, S.M., and M.A. Lazar. 2000. Transcriptional control of adipogenesis. *Annual review of nutrition*. 20:535-559.

Reaven, G.M. 1988. Banting lecture 1988. Role of insulin resistance in human disease. *Diabetes*. 37:1595-1607.

Redondo, M.J., L.M. Rodriguez, M.W. Haymond, C.S. Hampe, E.O. Smith, A. Balasubramanyam, and S. Devaraj. 2014. Serum adiposity-induced biomarkers in obese and lean children with recently diagnosed autoimmune type 1 diabetes. *Pediatric diabetes*. 15:543-549.

Reilly, M.P., and D.J. Rader. 2003. The metabolic syndrome: more than the sum of its parts? *Circulation*. 108:1546-1551.

Ren, D., T.N. Collingwood, E.J. Rebar, A.P. Wolffe, and H.S. Camp. 2002. PPARgamma knockdown by engineered transcription factors: exogenous PPARgamma2 but not PPARgamma1 reactivates adipogenesis. *Genes & development*. 16:27-32.

Reya, T., and H. Clevers. 2005. Wnt signalling in stem cells and cancer. *Nature*. 434:843-850.

Reznikoff, C.A., D.W. Brankow, and C. Heidelberger. 1973. Establishment and characterization of a cloned line of C3H mouse embryo cells sensitive to postconfluence inhibition of division. *Cancer research*. 33:3231-3238.

Ricklin, D., G. Hajishengallis, K. Yang, and J.D. Lambris. 2010. Complement: a key system for immune surveillance and homeostasis. *Nature immunology*. 11:785-797.

Roche, H.M., E. Noone, C. Sewter, S. Mc Bennett, D. Savage, M.J. Gibney, S. O'Rahilly, and A.J. Vidal-Puig. 2002. Isomer-dependent metabolic effects of conjugated linoleic acid: insights from molecular markers sterol regulatory element-binding protein-1c and LXRalpha. *Diabetes*. 51:2037-2044.

Rodbell, M. 1964. Metabolism of Isolated Fat Cells. I. Effects of Hormones on Glucose Metabolism and Lipolysis. *The Journal of biological chemistry*. 239:375-380.

Rodeheffer, M.S., K. Birsoy, and J.M. Friedman. 2008. Identification of white adipocyte progenitor cells in vivo. *Cell*. 135:240-249.

Rolland, C., M. Hession, and I. Broom. 2011. Effect of weight loss on adipokine levels in obese patients. *Diabetes, metabolic syndrome and obesity : targets and therapy*. 4:315-323.

Roman, A.A., S.D. Parlee, and C.J. Sinal. 2012. Chemerin: a potential endocrine link between obesity and type 2 diabetes. *Endocrine*. 42:243-251.

Rosen, B.S., K.S. Cook, J. Yaglom, D.L. Groves, J.E. Volanakis, D. Damm, T. White, and B.M. Spiegelman. 1989. Adipsin and complement factor D activity: an immune-related defect in obesity. *Science*. 244:1483-1487.

Ross, S.E., R.L. Erickson, N. Hemati, and O.A. MacDougald. 1999. Glycogen synthase kinase 3 is an insulin-regulated C/EBPalpha kinase. *Molecular and cellular biology*. 19:8433-8441.

Ross, S.E., N. Hemati, K.A. Longo, C.N. Bennett, P.C. Lucas, R.L. Erickson, and O.A. MacDougald. 2000. Inhibition of adipogenesis by Wnt signaling. *Science*. 289:950-953.

Rothwell, N.J., and M.J. Stock. 1988. The cafeteria diet as a tool for studies of thermogenesis. *The Journal of nutrition*. 118:925-928.

Rovedo, M. A., N. L. Krett, et al. (2011). "Inhibition of glycogen synthase kinase-3 increases the cytotoxicity of enzastaurin." J Invest Dermatol 131(7): 1442-1449.

Rubin, C.S., A. Hirsch, C. Fung, and O.M. Rosen. 1978. Development of hormone receptors and hormonal responsiveness in vitro. Insulin receptors and insulin sensitivity in the preadipocyte and adipocyte forms of 3T3-L1 cells. *The Journal of biological chemistry*. 253:7570-7578.

Russell, J.S., S.O. McGee, M.M. Ip, D. Kuhlmann, and P.A. Masso-Welch. 2007. Conjugated linoleic acid induces mast cell recruitment during mouse mammary gland stromal remodeling. *The Journal of nutrition*. 137:1200-1207.

Russell, T.R., and R. Ho. 1976. Conversion of 3T3 fibroblasts into adipose cells: triggering of differentiation by prostaglandin F2alpha and 1-methyl-3-isobutyl xanthine. *Proceedings of the National Academy of Sciences of the United States of America*. 73:4516-4520.

Sakaue, H., M. Konishi, W. Ogawa, T. Asaki, T. Mori, M. Yamasaki, M. Takata, H. Ueno, S. Kato, M. Kasuga, and N. Itoh. 2002. Requirement of fibroblast growth factor 10 in development of white adipose tissue. *Genes & development*. 16:908-912.

Samad, F., K. Yamamoto, M. Pandey, and D.J. Loskutoff. 1997. Elevated expression of transforming growth factor-beta in adipose tissue from obese mice. *Molecular medicine*. 3:37-48.

Samal, B., Y. Sun, G. Stearns, C. Xie, S. Suggs, and I. McNiece. 1994. Cloning and characterization of the cDNA encoding a novel human pre-B-cell colony-enhancing factor. *Molecular and cellular biology*. 14:1431-1437.

Sampson, S.R., and D.R. Cooper. 2006. Specific protein kinase C isoforms as transducers and modulators of insulin signaling. *Molecular genetics and metabolism*. 89:32-47.

Samsa, M.M., J.A. Mondotte, N.G. Iglesias, I. Assuncao-Miranda, G. Barbosa-Lima, A.T. Da Poian, P.T. Bozza, and A.V. Gamarnik. 2009. Dengue virus capsid protein usurps lipid droplets for viral particle formation. *PLoS pathogens*. 5:e1000632.

Sassi, F. 2010. OBESITY AND THE ECONOMICS OF PREVENTION: FIT NOT FAT. *OECD*.

Savona-Ventura, C., and S. Savona-Ventura. 2015. The inheritance of obesity. *Best practice & research. Clinical obstetrics & gynaecology*. 29:300-308.

Schachtrup, C., T. Emmler, B. Bleck, A. Sandqvist, and F. Spener. 2004. Functional analysis of peroxisome-proliferator-responsive element motifs in genes of fatty acid-binding proteins. *The Biochemical journal*. 382:239-245.

Schaffler, A., and J. Scholmerich. 2010. Innate immunity and adipose tissue biology. *Trends in immunology*. 31:228-235.

Schenk, S., M. Saberi, and J.M. Olefsky. 2008. Insulin sensitivity: modulation by nutrients and inflammation. *The Journal of clinical investigation*. 118:2992-3002.

Scherer, P.E., S. Williams, M. Fogliano, G. Baldini, and H.F. Lodish. 1995. A novel serum protein similar to C1q, produced exclusively in adipocytes. *J Biol Chem*. 270:26746-26749.

Schipper, H.S., M. Rakhshandehroo, S.F. van de Graaf, K. Venken, A. Koppen, R. Stienstra, S. Prop, J. Meerding, N. Hamers, G. Besra, L. Boon, E.E. Nieuwenhuis, D. Elewaut, B. Prakken, S. Kersten, M. Boes, and E. Kalkhoven. 2012. Natural killer T cells in adipose tissue prevent insulin resistance. *The Journal of clinical investigation*. 122:3343-3354.

Schmidt, J., K. Liebscher, et al. (2011). "Conjugated linoleic acids mediate insulin release through islet G protein-coupled receptor FFA1/GPR40." J Biol Chem 286(14): 11890-11894.

Schmierer, B., A.L. Tournier, P.A. Bates, and C.S. Hill. 2008. Mathematical modeling identifies Smad nucleocytoplasmic shuttling as a dynamic signal-interpreting system. *Proceedings of the National Academy of Sciences of the United States of America*. 105:6608-6613.

Schmitz-Peiffer, C. 2013. The tail wagging the dog--regulation of lipid metabolism by protein kinase C. *The FEBS journal*. 280:5371-5383.

Schoonjans, K., J. Peinado-Onsurbe, A.M. Lefebvre, R.A. Heyman, M. Briggs, S. Deeb, B. Staels, and J. Auwerx. 1996. PPARalpha and PPARgamma activators direct a distinct tissue-specific transcriptional response via a PPRE in the lipoprotein lipase gene. *The EMBO journal*. 15:5336-5348.

Schoonjans, K., M. Watanabe, H. Suzuki, A. Mahfoudi, G. Krey, W. Wahli, P. Grimaldi, B. Staels, T. Yamamoto, and J. Auwerx. 1995. Induction of the acyl-coenzyme A synthetase gene by fibrates and fatty acids is mediated by a peroxisome proliferator response element in the C promoter. *The Journal of biological chemistry*. 270:19269-19276.

Schraw, T., Z.V. Wang, N. Halberg, M. Hawkins, and P.E. Scherer. 2008. Plasma adiponectin complexes have distinct biochemical characteristics. *Endocrinology*. 149:2270-2282.

Schulman, I.G., G. Shao, and R.A. Heyman. 1998. Transactivation by retinoid X receptor-peroxisome proliferator-activated receptor gamma (PPARgamma) heterodimers: intermolecular synergy requires only the PPARgamma hormone-dependent activation function. *Molecular and cellular biology*. 18:3483-3494.

Schulz, T.J., T.L. Huang, T.T. Tran, H. Zhang, K.L. Townsend, J.L. Shadrach, M. Cerletti, L.E. McDougall, N. Giorgadze, T. Tchkonia, D. Schrier, D. Falb, J.L. Kirkland, A.J. Wagers, and Y.H. Tseng. 2011. Identification of inducible brown adipocyte progenitors residing in skeletal muscle and white fat. *Proceedings of the National Academy of Sciences of the United States of America*. 108:143-148.

Schwarz, E.J., M.J. Reginato, D. Shao, S.L. Krakow, and M.A. Lazar. 1997. Retinoic acid blocks adipogenesis by inhibiting C/EBPbeta-mediated transcription. *Molecular and cellular biology*. 17:1552-1561.

Schweiger, M., R. Schreiber, G. Haemmerle, A. Lass, C. Fledelius, P. Jacobsen, H. Tornqvist, R. Zechner, and R. Zimmermann. 2006. Adipose triglyceride lipase and hormone-sensitive lipase are the major enzymes in adipose tissue triacylglycerol catabolism. *The Journal of biological chemistry*. 281:40236-40241.

Sclafani, A., and D. Springer. 1976. Dietary obesity in adult rats: similarities to hypothalamic and human obesity syndromes. *Physiology & behavior*. 17:461-471.

Sell, H., J. Laurencikiene, A. Taube, K. Eckardt, A. Cramer, A. Horrighs, P. Arner, and J. Eckel. 2009. Chemerin is a novel adipocyte-derived factor inducing insulin resistance in primary human skeletal muscle cells. *Diabetes*. 58:2731-2740.

Sengenes, C., A. Bouloumie, H. Hauner, M. Berlan, R. Busse, M. Lafontan, and J. Galitzky. 2003. Involvement of a cGMP-dependent pathway in the natriuretic peptide-mediated hormone-sensitive lipase phosphorylation in human adipocytes. *The Journal of biological chemistry*. 278:48617-48626.

Shah, S.A., N. Mahmud, M. Mftah, H.M. Roche, and D. Kelleher. 2006. Chronic but not acute conjugated linoleic acid treatment inhibits deoxycholic acid-induced protein kinase C and nuclear factor-kappaB activation in human colorectal cancer cells. *European journal of cancer prevention : the official journal of the European Cancer Prevention Organisation*. 15:125-133.

Shapiro, H., T. Pecht, R. Shaco-Levy, I. Harman-Boehm, B. Kirshtein, Y. Kuperman, A. Chen, M. Bluher, I. Shai, and A. Rudich. 2013. Adipose tissue foam cells are present in human obesity. *The Journal of clinical endocrinology and metabolism*. 98:1173-1181.

Sharma, A.M., S. Engeli, and T. Pischon. 2001. New developments in mechanisms of obesity-induced hypertension: role of adipose tissue. *Current hypertension reports*. 3:152-156.

Shen, H.M., and P. Codogno. 2011. Autophagic cell death: Loch Ness monster or endangered species? *Autophagy*. 7:457-465.

Shen, W.J., Y. Liang, R. Hong, S. Patel, V. Natu, K. Sridhar, A. Jenkins, D.A. Bernlohr, and F.B. Kraemer. 2001. Characterization of the functional interaction of adipocyte lipid-binding protein with hormone-sensitive lipase. *The Journal of biological chemistry*. 276:49443-49448.

Shen, W.J., Z. Yu, S. Patel, D. Jue, L.F. Liu, and F.B. Kraemer. 2011. Hormone-sensitive lipase modulates adipose metabolism through PPARgamma. *Biochimica et biophysica acta*. 1811:9-16.

Sherwood, V. 2015. WNT signaling: an emerging mediator of cancer cell metabolism? *Molecular and cellular biology*. 35:2-10.

Shi, Y., and J. Massague. 2003. Mechanisms of TGF-beta signaling from cell membrane to the nucleus. *Cell*. 113:685-700.

Shimizu, S., T. Kanaseki, N. Mizushima, T. Mizuta, S. Arakawa-Kobayashi, C.B. Thompson, and Y. Tsujimoto. 2004. Role of Bcl-2 family proteins in a non-apoptotic programmed cell death dependent on autophagy genes. *Nature cell biology*. 6:1221-1228.

Shore, S.A. 2007. Obesity and asthma: lessons from animal models. *Journal of applied physiology*. 102:516-528.

Siersbaek, R., R. Nielsen, and S. Mandrup. 2012. Transcriptional networks and chromatin remodeling controlling adipogenesis. *Trends in endocrinology and metabolism: TEM*. 23:56-64.

Simpson, E.R. 2003. Sources of estrogen and their importance. *The Journal of steroid biochemistry and molecular biology*. 86:225-230.

Singh, R., Y. Xiang, Y. Wang, K. Baikati, A.M. Cuervo, Y.K. Luu, Y. Tang, J.E. Pessin, G.J. Schwartz, and M.J. Czaja. 2009. Autophagy regulates adipose mass and differentiation in mice. *The Journal of clinical investigation*. 119:3329-3339.

Skillington, J., L. Choy, and R. Derynck. 2002. Bone morphogenetic protein and retinoic acid signaling cooperate to induce osteoblast differentiation of preadipocytes. *The Journal of cell biology*. 159:135-146.

Skinner, J.R., L.A. Harris, T.M. Shew, N.A. Abumrad, and N.E. Wolins. 2013. Perilipin 1 moves between the fat droplet and the endoplasmic reticulum. *Adipocyte*. 2:80-86.

Skinner, J.R., T.M. Shew, D.M. Schwartz, A. Tzekov, C.M. Lepus, N.A. Abumrad, and N.E. Wolins. 2009. Diacylglycerol enrichment of endoplasmic reticulum or lipid droplets

recruits perilipin 3/TIP47 during lipid storage and mobilization. *The Journal of biological chemistry*. 284:30941-30948.

Smathers, R.L., and D.R. Petersen. 2011. The human fatty acid-binding protein family: evolutionary divergences and functions. *Human genomics*. 5:170-191.

Smink, J.J., and A. Leutz. 2010. Rapamycin and the transcription factor C/EBPbeta as a switch in osteoclast differentiation: implications for lytic bone diseases. *Journal of molecular medicine*. 88:227-233.

Smith, P.J., L.S. Wise, R. Berkowitz, C. Wan, and C.S. Rubin. 1988. Insulin-like growth factor-I is an essential regulator of the differentiation of 3T3-L1 adipocytes. *The Journal of biological chemistry*. 263:9402-9408.

So, M.H., I.M. Tse, and E.T. Li. 2009. Dietary fat concentration influences the effects of trans-10, cis-12 conjugated linoleic acid on temporal patterns of energy intake and hypothalamic expression of appetite-controlling genes in mice. *The Journal of nutrition*. 139:145-151.

Song, H.J., A.A. Sneddon, P.A. Barker, C. Bestwick, S.N. Choe, S. McClinton, I. Grant, D. Rotondo, S.D. Heys, and K.W. Wahle. 2004. Conjugated linoleic acid inhibits proliferation and modulates protein kinase C isoforms in human prostate cancer cells. *Nutrition and cancer*. 49:100-108.

Song, L., M. Liu, N. Ono, F.R. Bringhurst, H.M. Kronenberg, and J. Guo. 2012. Loss of wnt/beta-catenin signaling causes cell fate shift of preosteoblasts from osteoblasts to adipocytes. *Journal of bone and mineral research : the official journal of the American Society for Bone and Mineral Research*. 27:2344-2358.

Sottile, V., and K. Seuwen. 2000. Bone morphogenetic protein-2 stimulates adipogenic differentiation of mesenchymal precursor cells in synergy with BRL 49653 (rosiglitazone). *FEBS letters*. 475:201-204.

Souza, S.C., K.V. Muliro, L. Liscum, P. Lien, M.T. Yamamoto, J.E. Schaffer, G.E. Dallal, X. Wang, F.B. Kraemer, M. Obin, and A.S. Greenberg. 2002. Modulation of hormone-sensitive lipase and protein kinase A-mediated lipolysis by perilipin A in an adenoviral reconstituted system. *The Journal of biological chemistry*. 277:8267-8272.

Spalding, K.L., E. Arner, P.O. Westermark, S. Bernard, B.A. Buchholz, O. Bergmann, L. Blomqvist, J. Hoffstedt, E. Naslund, T. Britton, H. Concha, M. Hassan, M. Ryden, J. Frisen, and P. Arner. 2008. Dynamics of fat cell turnover in humans. *Nature*. 453:783-787.

Speakman, J.R., and S. O'Rahilly. 2012. Fat: an evolving issue. *Disease models & mechanisms*. 5:569-573.

Spiegelman, B.M., M. Frank, and H. Green. 1983. Molecular cloning of mRNA from 3T3 adipocytes. Regulation of mRNA content for glycerophosphate dehydrogenase and other differentiation-dependent proteins during adipocyte development. *The Journal of biological chemistry*. 258:10083-10089.

Statcan. 2004. Prevalence of Canadian child OW and OB compared between 1978/9

and 2004. *statcan.gc.ca/pub/82 -003- x/2005003/article/9277 -eng.pdf*.

Stefanovic-Racic, M., X. Yang, M.S. Turner, B.S. Mantell, D.B. Stolz, T.L. Sumpter, I.J. Sipula, N. Dedousis, D.K. Scott, P.A. Morel, A.W. Thomson, and R.M. O'Doherty. 2012. Dendritic cells promote macrophage infiltration and comprise a substantial proportion of obesity-associated increases in CD11c+ cells in adipose tissue and liver. *Diabetes*. 61:2330-2339.

Steinberg, S.F. 2008. Structural basis of protein kinase C isoform function. *Physiological reviews*. 88:1341-1378.

Steinhart, H., R. Rickert, and K. Winkler. 2003. Identification and analysis of conjugated linoleic acid isomers (CLA). *European journal of medical research*. 8:370-372.

Steppan, C.M., E.J. Brown, C.M. Wright, S. Bhat, R.R. Banerjee, C.Y. Dai, G.H. Enders, D.G. Silberg, X. Wen, G.D. Wu, and M.A. Lazar. 2001. A family of tissue-specific resistin-like molecules. *Proceedings of the National Academy of Sciences of the United States of America*. 98:502-506.

Stevens, G.A., G.M. Singh, Y. Lu, G. Danaei, J.K. Lin, M.M. Finucane, A.N. Bahalim, R.K. McIntire, H.R. Gutierrez, M. Cowan, C.J. Paciorek, F. Farzadfar, L. Riley, M. Ezzati, and G. Global Burden of Metabolic Risk Factors of Chronic Diseases Collaborating. 2012. National, regional, and global trends in adult overweight and obesity prevalences. *Population health metrics*. 10:22.

Stocco, C. 2012. Tissue physiology and pathology of aromatase. *Steroids*. 77:27-35.

Styner, M., B. Sen, Z. Xie, N. Case, and J. Rubin. 2010. Indomethacin promotes adipogenesis of mesenchymal stem cells through a cyclooxygenase independent mechanism. *Journal of cellular biochemistry*. 111:1042-1050.

Subramanian, V., A. Rothenberg, C. Gomez, A.W. Cohen, A. Garcia, S. Bhattacharyya, L. Shapiro, G. Dolios, R. Wang, M.P. Lisanti, and D.L. Brasaemle. 2004. Perilipin A mediates the reversible binding of CGI-58 to lipid droplets in 3T3-L1 adipocytes. *The Journal of biological chemistry*. 279:42062-42071.

Suganami, T., M. Tanaka, and Y. Ogawa. 2012. Adipose tissue inflammation and ectopic lipid accumulation. *Endocrine journal*. 59:849-857.

Sun, Z., R.A. Miller, R.T. Patel, J. Chen, R. Dhir, H. Wang, D. Zhang, M.J. Graham, T.G. Unterman, G.I. Shulman, C. Sztalryd, M.J. Bennett, R.S. Ahima, M.J. Birnbaum, and M.A. Lazar. 2012. Hepatic Hdac3 promotes gluconeogenesis by repressing lipid synthesis and sequestration. *Nature medicine*. 18:934-942.

Surwit, R.S., M.N. Feinglos, J. Rodin, A. Sutherland, A.E. Petro, E.C. Opara, C.M. Kuhn, and M. Rebuffe-Scrive. 1995. Differential effects of fat and sucrose on the development of obesity and diabetes in C57BL/6J and A/J mice. *Metabolism: clinical and experimental*. 44:645-651.

Sztalryd, C., G. Xu, H. Dorward, J.T. Tansey, J.A. Contreras, A.R. Kimmel, and C. Londos. 2003. Perilipin A is essential for the translocation of hormone-sensitive lipase during lipolytic activation. *The Journal of cell biology*. 161:1093-1103.

Taicher, G.Z., F.C. Tinsley, A. Reiderman, and M.L. Heiman. 2003. Quantitative magnetic resonance (QMR) method for bone and whole-body-composition analysis. *Analytical and bioanalytical chemistry*. 377:990-1002.

Takada, I., M. Mihara, M. Suzawa, F. Ohtake, S. Kobayashi, M. Igarashi, M.Y. Youn, K. Takeyama, T. Nakamura, Y. Mezaki, S. Takezawa, Y. Yogiashi, H. Kitagawa, G. Yamada, S. Takada, Y. Minami, H. Shibuya, K. Matsumoto, and S. Kato. 2007. A histone lysine methyltransferase activated by non-canonical Wnt signalling suppresses PPAR-gamma transactivation. *Nature cell biology*. 9:1273-1285.

Takada, I., M. Suzawa, and S. Kato. 2005. Nuclear receptors as targets for drug development: crosstalk between peroxisome proliferator-activated receptor gamma and cytokines in bone marrow-derived mesenchymal stem cells. *Journal of pharmacological sciences*. 97:184-189.

Takahashi, Y., M. Kushiro, K. Shinohara, and T. Ide. 2002. Dietary conjugated linoleic acid reduces body fat mass and affects gene expression of proteins regulating energy metabolism in mice. *Comparative biochemistry and physiology. Part B, Biochemistry & molecular biology*. 133:395-404.

Tan, N.S., N.S. Shaw, N. Vinckenbosch, P. Liu, R. Yasmin, B. Desvergne, W. Wahli, and N. Noy. 2002. Selective cooperation between fatty acid binding proteins and peroxisome proliferator-activated receptors in regulating transcription. *Molecular and cellular biology*. 22:5114-5127.

Tanaka, M., M. Nozaki, A. Fukuhara, K. Segawa, N. Aoki, M. Matsuda, R. Komuro, and I. Shimomura. 2007. Visfatin is released from 3T3-L1 adipocytes via a non-classical pathway. *Biochemical and biophysical research communications*. 359:194-201.

Tanaka, T., N. Yoshida, T. Kishimoto, and S. Akira. 1997. Defective adipocyte differentiation in mice lacking the C/EBPbeta and/or C/EBPdelta gene. *The EMBO journal*. 16:7432-7443.

Tang, Q.Q., M. Gronborg, H. Huang, J.W. Kim, T.C. Otto, A. Pandey, and M.D. Lane. 2005. Sequential phosphorylation of CCAAT enhancer-binding protein beta by MAPK and glycogen synthase kinase 3beta is required for adipogenesis. *Proceedings of the National Academy of Sciences of the United States of America*. 102:9766-9771.

Tang, Q.Q., and M.D. Lane. 1999. Activation and centromeric localization of CCAAT/enhancer-binding proteins during the mitotic clonal expansion of adipocyte differentiation. *Genes & development*. 13:2231-2241.

Tang, Q.Q., and M.D. Lane. 2012. Adipogenesis: from stem cell to adipocyte. *Annual review of biochemistry*. 81:715-736.

Tang, Q.Q., T.C. Otto, and M.D. Lane. 2004. Commitment of C3H10T1/2 pluripotent stem cells to the adipocyte lineage. *Proceedings of the National Academy of Sciences of the United States of America*. 101:9607-9611.

Tansey, J.T., A.M. Huml, R. Vogt, K.E. Davis, J.M. Jones, K.A. Fraser, D.L. Brasaemle, A.R. Kimmel, and C. Londos. 2003. Functional studies on native and mutated forms of perilipins. A role in protein kinase A-mediated lipolysis of triacylglycerols. *The Journal of biological chemistry*. 278:8401-8406.

Taylor, C.G., and P. Zahradka. 2004. Dietary conjugated linoleic acid and insulin sensitivity and resistance in rodent models. *The American journal of clinical nutrition*. 79:1164S-1168S.

Taylor-Jones, J.M., R.E. McGehee, T.A. Rando, B. Lecka-Czernik, D.A. Lipschitz, and C.A. Peterson. 2002. Activation of an adipogenic program in adult myoblasts with age. *Mechanisms of ageing and development*. 123:649-661.

Tchoukalova, Y.D., S.B. Votruba, T. Tchkonia, N. Giorgadze, J.L. Kirkland, and M.D. Jensen. 2010. Regional differences in cellular mechanisms of adipose tissue gain with overfeeding. *Proceedings of the National Academy of Sciences of the United States of America*. 107:18226-18231.

Terpstra, A.H. 2001. Differences between humans and mice in efficacy of the body fat lowering effect of conjugated linoleic acid: role of metabolic rate. *The Journal of nutrition*. 131:2067-2068.

Terpstra, A.H., M. Javadi, A.C. Beynen, S. Kocsis, A.E. Lankhorst, A.G. Lemmens, and I.C. Mohede. 2003. Dietary conjugated linoleic acids as free fatty acids and triacylglycerols similarly affect body composition and energy balance in mice. *The Journal of nutrition*. 133:3181-3186.

Timmons, J.A., K. Wennmalm, O. Larsson, T.B. Walden, T. Lassmann, N. Petrovic, D.L. Hamilton, R.E. Gimeno, C. Wahlestedt, K. Baar, J. Nedergaard, and B. Cannon. 2007. Myogenic gene expression signature establishes that brown and white adipocytes originate from distinct cell lineages. *Proceedings of the National Academy of Sciences of the United States of America*. 104:4401-4406.

Toh, S.Y., J. Gong, G. Du, J.Z. Li, S. Yang, J. Ye, H. Yao, Y. Zhang, B. Xue, Q. Li, H. Yang, Z. Wen, and P. Li. 2008. Up-regulation of mitochondrial activity and acquirement of brown adipose tissue-like property in the white adipose tissue of fsp27 deficient mice. *PloS one*. 3:e2890.

Tomas, E., T.S. Tsao, A.K. Saha, H.E. Murrey, C. Zhang Cc, S.I. Itani, H.F. Lodish, and N.B. Ruderman. 2002. Enhanced muscle fat oxidation and glucose transport by ACRP30 globular domain: acetyl-CoA carboxylase inhibition and AMP-activated protein kinase activation. *Proceedings of the National Academy of Sciences of the United States of America*. 99:16309-16313.

Tomlinson, E., L. Fu, L. John, B. Hultgren, X. Huang, M. Renz, J.P. Stephan, S.P. Tsai, L. Powell-Braxton, D. French, and T.A. Stewart. 2002. Transgenic mice expressing human fibroblast growth factor-19 display increased metabolic rate and decreased adiposity. *Endocrinology*. 143:1741-1747.

Tong, Q., J. Tsai, G. Tan, G. Dalgin, and G.S. Hotamisligil. 2005. Interaction between GATA and the C/EBP family of transcription factors is critical in GATA-mediated suppression of adipocyte differentiation. *Molecular and cellular biology*. 25:706-715.

Tontonoz, P., R.A. Graves, A.I. Budavari, H. Erdjument-Bromage, M. Lui, E. Hu, P. Tempst, and B.M. Spiegelman. 1994. Adipocyte-specific transcription factor ARF6 is a heterodimeric complex of two nuclear hormone receptors, PPAR gamma and RXR alpha. *Nucleic acids research*. 22:5628-5634.

Tontonoz, P., E. Hu, R.A. Graves, A.I. Budavari, and B.M. Spiegelman. 1994. mPPAR gamma 2: tissue-specific regulator of an adipocyte enhancer. *Genes & development*. 8:1224-1234.

Tontonoz, P., and B.M. Spiegelman. 2008. Fat and beyond: the diverse biology of PPARgamma. *Annual review of biochemistry*. 77:289-312.

Trayhurn, P. 1979. Thermoregulation in the diabetic-obese (db/db) mouse. The role of non-shivering thermogenesis in energy balance. *Pflugers Archiv : European journal of physiology*. 380:227-232.

Trewhella, J. 2006. Protein kinase A targeting and activation as seen by small-angle solution scattering. *European journal of cell biology*. 85:655-662.

Trujillo, M.E., and P.E. Scherer. 2005. Adiponectin--journey from an adipocyte secretory protein to biomarker of the metabolic syndrome. *Journal of internal medicine*. 257:167-175.

Tseng, Y.H., A.M. Cypess, and C.R. Kahn. 2010. Cellular bioenergetics as a target for obesity therapy. *Nature reviews. Drug discovery*. 9:465-482.

Tseng, Y.H., E. Kokkotou, T.J. Schulz, T.L. Huang, J.N. Winnay, C.M. Taniguchi, T.T. Tran, R. Suzuki, D.O. Espinoza, Y. Yamamoto, M.J. Ahrens, A.T. Dudley, A.W. Norris, R.N. Kulkarni, and C.R. Kahn. 2008. New role of bone morphogenetic protein 7 in brown adipogenesis and energy expenditure. *Nature*. 454:1000-1004.

Tseng, Y.H., K.M. Kriauciunas, E. Kokkotou, and C.R. Kahn. 2004. Differential roles of insulin receptor substrates in brown adipocyte differentiation. *Molecular and cellular biology*. 24:1918-1929.

Tsuboyama-Kasaoka, N., M. Takahashi, K. Tanemura, H.J. Kim, T. Tange, H. Okuyama, M. Kasai, S. Ikemoto, and O. Ezaki. 2000. Conjugated linoleic acid supplementation reduces adipose tissue by apoptosis and develops lipodystrophy in mice. *Diabetes*. 49:1534-1542.

Tsukada, J., Y. Yoshida, Y. Kominato, and P.E. Auron. 2011. The CCAAT/enhancer (C/EBP) family of basic-leucine zipper (bZIP) transcription factors is a multifaceted highly-regulated system for gene regulation. *Cytokine*. 54:6-19.

Unal, R., I. Pokrovskaya, P. Tripathi, B.P. Monia, P.A. Kern, and G. Ranganathan. 2008. Translational regulation of lipoprotein lipase in adipocytes: depletion of cellular protein kinase Calpha activates binding of the C subunit of protein kinase A to the 3'-untranslated region of the lipoprotein lipase mRNA. *The Biochemical journal*. 413:315-322.

Uysal, K.T., L. Scheja, S.M. Wiesbrock, S. Bonner-Weir, and G.S. Hotamisligil. 2000. Improved glucose and lipid metabolism in genetically obese mice lacking aP2. *Endocrinology*. 141:3388-3396.

Varjosalo, M., and J. Taipale. 2008. Hedgehog: functions and mechanisms. *Genes & development*. 22:2454-2472.

Vertino, A.M., J.M. Taylor-Jones, K.A. Longo, E.D. Bearden, T.F. Lane, R.E. McGehee, Jr., O.A. MacDougald, and C.A. Peterson. 2005. Wnt10b deficiency promotes coexpression of myogenic and adipogenic programs in myoblasts. *Molecular biology of the cell*. 16:2039-2048.

Wahle, K.W., S.D. Heys, and D. Rotondo. 2004. Conjugated linoleic acids: are they beneficial or detrimental to health? *Progress in lipid research*. 43:553-587.

Wakabayashi, K., M. Okamura, S. Tsutsumi, N.S. Nishikawa, T. Tanaka, I. Sakakibara, J. Kitakami, S. Ihara, Y. Hashimoto, T. Hamakubo, T. Kodama, H. Aburatani, and J. Sakai. 2009. The peroxisome proliferator-activated receptor gamma/retinoid X receptor alpha heterodimer targets the histone modification enzyme PR-Set7/Setd8 gene and regulates adipogenesis through a positive feedback loop. *Molecular and cellular biology*. 29:3544-3555.

Waki, H., T. Yamauchi, J. Kamon, Y. Ito, S. Uchida, S. Kita, K. Hara, Y. Hada, F. Vasseur, P. Froguel, S. Kimura, R. Nagai, and T. Kadowaki. 2003. Impaired multimerization of human adiponectin mutants associated with diabetes. Molecular structure and multimer formation of adiponectin. *J Biol Chem*. 278:40352-40363.

Wallace, R.J., N. McKain, K.J. Shingfield, and E. Devillard. 2007. Isomers of conjugated linoleic acids are synthesized via different mechanisms in ruminal digesta and bacteria. *Journal of lipid research*. 48:2247-2254.

Wang, H., U. Sreenivasan, H. Hu, A. Saladino, B.M. Polster, L.M. Lund, D.W. Gong, W.C. Stanley, and C. Sztalryd. 2011. Perilipin 5, a lipid droplet-associated protein, provides physical and metabolic linkage to mitochondria. *Journal of lipid research*. 52:2159-2168.

Wang, L., Q. Jin, J.E. Lee, I.H. Su, and K. Ge. 2010. Histone H3K27 methyltransferase Ezh2 represses Wnt genes to facilitate adipogenesis. *Proceedings of the National Academy of Sciences of the United States of America*. 107:7317-7322.

Wang, N.D., M.J. Finegold, A. Bradley, C.N. Ou, S.V. Abdelsayed, M.D. Wilde, L.R. Taylor, D.R. Wilson, and G.J. Darlington. 1995. Impaired energy homeostasis in C/EBP alpha knockout mice. *Science*. 269:1108-1112.

Wang, Q.A., C. Tao, R.K. Gupta, and P.E. Scherer. 2013. Tracking adipogenesis during white adipose tissue development, expansion and regeneration. *Nature medicine*. 19:1338-1344.

Wang, W., B. Poole, A. Mitra, S. Falk, G. Fantuzzi, S. Lucia, and R. Schrier. 2004. Role of leptin deficiency in early acute renal failure during endotoxemia in ob/ob mice. *Journal of the American Society of Nephrology : JASN*. 15:645-649.

Way, J.M., C.Z. Gorgun, Q. Tong, K.T. Uysal, K.K. Brown, W.W. Harrington, W.R. Oliver, Jr., T.M. Willson, S.A. Kliewer, and G.S. Hotamisligil. 2001. Adipose tissue resistin expression is severely suppressed in obesity and stimulated by peroxisome proliferator-activated receptor gamma agonists. *The Journal of biological chemistry*. 276:25651-25653.

Weisberg, S.P., D. McCann, M. Desai, M. Rosenbaum, R.L. Leibel, and A.W. Ferrante, Jr. 2003. Obesity is associated with macrophage accumulation in adipose tissue. *The Journal of clinical investigation*. 112:1796-1808.

Wendel, A.A., A. Purushotham, L.F. Liu, and M.A. Belury. 2008. Conjugated linoleic acid fails to worsen insulin resistance but induces hepatic steatosis in the presence of leptin in ob/ob mice. *Journal of lipid research*. 49:98-106.

West, D.B., J.P. Delany, P.M. Camet, F. Blohm, A.A. Truett, and J. Scimeca. 1998. Effects of conjugated linoleic acid on body fat and energy metabolism in the mouse. *The American journal of physiology*. 275:R667-672.

Whitaker, R.C., J.A. Wright, M.S. Pepe, K.D. Seidel, and W.H. Dietz. 1997. Predicting obesity in young adulthood from childhood and parental obesity. *The New England journal of medicine*. 337:869-873.

White, B.D., and R.J. Martin. 1997. Evidence for a central mechanism of obesity in the Zucker rat: role of neuropeptide Y and leptin. *Proceedings of the Society for Experimental Biology and Medicine. Society for Experimental Biology and Medicine*. 214:222-232.

White, R.T., D. Damm, N. Hancock, B.S. Rosen, B.B. Lowell, P. Usher, J.S. Flier, and B.M. Spiegelman. 1992. Human adipsin is identical to complement factor D and is expressed at high levels in adipose tissue. *The Journal of biological chemistry*. 267:9210-9213.

White, U.A., and Y.D. Tchoukalova. 2014. Sex dimorphism and depot differences in adipose tissue function. *Biochimica et biophysica acta*. 1842:377-392.

WHO. 2009. World Health Organization, Global health risks, mortality and burden of disease attributable to selected major risks. Retrived June 26,2015, from http://www.who.int/healthinfo/global_burden_disease/GlobalHealthRisks_report_full.pdf *WHO press*.

WHO, P.H.A.o.C. 2005. Preventing chronic diseases: a vital investment. *Geneva, World Health Organization, 2005*.

Wilfling, F., H. Wang, J.T. Haas, N. Krahmer, T.J. Gould, A. Uchida, J.X. Cheng, M. Graham, R. Christiano, F. Frohlich, X. Liu, K.K. Buhman, R.A. Coleman, J. Bewersdorf, R.V. Farese, Jr., and T.C. Walther. 2013. Triacylglycerol synthesis enzymes mediate lipid droplet growth by relocalizing from the ER to lipid droplets. *Developmental cell*. 24:384-399.

Wittamer, V., J.D. Franssen, M. Vulcano, J.F. Mirjolet, E. Le Poul, I. Migeotte, S. Brezillon, R. Tyldesley, C. Blanpain, M. Detheux, A. Mantovani, S. Sozzani, G. Vassart, M. Parmentier, and D. Communi. 2003. Specific recruitment of antigen-presenting cells by chemerin, a novel processed ligand from human inflammatory fluids. *The Journal of experimental medicine*. 198:977-985.

Wolf, A.M., D. Wolf, H. Rumpold, B. Enrich, and H. Tilg. 2004. Adiponectin induces the anti-inflammatory cytokines IL-10 and IL-1RA in human leukocytes. *Biochemical and biophysical research communications*. 323:630-635.

Wolins, N.E., B.K. Quaynor, J.R. Skinner, M.J. Schoenfish, A. Tzekov, and P.E. Bickel. 2005. S3-12, Adipophilin, and TIP47 package lipid in adipocytes. *The Journal of biological chemistry*. 280:19146-19155.

Wolins, N.E., J.R. Skinner, M.J. Schoenfish, A. Tzekov, K.G. Bensch, and P.E. Bickel. 2003. Adipocyte protein S3-12 coats nascent lipid droplets. *The Journal of biological chemistry*. 278:37713-37721.

Worldobesity. 2015. http://www.worldobesity.org/aboutobesity/child-obesity/ 2015.

Wu, C., Y. Zhang, Z. Sun, and P. Li. 2008. Molecular evolution of Cide family proteins: novel domain formation in early vertebrates and the subsequent divergence. *BMC evolutionary biology*. 8:159.

Wu, J., P. Bostrom, L.M. Sparks, L. Ye, J.H. Choi, A.H. Giang, M. Khandekar, K.A. Virtanen, P. Nuutila, G. Schaart, K. Huang, H. Tu, W.D. van Marken Lichtenbelt, J. Hoeks, S. Enerback, P. Schrauwen, and B.M. Spiegelman. 2012. Beige adipocytes are a distinct type of thermogenic fat cell in mouse and human. *Cell*. 150:366-376.

Wu, J., W.J. Yan, J. Mo, H.B. Yang, Z.Z. Wang, M.X. Lei, and L.W. Peng. 2011. [Association of adiponectin gene polymorphism with obesity in children]. *Zhongguo dang dai er ke za zhi = Chinese journal of contemporary pediatrics*. 13:539-542.

Wu, L., V.V. Parekh, C.L. Gabriel, D.P. Bracy, P.A. Marks-Shulman, R.A. Tamboli, S. Kim, Y.V. Mendez-Fernandez, G.S. Besra, J.P. Lomenick, B. Williams, D.H. Wasserman, and L. Van Kaer. 2012. Activation of invariant natural killer T cells by lipid excess promotes tissue inflammation, insulin resistance, and hepatic steatosis in obese mice. *Proceedings of the National Academy of Sciences of the United States of America*. 109:E1143-1152.

Wu, L., L. Zhou, C. Chen, J. Gong, L. Xu, J. Ye, D. Li, and P. Li. 2014. Cidea controls lipid droplet fusion and lipid storage in brown and white adipose tissue. *Science China. Life sciences*. 57:107-116.

Wu, X., H. Motoshima, K. Mahadev, T.J. Stalker, R. Scalia, and B.J. Goldstein. 2003. Involvement of AMP-activated protein kinase in glucose uptake stimulated by the globular domain of adiponectin in primary rat adipocytes. *Diabetes*. 52:1355-1363.

Wulster-Radcliffe, M.C., K.M. Ajuwon, J. Wang, J.A. Christian, and M.E. Spurlock. 2004. Adiponectin differentially regulates cytokines in porcine macrophages. *Biochemical and biophysical research communications*. 316:924-929.

Xiao, L., T. Sobue, A. Esliger, M.S. Kronenberg, J.D. Coffin, T. Doetschman, and M.M. Hurley. 2010. Disruption of the Fgf2 gene activates the adipogenic and suppresses the osteogenic program in mesenchymal marrow stromal stem cells. *Bone*. 47:360-370.

Xing, H., J.P. Northrop, J.R. Grove, K.E. Kilpatrick, J.L. Su, and G.M. Ringold. 1997. TNF alpha-mediated inhibition and reversal of adipocyte differentiation is accompanied by suppressed expression of PPARgamma without effects on Pref-1 expression. *Endocrinology*. 138:2776-2783.

Xu, H., G.T. Barnes, Q. Yang, G. Tan, D. Yang, C.J. Chou, J. Sole, A. Nichols, J.S. Ross, L.A. Tartaglia, and H. Chen. 2003. Chronic inflammation in fat plays a crucial role in the development of obesity-related insulin resistance. *The Journal of clinical investigation*. 112:1821-1830.

Xu, P., W. Ye, S. Zhong, H. Li, E. Feng, S.H. Lin, C.T. Kuo, J.Y. Liu, and Y.C. Lin. 2010. Leptin and zeranol up-regulate cyclin D1 expression in primary cultured normal human breast pre-adipocytes. *Molecular medicine reports*. 3:983-990.

Xu, Q., Y. Wang, A. Dabdoub, P.M. Smallwood, J. Williams, C. Woods, M.W. Kelley, L. Jiang, W. Tasman, K. Zhang, and J. Nathans. 2004. Vascular development in the retina and inner ear: control by Norrin and Frizzled-4, a high-affinity ligand-receptor pair. *Cell*. 116:883-895.

Xu, X., J. Storkson, S. Kim, K. Sugimoto, Y. Park, and M.W. Pariza. 2003. Short-term intake of conjugated linoleic acid inhibits lipoprotein lipase and glucose metabolism but does not enhance lipolysis in mouse adipose tissue. *The Journal of nutrition*. 133:663-667.

Yadav, H., C. Quijano, A.K. Kamaraju, O. Gavrilova, R. Malek, W. Chen, P. Zerfas, D. Zhigang, E.C. Wright, C. Stuelten, P. Sun, S. Lonning, M. Skarulis, A.E. Sumner, T. Finkel, and S.G. Rane. 2011. Protection from obesity and diabetes by blockade of TGF-beta/Smad3 signaling. *Cell metabolism*. 14:67-79.

Yamaguchi, T. 2010. Crucial role of CGI-58/alpha/beta hydrolase domain-containing protein 5 in lipid metabolism. *Biological & pharmaceutical bulletin*. 33:342-345.

Yamauchi, T., J. Kamon, Y. Minokoshi, Y. Ito, H. Waki, S. Uchida, S. Yamashita, M. Noda, S. Kita, K. Ueki, K. Eto, Y. Akanuma, P. Froguel, F. Foufelle, P. Ferre, D. Carling, S. Kimura, R. Nagai, B.B. Kahn, and T. Kadowaki. 2002. Adiponectin stimulates glucose utilization and fatty-acid oxidation by activating AMP-activated protein kinase. *Nature medicine*. 8:1288-1295.

Yamauchi, T., J. Kamon, H. Waki, Y. Terauchi, N. Kubota, K. Hara, Y. Mori, T. Ide, K. Murakami, N. Tsuboyama-Kasaoka, O. Ezaki, Y. Akanuma, O. Gavrilova, C. Vinson, M.L. Reitman, H. Kagechika, K. Shudo, M. Yoda, Y. Nakano, K. Tobe, R. Nagai, S. Kimura, M. Tomita, P. Froguel, and T. Kadowaki. 2001. The fat-derived hormone adiponectin reverses insulin resistance associated with both lipoatrophy and obesity. *Nat Med*. 7:941-946.

Yang, H., A. Galea, V. Sytnyk, and M. Crossley. 2012. Controlling the size of lipid droplets: lipid and protein factors. *Current opinion in cell biology*. 24:509-516.

Yang, H., Y.H. Youm, B. Vandanmagsar, A. Ravussin, J.M. Gimble, F. Greenway, J.M. Stephens, R.L. Mynatt, and V.D. Dixit. 2010. Obesity increases the production of proinflammatory mediators from adipose tissue T cells and compromises TCR repertoire diversity: implications for systemic inflammation and insulin resistance. *Journal of immunology*. 185:1836-1845.

Yang, V.W., R.J. Christy, J.S. Cook, T.J. Kelly, and M.D. Lane. 1989. Mechanism of regulation of the 422(aP2) gene by cAMP during preadipocyte differentiation. *Proceedings of the National Academy of Sciences of the United States of America*. 86:3629-3633.

Yang, X., P.A. Jansson, I. Nagaev, M.M. Jack, E. Carvalho, K.S. Sunnerhagen, M.C. Cam, S.W. Cushman, and U. Smith. 2004. Evidence of impaired adipogenesis in insulin resistance. *Biochemical and biophysical research communications*. 317:1045-1051.

Yang-Snyder, J., J.R. Miller, J.D. Brown, C.J. Lai, and R.T. Moon. 1996. A frizzled homolog functions in a vertebrate Wnt signaling pathway. *Current biology : CB*. 6:1302-1306.

Ye, J., J.Z. Li, Y. Liu, X. Li, T. Yang, X. Ma, Q. Li, Z. Yao, and P. Li. 2009. Cideb, an ER- and lipid droplet-associated protein, mediates VLDL lipidation and maturation by interacting with apolipoprotein B. *Cell metabolism*. 9:177-190.

Yeganeh, A. 2008. Role of connexin 43 and conjugated linoleic acid isomers during adipocyte differentiation. *In* Department of Human Nutritional Sciences-. Vol. Master of scienses. University of Manitoba. 131.

Yeganeh, A., G.L. Stelmack, R.R. Fandrich, A.J. Halayko, E. Kardami, and P. Zahradka. 2012. Connexin 43 phosphorylation and degradation are required for adipogenesis. *Biochimica et biophysica acta*. 1823:1731-1744.

Yeh, W.C., Z. Cao, M. Classon, and S.L. McKnight. 1995. Cascade regulation of terminal adipocyte differentiation by three members of the C/EBP family of leucine zipper proteins. *Genes & development*. 9:168-181.

Yu, J.G., S. Javorschi, A.L. Hevener, Y.T. Kruszynska, R.A. Norman, M. Sinha, and J.M. Olefsky. 2002. The effect of thiazolidinediones on plasma adiponectin levels in normal, obese, and type 2 diabetic subjects. *Diabetes*. 51:2968-2974.

Yu, Y., P.H. Correll, and J.P. Vanden Heuvel. 2002. Conjugated linoleic acid decreases production of pro-inflammatory products in macrophages: evidence for a PPAR gamma-dependent mechanism. *Biochimica et biophysica acta*. 1581:89-99.

Zabel, B.A., S.J. Allen, P. Kulig, J.A. Allen, J. Cichy, T.M. Handel, and E.C. Butcher. 2005. Chemerin activation by serine proteases of the coagulation, fibrinolytic, and inflammatory cascades. *The Journal of biological chemistry*. 280:34661-34666.

Zabel, B.A., S. Nakae, L. Zuniga, J.Y. Kim, T. Ohyama, C. Alt, J. Pan, H. Suto, D. Soler, S.J. Allen, T.M. Handel, C.H. Song, S.J. Galli, and E.C. Butcher. 2008. Mast cell-expressed orphan receptor CCRL2 binds chemerin and is required for optimal induction of IgE-mediated passive cutaneous anaphylaxis. *The Journal of experimental medicine*. 205:2207-2220.

Zamani, N., and C.W. Brown. 2011. Emerging roles for the transforming growth factor-{beta} superfamily in regulating adiposity and energy expenditure. *Endocrine reviews*. 32:387-403.

Zernecke, A., and C. Weber. 2005. Inflammatory mediators in atherosclerotic vascular disease. *Basic research in cardiology*. 100:93-101.

Zezulak, K.M., and H. Green. 1985. Specificity of gene expression in adipocytes. *Molecular and cellular biology*. 5:419-421.

Zhai, J.J., Z.L. Liu, J.M. Li, J.P. Chen, L. Jiang, D.M. Wang, J. Yuan, J.G. Shen, D.P. Yang, and J.Q. Chen. 2010. Different mechanisms of cis-9,trans-11- and trans-10,cis-12- conjugated linoleic acid affecting lipid metabolism in 3T3-L1 cells. *The Journal of nutritional biochemistry*. 21:1099-1105.

Zhang, H.H., S.C. Souza, K.V. Muliro, F.B. Kraemer, M.S. Obin, and A.S. Greenberg. 2003. Lipase-selective functional domains of perilipin A differentially regulate constitutive and protein kinase A-stimulated lipolysis. *The Journal of biological chemistry*. 278:51535-51542.

Zhang, Y., S. Goldman, R. Baerga, Y. Zhao, M. Komatsu, and S. Jin. 2009. Adipose-specific deletion of autophagy-related gene 7 (atg7) in mice reveals a role in adipogenesis.

Proceedings of the National Academy of Sciences of the United States of America. 106:19860-19865.

Zhang, Y., R. Proenca, M. Maffei, M. Barone, L. Leopold, and J.M. Friedman. 1994. Positional cloning of the mouse obese gene and its human homologue. *Nature*. 372:425-432.

Zhang, Y., X. Zeng, and S. Jin. 2012. Autophagy in adipose tissue biology. *Pharmacological research : the official journal of the Italian Pharmacological Society*. 66:505-512.

Zhao, M., M. Qiao, S.E. Harris, D. Chen, B.O. Oyajobi, and G.R. Mundy. 2006. The zinc finger transcription factor Gli2 mediates bone morphogenetic protein 2 expression in osteoblasts in response to hedgehog signaling. *Molecular and cellular biology*. 26:6197-6208.

Zheng, Q., S.D. Hursting, and O. Reizes. 2012. Leptin regulates cyclin D1 in luminal epithelial cells of mouse MMTV-Wnt-1 mammary tumors. *Journal of cancer research and clinical oncology*. 138:1607-1612.

Zhou, L., S.Y. Park, L. Xu, X. Xia, J. Ye, L. Su, K.H. Jeong, J.H. Hur, H. Oh, Y. Tamori, C.M. Zingaretti, S. Cinti, J. Argente, M. Yu, L. Wu, S. Ju, F. Guan, H. Yang, C.S. Choi, D.B. Savage, and P. Li. 2015. Insulin resistance and white adipose tissue inflammation are uncoupled in energetically challenged Fsp27-deficient mice. *Nature communications*. 6:5949.

Zhou, Z., S. Yon Toh, Z. Chen, K. Guo, C.P. Ng, S. Ponniah, S.C. Lin, W. Hong, and P. Li. 2003. Cidea-deficient mice have lean phenotype and are resistant to obesity. *Nature genetics*. 35:49-56.

Zhu, Y., C. Qi, J.R. Korenberg, X.N. Chen, D. Noya, M.S. Rao, and J.K. Reddy. 1995. Structural organization of mouse peroxisome proliferator-activated receptor gamma (mPPAR gamma) gene: alternative promoter use and different splicing yield two mPPAR gamma isoforms. *Proceedings of the National Academy of Sciences of the United States of America*. 92:7921-7925.

Zierath, J.R., J.W. Ryder, T. Doebber, J. Woods, M. Wu, J. Ventre, Z. Li, C. McCrary, J. Berger, B. Zhang, and D.E. Moller. 1998. Role of skeletal muscle in thiazolidinedione insulin sensitizer (PPARgamma agonist) action. *Endocrinology*. 139:5034-5041.

Zimmermann, R., J.G. Strauss, G. Haemmerle, G. Schoiswohl, R. Birner-Gruenberger, M. Riederer, A. Lass, G. Neuberger, F. Eisenhaber, A. Hermetter, and R. Zechner. 2004. Fat mobilization in adipose tissue is promoted by adipose triglyceride lipase. *Science*. 306:1383-1386.

Zuk, P.A., M. Zhu, P. Ashjian, D.A. De Ugarte, J.I. Huang, H. Mizuno, Z.C. Alfonso, J.K. Fraser, P. Benhaim, and M.H. Hedrick. 2002. Human adipose tissue is a source of multipotent stem cells. *Molecular biology of the cell*. 13:4279-4295.

Zweytick, D., K. Athenstaedt, and G. Daum. 2000. Intracellular lipid particles of eukaryotic cells. *Biochimica et biophysica acta*. 1469:101-120.

#

11. Appendix

11.1 Appendix A. Representative flow cytometry plots

Figure A1. Representative flow cytometry plots from lineage markers (tube 1) in SVF from lean C57BL/6 mice

(a) Viable cell population defined by forward-scattered light (FSC) and side-scattered light (SSC).

(b) Cell population of $CD45^{-}CD31^{-}$, shown in Q3, are the non-hematopoietic and non-endothelial cells, which were gated next.

(c) Cell populations of $CD34^{+}CD29^{+}$, shown in Q1, are mesenchymal stem cells, which were gated next.

(d) Cell population of $CD24^{-}Sca\text{-}1^{+}$, shown in Q1, are preadipocytes; cell population of $CD24^{+}Sca\text{-}1^{+}$, shown in Q2, are adipocyte stem cells; cell population of $CD24^{-}Sca\text{-}1^{-}$, shown in Q3, are immature adipocytes.

(a)

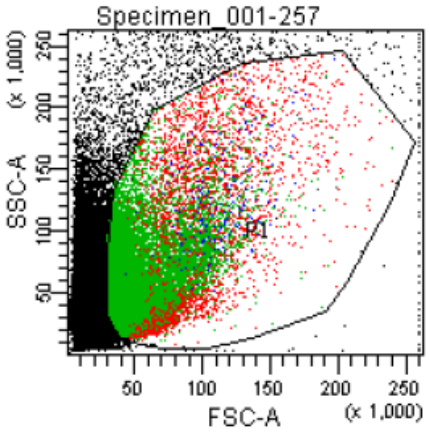
Specimen_001-257
SSC-A
(x 1,000)
FSC-A
(x 1,000)
P1

(b)

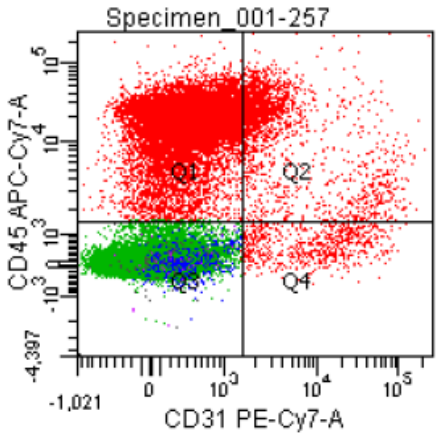
Specimen_001-257
CD45 APC-Cy7-A
CD31 PE-Cy7-A
Q1
Q2
Q3
Q4

(c)

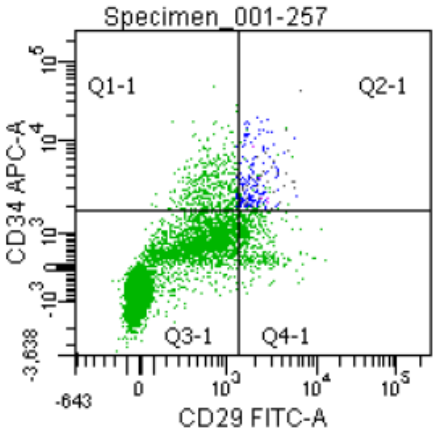
Specimen_001-257
CD34 APC-A
CD29 FITC-A
Q1-1
Q2-1
Q3-1
Q4-1

(d)

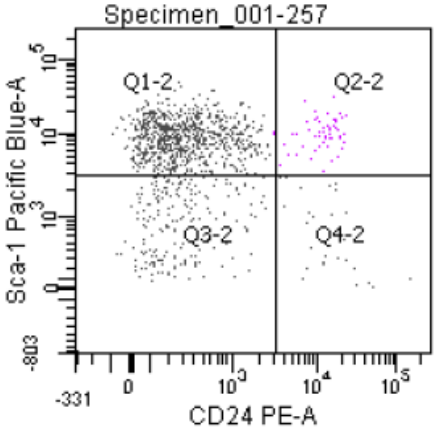
Specimen_001-257
Sca-1 Pacific Blue-A
CD24 PE-A
Q1-2
Q2-2
Q3-2
Q4-2

Figure A2. Representative flow cytometry plots from lineage markers (tube 1) in SVF from obese *db/db* mice

(a) Viable cell population defined by forward-scattered light (FSC) and side-scattered light (SSC)

(b) Cell population of $CD45^{-}CD31^{-}$, shown in Q3, are the non-hematopoietic and non-endothelial cells, which were gated next.

(c) Cell population of $CD34^{+}CD29^{+}$, shown in Q1, are mesenchymal stem cells, which were gated next.

(d) Cell population of $CD24^{-}Sca\text{-}1^{+}$, shown in Q1, are preadipocytes; cell populations of $CD24^{+}Sca\text{-}1^{+}$, shown in Q2, are adipocyte stem cells; cell population of $CD24^{-}Sca\text{-}1^{-}$, shown in Q3, are immature adipocytes.

(a)

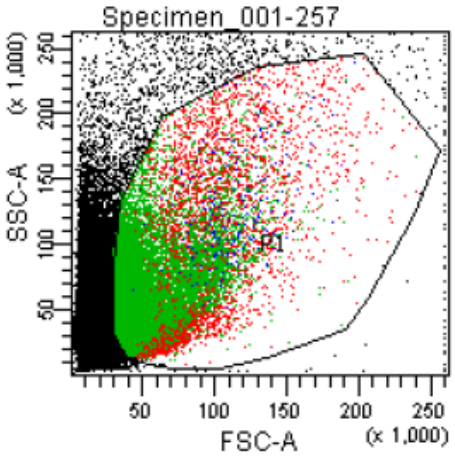
Specimen_001-257
SSC-A
(x 1,000)
FSC-A
(x 1,000)
P1

(b)

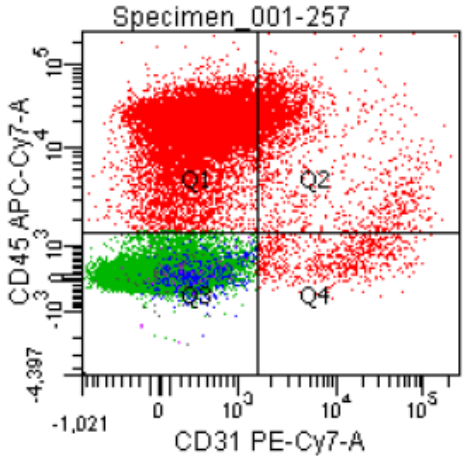
Specimen_001-257
CD45 APC-Cy7-A
CD31 PE-Cy7-A
Q1
Q2
Q3
Q4

(c)

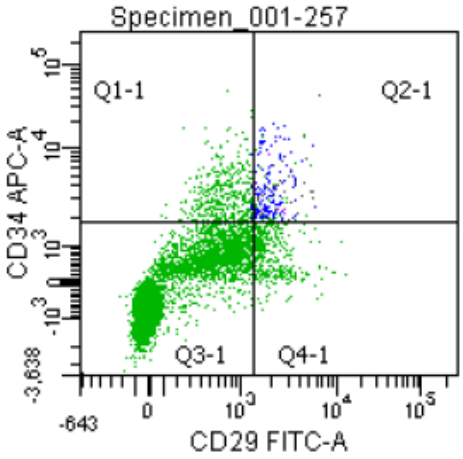
Specimen_001-257
CD34 APC-A
CD29 FITC-A
Q1-1
Q2-1
Q3-1
Q4-1

(d)

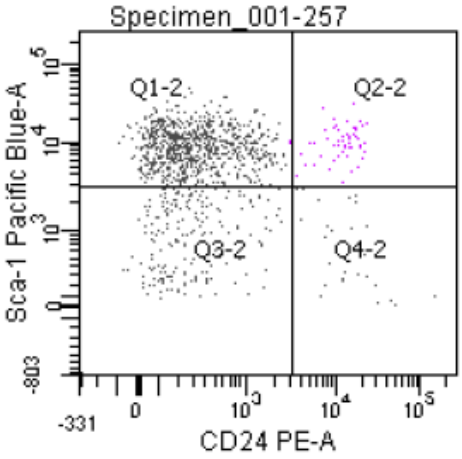
Specimen_001-257
Sca-1 Pacific Blue-A
CD24 PE-A
Q1-2
Q2-2
Q3-2
Q4-2

Figure A3. Representative flow cytometry plots from immune markers (tube 2) in SVF from lean C57BL/6 mice.

(a) Viable cell population defined by forward-scattered light (FSC) and side-scattered light (SSC)

(b) Cell population of $CD3^+$, which are T lymphocytes.

(c) Cell populations of $CD11c^+$, which are DC and macrophages. They are distinguished by the levels of auto-fluorescence and their size, as the macrophages are larger and have high auto-fluorescence.

(d) The DC from plot (c) were gated for MHCII and CD11c. The $CD11c^+MHCII^+$, shown in Q2, are mature DCs and the $CD11c^+MHCII^-$, shown in Q4, are immature dendritic cells.

(e) The macrophages from plot (c) were gated for F4/80 and CD11c. The $F4/80^+CD11c^+$ cells, shown in Q2, are M1 macrophages and the $F4/80^+CD11c^-$ cells, shown in Q4, are M2 macrophages.

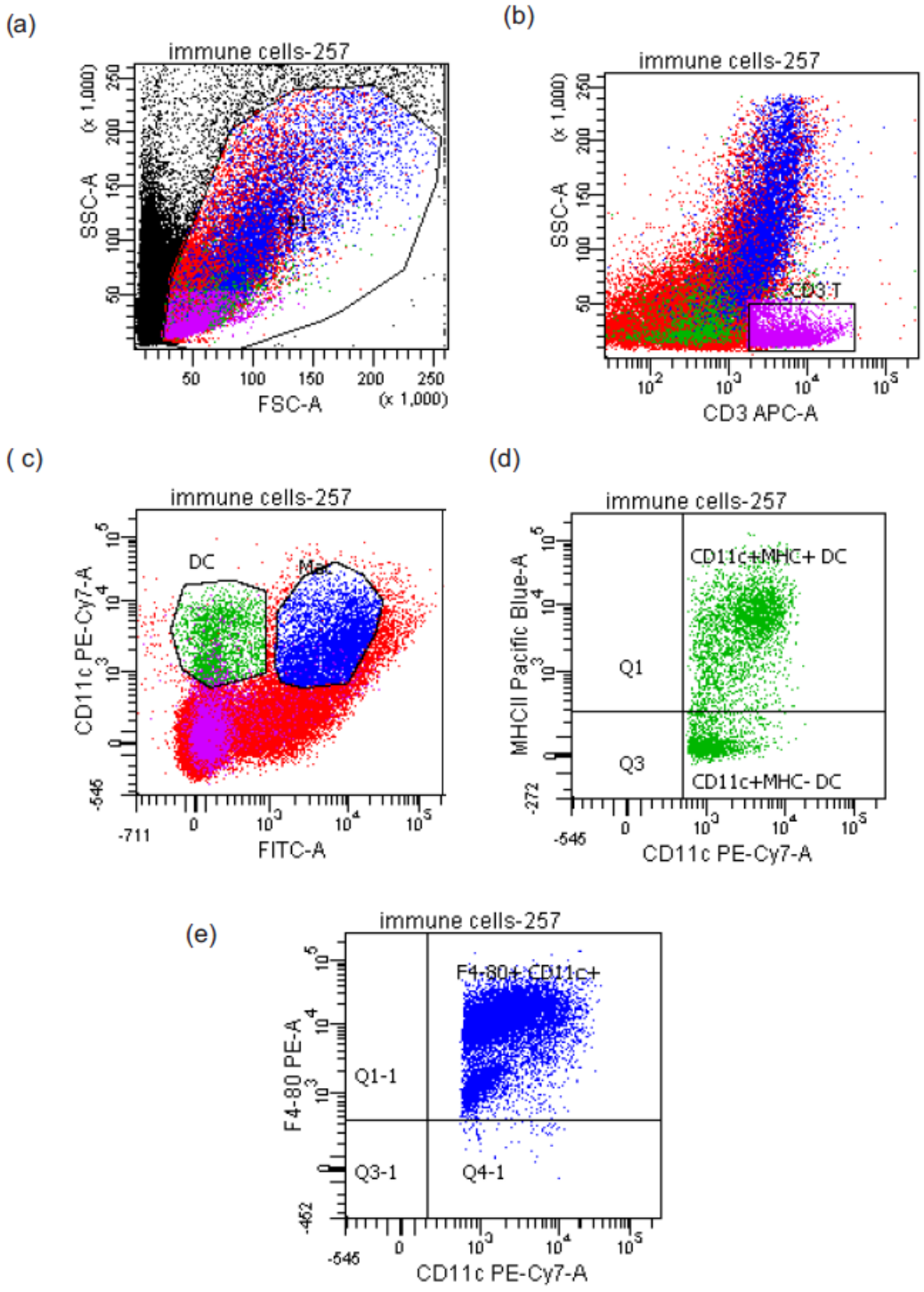
(a)
immune cells-257
SSC-A
(x 1,000)
FSC-A
(x 1,000)
(b)
immune cells-257
SSC-A
CD3+T
CD3 APC-A
(c)
immune cells-257
DC
Mac
CD11c PE-Cy7-A
FITC-A
(d)
immune cells-257
CD11c+MHC+ DC
Q1
Q3
CD11c+MHC- DC
MHCII Pacific Blue-A
CD11c PE-Cy7-A
(e)
immune cells-257
F4-80+ CD11c+
Q1-1
Q3-1
Q4-1
F4-80 PE-A
CD11c PE-Cy7-A

Figure A4. Representative flow cytometry plots from immune markers (tube 2) in SVF from obese *db/db* mice

(a) Viable cell population defined by forward-scattered light (FSC) and side-scattered light (SSC)

(b) Cell population of $CD3^+$, which are T lymphocytes

(c) Cell populations of $CD11c^+$, which are DCs and macrophages. They are distinguished by the levels of auto-fluorescence and their size, as the macrophages are larger and have high auto-fluorescence.

(d) The DCs from plot (c) were gated for MHCII and CD11c. The $CD11c^+MHCII^+$, shown in Q2, are mature DCs and the $CD11c^+MHCII^-$, shown in Q4, are immature dendritic cells.

(e) The macrophages from plot (c) were gated for F4/80 and CD11c. The $F4/80^+CD11c^+$ cells, shown in Q2, are M1 macrophages and the $F4/80^+CD11c^-$ cells, shown in Q4, are M2 macrophages.

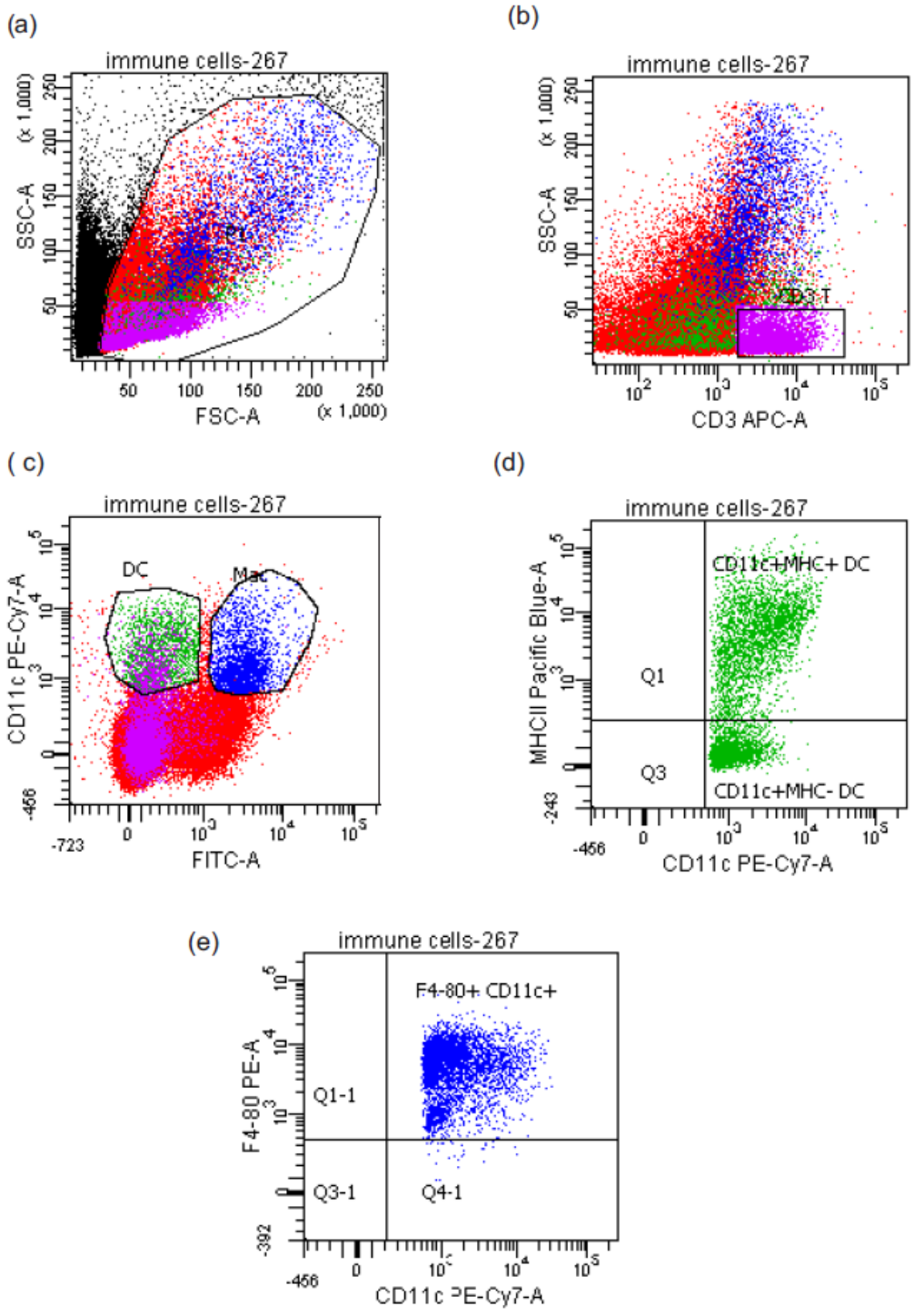
(a)
immune cells-267
SSC-A (x 1,000)
FSC-A (x 1,000)
P1
(b)
immune cells-267
SSC-A (x 1,000)
CD3 APC-A
CD3+T
(c)
immune cells-267
CD11c PE-Cy7-A
FITC-A
DC
Mac
(d)
immune cells-267
MHCII Pacific Blue-A
CD11c PE-Cy7-A
Q1
Q3
CD11c+MHC+ DC
CD11c+MHC- DC
(e)
immune cells-267
F4-80 PE-A
CD11c PE-Cy7-A
Q1-1
Q3-1
Q4-1
F4-80+ CD11c+

11.2 Appendix B. Physiological parameters and PPARγ in adipose tissue

Table B1. Organ weights and urine volume[1]

	db/db				C57BL/6			
Parameter	**CTL**	***c*9-*t*11 CLA**	***t*10-*c*12 CLA**	**PW**	**CTL**	***c*9-*t*11 CLA**	***t*10-*c*12 CLA**	**PW**
Liver Wt	3.08 ±0.29^{b}	3.58 ±0.23^{a}	3.99 ±0.18^{c}	1.61 ±0.15^{d}	1.02 ±0.04^{xy}	0.96 ±0.03^{x}	1.44 ±0.14^{y}	0.91 ±0.04^{x}
Liver /100 g BW	6.98 ±0.54^{a}	7.92 ±0.33^{a}	13.3 ±0.46^{b}	4.78 ±0.38^{c}	4.08 ±0.06^{a}	4.15 ±0.11^{a}	6.19 ±0.56^{b}	4.00 ±0.13^{a}
Heart Wt	0.156 ±0.008^{a}	0.146 ±0.006^{ab}	0.136 ±0.006^{bc}	0.124 ±0.010^{c}	0.154 ±0.003^{y}	0.132 ±0.006^{x}	0.143 ±0.004^{xy}	0.140 ±0.008^{xy}
Heart /100 g BW	0.371 ±0.026^{a}	0.328 ±0.016^{a}	0.454 ±0.022^{b}	0.369 ±0.004^{a}	0.621 ±0.027	0.572 ±0.024	0.621 ±0.011	0.619 ±0.035
Urine (ml/5 hours)	0.625 ±0.080^{a}	0.925 ±0.231^{a}	0.582 ±0.127^{a}	0.240 ±0.060^{b}	0.225 ±0.068^{x}	0.113 ±0.040^{xz}	0.792 ±0.111^{y}	0.150 ±0.038^{z}

[1]The absolute organs weights and organs weight adjusted to total body weight; urine was collected in metabolic cages, means ± SEM; n=12 for C57BL/6 *t*10-*c*12 CLA, n=11 for *db/db* *t*10-*c*12 CLA, n=7 for *db/db* PW and n=8 for all other groups. Statistical analysis was performed using two-way ANOVA and SAS software; contrast statements for pre-planned comparisons were used for means testing. Statistical differences ($P \leq 0.05$) among means are indicated by different lower case letters within a genotype.

Interpretation: The increase in liver weight (both absolut and relative) in *t*10-*c*12 CLA groups compared to the rest of the groups within their respective genotype, could indicate fat accumulation is occurring in the liver, which results in fatty liver. The increased heart weight relative to body weight in the *db/db* *t*10-*c*12 CLA fed mice could suggest hypertrophy of the heart and increased cardiac output. The increased amount of urine from *db/db* CTL, *c*9-*t*11 CLA and *t*10-*c*12 CLA fed mice could possibly be a factor associated with the increase of blood glucose and advancement of diabetes. The increased amount of urine from C57BL/6 *t*10-*c*12 CLA group, which had elevated blood glucose were also observed. In contrast, the lower amount of urine from calorie restricted mice could be suggestive of improvements in blood glucose and diabetes. However, further investigation is required to confirm these speculations.

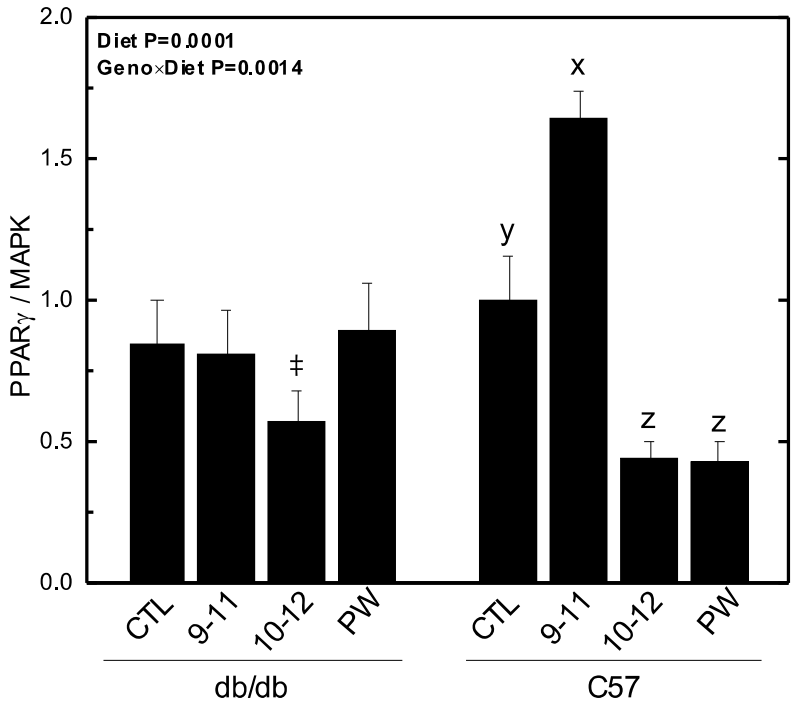

Figure B1. Levels of PPARγ in the epididymal adipose tissue of the obese *db/db* and lean C57BL/6 mice

Densitometry was used to quantify the intensity of the Western blot bands of PPARγ. Data were normalized to the loading control (MAPK). The results are presented as means ± SEM for n=9 for *db/db* *t*10-*c*12 group, n=8 for *db/db* CTL and *db/db* *c*9-*t*11 groups, n=7 for *db/db* PW group, n=6 for the C57BL/6 *t*10-*c*12 group and n=4 for C57BL/6 CTL, C57BL/6 *c*9-*t*11 and C57BL/6 PW groups. Statistical analysis was performed using two-way ANOVA and SAS software; contrast statements for preplanned comparison were used for means testing. Statistical differences ($P \leq 0.05$) among means are indicated by

different lower case letters within a genotype. The ‡ indicates a trend (P=0.08) for lower PPARγ in the *db/db* *t*10-*c*12 compared to the *db/db* PW and *db/db* CTL groups.

Interpretation: Lower PPARγ levels in epididymal adipose tissue of the obese *db/db* and lean C57BL/6 mice fed *t*10-*c*12 CLA compared to their respective CTL group could indicate that adipogenesis is reduced in the adipose tissue. These data are supported of published findings that *t*10-*c*12 CLA increases the levels of inflammatory cytokines such as TNFα, which inhibits PPARγ and consequently adipogenesis. In contrast, the C57BL/6 mice fed *c*9-*t*11 CLA had elevated levels of PPARγ. Since an increase in body weight and/or fat mass was not observed in *c*9-*t*11 CLA fed mice, the increase in PPARγ levels may not affect adipogenesis, however, it could possibly increase other factors such as lipid droplet formation. Interestingly, the levels of PPARγ were reduced in calorie restricted C57BL/6 mice, suggesting diminished recruitment of new adipocytes in this group.